Characterisation of the SIX6 effector protein from *Fusarium oxysporum* f. sp. *lycopersici*

A thesis submitted for the degree of Doctor of Philosophy of
The Australian National University

By

Pravin Bhanudas Khambalkar

October 2025

© Copyright by Pravin Bhanudas Khambalkar 2025

All Rights Reserved

Declaration

I hereby declare that this thesis is solely my work and has not been presented in any manner for another academic award at any university or similar institution of higher education. The text acknowledges information derived from the work of others and gives a list of references. The text recognises materials generated by others obtained for use in this study.

Pravin Bhanudas Khambalkar

October 2025

Acknowledgements

First, I would like to acknowledge my supervisor and honorary group leader of the plant disease resistance Lab, David Jones, who has supported me from the first email contact for the PhD position. His support was continuously there even during the difficult times during the COVID pandemic, when I was stuck in India for two years. I would like to acknowledge Dr Simon Williams for his co-supervision. I appreciate all his help and advice during this project.

A big thanks goes to Daniel Yu, who helped me in purifying proteins and discussing all the experiments regarding protein purification, along with crystallisation. Moreover, he was generous enough to give some of his protein to me for doing the functional and in planta experiments. We have achieved so much more together as a team than we would have individually.

I would also like to acknowledge Dr Ann Maree Catanzariti and Dr Lisong Ma for their valuable guidance in the lab during this project and Dr Florian Busch from Farquhar's lab for his help in measuring stomatal conductance. I would also like to highlight my colleagues Della, who helped me with initial laboratory work, Dr Jaime Simbaqueba for his guidance in the pathogenicity test and Sharmin, Ayesha, Farhad, Sun, and Suresh for being part of the Jones Lab, sharing and discussing relevant issues in the group.

I wish to express my sincere appreciation to the plant services team for their meticulous care of my various plant specimens during the protein functional testing phase. I am particularly grateful to Jenny, whose keen awareness and responsiveness to our requirements proved indispensable. My thanks also extend to Christine and Gavin for their diligent support in managing my plants in the Controlled Environmental Facility (CEF).

I am deeply grateful to Professor Barry Pogson for providing me with the opportunity to work in his laboratory. I owe special recognition to Dr Marten Moore, my direct supervisor, whose unwavering support, guidance, and encouragement were instrumental in the completion of my thesis, and I cannot express enough gratitude for his exceptional character. I would like to extend my sincere thanks to my colleagues in the Pogson Laboratory: Derek, Nat, Bec, Garima, Andrew, Mat, Brea, and Julie for creating a collaborative and supportive environment. I also wish to acknowledge my former colleagues from Furbank's laboratory, particularly Florence, Kavya, Riya, and Ding, for their friendly nature throughout my working period.

I would like to thank my parents for their constant love and support, especially during tough COVID times. A big thanks goes to my wife, Swati, for choosing me as her husband, even though I did not have much at that point of time in my life and was stuck in India during COVID. Her support continued unwaveringly after our return to Australia. I would also like to thank my younger brothers, Chetan and Deepak, for their unconditional love and support. To my colleagues from other Labs in the Research School of Biology, including Ramawatar, Suresh, Sam, Bayantes, Yiheng, Alex, Tamene, Reynaldi, and Yi Chang. To my friends in Australia, Sana, Roshan, Nabeel, Omkar, Rahul sir and family, Akshay sir and family, thank you for being there for me throughout my journey. Your company and support are very much appreciated. I would also like to thank my friends in India, Vikas, Ruturaj, Shashikant, Mahesh, Satish, Raj, Sachin, Pradip, Rupesh, and Roshan, who were overseas but still reachable whenever I needed them.

Finally, I wish to express my deep gratitude to the Indian Council of Agricultural Research (ICAR) for awarding me the Netaji Subhas-ICAR International Fellowship, and to the Research School of Biology at the Australian National University for providing the Fee Remission Scholarship and research facilities essential to this work.

Abstract

The phytopathogenic fungus *Fusarium oxysporum* f. sp. *lycopersici* (*Fol*) causes vascular wilt disease in tomato. During host colonisation, *Fol* secretes multiple effector proteins into the xylem sap, including fourteen SIX (Secreted In Xylem) proteins. Three of these SIX proteins function as the avirulence determinants Avr1 (SIX4), Avr2 (SIX3) and Avr3 (SIX1) recognised by tomato resistance proteins I, I-2 and I-3, respectively. Despite identifying the *I-7* resistance gene, which encodes a leucine-rich repeat receptor protein, its corresponding avirulence gene remains undetermined. This work initially aimed to identify *Avr7* by evaluating untested *SIX* genes and novel effector candidates. Effector candidates from transcriptomic analysis of infected tomato roots were assessed via *Agrobacterium*-mediated co-expression with *I-7* in *Nicotiana benthamiana*. *I-7*-dependent leaf cell death would indicate recognition. None of the examined candidates exhibited *I-7*-dependent cell death, but *SIX6* induced cell death independently of *I-7* (Chapter 2). This observation prompted experiments to characterise SIX6 function *in planta*.

In collaboration with Daniel Yu from the Williams Laboratory at ANU, *Fol SIX6* was expressed in *E. coli* and the recombinant protein purified for functional analyses. Purified recombinant *Fol* SIX6 induced cell death in *N. benthamiana* and tomato (Chapter 3). Subsequently, SIX6 homologues from *F. oxysporum* ff. spp. *cubense* TR4, *melonis* and *vasinfectum* (*Foc*, *Fom* and *Fov* SIX6) were expressed and purified, and found to induce cell death responses in *N. benthamiana* and tomato (Chapter 3). Testing purified *Fol*, *Foc* and *Fom* SIX6 proteins in foliar tissues of representatives from multiple taxonomic families (Solanaceae, Cucurbitaceae, Brassicaceae and Leguminosae) revealed broad yet differential plant sensitivity (Chapter 3). Notably, *Fol* and *Fov* SIX6 induced stronger cell death in the corresponding tomato and cotton hosts than vice versa.

VIGS of known plant defence-signalling components in *N. benthamiana* was used to test whether *Fol* SIX6-induced cell death might constitute a plant immune response. VIGS targets included pattern recognition co-receptors BAK1, SOBIR1, and mitogen-activated protein kinases WIPK and SIPK. VIGS-mediated depletion of these signalling components failed to attenuate *Agrobacterium*-mediated *Fol* SIX6-induced cell death (Chapter 4). These experiments were complemented by challenging mutant tomato lines compromised in defence signalling with *Fol* SIX6 protein. The ethylene-insensitive *Never ripe* mutant and *sun1-1* mutant deficient in EDS1-mediated resistance exhibited cell-death responses comparable to

wild-type controls following SIX6 infiltration (Chapter 4). These findings suggested SIX6 induced cell death through a mechanism distinct from these plant defence pathways.

A microscopic investigation of cellular responses leading to SIX6-induced cell death revealed that *Fol* SIX6 protein causes stomatal opening in tomato and *N. benthamiana* before visible cell death (Chapter 5). Physiological measurements demonstrated that *Fol* SIX6 infiltration significantly increased stomatal conductance and transpiration rates in *N. benthamiana* leaves, regardless of light conditions (Chapter 5). Confocal fluorescence microscopy following *Agrobacterium*-mediated expression of a vacuole-targeted fluorescent protein revealed that SIX6 treatment caused vacuolar shrinkage and leakage in *N. benthamiana* leaf epidermal cells (Chapter 5).

An examination of the effect of *Fol* SIX6 on *N. benthamiana* and tomato roots showed that *Fol* SIX6 protein caused electrolyte leakage (Chapter 6). *In vitro* growth assays on medium supplemented with purified *Fol* SIX6 protein resulted in significant inhibition of primary root elongation in tomato seedlings (Chapter 6). These findings suggest SIX6 exerts physiological effects on root tissues that may contribute to *Fol* pathogenicity during infection.

Abbreviations

ABA	abscisic acid
ACC synthase	1-aminocyclopropane-1-carboxylic acid synthase
ADR1	activated disease resistance 1
AtMPK3	*Arabidopsis thaliana* mitogen-activated kinase 3
AtMPK6	*Arabidopsis thaliana* mitogen-activated kinase 6
Avr	avirulence
BAK1	BRI1-associated receptor kinase 1
CC	coiled-coil domain
CC-NLRs	coiled-coil domain NLRs
CERK1	chitin elicitor receptor kinase 1
CNL	coiled-coil–nucleotide-binding leucine-rich repeat
CTR1	constitutive triple response 1
DAMPs	damage-associated molecular patterns
DNA	deoxyribonucleic acid
dpi	days post infiltration
DTT	dithiothreitol
EDS1	enhanced disease susceptibility 1
EIN2	ethylene insensitive 2
EIN3	ethylene insensitive 3
ERFs	ethylene response factors
ETI	effector-triggered immunity
ETR1	ethylene receptor 1
ETS	effector-triggered susceptibility

FLS2	flagellin sensing 2
Fg	*Fusarium graminearum*
Foc	*F. oxysporum* f. sp. *cubense*
Fof	*F. oxysporum* f. sp. *fragariae*
Fol	*F. oxysporum* f. sp. *lycopersici*
FOLD	*Fusarium oxysporum* f. sp. *lycopersici* dual domain
Fom	*F. oxysporum* f. sp. *melonis*
Fon	*F. oxysporum* f. sp. *niveum*
FOSC	*Fusarium oxysporum* species complex
Fov	*F. oxysporum* f. sp. *vasinfectum*
Fv	*Fusarium verticillioides*
HR	hypersensitive response
JA	jasmonic acid
kb	kilo base pairs
LB/LBA	lysogeny broth/ lysogeny broth agar
LIC	ligation-independent cloning
LOV	locus orchestrating victorin
LRR-RKs	leucine-rich repeat receptor kinases
LRR-RPs	leucine-rich repeat receptor proteins
LS	lineage-specific
MAMPs	microbe-associated molecular patterns
MAPK	mitogen-activated protein kinase
MAPKs	mitogen-activated protein kinases
MLRKs	Malectin-like receptor kinases

MS	Murashige and Skoog
NEP1	NEP1-like proteins
NIPs	Nodulin-26-like intrinsic proteins
NLPs	necrosis and ethylene-inducing peptide 1-like proteins
NLRs	nucleotide-binding leucine-rich repeat proteins
NHR	Non-host resistance
NRG1	N requirement gene 1
OD	optical density
PAD4	phytoalexin-deficient 4
PAMPs	pathogen-associated molecular patterns
PBL31	PBS1-like 31
PCD	programmed cell death
PCR	polymerase chain reaction
PDB	potato dextrose broth
PG	polygalacturonase
PIPs	plasma membrane intrinsic proteins
PRRs	pattern recognition receptors
PTI	pattern-triggered immunity
RALFs	rapid alkalinisation factors
ROS	reactive oxygen species
SA	salicylic acid
SAG101	senescence-associated gene 101
SAP	stress-associated protein
SDS-PAGE	sodium dodecyl-sulphate polyacrylamide gel electrophoresis

SIPK	salicylic acid-induced protein kinases
SIX	secreted in xylem
SOBIR1	suppressor of BAK1-interacting receptor-like kinase 1
SRLK	self-incompatibility receptor-like kinase
SRLKs	S-locus receptor kinases
TIPs	tonoplast intrinsic proteins
TIR	toll/interleukin-1 receptor
TIR-NLRs	Toll/interleukin-1 receptor cytosolic domain NLRs
TNL	toll/interleukin-1 receptor–nucleotide-binding leucine-rich repeat
TRV	tobacco rattle virus
VCGs	vegetative compatibility groups
VIGS	virus-induced gene silencing
VPEs	vacuolar processing enzymes
VSP	vegetative storage protein
WAK	wall-associated kinase
WAKs	wall-associated kinases
WIPK	wound-induced protein kinase
XIPs	X intrinsic proteins

Table of Contents

Declaration 1

Acknowledgements 2

Abstract 4

Abbreviations 6

List of Figures 18

List of Tables 22

Chapter 1: Introduction 23

1.1 Plant pathogens 24

1.1.1 Plant pathogens 24

1.1.2 Fungal Pathogens 24

1.1.3 *Fusarium* 25

1.1.4 *Fusarium oxysporum* 25

1.1.5 *Fusarium oxysporum* f. sp. *lycopersici* (*Fol*) 27

1.1.6 *Fol* infection process 28

1.1.7 Disease symptoms 29

1.2 Plant immunity 31

1.2.1 Plant Immunity: A General Overview 31

1.2.2 Non-host resistance: a broad-spectrum barrier against pathogens 31

1.2.2.1 PRRs 33

1.2.2.2 Induction of PTI by LRR-RKs and LRR-RPs 36

1.2.3 Host-specific resistance: Pathogen strain-specific resistance 37

1.2.3.1 Resistance proteins 39

1.2.3.2 Induction of ETI and cell death by TIR-NLRs 41

1.2.3.3 Induction of ETI and cell death by CC-NLRs 43

1.3 Pathogen effectors 44

1.3.1 Fungal effectors in pathogen nutrition and the avoidance of recognition 44

1.3.2 Fungal effectors causing cell death 47

1.3.3 *Fol* effectors and their function 49

1.3.4 Tomato genes conferring resistance to *Fol* 56

1.4 Aims of the research project 59

References 60

Chapter 2: Attempts to identify the *Avr7* effector gene from *Fusarium oxysporum* f. sp. *lycopersici* enable the identification of *SIX6* as an inducer of plant cell death **77**

2.1 Introduction 78

2.2 Materials and Methods 79

2.2.1 Plant growth conditions 79

2.2.2 Testing of *Avr7* candidates 79

2.2.3 *Fol* genomic DNA extraction protocol 79

2.2.4 Total RNA extraction and cDNA synthesis 80

2.2.5 Ligation Independent Cloning (LIC) 80

2.2.5.1 Amplification of target sequences 82

2.2.5.2 Preparation of the LIC Vector 82

2.2.5.3 T4 DNA polymerase treatment 82

2.2.5.4 Annealing 83

2.2.6 *E. coli* transformation 83

2.2.7 Colony screening 83

2.2.8 DNA sequencing 84

2.2.9 Transformation of *Agrobacterium* 84

2.2.10 *Agrobacterium*-mediated gene expression 84

2.3 Results 85

2.3.1 Co-expression of candidate *Avr7* genes with *I-7* in *N. benthamiana* leaves 85

2.4 Discussion 90

2.4.1 Testing of seven *Avr7* candidates has not enabled the identification of *Avr7* 90

2.4.2 *Fol SIX6* is an effector that causes cell death 93

References 94

Appendix 2.1 Map of pSL vector used in this study 98

Appendix 2.2 Map of pSLG vector used in this study 98

Appendix 2.3 Primers used for amplification of the target sequence (*Avr7* candidates) 99

Appendix 2.4 Co-agroinfiltration of *Avr7* candidates and *I-7* in *N. benthamiana* leaves 107

Appendix 2.5 Agroinfiltration of *I-7* and *Fol SIX6* in *Nicotiana benthamiana* leaves 109

Chapter 3: *Fol* SIX6 is a cell death-inducing effector **110**

3.1 Introduction 111

3.2 Materials and Methods 113

3.2.1 Plant material 113

3.2.2 Bacterial strains and vectors 113

3.2.3 Purification of plasmid DNA 114

3.2.4 DNA gel electrophoresis 114

3.2.5 Purification of DNA from PCR samples 114

3.2.6 Transformation of *E. coli* 114

3.2.7 Transformation of *Agrobacterium* (GV3101) 115

3.2.8 Colony PCR screening 115

3.2.9 SDS-PAGE (Sodium Dodecyl-Sulphate Polyacrylamide Gel Electrophoresis) 116

3.2.10 Generation of binary vector constructs by ligation-independent cloning (LIC) 116

3.2.11 *Agrobacterium*-mediated gene expression 117

3.2.12 Generation of protein expression constructs by Golden Gate cloning 117

3.2.13 Preparation and infiltration of recombinant SIX6 proteins 118

3.3 Results 119

3.3.1 *Agrobacterium*-mediated expression of *Fol* SIX6 and its homologues induces plant cell death 119

3.3.2 *Fol* SIX6 protein induces cell death in tomato 121

3.3.3 DTT treatment but not heat treatment affects the cell death-inducing activity of *Fol* SIX6 protein 123

3.3.4 Homologues of *Fol* SIX6 induce cell death responses of different intensities 125

3.3.5 *Fol* SIX6 induces a variety of responses in different plant species 127

3.3.6 *Fom* SIX6 and *Foc* SIX6 proteins induce similar responses compared to *Fol* SIX6 with some variations 133

3.3.7 SIX6 proteins from different ff. spp. induce stronger cell death in their corresponding host plants than in non-host plants 149

3.4 Discussion 150

3.4.1 *Fol* SIX6 is a semi-specific cell death-inducing protein 150

3.4.2 *Fol* SIX6 homologues cause cell death and other phenotypes in different plant families 153

References 158

Appendix 3.1 Plant species used in the study 164

Appendix 3.2 Gene blocks used in the study 165

Appendix 3.3 Primers used in this study 166

Appendix 3.4 Agroinfiltration of *Fol* SIX6 and Avr1 (*Fol* SIX4 used as a positive control) into leaves of tomato cv. M82 (which carried the I gene) did not induce a cell death response 167

Appendix 3.5 Protein gel blot of 6xHis-GB1-FolSIX6 protein at various steps during its purification, probed using HRP-conjugated anti-His antibodies 168

Appendix 3.6 Agroinfiltration of protein extracted from a vector-only control into leaves of *N. benthamiana* tomato did not induce a cell death response 169

Appendix 3.7 *Fol* SIX6 protein 100 µg/ml and water (control) infiltration in wheat varieties Currawong and WW2249 170

Appendix 3.8 Leaves of banana lines resistant or susceptible to *Foc* TR4 were infiltrated with *Foc* SIX protein (100 µg/ml), NLP protein (100 µg/ml) or buffer 171

Chapter 4: Is *Fol*-SIX6-induced cell death a plant-defence response? 172

4.1 Introduction 173

4.2 Materials and Methods 179

4.2.1 Plant material 179

4.2.2 *Fol* SIX6 protein infiltration in tomato and *N. benthamiana* 179

4.2.3 VIGS constructs used in *N. benthamiana* 180

4.2.4 VIGS assay in *N. benthamiana* 180
4.3 Results 182
4.3.1 Virus-induced gene silencing of *BAK1*, *SOBIR1* or *WIPK* and *SIPK* does not reduce the cell death response induced by expression of *Fol* SIX6 in *N. benthamiana* 182
4.3.2 Mutations affecting *EDS1* and ethylene perception do not reduce the cell death response induced by *Fol* SIX6 in tomato 185
4.4 Discussion 187
4.4.1 *Fol* SIX6-mediated cell death is not dependent on defence signalling 187
References 190

Chapter 5: *Fol* SIX6 induces stomatal opening and increases leaf transpiration 201
5.1 Introduction 202
5.2 Materials and Methods 207
5.2.1 Plant Materials 207
5.2.2 Preparation of epidermal peels and measurements of stomatal length and aperture 207
5.2.3 Gas exchange measurements 208
5.2.4 Measurement of electrolyte leakage from leaf discs 209
5.2.5 Confocal fluorescence microscopy of mTurquoise2-labelled vacuoles 210
5.2.6 Preparation of *Fol* inoculum 211
5.2.7 *Fol* pathogenicity test 211
5.3 Results 211
5.3.1 *Fol* SIX6 causes stomatal opening in *Nicotiana benthamiana* 211
5.3.2 *Fol* SIX6 causes stomatal opening in a light-independent manner and increases transpiration 214
5.3.3 *Fol* SIX6 protein causes electrolyte leakage in leaves of *N. benthamiana an*d tomato 215
5.3.4 *Fol* SIX6 causes vacuolar shrinkage 217
5.3.5 ABA has a minor effect on the ability of *Fol* SIX6 to open stomata, but does not appear to affect cell death induction 220
5.3.6 *Fol* SIX6 does not cause stomatal opening during infection 224
5.4 Discussion 225

5.4.1 *Fol* SIX6 induces stomatal opening 225
5.4.2 *Fol* SIX6 protein causes vacuolar shrinkage 228
5.4.3 ABA has a minor negative effect on *Fol* SIX6-induced stomatal opening but a positive effect on cell death induction 229
5.4.4 *Fol* infection fails to induce stomatal opening 230
References 231
Appendix 5.1 Coding and protein sequence of vacuole-targeted mTurquoise2 237
Appendix 5.2 Stomatal response to Agrobacterium-mediated expression of *Fol* SIX6 and Avr1 (*Fol* SIX4) 238
Appendix 5.3 Microscopic analysis of radish and zucchini stomata from leaves infiltrated with *Fol* SIX6 239
Appendix 5.4 Disease symptoms in M82 tomato 21 days after inoculation with *Fol* race 3 240

Chapter 6: Functional analysis of the effect of *Fol* SIX6 protein on roots 241
6.1 Introduction 242
6.2 Materials and Methods 243
6.2.1 Measurement of ion leakage from *N. benthamiana* root sections 243
6.2.2 Measurement of ion leakage from tomato root sections 245
6.2.3 Tomato root growth measurement 246
6.3 Results 247
6.3.1 *Fol* SIX6 protein causes electrolyte leakage from roots of *N. benthamiana* and tomato 247
6.3.2 *Fol* SIX6 protein inhibits primary root elongation and promotes the formation of secondary roots of tomato 249
6.4 Discussion 255
6.4.1 *Fol* SIX6 causes electrolyte leakage in roots of *N. benthamiana* and tomato 255
6.4.2 *Fol* SIX6 affects root growth in tomato 257
References 259
Appendix 6.1 Primary root lengths and secondary root numbers used to generate Figure 6.5 262

Appendix 6.2 Primary root lengths and secondary root numbers used to generate Figure 6.6 263
Appendix 6.3 Primary root lengths and secondary root numbers used to generate Figure 6.7 264
Appendix 6.4 Primary root lengths and secondary root numbers used to generate Figure 6.8 265

Chapter 7: General Discussion **266**
7.1 Avr7 gene identification efforts and prospects 267
7.2 SIX6 cell death-inducing activity: potential for novel herbicide development 268
7.3 SIX6 cell death-inducing activity: independence from some defence pathways and future genetic approaches to test others 270
7.4 SIX6 impact on leaves: stomatal opening, water loss and the induction of leaf cell death 271
7.5 SIX6 impact on root systems: physiological disruption 273
7.6 Concluding remarks 274
References 277

List of Figures

Figure 1.1: *Fusarium oxysporum* causes wilt diseases in economically important crops like tomato, banana, cotton and watermelon.

Figure 1.2: The life cycle of *F. oxysporum*.

Figure 1.3: Disease symptoms of tomato Fusarium wilt.

Figure 1.4: Non-host resistance mechanisms in plants.

Figure 1.5: Diversity of plant extracellular immune receptors and downstream immune signalling.

Figure 1.6: Host-specific resistance mechanism in plant-pathogen interactions.

Figure 1.7: Plant immune receptors and effector-triggered immunity.

Figure 1.8: TIR-NLR immune signalling in plants.

Figure 1.9: CC-NLRs in plant immunity and cell death.

Figure 1.10: A graphical illustration of the tomato/*Fol* interaction and the R/Avr involved.

Figure 1.11: Graphic representation of the predicted I-7 protein.

Figure 2.1: Graphic representation of Ligation Independent Cloning (LIC).

Figure 2.2: Schematic representation of the pL-*I-7* vector and *Avr7*-candidate constructs in pSL and pSLG.

Figure 2.3: Patterns of agroinfiltration used in *N. benthamiana* leaves.

Figure 2.4: Co-agroinfiltration of *Avr7* candidates and *I-7* in *N. benthamiana* leaves.

Figure 2.5: Agroinfiltration of *I-7* and *Fol SIX6* in *Nicotiana benthamiana* leaves.

Figure 3.1: Cell death responses caused by *Agrobacterium*-mediated expression of *Fol SIX6* and its homologues.

Figure 3.2: Multiple sequence alignment of *Fol SIX6* and homologues.

Figure 3.3: SDS-PAGE analysis of SIX6 proteins during and after purification.

Figure 3.4: *Fol* SIX6 protein causes cell death in *N. benthamiana* and tomato.

Figure 3.5: Effects of heat and DTT treatments on cell death induced by *Fol* SIX6 in *N. benthamiana.*

Figure 3.6: Cell death induced by recombinant SIX6 proteins in *N. benthamiana.*

Figure 3.7: *Fol* SIX6 causes cell death in some plant species, but different responses or no response in other species.

Figure 3.8: *Fom* SIX6 causes cell death in some plant species but different responses or no response in other species.

Figure 3.9: *Foc* SIX6 causes cell death in some plant species but a different response or no response in other species.

Figure 3.10: *SIX*6 causes wilting and curling of cotyledons in some plant species.

Figure 3.11: A graphic comparison of the effects of *Fol*, *Fom* and *Foc* SIX6 on different plant species.

Figure 3.12: Recombinant *Fol*, *Fom* and *Fov* SIX6 proteins induce strong cell death responses in their respective plant hosts.

Figure 3.13: Cell death responses induced by *Fol* SIX6 and *Fov* SIX6 proteins in tomato and cotton.

Figure 3.14: Comparison of SIX6 sequences expressed by Gawehns et al. (2014) and in this study.

Figure 3.15: Phylogenetic distribution of plant species tested for responses to SIX6.

Figure 4.1: Simplified diagram showing where 1) *BAK1*, 2) *SOBIR1*, 3) *EDS1*, 4) ethylene and 5) Arabidopsis orthologues of tobacco *WIPK* and *SIPK* act in Arabidopsis defence-signalling pathways leading to cell death.

Figure 4.2: An overview of the VIGS study in *N. benthamiana* used to test the requirement for defence-related genes in *Fol-SIX6*-mediated cell death.

Figure 4.3: Virus-Induced Gene Silencing (VIGS) with CITRX to examine the establishment of VIGS in *N. benthamiana*.

Figure 4.4: Virus-Induced Gene Silencing (VIGS) testing for a requirement for *BAK1*, *SOBIR1* or *WIPK* and *SIPK* in *Fol-SIX6*-mediated cell death in *N. benthamiana*.

Figure 4.5: Cell death response induced by *Fol* SIX6 protein infiltrations in mutant tomato lines.

Figure 5.1: Simple illustration of various ion channels and transporters involved in the process of ion movement in guard cells, leading to stomatal opening and closure.

Figure 5.2: Simple illustration of aquaporin involvement in the process of stomatal opening and closing.

Figure 5.3: Simple illustration of the role of ABA in stomatal closure.

Figure 5.4: Stomatal pore length and width measurements from leaves of *Nicotiana benthamiana* infiltrated with *Fol* SIX6 protein.

Figure 5.5: Gas exchange measurements of leaves of *Nicotiana benthamiana* infiltrated with *Fol* SIX6 protein.

Figure 5.6: Measurement of electrolyte leakage from leaf discs taken from leaves of *N. benthamiana* or tomato plants infiltrated with *Fol* SIX6.

Figure 5.7: *Fol* SIX6 protein induces stomatal opening in *Nicotiana benthamiana*.

Figure 5.8: Stomatal opening in *Nicotiana benthamiana* is dependent on intact *Fol* SIX6 and is not an artefact of heterologous protein expression and purification.

Figure 5.9: SIX6 causes stomatal opening in tomato.

Figure 5.10: *Fol* SIX6 causes irreversible light-independent stomatal opening.

Figure 5.11: SIX6 causes electrolyte leakage in *N. benthamiana* leaves.

Figure 5.12: SIX6 causes electrolyte leakage in tomato leaves.

Figure 5.13: *Fol* SIX6 causes vacuolar shrinkage in *N. benthamiana.*

Figure 5.14: Repeated application of ABA did not stop cell death induced by *Fol* SIX6.

Figure 5.15: ABA causes a small reduction in stomatal opening caused by *Fol* SIX6.

Figure 5.16: Stomatal behaviour during infection.

Figure 6.1: Measurement of electrolyte leakage from *N. benthamiana* root sections.

Figure 6.2: Measurement of electrolyte leakage from tomato root sections.

Figure 6.3: Measuring electrolyte leakage from roots of *N. benthamiana* incubated with *Fol* SIX6 or Control.

Figure 6.4: Measuring electrolyte leakage from roots of tomato incubated with *Fol* SIX6 or control.

Figure 6.5: Measurement of primary root lengths and numbers of secondary roots for tomato seedlings grown on media containing BSA, *Fol* SIX6 protein or water.

Figure 6.6: Measurement of primary root lengths and numbers of secondary roots for tomato seedlings grown on media containing BSA, *Fol* SIX6 protein or water.

Figure 6.7: Measurement of primary root length and number of secondary roots of tomato c.v. M82 grown on half-strength media containing BSA, or *Fol* SIX6 protein or water.

Figure 6.8: Measurement of primary root lengths and numbers of secondary roots for tomato seedlings grown on half-strength media containing BSA, or *Fol* SIX1, or *Fol* SIX6 or *Fol* SIX8 or water.

Figure 6.9: Phenotypes of tomato seedlings after 20 days of growth on media containing BSA, *Fol* SIX6 protein or water.

Figure 7.1: Possible models for the induction of leaf cell death by SIX6

List of Tables

Table 1.1. List of effector proteins reported to date in *Fol*.

Table 2.1: List of effector candidates encoding small, secreted mostly cysteine-rich proteins, excluding those already tested as *Avr7* candidates, that had transcript per million values exceeding or equal to that of *SIX13* during *Fol* infection (Sun et al., 2022).

Chapter 1: Introduction

1.1 Plant pathogens

1.1.1 Plant pathogens

Many biotic and abiotic factors influence plant growth. Biotic factors include insects, weeds and plant pathogens, including parasitic plants, nematodes, oomycetes, fungi, bacteria and viruses, while abiotic factors consist of high or low light stress, high or low nutrient stress, flooding, high humidity, salt stress and drought stress. Any of these factors can adversely affect plant development, quality and productivity. Plant pathogens have been classified into three categories based on their feeding habit and reproduction. Biotrophic pathogens feed and reproduce on living plant tissues. Hemibiotrophic pathogens start feeding on living host tissue like a biotroph, but in later stages of infection, they kill host tissue and feed and reproduce on the dead tissue using secreted enzymes such as cellulases, pectinases and proteases to break down the plant cell wall and access nutrients from the dead cells (Mayer et al., 2001). In contrast, necrotrophic pathogens kill plant tissues at the beginning of infection. Plants try to stop pathogen invasion by using defence mechanisms targeted to the pathogen's lifestyle and mechanism of pathogenesis. Pathogen success, called a compatible interaction, is an infection that results in plant disease and the production of new pathogen propagules. Conversely, pathogen failure, called an incompatible interaction, is an attempted infection that is slowed or halted by the plant and results in the failure or limited ability to produce new pathogen propagules.

1.1.2 Fungal Pathogens

Examples of biotrophic fungi include the *Erysiphales*, which cause powdery mildews and the *Pucciniales,* which cause rust diseases. Examples of hemibiotrophic fungi, include *Magnaporthe oryzae*, which causes rice blast disease, *Colletotrichum* spp., which cause anthracnose diseases and *Fusarium oxysporum,* which causes wilt disease. *Botrytis cinerea,* which causes grey mould, is an example of a necrotrophic fungus. Pathogenic fungi reproduce and spread through spores, which are carried by different means such as wind, water, insects, soil or human activities, with some dispersal mechanisms enabling rapid dissemination of spores across widespread areas. The ability of pathogens to spread over vast areas in a relatively short period of time has a major effect on the yield of affected crops and a lot of economic consequences.

Fungal diseases of plants are usually managed by the development of genetically resistant plant cultivars, the application of biological control agents, such as antagonistic microorganisms, environmental controls or the strategic use of chemical fungicides. However, the increasing prevalence of fungicide-resistant strains highlights the urgent need for sustainable, integrated disease management practices that combine multiple control measures to ensure long-term efficacy. Advances in molecular biology, transcriptomics and genomics are revolutionising our understanding of fungal pathogenesis and plant immune responses, enabling the identification of pathogenicity factors and host resistance mechanisms. These insights are paving the way for innovative solutions, such as genome editing and molecular breeding, to enhance crop resilience. Therefore, elucidating the molecular and biochemical pathways underpinning fungal pathogenesis remains important for the development of targeted, effective and sustainable disease management strategies.

1.1.3 *Fusarium*

The genus *Fusarium* contains species that range from pathogens on plants and arthropods and opportunistic pathogens on mammals. Many soil-borne species of *Fusarium* have been recognised as significant plant pathogens and are found all over the world (Moss and Smith 1984), although more prevalent in tropical and subtropical ecosystems (Summerell, 2019). There are no less than 300 phylogenetically different species in the genus *Fusarium* and most of them lack a formal name (Geiser et al., 2013; Summerell, 2019). The genus also contains 20 species complexes that contain at least 60 different subspecies or *formae speciales* (Ma et al., 2013; Geiser et al., 2013; O'Donnell et al., 2015; Summerell, 2019). Some of the most prevalent plant pathogens in the genus are found in the *Fusarium oxysporum* and *Fusarium solani* species complexes (Dean et al., 2012).

1.1.4 *Fusarium oxysporum*

Members of the *Fusarium oxysporum* species complex (FOSC) are found in agricultural soils across the world. Plant-pathogenic members of the FOSC are capable of causing a range of diseases across a broad spectrum of plant hosts, including root and bulb rots as well as vascular wilts. Hosts include numerous economically important field crops, vegetables and ornamentals. Some of the economically important crops severely affected by *F. oxysporum* include banana, date palm, oil palm, chickpea, beans, melon, soybean, cotton, onion, cucurbits, brassicas,

legumes and members of the Solanaceae such as tomato, chilli, eggplant and cape gooseberry (Michielse and Rep, 2009; Ma et al., 2013).

Although there is no sexual reproduction in the FOSC, horizontal gene transfer contributes significantly to pathogenic strain diversification (Laurence et al., 2015; Van Dam and Rep, 2017; Gordon, 2017; Czislowski et al., 2018; Simbaqueba et al., 2018; Liu et al., 2019). The parasexual cycle has also been linked to genetic diversification via heterokaryon formation, which assists mitotic genetic exchange between two separate nuclei (Glass et al., 2000; Di Pietro et al., 2003). Vegetative compatibility loci restrict heterokaryon formation by only allowing hyphae from vegetatively compatible isolates to fuse and form heterokaryons. Individual isolates of *F. oxysporum* may be members of different VCGs (Vegetative Compatibility Groups), which are genetically distinct from each other and are basically distinct subspecies within the FOSC, each with a monophyletic distribution (Elias and Schneider, 1991).

Economically important *formae speciales* (*ff. spp*.) of *F. oxysporum* include *F. oxysporum* f. sp. *lycopersici* (*Fol*), which infects tomato plants, blocks the vascular system and ultimately leads to wilting and plant death (Figure 1.1A), *F. oxysporum* f. sp. *cubense* (*Foc*) which infects banana plants and causes Panama disease also known as Banana wilt (Figure 1.1B), *F. oxysporum* f. sp. *vasinfectum* (*Fov*) which leads to Fusarium wilt in cotton (Figure 1.1C) and *F. oxysporum* f. sp. *melonis* (*Fom*) or *niveum* (*Fon*) which cause wilt disease in muskmelon and watermelon (Figure 1.1D).

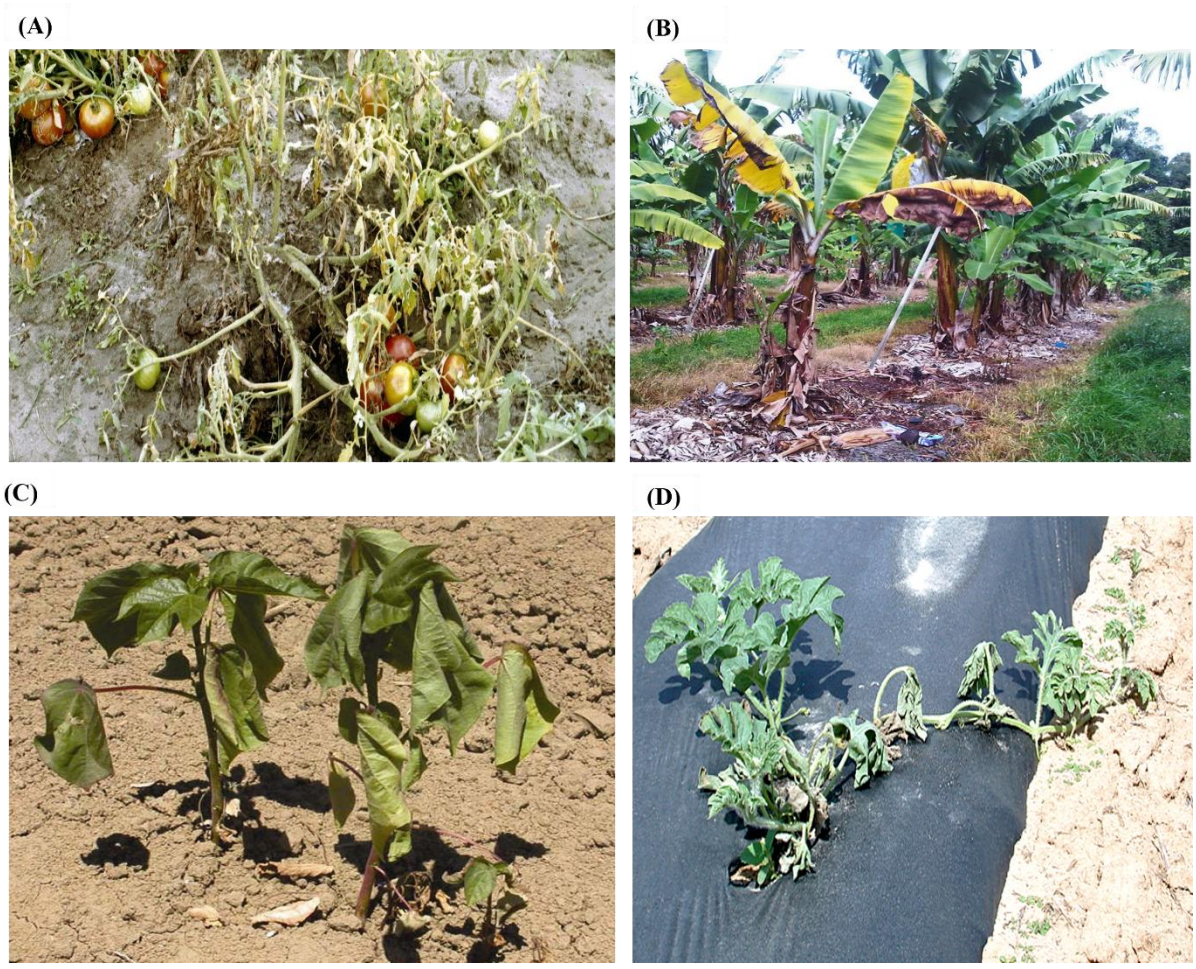

Figure 1.1 *Fusarium oxysporum* causes wilt diseases in economically important crops like tomato, banana, cotton and watermelon.

(A) *Fusarium* wilt caused by *Fol* in field-grown tomato **(**taken from https://extension.umd.edu/resource/fusarium-wilt-tomatoes-home-garden). **(B)** Wilted Cavendish banana plant infected by *Foc* race 1 (Pegg et al., 2019). (**C)** Wilted cotton plants infected by *Fov* (Davis et al., 2006). (**D)** Wilt of a watermelon plant caused by *Fon* (Egel and Martyn, 2007).

1.1.5 *Fusarium oxysporum* f. sp. *lycopersici* (*Fol*)

Fol specifically infects tomato plants and is considered one of the most important diseases of tomato. Three races, numbered 1, 2 and 3, have been described in *Fol*. They are distinguished by their differential capacity to infect tomato cultivars with one or more resistance genes. *Fol* race 1 was described by Bohn and Tucker (1939) and *Fol* race 2 was discovered by Alexander and Tucker (1945). Both races have been reported from agricultural regions across all continents. *Fol* race 3 was initially detected in Queensland, Australia in 1978 (Grattidge and O'Brien, 1982). During the 1980s, *Fol* race 3 was responsible for devastating losses of yield in

Australia. Race 3 has since spread to most parts of the world, including the USA and South America (Volin and Jones, 1982; Valenzuela-Ureta et al., 1996; Reis et al., 2005).

1.1.6 *Fol* infection process

Fol begins its life cycle as spores or mycelium in the soil (Figure 1.2). The germinating fungus secretes several enzymes, including polygalacturonases, xylanases and proteases to facilitate entry of fungal hyphae into the root (Beckman, 1987; Michielse and Rep, 2009; Perincherry et al., 2020). Hyphae then advance across the root cortex and start colonising xylem vessels (Figure 1.2). In an effort to combat this invasion and avoid the spread of the fungus to adjacent xylem vessels, plants form tyloses and secrete gums and pectin-rich gels, which lead to clogging of the vessels (Yadeta and Thomma, 2013). The combined effect of pathogen colonisation and plant responses results in blockage of xylem vessels, causing water stress and wilting symptoms to appear in lower leaves (Figure 1.2). During growth in the xylem, the pathogen switches to necrotrophy and secretes toxins and virulence factors that promote plant cell death (De Sain and Rep, 2015). Wilting and cell death spread to the entire plant which eventually dies from the disease (Figure 1.2). The fungus colonises the dead plant and fungal spores are released into the soil. *Fol* demonstrates remarkable environmental persistence through the production of chlamydospores, which are specialised survival spores that can remain dormant in soil for up to three decades before germinating under favourable conditions (Griffiths, 1973) and initiating new infections (Figure 1.2).

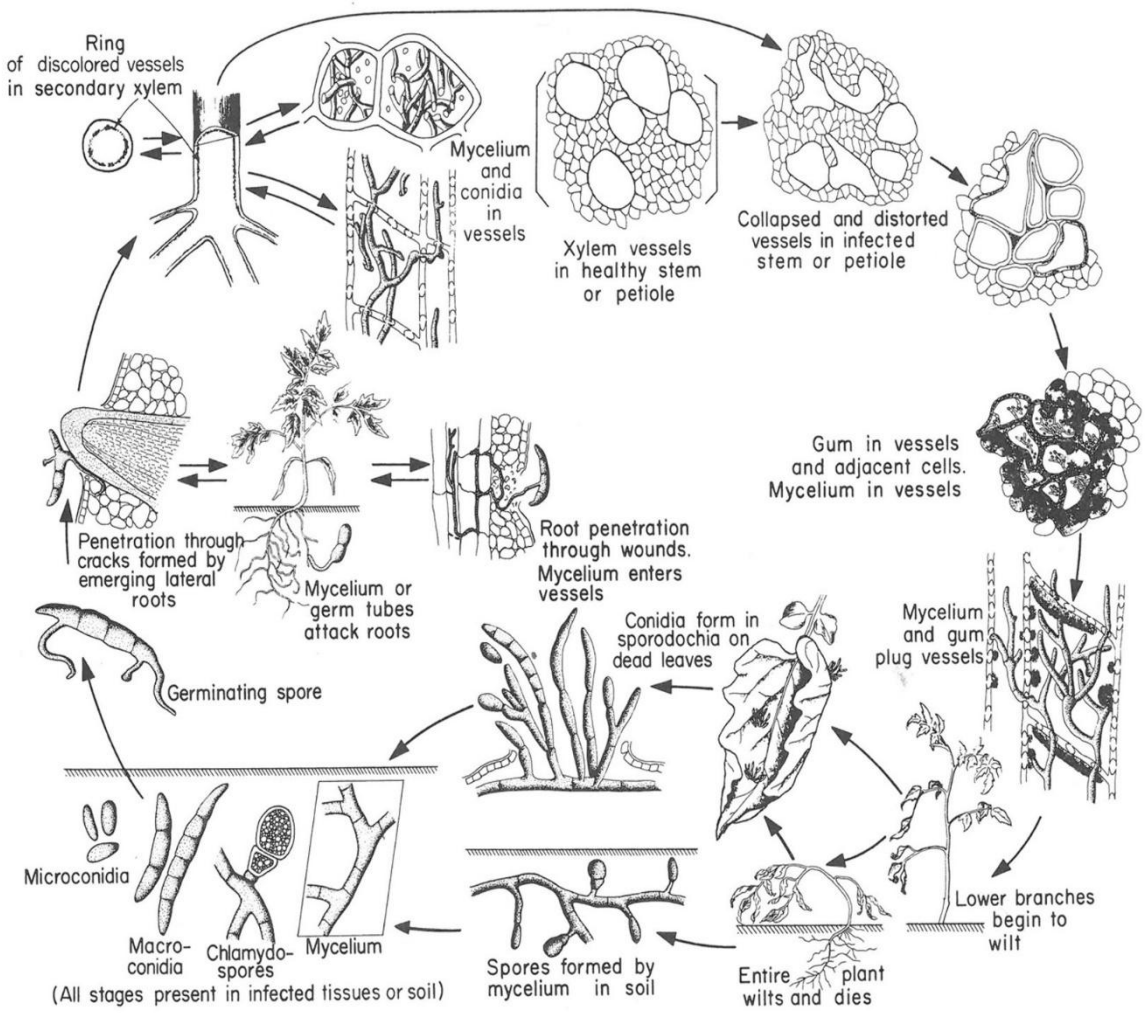

Figure 1.2 The life cycle of *F. oxysporum*.

Figure taken from Agrios (2005).

1.1.7 Disease symptoms

Fusarium wilt of tomato is characterised by yellowing of the leaves, commencing with the bottom leaves and moving to the top (Figure 1.3A). The disease symptoms can advance rapidly, causing progressive wilting, stunting, leaf death and ultimately death of the plant in severe infections (Figures 1.3B and 1.3C). Host plant defence responses, including the formation of callose, gels and balloon-like outgrowths called tyloses, which serve as barriers against the spread of the infection but disturb the flow of the water, can be visualised as vascular browning (Figure 1.3D).

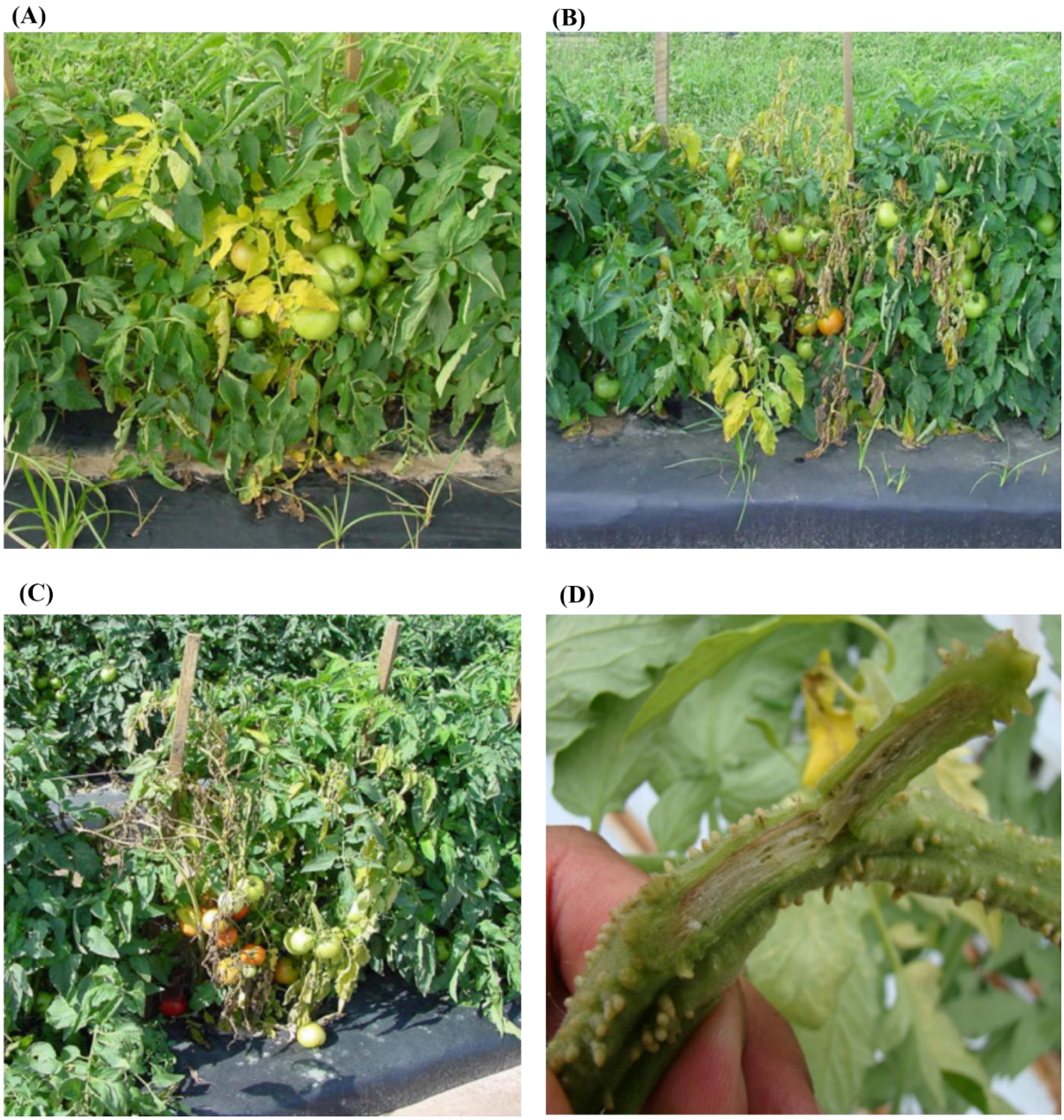

Figure 1.3 Disease symptoms of tomato Fusarium wilt.

(**A)** Initially, yellowing appears on a few leaves of the *Fol*-infected tomato plant. (**B)** and **(C)** After the spread of the fungus, disease advances rapidly, causing progressive yellowing, wilting and leaf death that eventually encompasses the whole plant. (**D)** A longitudinal section through a *Fol*-infected tomato plant shows browning of the vascular system and pith. Photos were sourced from https://plantpath.ifas.ufl.edu/u-scout/tomato/fusarium-wilt.html.

1.2 Plant immunity

1.2.1 Plant Immunity: A General Overview

Plants are constantly exposed to a wide range of pathogens in their growth environments. While pathogens have evolved numerous strategies to infect and cause disease, plants have developed complex immune systems to defend themselves. Plant diseases remain a major factor contributing to reduced yields and economic losses in key agricultural crops globally. To mitigate these impacts, various disease resistance strategies have been implemented in commercial crop breeding programs to lower disease incidence and boost productivity. Developing disease-resistant crops continues to be a crucial area of research. However, plant immune responses are highly intricate, involving multiple layers of defence to prevent infection. Pathogens, in turn, have adapted to bypass or suppress many of these defences, increasing their chances of successful infection. As a result, scientists are increasingly focused on studying plant-pathogen interactions at the molecular level. This includes exploring how plants identify harmful microbes, which defence pathways are activated upon detection and how pathogens attempt to evade these responses.

When a pathogen attempts to infect a plant, the outcome can go one of two ways: either the pathogen successfully enters, colonises and multiplies within the plant while suppressing immune responses, resulting in disease, or the plant detects the intruder early, activates defence mechanisms and halts the infection, resulting in disease resistance. Disease resistance is generally categorised into either non-host or host-specific resistance.

1.2.2 Non-host resistance: a broad-spectrum barrier against pathogens

Non-host resistance (NHR) is a crucial aspect of plant immunity, representing the inherent ability of the vast majority of plant species to resist infection by most potential pathogens. This broad-spectrum form of resistance can protect against prospective pathogens regardless of specific plant genotypes or cultivars (Heath, 2000; Senthil-Kumar and Mysore, 2013; Lee et al., 2017; Fonseca and Mysore, 2019). NHR represents a fundamental aspect of plant immunity, relying on two primary mechanisms to protect plants against potential pathogens (Heath, 2000; Senthil-Kumar and Mysore, 2013). The first mechanism, constitutive resistance, comprises preformed physical barriers including cell walls, thorns, trichomes, spines, cuticles and chemical barriers such as waxes, latex, oils, resins, sticky compounds and antimicrobial secondary metabolites, that function regardless of pathogen presence (Nürnberger and Lipka,

2005). These surface structures and chemical barriers create obstacles to pathogen entry (Underwood, 2012). Plants constitutively produce many antimicrobial compounds such as saponins, glucosinolates and phenolics that provide chemical defence against a wide range of microorganisms (Osbourn, 1996; VanEtten et al., 1994; Bednarek and Osbourn, 2009). Additionally, plants constitutively express various antimicrobial proteins, including defensins and thionins, which exhibit broad-spectrum activity against potential invaders (Broekaert et al., 1997; Stotz et al., 2009). These constitutive defences form the first layer of protection and are constantly maintained without requiring pathogen detection to initiate their formation (Figure 1.4).

The second mechanism involves pattern recognition receptors (PRRs) that recognise and relay pathogen presence to the plant (Jones and Dangl, 2006). These cell surface receptors recognise conserved molecular patterns associated with pathogens, including pathogen-associated molecular patterns (PAMPs) or more broadly, microbe-associated molecular patterns (MAMPs) and damage-associated molecular patterns (DAMPs) caused by pathogen-inflicted damage to plant tissues (Boller and Felix, 2009; Zipfel, 2014; Choi and Klessig, 2016). Upon recognition, PRRs initiate complex signalling cascades that activate various defence responses throughout the plant, collectively called pattern-triggered immunity (PTI) (Couto and Zipfel, 2016). Widely studied PRRs include FLS2, which perceives bacterial flagellin, EFR, which recognises the bacterial elongation factor Tu (EF-Tu), and CERK1, which mediates recognition of chitin, a major component of fungal cell walls (Gómez-Gómez and Boller, 2000; Zipfel et al., 2006; Miya et al., 2007). The activation of these receptors initiates numerous cellular responses, such as the production of reactive oxygen species, calcium signalling, activation of mitogen-activated protein kinases and extensive transcriptional reprogramming, which collectively inhibit pathogen growth and spread (Figure 1.4) (Li et al., 2016). While constitutive resistance provides immediate protection, PTI offers a more flexible response that can be activated upon pathogen detection. The combination of constitutive defences and PTI forms a comprehensive and effective defence system that enables most plants to withstand most microbial challenges in their environment and underpins the phenomenon of non-host resistance. Consequently, successful pathogen colonisation represents an exception rather than the norm, which in turn led to the evolution of host-specific resistance.

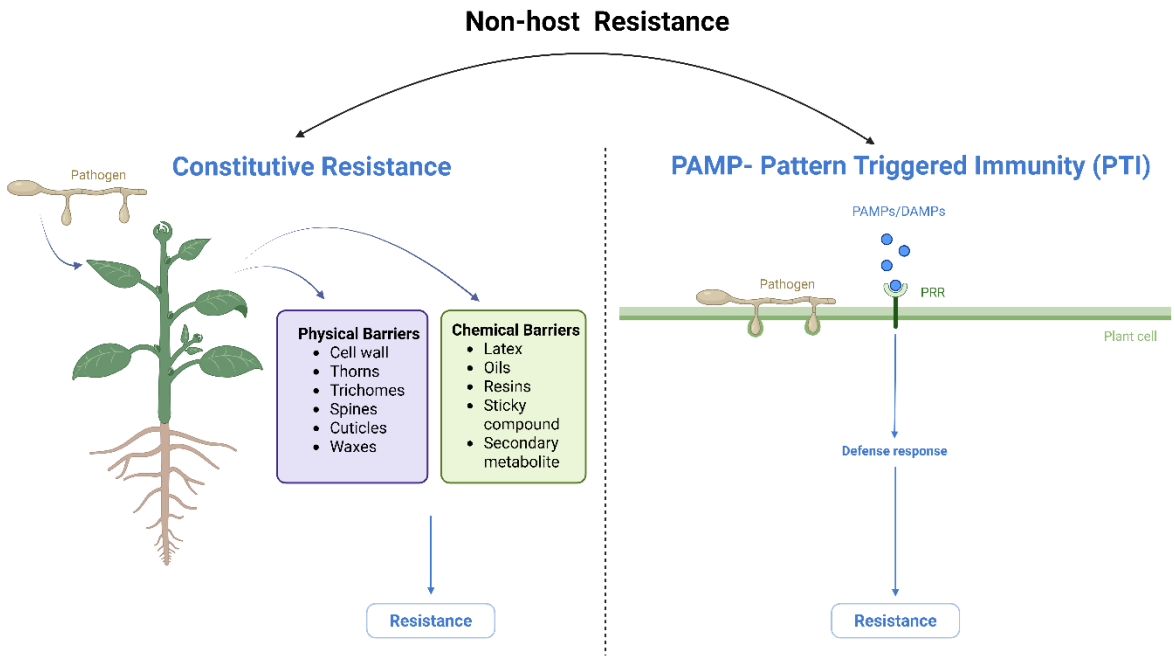

Figure 1.4 Non-host resistance mechanisms in plants

The diagram illustrates two major categories of non-host resistance in plants. On the left, constitutive resistance involves preformed barriers that function regardless of pathogen presence, including chemical barriers (latex, oils, resins, sticky compounds and secondary metabolites) and physical barriers (cell wall, thorns, trichomes, spines, cuticles and waxes). On the right, Pattern-Triggered Immunity (PTI) represents an inducible defence mechanism activated when plant PRRs detect PAMPs and DAMPs, initiating a signalling cascade that ultimately leads to various resistance responses. Figure adapted from Santamaria et al. (2013) and recreated using BioRender (https://biorender.com).

1.2.2.1 PRRs

Plant pattern recognition receptors (PRRs) are vital components of the innate immune system, detecting conserved molecular signatures from microbes or signals of cellular damage to trigger defence responses. PRR-mediated recognition can result in both broad-spectrum immunity through detection of conserved pathogen-associated molecular patterns (PAMPs) and race-specific immunity, as exemplified by receptors such as the tomato Cf-4 and Cf-9 proteins that recognise specific *Cladosporium fulvum* effectors Avr4 and Avr9, respectively (Joosten et al., 1994; Thomas et al., 1997). These receptors are classified into several major types based on their structural features and ligand specificities, including leucine-rich repeat receptor kinases (LRR-RKs), receptor-like proteins (RLPs), LysM-containing receptor kinases, malectin-like receptor kinases (MLRKs), wall-associated kinases (WAKs), and S-locus receptor kinases (SRLKs) (Figure 1.5). LRR-RKs, such as FLS2 and EFR, are among the most

extensively studied; FLS2 perceives bacterial flagellin-derived peptide flg22, prompting immune signalling, while EFR recognises the bacterial elongation factor Tu peptide elf18 (Macho and Zipfel, 2014) (Figure 1.5). The activation of these receptors commonly involves co-receptors like BAK1 (BRI1-associated kinase 1), a leucine-rich repeat receptor kinase that functions as a central signalling hub in plant immunity by heterodimerising with activated PRRs to enhance receptor complex formation and amplify downstream signalling. RLPs, such as the tomato Cf-4 and Cf-9 receptors, recognise fungal effectors like Avr4 and Avr9 through association with co-receptors, including SOBIR1 and BAK1, leading to immune activation (Liebrand et al., 2013; Huang et al., 2024) (Figure 1.5). In fungal pathogen detection, LysM receptor kinases like CERK1 are central; CERK1 binds chitin fragments generated from fungal cell walls, which is crucial for triggering defence responses against fungi such as *Colletotrichum* and *Magnaporthe* spp. (Miya et al., 2007). WAK1 has been implicated in sensing pectin-derived oligogalacturonides from the cell wall, although recent evidence has challenged this direct receptor-ligand relationship (Herold et al., 2025). However, recent studies by Herold et al. (2025) have cast doubt on this function, questioning direct binding and suggesting alternative recognition mechanisms or accessory proteins may be involved (Herold et al., 2025). Notably, WAKs can provide race-specific resistance in crops; for example, the *Brassica napus Rlm9* resistance gene encodes a WAK-like (WAKL) receptor kinase that triggers BAK1- and SOBIR1-independent cell death following recognition of the *Leptosphaeria maculans AvrLm5-9* effector (Larkan et al., 2020), while the *Stb6* gene in wheat confers resistance to *Zymoseptoria tritici* (Saintenac et al., 2018). Malectin-like receptor kinases (MLRKs), which resemble animal malectin proteins, also participate in carbohydrate recognition, though their exact ligands are still under investigation (Guerreiro and Marhavy, 2023) (Figure 1.5). SRLKs are mostly known for their role in the self-incompatibility response but demonstrate the extensive diversity of the receptor family (Takayama & Isogai, 2005). Collectively, these PRRs form a sophisticated surveillance network, often working in concert or crosstalk, to detect various MAMPs, effectors, or DAMPs and activate immune signalling pathways such as MAPKs, ROS production, and transcriptional reprogramming (Macho and Zipfel, 2014) (Figure 1.5).

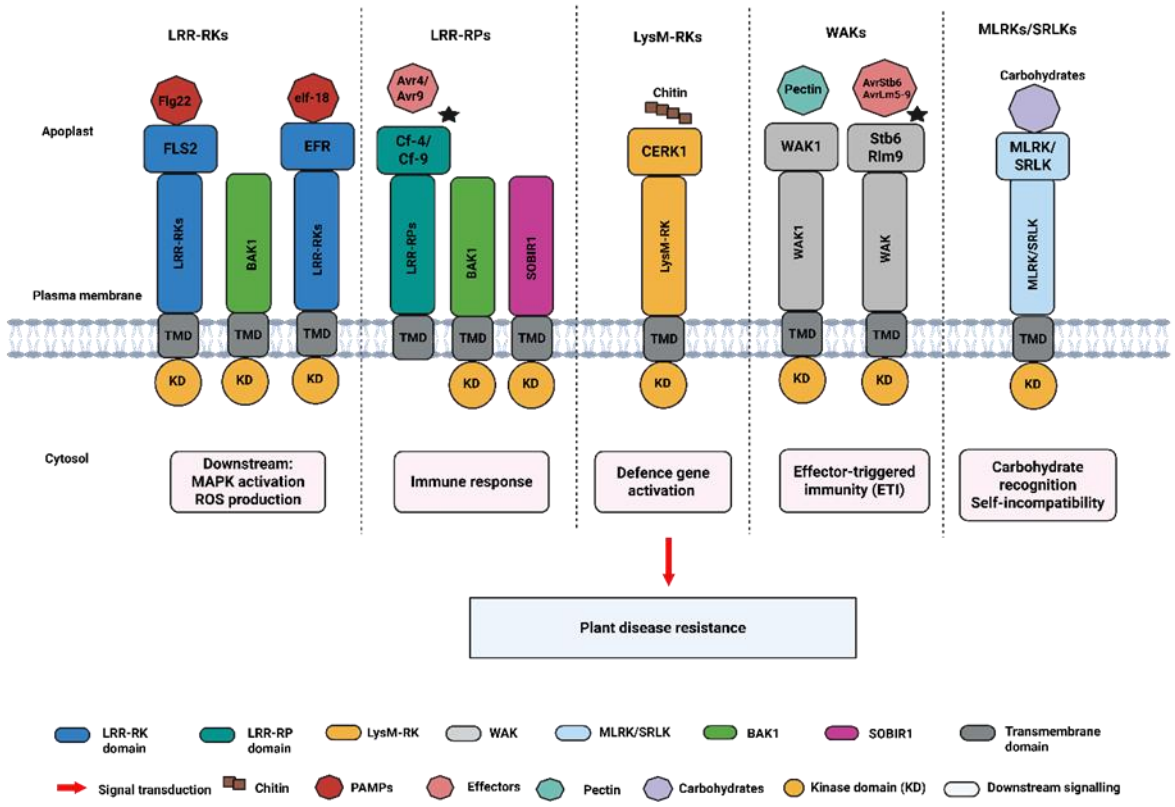

Figure 1.5 Diversity of plant extracellular immune receptors and downstream immune signalling.

Avr4, Avr9: *Cladosporium fulvum* avirulence proteins 4 and 9; AvrStb6: *Zymoseptoria tritici* avirulence protein recognised by the wheat Stb6 resistance protein; AvrLm5-9: *Leptosphaeria maculans* avirulence protein recognised by the *Brassica napus* Rlm9 resistance protein; BAK1: BRI1-associated kinase 1; Ca^{2+}: Calcium ion; CERK1: chitin elicitor receptor kinase 1; Cf-4, Cf-9: tomato resistance proteins that recognise *Cladosporium fulvum* Avr4 and Avr9, respectively; DAMP: damage-associated molecular pattern; EFR: elongation factor-Tu receptor; elf18: elongation factor-Tu-derived 18-amino-acid peptide; ETI: effector-triggered immunity; flg22: flagellin-derived 22-aminio-acid peptide; FLS2: flagellin sensing 2; LRR-RK: leucine-rich repeat receptor kinase; LRR-RP: leucine-rich repeat receptor protein; LysM-RK: lysin motif receptor kinase; MAPK: mitogen-activated protein kinase; MLRK: malectin-like receptor kinase; OG: oligogalacturonide; PAMP: pathogen-associated molecular pattern; ROS: reactive oxygen species; Rlm9: Resistance to *Leptosphaeria maculans* 9; SOBIR1: suppressor of bir1-1; SRLK: S-receptor-like kinase; Stb6: *Septoria tritici* blotch resistance 6; TMD: transmembrane domain; WAK: wall-associated kinase; WAK1: wall-associated kinase 1. Plant extracellular immune receptors detect diverse PAMPs, DAMPs and pathogen effectors through distinct receptor classes: LRR-RKs include PAMP receptors (FLS2/EFR, blue); LRR-RPs functioning as R proteins (Cf-4/Cf-9★, cyan); LysM-RKs (CERK1, orange); WAKs include potential PAMP receptors (WAK1, grey) and effector receptors (Stb6★, Rlm9★, grey);

and MLRKs/SRLKs (light blue). ★ denotes receptors mediating race-specific immunity through effector recognition (ETI) rather than broad-spectrum recognition of conserved PAMPs (PTI). Co-receptors BAK1 (green) and SOBIR1 (pink) facilitate signal transduction. Receptor activation triggers MAPK cascades, ROS production, Ca^{2+} signalling, and defence gene expression. The illustration was generated using BioRender (https://app.biorender.com).

1.2.2.2 Induction of PTI by LRR-RKs and LRR-RPs

Leucine-rich repeat receptor kinases (LRR-RKs) and leucine-rich repeat receptor-like proteins (LRR-RLPs) are key components of plant immune systems, primarily responsible for detecting external signals such as PAMPs, DAMPs, and effectors. As described above, FLS2 detects bacterial flagellin (flg22), while EFR recognises elongation factor EF-Tu (elf18), and the tomato Cf proteins (such as Cf-4 and Cf-9) recognise *Cladosporium fulvum* effectors Avr4 and Avr9, respectively (Macho and Zipfel, 2014; Liebrand et al., 2013; Huang et al., 2024).

Crucial to the signalling function of LRR-RKs and LRR-RLPs are co-receptors and regulatory proteins that facilitate or modulate immune activation. BAK1 (BRI1-associated kinase 1) is a central co-receptor for both LRR-RKs and LRR-RLPs. Upon ligand perception by receptors such as FLS2 or EFR, BAK1 forms heterodimeric complexes with the activated receptor, facilitating receptor activation through phosphorylation events that trigger downstream defences, including MAPK cascades (Chinchilla et al., 2007; Heese et al., 2007). Similarly, LRR-RLPs such as the tomato Cf proteins also associate with BAK1 to transduce immune signals (Liebrand et al., 2013).

In addition to BAK1, LRR-RLPs require SOBIR1 (suppressor of BIR1-1) for signalling because they lack intrinsic kinase activity. SOBIR1 is a constitutively active receptor-like kinase that functions as an essential adaptor protein, forming pre-association complexes with LRR-RLPs at the plasma membrane (Liebrand et al., 2013; Bi et al., 2016). Upon ligand perception, SOBIR1 recruits BAK1 to form a tripartite receptor-SOBIR1-BAK1 complex that enables signal transduction (Liebrand et al., 2013; Postma et al., 2016). This SOBIR1-dependent mechanism is essential for LRR-RLP signalling; for example, Ve1 detection of the *Verticillium Ave1* effector and Cf protein recognition of *C. fulvum* effectors both require SOBIR1 for immune activation (Liebrand et al., 2013; Boshoven et al., 2015). Notably, some WAK-mediated race-specific resistance, such as *Brassica napus* Rlm9 recognition of the *Leptosphaeria maculans AvrLm5-9* effector, functions independently of both BAK1 and SOBIR1, demonstrating alternative signalling mechanisms (Larkan et al., 2020).

EDS1 (enhanced disease susceptibility 1) plays a crucial role in amplifying immune signals downstream of both LRR-RKs and LRR-RLPs, often linking receptor activation to effector-triggered responses and acting as a bridge between PTI and ETI (Dongus and Parker, 2021; Pruitt et al., 2021). In contrast, BIR1 (BAK1-interacting receptor-like kinase 1) functions as a negative regulator within these signalling pathways. BIR1 interacts with receptor complexes to prevent unwarranted activation, thereby maintaining immune homeostasis and preventing autoimmunity (Gao et al., 2009; Liu et al., 2016). The balance between positive regulation by BAK1, SOBIR1, and EDS1, and negative regulation by BIR1, ensures appropriate immune responses while preventing excessive or inappropriate immune activation (Van der Burgh and Joosten, 2019; McCombe et al., 2022).

1.2.3 Host-specific resistance: Pathogen strain-specific resistance

When pathogens evolved the ability to bypass both constitutive and inducible components of non-host resistance, host-specific resistance came into play. Host-specific resistance refers to the ability of certain genotypes or cultivars within a plant species to resist specific races or strains of a particular pathogen (van der Burgh and Joosten, 2019). Effectors may include secondary metabolites, small RNAs (sRNAs) or secreted proteins that are often small and cysteine-rich (Stergiopoulos and de Wit, 2009; Pieterse et al., 2012; Weiberg et al., 2013). Depending on their function, they are secreted into the apoplastic space or translocated into host cells, where they interfere with immune responses and facilitate pathogen colonisation (Dou and Zhou, 2012).

Effectors commonly function by suppressing PTI or otherwise reducing plant defences by degrading or counteracting constitutive barriers. This mechanism, whereby effectors promote successful pathogen colonisation, is known as effector-triggered susceptibility (ETS) (Jones and Dangl, 2006). In response to this evolutionary pressure, plants have developed specialised receptor proteins, known as resistance (R) proteins, that can recognise and respond to specific pathogen effectors. When an R protein successfully recognises an effector, it activates a robust defence response termed effector-triggered immunity (ETI) (Jones and Dangl, 2006) (Figure 1.6).

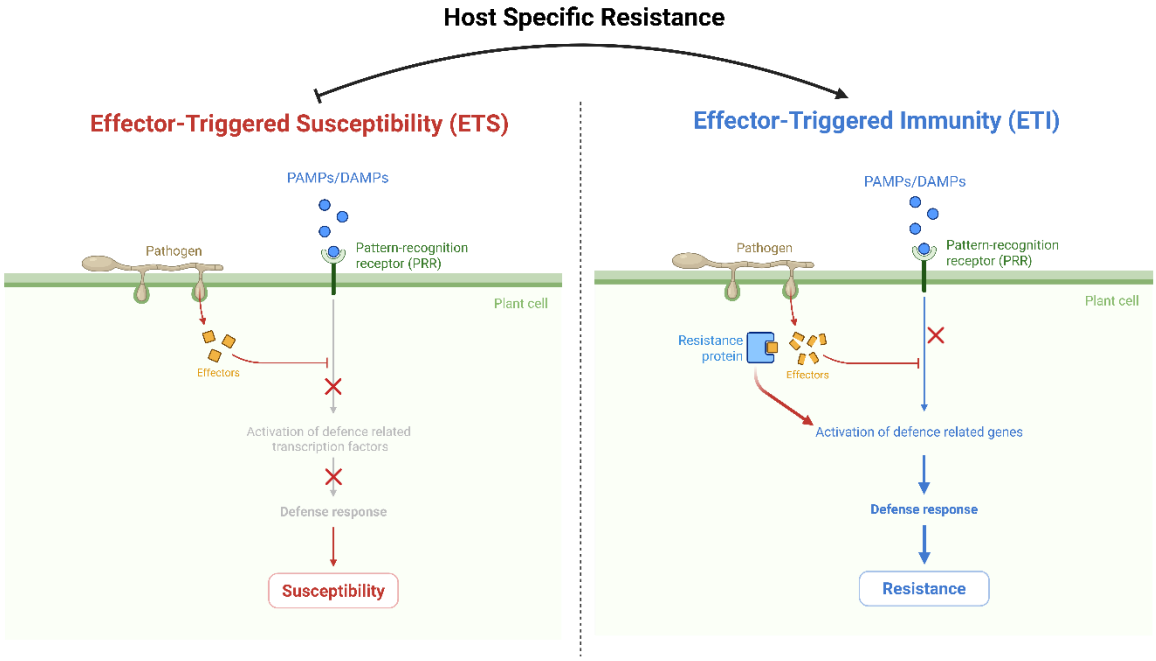

Figure 1.6 Host-specific resistance mechanism in plant-pathogen interactions.

The diagram depicts host-specific resistance in plant-pathogen interactions. On the left, Effector-Triggered Susceptibility (ETS) occurs when pathogen-secreted effector molecules are translocated into the host and successfully suppress PTI, blocking the activation of downstream defence responses, ultimately resulting in plant infection. On the right, Effector-Triggered Immunity (ETI) occurs when plant resistance proteins recognise specific pathogen effectors, enabling the activation of a strong defence responses that lead to resistance often accompanied by a hypersensitive response (HR). Both processes involve the initial detection of PAMPs or DAMPs by PRRs but differ in whether pathogen effectors succeed in subverting host immunity or fail owing to detection of one or more of them by the plant surveillance system. This figure, which does not include effectors that act and are detected at the cell surface, was adapted from Jones and Dangl (2006) and recreated using BioRender (https://biorender.com).

This type of resistance often follows a gene-for-gene model (Flor, 1971), where a specific plant resistance (*R*) gene enables recognition of a pathogen isolate carrying the corresponding avirulence (*Avr*) gene (now often referred to as an effector gene) (Jones and Dangl, 2006). The presence of both a functional *R* gene in the plant and its matching *Avr*/effector gene in the pathogen leads to an incompatible interaction and plant disease resistance. Conversely, if the pathogen lacks the *Avr*/effector gene or the plant lacks the corresponding *R* gene, a compatible interaction and successful plant infection occur (Jones and Dangl, 2006). For instance, the tomato *Cf-4 R* gene enables recognition of *Cladosporium fulvum* isolates carrying the *Avr4* effector gene, triggering a strong defence response, including the hypersensitive response (HR) (Thomas et al., 1997).

1.2.3.1 Resistance proteins

Plants employ various membrane-anchored immune receptors such as receptor-like kinases (RLKs) and receptor-like proteins (RLPs). These receptors typically possess extracellular leucine-rich repeat domains that detect pathogen-associated molecules or effectors at the cell surface. They initiate signalling cascades internally through kinase domains or through partnerships with co-receptors (McCombe et al., 2022). Wall-associated kinases (WAKs) are a subset of RLKs that sense damage signals (DAMPs) and promote immune pathways by forming heterodimers with other receptor kinases like CERK1 or LYK5, enhancing the plant's ability to perceive pathogenic threats (Ngou et al., 2021). Similarly, S-locus receptor kinases (SRLKs) participate in immune responses, often contributing to pathways of ETI, expanding the repertoire of receptor-mediated defences (Ngou et al., 2021). In addition to these extracellular receptors, plants' intracellular resistance proteins known as NB-LRRs are also fundamental components of effector-triggered immunity (ETI). These proteins typically feature a tripartite domain architecture: an N-terminal domain, either a Toll/Interleukin-1 receptor (TIR) or coiled-coil (CC), which initiates intracellular signalling; a central nucleotide-binding (NB) domain, acting as a molecular switch that is activated by ATP or ADP binding; and a C-terminal leucine-rich repeat (LRR) region that confers specificity for recognising pathogen effectors (Gabriels et al., 2007). Upon effector detection, conformational shifts in the NB-LRR proteins activate defence pathways, including localised cell death, which restricts pathogen growth (Gabriels et al., 2007). Together, these different classes of resistance proteins work synergistically to detect pathogens, hypersensitivity response, ROS burst, MAPK cascade, hormonal response and SAR response (Figure 1.7). The coordination among NB-LRRs, RLKs, RLPs, WAKs, and SRLKs forms a complex network for effective and resilient plant immunity (Yuan et al., 2021; Ngou et al., 2021) (Figure 1.7).

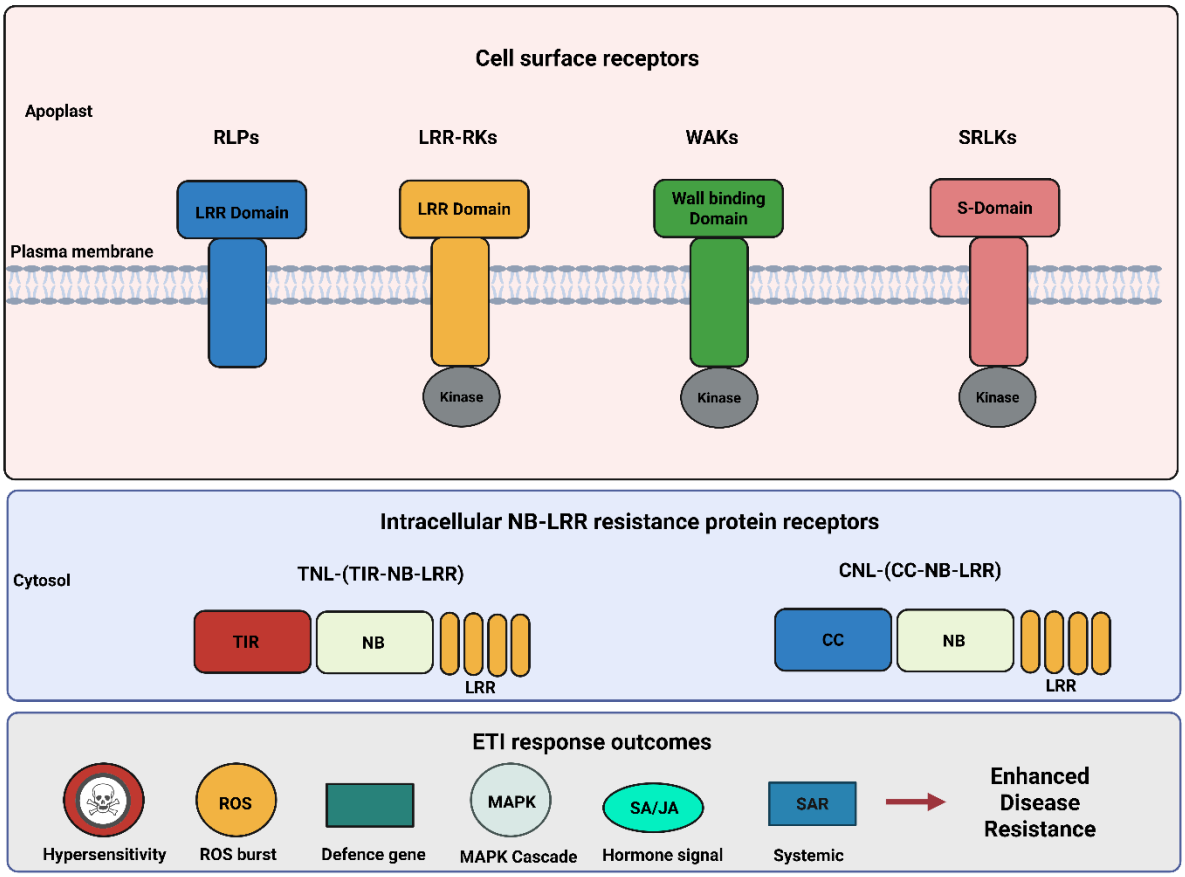

Figure 1.7 Plant immune receptors and effector-triggered immunity

RLPs: receptor-like proteins; LRR-RKs: leucine-rich repeat receptor kinases; WAKs: wall-associated kinases; SRLKs: S-domain receptor-like kinases; NB-LRR: nucleotide-binding leucine-rich repeat; TNL: toll/interleukin-1 receptor–nucleotide-binding leucine-rich repeat; CNL: coiled-coil–nucleotide-binding leucine-rich repeat; TIR: toll/interleukin-1 receptor; CC: coiled-coil domain; LRR: leucine-rich repeat domain; ROS: reactive oxygen species; MAPK: mitogen-activated protein kinase; SA: salicylic acid; JA: jasmonic acid; SAR: systemic acquired resistance; ETI: effector-triggered immunity

Cell-surface receptors (RLPs, LRR-RKs, WAKs, SRLKs) and intracellular NB-LRR proteins (TNLs, CNLs) perceive pathogen signals and effectors to activate ETI. This response triggers HR, ROS burst, defence gene expression, MAPK cascades, SA/JA signalling, and SAR, collectively enhancing disease resistance. The image is created by using BioRender (https://biorender.com).

1.2.3.2 Induction of ETI and cell death by TIR-NLRs

TIR-NLRs (Toll/interleukin-1 receptor nucleotide binding leucine-rich repeat proteins) are a specialised class of intracellular immune receptors in plants that play a role in pathogen recognition and activation of immune signalling pathways (e.g. RRS1-R) (Deslandes et al., 2003). These NLRs are sometimes organised in pairs, consisting of sensor NLRs that directly or indirectly recognise pathogen effectors, and executor NLRs that trigger immune signalling once activation occurs (Wang et al., 2023; Yu et al., 2024). Sensor NLRs frequently contains integrated domains derived from host effector targets, such as WRKY or kinase domains, which serve as decoys or bait for pathogen effectors, enhancing detection sensitivity. Their function heavily depends on several signalling components, notably EDS1 (enhanced disease susceptibility 1), SAG101 (senescence-associated gene 101), and PAD4 (phytoalexin deficient 4). These proteins form complexes that transduce signals downstream of TIR domains, facilitating the activation of defence responses. TIR domains possess NADase activity, which catalyses the cleavage of nicotinamide adenine dinucleotide (NAD+) into various products, including cyclic ADP-ribose and other cyclic ADP-ribose derivatives, which are believed to act as second messengers in immune signalling. These molecules can promote calcium fluxes and other downstream responses critical for amplifying immune activation including hypersensitive cell death, production of defence-related hormones such as salicylic acid, activation of defence gene expression, callose deposition at infection sites to reinforce cell walls, and the initiation of systemic acquired resistance (SAR) that primes the entire plant for enhanced defence against future attacks (Wang et al., 2023; Yu et al., 2024).

Additionally, signal transduction often involves paired NLRs, with sensor NLRs responsible for recognising specific pathogen effectors directly or indirectly, and executor NLRs that execute the immune response, such as inducing hypersensitive cell death. Helper NLRs, such as ADR1 (activated disease resistance 1) and NRG1 (N requirement gene 1), serve as essential mediators that amplify or relay the signal initiated by sensor NLRs, often working in concert with EDS1-PAD4-SAG101 complexes. For example, NRG1 and ADR1 are auxiliary proteins that help propagate signals downstream of TIR-NLR activation, ultimately leading to defence gene expression and programmed cell death (Kourelis and Adachi, 2022). These helper NLRs can operate as either single or paired units, forming immune networks that confer robustness and specificity to plant immune responses (Ngou et al., 2021). Integrative domains within NLRs can also enhance immune specificity by acting as decoys or novel sensors for pathogen effectors, further diversifying the plant's immune repertoire. Overall, TIR domains with

NADase activity work together with helper signalling proteins like EDS1, SAG101, PAD4, ADR1, and NRG1, and with the modular structure of NLRs. This interaction shows the complexity and sophistication of plant immunity (Figure 1.8).

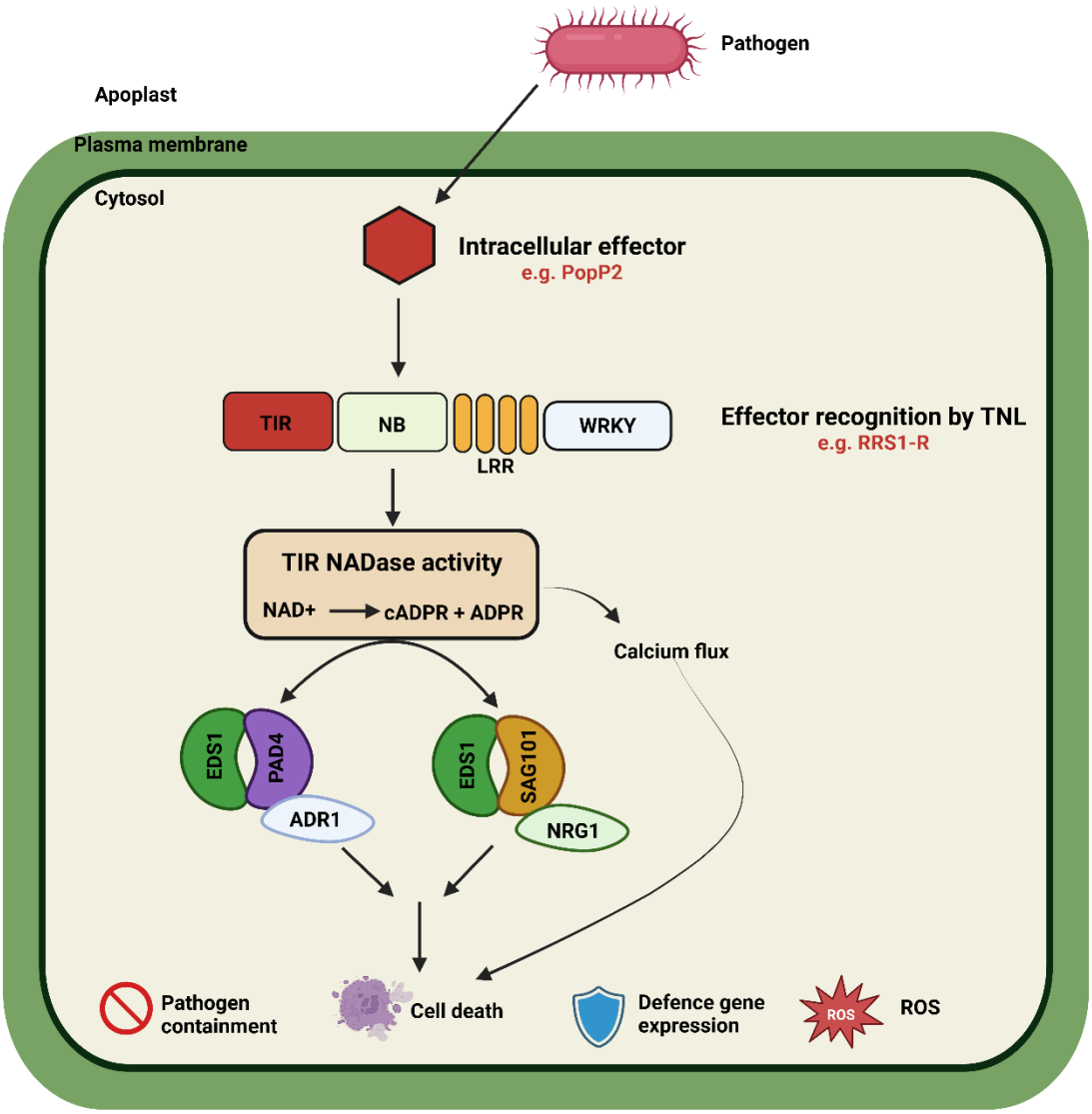

Figure 1.8 TIR-NLR immune signalling in plants.

cADPR: cyclic ADP-ribose; ADPR: ADP-ribose; ADP: adenosine diphosphate.

Pathogen effectors are recognised by sensor TNL receptors (e.g., RRS1-R), activating TIR NADase activity that produces cADPR and ADPR. These molecules activate EDS1-PAD4/ADR1 and EDS1-SAG101/NRG1 complexes, leading to immune responses including cell death, defence gene expression, and ROS production. The image is created by using BioRender (https://biorender.com).

1.2.3.3 Induction of ETI and cell death by CC-NLRs

Coiled-coil nucleotide-binding leucine-rich repeat receptors (CC-NLRs) constitute a substantial class of intracellular immune receptors in plants that play roles in detecting pathogen-derived effectors and activating immune responses. These receptors are characterised by an N-terminal coiled-coil (CC) domain, a central nucleotide-binding (NB) domain, and a C-terminal leucine-rich repeat (LRR) region (Adachi et al., 2019; Adachi and Kamoun, 2022; Wang et al., 2023; Yu et al., 2024). Upon recognition of specific effectors, CC-NLRs undergo conformational changes that trigger their activation. A key feature of many CC-NLRs, such as ZAR1, is their ability to form large resistosome complexes (Bi et al., 2021). Specifically, ZAR1 forms a pentameric resistosome that inserts into the plasma membrane, creating a pore that functions as a Ca^{2+}-permeable channel, thereby facilitating a rapid influx of calcium ions essential for downstream signalling and cell death programs (Bi et al., 2021). Helper NLRs, such as ADR1 and NRG1, which also belong to the CC-NLR family, facilitate signal transduction and amplify defence response. Sometimes helper NLRs also undergo a similar oligomerisation process upon activation, forming resistosomes that directly serve as calcium channels, thereby amplifying the calcium signalling necessary for immune responses. This multimerisation and pore formation allow CC-NLRs to act as both sensors of pathogenic effectors and active executors that modulate ion fluxes at the plasma membrane, effectively translating pathogen detection into cellular defence actions. Additional NLRs, such as NRCs, collaborate within these signalling networks, further fine-tuning immune responses. In summary, CC-NLRs are adaptable immune receptors that can attach to the cell membrane and form pores that let calcium in, which is vital for starting a strong immune response in plants (Adachi et al., 2019; Bi et al., 2021) (Figure 1.9).

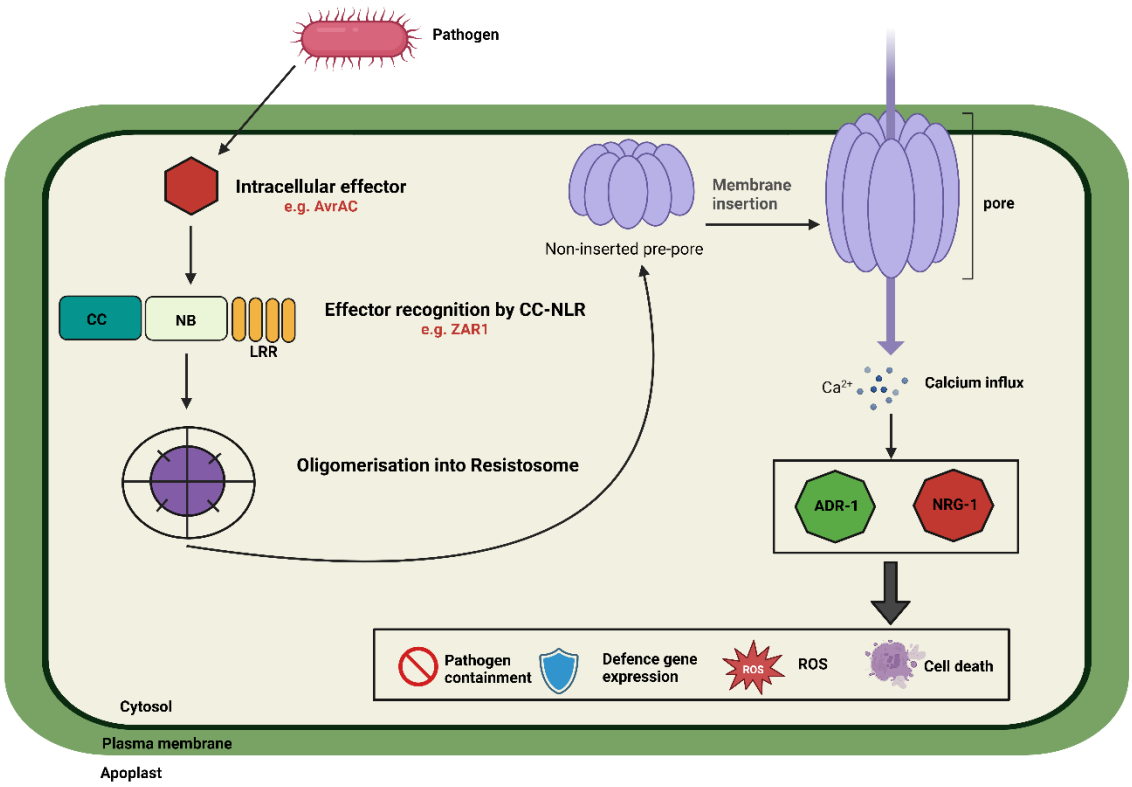

Figure 1.9 CC-NLRs in plant immunity and cell death.

Sensor CC-NLRs (e.g., ZAR1) recognise intracellular pathogen effector (AvrAC) and oligomerize into resistosome complexes. The resistosome inserts into the plasma membrane, forming a Ca^{2}-permeable pore that triggers calcium influx. Elevated cytoplasmic Ca^{2+} activates helper NLRs (ADR1-1 and NRG-1), leading to amplified defence responses including pathogen containment, cell death, defence gene expression, and ROS production. The image is created by using BioRender (https://biorender.com).

1.3 Pathogen effectors

Effectors are produced by various pathogens, including viruses, bacteria, fungi, oomycetes, nematodes, insects and even parasitic plants. Here, I will primarily focus on fungal effectors that induce plant cell death as part of their virulence strategy.

1.3.1 Fungal effectors in pathogen nutrition and the avoidance of recognition

Effectors exhibit remarkable diversity in structure, function, and mechanisms of action. A single pathogen species can secrete dozens to hundreds of effectors, constituting a highly complex repertoire of virulence factors. Structurally, effectors encompass small cysteine-rich proteins, large modular proteins, enzymes with defined catalytic domains, proteins containing

host-mimicking motifs, as well as intrinsically disordered or unstructured proteins. Functionally, they include proteases and peptidases, kinases and phosphatases, E3 ubiquitin ligases, transcription factor-like proteins, and enzymes that modify nucleic acids. The effector not only functions in the suppression of plant immunity, as explained previously, but also plays a role in pathogen nutrition (Zhang et al., 2022).

Many effectors actively reprogram host metabolism and physiology to increase the availability of sugars, amino acids, and other metabolites in the apoplast or vascular tissues. For instance, in *Fusarium oxysporum* f. sp. *lycopersici*, several Secreted in Xylem (SIX) proteins contribute to virulence beyond recognition by resistance genes. *SIX1* and *SIX6* effectors have been shown to influence host physiology, altering water and nutrient balance in the xylem to create conditions favourable for fungal proliferation (Gawehns et al., 2014; van der Does et al., 2008). Similarly, effectors from *Cladosporium fulvum*, such as *Avr2* and *Avr4*, protect fungal hyphae from plant defence enzymes, including proteases and chitinases. While their primary role lies in suppressing apoplastic defence, this indirectly ensures continued nutrient leakage and accessibility for the fungus (van den Burg et al., 2006; van Esse et al., 2007). In the maize smut fungus *Ustilago maydis*, the effector *Cmu1* is an enzyme that diverts chorismate away from making salicylic acid (a defence signal). This weakens the plant's immunity and instead directs metabolism toward normal growth processes, which provides more nutrients for the fungus (Djamei et al., 2011). The rice blast fungus *Magnaporthe oryzae* also deploys a wide effector repertoire. For example, *AvrPiz-t* interacts with a rice E3 ubiquitin ligase to suppress immunity and sustain colonisation, while other effectors manipulate the expression of host SWEET sugar transporters, thereby enhancing the efflux of sugars into the apoplast for fungal consumption (Park et al., 2012; Chen et al., 2010). More broadly, apoplastic effectors across fungal pathogens commonly prevent host reinforcement of cell walls or occlusion of vascular tissue, processes that would otherwise restrict nutrient access. By protecting feeding structures such as haustoria, or by manipulating host transport and metabolic pathways, these effectors ensure a continuous supply of assimilates for the invading fungus. Thus, effector activity is intimately tied not only to suppression of host defence but also to the manipulation of host nutrient allocation, a dual strategy that underpins the success of many fungal pathogens.

Fungal pathogens need to hide their molecular fingerprints to avoid triggering plant immune responses. The most critical issue for fungi is chitin which is a major cell wall component that plants recognise as a danger signal through receptors like CERK1. To overcome this, many

fungi secrete LysM effector proteins that act like molecular sponges, soaking up chitin fragments before plants can detect them. A classic example is Ecp6 from the tomato pathogen *Cladosporium fulvum*, which has three LysM domains that can simultaneously bind three chitin chains with extremely high affinity, effectively hiding them from plant surveillance (de Jonge et al., 2010). Similarly, the rice blast fungus *Magnaporthe oryzae* uses *Slp1*, another LysM effector that shields chitin during infection, and mutants lacking this protein are much less virulent because the plant quickly spots the invasion (Mentlak et al., 2012). These camouflage strategies are essential because they give pathogens those critical early hours to establish infection before the plant's defences kick in.

Some fungal effectors are remarkably efficient because they can affect multiple host processes with a single enzymatic activity, particularly when they target enzyme families or proteins with broad cellular roles. An excellent example of this is *Pep1* from *Ustilago maydis*, the corn smut fungus. Pep1 is a secreted peroxidase inhibitor, but rather than blocking just one specific peroxidase, it inhibits an entire family of plant peroxidases. Hemetsberger et al. (2012) showed that this broad inhibitory activity creates a cascade of beneficial effects for the pathogen: it suppresses the oxidative burst by reducing reactive oxygen species (ROS) accumulation, prevents lignin deposition in plant cell walls (since lignification requires peroxidase activity), maintains tissue penetrability for fungal hyphae, and protects the fungus from oxidative damage. All of these outcomes, immune suppression, enhanced colonisation, and improved nutritional access, stem from one effector targeting multiple members of the peroxidase enzyme family.

Effector-induced host cell death is a strategic virulence mechanism predominantly utilised by necrotrophic fungi, which deliberately trigger host tissue necrosis to facilitate nutrient acquisition and disease progression. Necrotrophs secrete specific effectors that manipulate host cell death pathways, causing the host plant to undergo cell death or necrosis, thus transforming healthy tissue into resource-rich dead tissue that supports pathogen proliferation. In the case of hemibiotrophic pathogens, which initially establish infection in living host tissue (biotrophy), effectors play a crucial role in their transition to necrotrophy. During early infection stages, these pathogens may evade host defences and maintain host cell viability; however, as infection progresses, they secrete necrosis-inducing effectors that induce targeted host cell death. This switch from a biotrophic to a necrotrophic lifestyle involves a deliberate manipulation of host cell death pathways, allowing the pathogen to exploit necrotic tissue for expansion and nutrient

access. The ability to induce cell death at specific stages is thus a key virulence strategy that determines the success of hemibiotrophs in completing their infection cycle and underscores the importance of effectors in modulating host immunity and cell fate decisions. In summary, effector-triggered host cell death is a fundamental virulence strategy for necrotrophic fungi and hemibiotrophs during their transition from biotrophy to necrotrophy, enabling them to overcome host defences, access nutrients, and establish persistent infections (Lee and Rose, 2010).

1.3.2 Fungal effectors causing cell death

Fungal pathogens deploy diverse effector proteins to induce cell death in plants as part of their infection strategy. Many fungal pathogens produce necrosis and ethylene-inducing peptide 1 (NEP1)-like proteins (NLPs) that directly disrupt plant cell membranes, causing widespread necrosis in host tissues which then act as a substrate for fungal nutrition. Examples include *BcNEP1* and *BcNEP2* from *Botrytis cinerea* and *MpNEP1* and *MpNEP2* from *Moniliophthora perniciosa* (Gijzen and Nürnberger, 2006; Schouten et al., 2008). Some cerato-platanin proteins, such as BcSpl1 from *Botrytis cinerea* (Frias et al., 2011) represent another class of cell death elicitors.

However, a particularly intriguing class of fungal effectors operates through an inverse gene-for-gene relationship, where pathogen recognition by the host leads to susceptibility rather than resistance. In these cases, effectors trigger R protein-mediated cell death as a pathogenicity mechanism, exploiting the host's own defence machinery for the pathogen's benefit. A prominent example of this phenomenon is the ToxA protein, an extracellular effector produced by the wheat pathogen *Parastagonospora nodorum*. ToxA triggers cell death specifically in wheat cultivars carrying the *Tsn1* gene, which encodes a nucleotide-binding leucine-rich repeat (NLR) protein (Faris et al., 2010). Mechanistically, ToxA appears to interact with TaNHL10, a wheat homologue of Arabidopsis NDR1 that is required for Rpm1 and Rps2-mediated resistance triggered by AvrB, AvrRpm1, and AvrRpt2. Like NDR1, TaNHL10 is a type II membrane-anchored protein with its C-terminus positioned extracellularly. It may facilitate the translocation of ToxA into the cytosol, where it is subsequently recognised by Tsn1, leading to necrosis (Dagvadorj et al., 2022). This represents a sophisticated hijacking of the host's resistance machinery, where the pathogen has evolved to exploit components normally involved in defence responses.

The *P. nodorum* pathosystem provides another example through the *Snn1* gene, which encodes a wall-associated kinase (WAK) that serves as a target for the fungal effector Tox1. This interaction demonstrates how WAKs can function either in resistance or as susceptibility targets, depending on the pathogen effector involved (Shi et al., 2016).

Beyond the ToxA-Tsn1 system, other NLR genes have been shown to function as susceptibility factors in inverse gene-for-gene interactions. In Arabidopsis, the *LOV1* (locus orchestrating victorin effects 1) gene encodes a coiled-coil NLR protein that mediates sensitivity to victorin, a cyclic pentapeptide toxin produced by *Cochliobolus victoriae*, which causes Victoria blight on oats (Lorang et al., 2007). Rather than binding victorin directly, LOV1 acts as a guard protein that monitors the thioredoxin TRX-h5, the actual target of victorin (Sweat and Wolpert, 2007; Lorang et al., 2012). When victorin binds TRX-h5, LOV1 becomes activated and triggers cell death alongside typical defence responses such as PR-1 gene induction and camalexin accumulation, thereby promoting disease development. This system has particular historical significance in oats, where the *Vb* gene conferring victorin sensitivity appears to be identical to *Pc-2*, a gene that provides resistance to crown rust caused by *Puccinia coronata* f. sp. *avenae*. This situation exemplifies how a single gene can confer resistance to one pathogen while simultaneously rendering the plant susceptible to another (Faris and Friesen, 2020).

Another well-studied example involves the *Pc* gene in sorghum, which also belongs to the coiled-coil NLR family and governs sensitivity to PC-toxin from *Periconia circinata*, the causal agent of milo disease (Nagy and Bennetzen, 2008). PC-toxin is a hybrid molecule composed of a peptide linked to a chlorinated polyketide. When Pc recognises PC-toxin, it initiates programmed cell death accompanied by various cellular disruptions, including mitosis inhibition, chromatin condensation, electrolyte leakage, and potassium ion flux (Dunkle and Macko, 1995). Interestingly, the *Pc* locus resides within a cluster of NLR genes that frequently undergoes unequal recombination, spontaneously generating PC-toxin-insensitive variants at notably high rates while simultaneously producing allelic diversity (Nagy and Bennetzen, 2008). Together with the ToxA-Tsn1 interaction, these examples demonstrate how necrotrophic pathogens have evolved to hijack plant resistance mechanisms that normally function against biotrophic pathogens (Faris and Friesen, 2020).

1.3.3 *Fol* effectors and their function

The *Fol* genome has been organised into 15 chromosomes, out of which 11 are considered core chromosomes and four are considered lineage-specific (LS) chromosomes based on comparative genome analysis with *F. graminearum* (*Fg*) and *F. verticillioides* (*Fv*) (Ma et al., 2010). Several LS regions were also found on a number of conserved chromosomes. The LS chromosomes and regions are rich in transposons and genes related to pathogenicity that are only present in the *Fol* genome and not in the *Fg* or *Fv* genomes (Ma et al., 2010). A number of these genes encode proteins found in the xylem sap of *Fol*-infected tomato plants (Rep et al., 2004; Houterman et al., 2007; Schmidt et al., 2013). Most of these *SIX* (secreted in xylem) genes are found on LS chromosome 14 of *Fol* strain 4287, which is a mobile pathogenicity chromosome that can transfer, albeit at a very low frequency, to a non-pathogenic isolate of *F. oxysporum* in a different VCG and convert it into a strain pathogenic on tomato (Ma et al., 2010; Schmidt et al., 2013; van Dam et al., 2017). Of these 14 SIX proteins, SIX1 (Avr3), SIX2, SIX3 (Avr2), SIX5, SIX6 and SIX8 have been shown to be required for full *Fol* pathogenicity on susceptible tomato plants (Rep et al., 2004; Houterman et al., 2009; Gawehns et al., 2014, 2015; Ma et al., 2015; Aalders et al., 2024). Interestingly, SIX4 (Avr1) does not contribute to *Fol* pathogenicity on susceptible tomato plants, but has been found to suppress I-2- and I-3-mediated resistance (Houterman et al., 2008). In contrast, the SIX4 orthologue in *F. oxysporum* f. sp. *conglutinans* has been shown to contribute to pathogenicity on Arabidopsis (Thatcher et al., 2012).

Avr2 and *SIX5* are adjacent genes that are transcribed divergently from a shared promoter (Cao et al., 2018). Avr2 is detected by the I-2 resistance protein, which is a cytosolic protein. This suggests Avr2 acts in the cytosol of the host plant cell (Simons et al., 1998; Houterman et al., 2009). *In planta* cytosolic expression of *Avr2* alone was found to be sufficient to induce I-2-mediated cell death in *N. benthamiana* and tomato, but both effectors were required for I-2-mediated *Fol* resistance in tomato (Cao et al., 2018). SIX5 was found to interact with Avr2 and facilitate its movement from one cell to another via plasmodesmata, which contributes to virulence in susceptible plants (Cao et al., 2018).

SIX6 is expressed at early as well as late stages of infection and requires a living host to induce its expression (Gawehns et al., 2014). *Fol SIX6* contributes to pathogen virulence as plants inoculated with *Fol SIX6* deletion mutants showed greater plant weight and a lower disease index compared to plants inoculated with wild-type *Fol* (Gawehns et al., 2014). However, in a

different study, a strain of *Fol* containing a deletion of *SIX6*, *SIX9* and *SIX11* did not display a decrease in virulence (Vlaardingerbroek et al., 2016). *SIX6* is present in other *formae speciales* of *F. oxysporum* that infect melon, cotton, watermelon, passion fruit and cucumber (Lievens et al., 2009; Chakrabarti et al., 2011; Gawehns et al., 2014). The *SIX6* gene in *F. oxysporum* f. sp. *phaseoli* was found to be positively associated with the induction of wilt symptoms in soybean (Lanubile et al., 2016) and *SIX*6 was shown to play a role in virulence in watermelon-infecting *F. oxysporum* f. sp. *niveum* (Niu et al., 2016) and cucurbit-infecting strain *Forc016* of *F. oxysporum* f. sp *radicis-cucumerinum* (Van Dam et al., 2017). However, *SIX6* deletion strains of *F. oxysporum* f. sp. *melonis* (*Fom*) showed no loss of virulence on melon plants compared to wild-type strains, suggesting that *SIX6* does not play a role in virulence in *Fom* (Li et al., 2020). *SIX6* homologues are also present in *Colletotrichum* (Gawehns et al., 2014). Collectively, these studies underscore the context-dependent and, in certain instances, paradoxical role of SIX6 in *F. oxysporum* pathogenicity. While targeted gene deletion analyses across multiple *formae speciales* have demonstrated a measurable contribution of SIX6 to disease phenotype severity, other investigations indicate functional redundancy or host-specific dispensability of this effector. The absence of an observable virulence phenotype in *Fol* strains harboring combinatorial deletions of multiple *SIX* genes (*SIX6*, *SIX9*, and *SIX11*) suggests that compensatory effector networks or parallel virulence mechanisms may obscure the individual contribution of specific effectors under defined experimental conditions (Vlaardingerbroek et al., 2016). Similarly, the failure to detect attenuation of virulence in *SIX6* deletion mutants of *F. oxysporum* f. sp. *melonis* indicates that SIX6 functionality may be contingent upon host genotype, the collective effector complement of the pathogenic strain, or the discrete infection microenvironment occupied by the pathogen (Li et al., 2020). Collectively, these observations demonstrate that SIX6-mediated pathogenic contribution is highly contingent upon the genetic architecture and physiological state of both the pathogen and host system, thereby highlighting the inherent complexity of effector biology and the inherent limitations of reductionist single-gene knockout methodologies for comprehensive elucidation of effector function *in planta*.

The SIX8 effector is translocated into host cells (Tintor et al., 2020) where it promotes *Fol* pathogenicity by interacting with the tomato TPL1 (TOPLESS 1) and TPL2 proteins and enhancing their function as transcriptional co-repressors of genes involved in plant defence (Aalders et al., 2024). The *SIX8* gene exists in multiple copies within the *Fol* genome, with copy numbers ranging from one to thirteen copies among different *Fol* strains (De Sain et al., 2015). Like *SIX3* and *SIX5*, the *Fol SIX8* gene is arranged in a divergently transcribed pair with

a putative effector gene designated *PSL1* (*PSE*1-like 1) (Ayukawa et al., 2021; Sun et al., 2022, 2025). *PSE1* (Paired with *SIX8*) encodes a small cysteine-rich protein secreted by *F. oxysporum* f. sp. *conglutinans* (*Focn*) that, together with *Focn* SIX8 suppresses phytoalexin-based defences in Arabidopsis (Aykawa et al. 2021). It is possible that PSL1 promotes the cell-to-cell movement of SIX8, similar to the role of SIX5 in promoting the cell-to-cell movement of SIX3 (Avr2). A *PSE1* orthologue is present in *Fol,* but it is paired with a *SIX8* homologue designated *SIX8b* that is neither transcribed nor translated (Schmidt et al., 2013; Sun et al., 2022).

Beyond the well-characterised SIX effector proteins, *Fol* also produces extracellular proteases that play an important role in overcoming chitinase-based defence of tomato. Two of these proteases, the fungalysin metalloprotease (FoMep1) and the subtilisin serine protease (FoSep1), work together to inactivate chitin-binding domain-containing chitinases, which are among the plant's primary antifungal defences (Jashni et al., 2015). FoMep1 is closely related to a similar metalloprotease found in *F. verticillioides* and can be detected in the xylem sap of infected tomato plants, indicating it is actively secreted during *Fol* infection. Interestingly, neither protease alone is particularly effective at disabling plant chitinases. FoMep1 can only partially cleave one type of chitinase (the class IV enzyme SlChi13), while FoSep1 on its own has minimal effect. However, when both proteases are present together, they completely remove the chitin-binding domains from two major tomato chitinases (SlChi1 and SlChi13), cutting them at different positions on their N-terminal regions. This cleavage reduces both the enzymatic activity and antifungal potency of these defence proteins. The importance of this cooperative protease activity becomes clear when looking at deletion mutants. Strains lacking just one of the two proteases show only minor decreases in virulence, but double mutants lacking both FoMep1 and FoSep1 are significantly less pathogenic, causing much milder disease symptoms that are comparable to mock-inoculated plants. This demonstrates that the synergistic action of these two proteases is essential for the full virulence of *Fol* on tomato (Jashni et al., 2015).

FoRnt2 is a secreted ribonuclease family protein (encoded by FOXG_12372) from *Fol* that contributes to fungal virulence on tomato. The protein contains an N-terminal signal peptide and a conserved RNase T2 domain with two critical active site residues (His80 and His142) that are essential for its RNA-degrading activity. FoRnt2 expression is strongly induced during infection, peaking at 8 hours post-inoculation and the protein localise to both the cytoplasm and nucleus of plant cells after secretion. While deletion of *FoRnt2* does not affect fungal

growth or conidiation, it significantly reduces virulence on tomato. RNA-seq analysis revealed that FoRnt2 down-regulates 1,463 plant genes enriched in defence-related pathways, including hormone signaling (auxin, ethylene, ABA), MAPK signalling, and ribosome biogenesis. Unlike other effectors, FoRnt2 does not induce cell death but instead suppresses plant immunity by degrading defence-related RNAs, thereby promoting fungal infection (Qian et al., 2022).

FolSvp1 (encoded by FOXG_11456) is another secreted effector from *Fol* that is essential for full fungal virulence on tomato. The protein contains both a signal peptide for secretion and a nuclear localisation signal, which allows it to enter the plant cell nucleus. A key aspect of FolSvp1 function is the acetylation of lysine 167 (K167) by the fungal enzyme FolArd1, which protects the protein from degradation. Without this acetylation, FolSvp1 becomes marked for destruction at three other lysine residues, resulting in approximately 75% reduction in protein levels. Once secreted into the plant, FolSvp1 targets SlPR1, a tomato defence protein normally located in the apoplast. FolSvp1 binds to SlPR1 and relocates it into the nucleus, preventing SlPR1 from generating CAPE1, a defence-signalling peptide that would normally enhance plant immunity. The K167 acetylation continues to protect FolSvp1 from degradation within plant cells, allowing it to complete its immune-suppressing function. Experiments show that deleting the *FolSvp1* gene or mutating K167 to prevent acetylation significantly reduces the fungus ability to cause disease, while mutations that mimic acetylation maintain full virulence. This demonstrates that a single acetylation event on one amino acid is essential for successful fungal infection (Li et al., 2022).

Fol produces eight polygalacturonases, but two dominate the secreted PG activity. Pg1 (encoded by FOXG_14695) is the major endopolygalacturonase that cleaves pectin chains internally, showing the highest expression levels when induced by galacturonic acid. Pgx6 (encoded by FOXG_15415) is the major exopolygalacturonase that degrades oligogalacturonides from chain ends to produce smaller fragments and monomers. Together, these enzymes account for approximately 90% of total secreted PG activity, working synergistically to degrade pectin. Despite their importance in pectin degradation, individual deletion of either *pg1* or *pgx6* did not significantly reduce virulence on tomato plants, even though the Δpg1 mutant showed dramatically decreased endoPG activity and Δpgx6 showed 16% reduction in total activity. However, the Δpg1Δpgx6 double mutant retained less than 10% of wild-type PG activity and was significantly attenuated in virulence, with only 40% plant mortality after 30 days compared to nearly complete mortality with wild-type or single

mutants. Thin-layer chromatography confirmed that the double mutant produced far fewer pectin degradation products. Complementation with intact *pg1* fully restored virulence. Interestingly, fungal colonisation levels and plant defence gene expression were similar across all strains, suggesting these PGs contribute to symptom development rather than tissue colonisation. This demonstrates that the combined action of endo and exopolygalacturonases is essential for full virulence of *Fol* (Bravo Ruiz et al., 2016).

Tom1 effector from *Fol* functions primarily as a detoxification effector, encoding a tomatinase enzyme that degrades α-tomatine, a potent antifungal saponin produced by tomato plants as a defence mechanism. By neutralising α-tomatine, *Tom1* facilitates the pathogen's ability to infect and cause disease in tomato hosts. Although not essential for pathogenicity, the presence and activity of *Tom1* significantly contribute to virulence, as disruption of the gene delays disease progression while overexpression accelerates symptom development. The genome of *Fol* contains at least five tomatinase-encoding genes, suggesting a redundant system that enhances the fungus's capacity to overcome plant defences. Overall, *Tom1* acts as a virulence factor that helps the pathogen evade host chemical defences, enabling successful infection (Pareja-Jaime et al., 2008).

Fol-milR1 is a microRNA-like RNA (milRNA) produced by the *Fol* that functions as a virulence effector by crossing kingdom boundaries to suppress plant immunity. Unlike conventional protein effectors, *Fol-milR1* represents a novel pathogenicity strategy where the fungus exports small RNA molecules directly into tomato host cells during infection. Once inside plant cells, *Fol-milR1* targets and cleaves the mRNA of *SlyFRG4* (Solyc06g007430), a gene encoding a CBL-interacting protein kinase essential for tomato wilt disease resistance. The pathogenic importance of *Fol-milR1* is demonstrated through genetic studies: fungal knockout mutants show attenuated virulence on susceptible tomato cultivars, while overexpression strains cause disease even in resistant plants. The discovery of *Fol-milR1* as a trans-kingdom RNA effector expands our understanding of plant-pathogen molecular warfare beyond protein-based interactions and suggests that cross-kingdom RNA interference may be a conserved evolutionary strategy employed by diverse pathogens to subvert host immunity and achieve successful colonisation (Ji et al., 2021).

Recently, Sun et al. (2022) have expanded the possible effector repertoire of *Fol* by identifying 40 candidate effector genes, which included 13 of the 14 characterised *SIX* genes (*SIX4* was not present in *Fol* 4287) and 27 novel effector gene candidates (Table 1.1). One of these

secreted effector genes, *Fol-EC19*, encodes a secreted guanyl-specific ribonuclease that induces cell death when expressed in *Nicotiana benthamiana*. Two other effector genes, *Fol-EC14* and *Fol-EC20*, encoding a secreted glucanase and a secreted trypsin, respectively, can suppress *Bax*-induced cell death as well as cell death responses triggered by *I-2/Avr2* and *I/Avr1* in *N. benthamiana* (Sun et al., 2022). The identification of these effectors underscores the diverse strategies employed by *Fol* to manipulate host immunity. Some effectors promote cell death while others suppress immune responses to enable sustained infection (Sun et al., 2022).

Table 1.1. List of effector proteins reported to date in *Fol.*

Effector gene	Effector status	Size (aa)	Cysteines	References
SIX1	Confirmed	284	8	Rep et al., 2004
SIX2	Putative	232	8	van der Does et al., 2008
SIX3	Confirmed	163	2	Houterman et al., 2009
SIX4	Confirmed	242	6	Houterman et al., 2008
SIX5	Confirmed	102	6	Ma et al., 2015
SIX6	Confirmed	225	9	Gawehns et al., 2014
SIX7	Putative	163	2	Gonzalez-Cendales et al., 2016
SIX8	Putative	141	2	Schmidt et al., 2013
PSL1	Putative	111	9	Ayukawa et al., 2021 Sun et al., 2022
PSE1	Putative	106	9	Ayukawa et al., 2021
SIX9	Putative	114	6	Schmidt et al., 2013
SIX10	Putative	149	2	Schmidt et al., 2013
SIX11	Putative	110	8	Schmidt et al., 2013
SIX12	Putative	127	10	Gonzalez-Cendales et al., 2016
SIX13	Putative	293	12	Schmidt et al., 2013
SIX14	Putative	88	6	Schmidt et al., 2013
SIX15	Putative	79	9	Gonzalez-Cendales et al., 2016 Simbaqueba et al., 2018
Fol Ave1	Confirmed	124	4	de Jonge et al., 2012 Boshoven et al., 2015
RALF-B	Confirmed	49	4	Thynne et al., 2017 Masachis et al., 2016
FoMEP1	Confirmed	632	5	Jashni et al., 2015
FoSEP1	Confirmed	414	1	Jashni et al., 2015

FoRnt2	Confirmed	263	11	Qian et al., 2022
FolSvp1	Confirmed	315	9	Li et al., 2022
PG1	Confirmed	371	10	Bravo Ruiz et al., 2016
PGX6	Confirmed	464	11	Bravo Ruiz et al., 2016
Tom1	Confirmed	370	5	Pareja-Jaime et al., 2008
Fol-milR1	Confirmed	N/A	N/A	Ji et al., 2021
Fol-EC14	Putative	113	4	Sun et al., 2022
Fol-EC19	Putative	211	6	Sun et al., 2022
Fol-EC20	Putative	204	7	Sun et al., 2022
FOXGR_015522	Putative	79	9	Sun et al., 2022
FOXGR_015533	Putative	114	3	Sun et al., 2022
FOXG_10949	Putative	107	8	Sun et al., 2022
FOXG_10950	Putative	152	9	Sun et al., 2022
FOXG_11033	Putative	226	0	Sun et al., 2022
FOXG_05750	Putative	265	12	Sun et al., 2022
FOXG_05755	Putative	157	3	Sun et al., 2022
FOXG_18699	Putative	96	10	Sun et al., 2022
FOXGR_007323	Putative	86	0	Sun et al., 2022
FOXG_10672	Putative	198	13	Sun et al., 2022
FOXG_04863	Putative	300	8	Sun et al., 2022
FOXG_04805	Putative	132	8	Sun et al., 2022
FOXG_02829	Putative	149	16	Sun et al., 2022
FOXGR_021626	Putative	294	3	Sun et al., 2022
FOXG_08899	Putative	148	1	Sun et al., 2022
FOXGR_010884	Putative	264	0	Sun et al., 2022
FOXG_11745	Putative	183	4	Sun et al., 2022
FOXG_10138	Putative	261	2	Sun et al., 2022
FOXGR_025639	Putative	61	2	Sun et al., 2022
FOXG_16600	Putative	164	0	Sun et al., 2022
FOXG_13233	Putative	131	4	Sun et al., 2022
FOXG_13248	Putative	248	6	Sun et al., 2022
FOXG_14607	Putative	275	7	Sun et al., 2022
FOXG_14684	Putative	168	14	Sun et al., 2022

1.3.4 Tomato genes conferring resistance to *Fol*

Out of fourteen SIX genes, three are known to encode effectors recognised by tomato plants carrying corresponding resistance genes. The *I* (immunity) gene, introgressed from *Solanum pimpinellifolium,* encodes a LRR-RP (Catanzariti et al., 2017) (Figure 1.10) that provides protection against *Fol* race 1 through recognition of the SIX4 effector, hence *SIX4* is also known as *Avr1* (Houterman et al., 2008). The *I-2* gene, also introgressed from *S. pimpinellifolium* (Stall and Walter, 1965), encodes a CC-NLR (Simons et al., 1998) that confers resistance to *Fol* race 2 through recognition of the SIX3 effector protein, also known as Avr2 (Houterman et al., 2009) (Figure 1.10).

Two genes have been identified that confer resistance against *Fol* race 3, one from *Solanum pennellii* accession LA716 (Scott and Jones, 1989) and the other from *S. pennelli* accession PI414773 (McGrath et al., 1987). Initially, both genes were called *I-3*, but additional analysis indicated that they were not identical (Lim et al., 2006). The *I-3* gene from LA716 encodes an SRLK (Catanzariti et al., 2015), while the gene from PI414773 was renamed *I-7* and shown to encode a LRR-RP (Gonzalez-Cendales et al., 2016) (Figure 1.11). The *I-3* resistance gene confers resistance through recognition of the SIX1 effector (Rep et al., 2004), also designated Avr3, but the effector recognised by I-7 remains unknown (Figure 1.10). The *I-7* gene provides resistance against all three races of *Fol* (Gonzalez-Cendales et al., 2016), in part because the *SIX4* (*Avr1*) gene carried by race 1 cannot overcome the protection conferred by *I-7* despite suppressing resistance mediated by *I* and *I-3*. Resistance conferred by the *I* and *I-7* resistance genes has been shown to be *EDS1* dependent (Hu et al., 2005; Gonzalez-Cendales et al., 2016) and the induction of cell death by *I* has been shown to be *BAK1* and *SOBIR1*-dependent (Catanzariti et al., 2017).

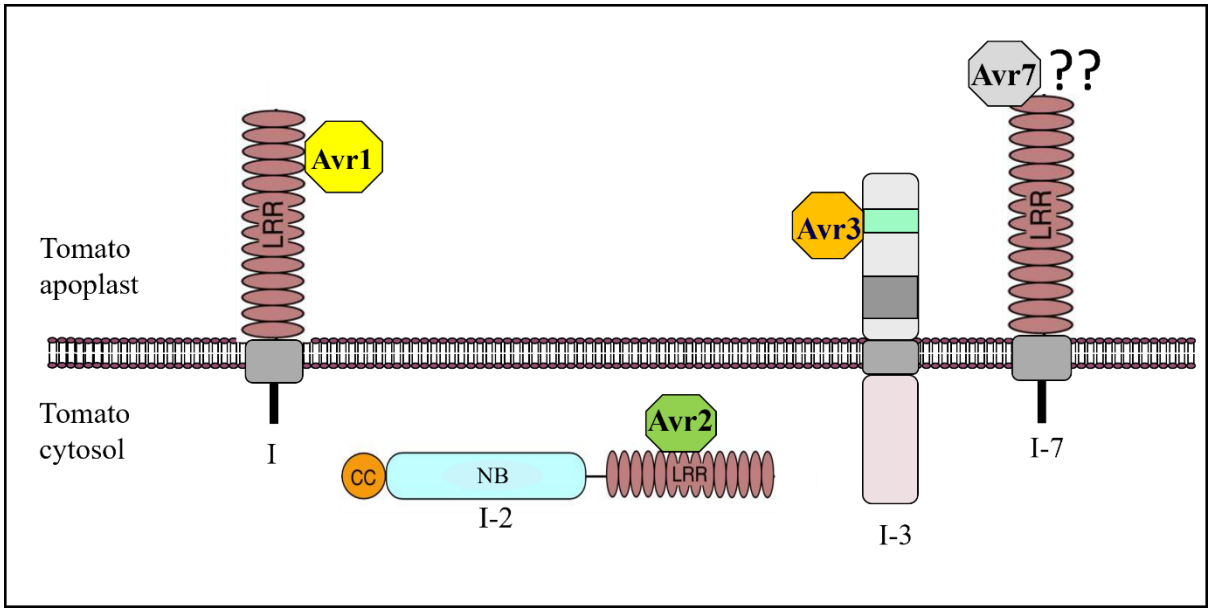

Figure 1.10 A graphical illustration of the tomato/*Fol* interaction and the R/Avr involved. Abbreviations: CC (coiled coil), LRR (leucine-rich repeat), NB (nucleotide binding), Avr (Avirulence).

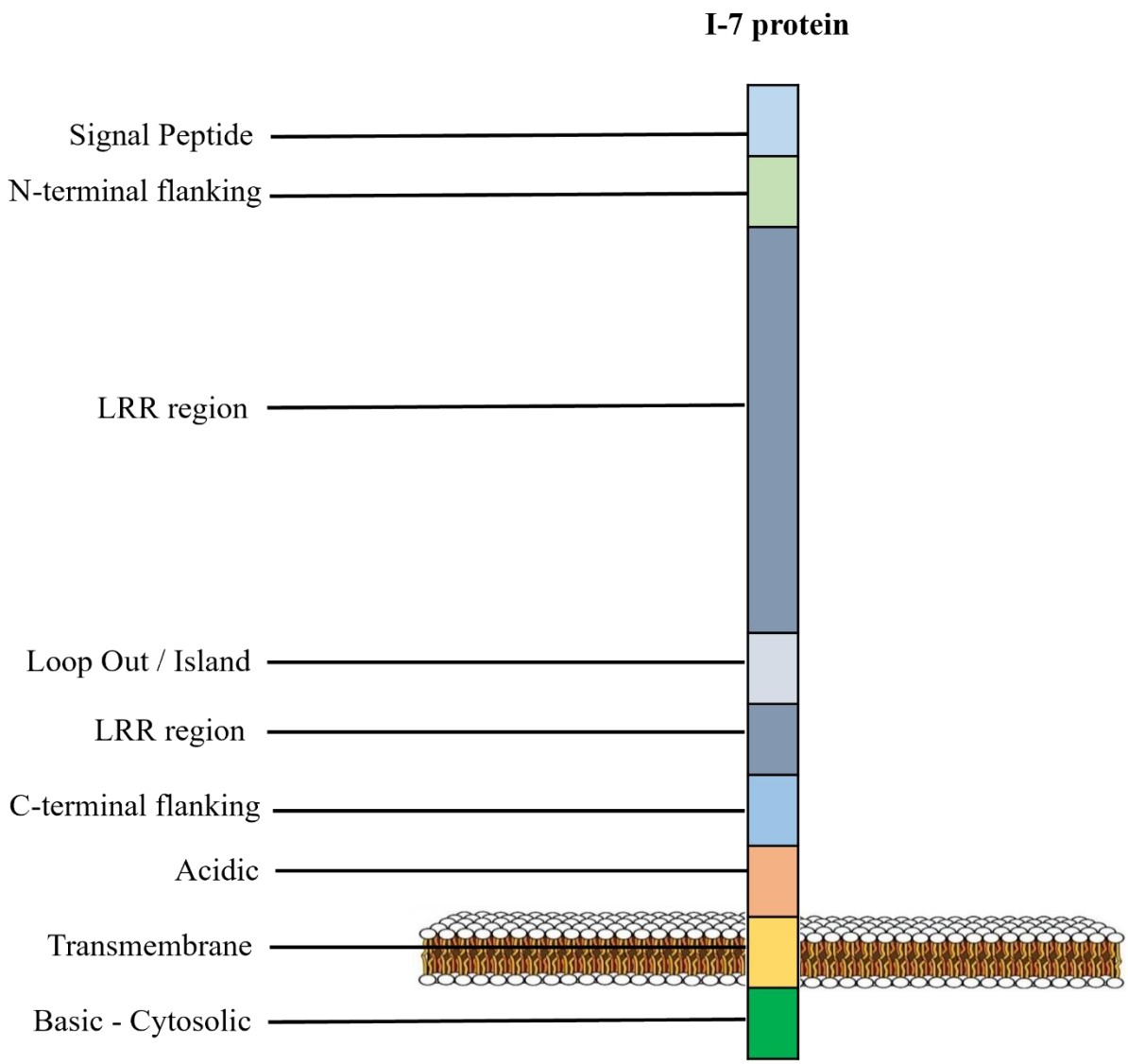

Figure 1.11 Graphic representation of the predicted I-7 protein.

The I-7 protein contains a signal peptide, two LRR regions separated by a so-called loop-out or island domain, an acidic extracytosolic juxtamembrane domain a transmembrane domain and a basic cytosolic juxtamembrane domain. (Diagram adapted from Gonzalez-Cendales et al., 2016).

1.4 Aims of the research project

The *I-7* resistance gene encoding an LRR-RP has been identified in tomato (Gonzalez-Cendales et al., 2016), but the corresponding *Fol Avr7* gene has not. The *Avr7* gene could be a *SIX* gene or a novel effector gene. The initial goal of my project was to identify and characterise the *Avr7* gene from *Fol*. All were screened before using RNA sequencing to identify LS genes encoding small, secreted proteins for subsequent testing. An RNA sequencing experiment had already been conducted on *I-7* resistant and susceptible tomato plants at 2 days post-inoculation with *Fol* race 3 (Gonzalez-Cendales, Catanzariti and Jones, unpublished). It showed early expression of the *SIX* genes as well as some other possible effector genes. Initially, my project involved cloning *Avr7* candidate genes into a plant expression vector and screening them for cell death induction following co-agroinfiltration with *I-7* in *Nicotiana benthamiana* leaves.

During this screening work, I discovered that *SIX6* triggered plant cell death by itself. I then decided to pursue characterisation of *SIX6*, so the second and ultimately main aim of my project was to obtain an improved understanding of *SIX6* function. Previous findings about *Fol SIX6* reveal that it contributes to pathogen virulence (Gawehns et al., 2014). Transient expression of *SIX6* was also reported to reduce cell death and ion leakage triggered by co-expression of *I-2* and *Avr2* in *N. benthamiana* leaves (Gawehns et al., 2014), but this result was based on a version of *SIX6* encoding a protein that lacked a signal peptide and contained a C-terminal truncation, and is not supported by the work described in this thesis. How *SIX6* contributed to pathogen virulence, therefore, remained unclear. The overall objective of my research was to gain a better understanding of *SIX6* function and the mechanism underlying its contribution to pathogen virulence. The specific aims of the project were to:

1. Identify the *Avr7* effector gene from *Fusarium oxysporum* f. sp. *lycopersici.*
2. Use recombinant SIX6 protein to characterise its cell-death-inducing activity in a range of plant species.
3. Investigate whether the cell death induced by *Fol* SIX6 is a defence response.
4. Examine how *Fol* SIX6 affects plant physiology by analysing its role in stomatal opening and vacuolar dynamics in leaf epidermal cells.
5. Investigate the effects of *Fol* SIX6 on root tissues, which are the primary site for *Fol* infection in tomato plants.

References

Aalders, T.R., de Sain, M., Gawehns, F., Oudejans, N., Jak, Y.D., Dekker, H.L., Rep, M., van den Burg, H.A., Takken, F.L.W. (2024). Specific members of the TOPLESS family are susceptibility genes for Fusarium wilt in tomato and Arabidopsis. *Plant Biotechnology Journal, 22*(1), 248-261.

Adachi, H., & Kamoun, S. (2022). NLR receptor networks in plants. *Essays in Biochemistry*, *66*(5), 541-549.

Adachi, H., Contreras, M.P., Harant, A., Wu, C.H., Derevnina, L., Sakai, T., Duggan, C., Moratto, E., Bozkurt, T.O., Maqbool, A., Kamoun, S. (2019). An N-terminal motif in NLR immune receptors is functionally conserved across distantly related plant species. *Elife*, *8*, e49956.

Agrios, G.N. (2005). Plant pathology (5th ed.). Elsevier Academic Press.

Alexander, L.J., & Tucker, C.M. (1945). Physiological specialization in the tomato wilt fungus *Fusarium oxysporum* f. sp. *lycopersici. Journal for Agriculture Research, 70,* 303-313.

Ayukawa, Y., Asai, S., Gan, P., Tsushima, A., Ichihashi, Y., Shibata, A., Komatsu, K., Houterman, P.M., Rep, M., Shirasu, K., Arie, T. (2021). A pair of effectors encoded on a conditionally dispensable chromosome of *Fusarium oxysporum* suppress host-specific immunity. *Communications Biology, 4*(1),707.

Beckman, C.H. (1987). The nature of wilt diseases of plants. St. Paul: APS Press.

Bednarek, P., & Osbourn, A. (2009). Plant-microbe interactions: chemical diversity in plant defence. *Science, 324*(5928), 746-748.

Bi, G., Su, M., Li, N., Liang, Y.U., Dang, S., Xu, J., Hu, M., Wang, J., Zou, M., Deng, Y., Zhou, J.M. (2021). The ZAR1 resistosome is a calcium-permeable channel triggering plant immune signaling. *Cell*, *184*(13), 3528-3541.

Bohn, G.W., & Tucker, C.M. (1939). Immunity to Fusarium wilt in the tomato. *Science, 89*(2322), 603-604.

Boller, T., & Felix, G. (2009). A renaissance of elicitors: perception of microbe-associated molecular patterns and danger signals by pattern-recognition receptors. *Annual Review of Plant Biology, 60*, 379-406.

Boshoven, J.C., Ebert, M.K., Song, Y., Rovenich, H., Rojas-Padilla, E., Bolton, M.D. Thomma, B.P. (2015). Homologs of *Verticillium dahliae* effector Ave1 contribute to virulence of fungal pathogens of diverse plant hosts. In *Book of Abstracts 28th Fungal Genetics Conference,* 208.

Bravo Ruiz, G., Di Pietro, A., Roncero, M.I.G. (2016). Combined action of the major secreted exo and endopolygalacturonases is required for full virulence of *Fusarium oxysporum*. *Molecular Plant Pathology, 17*(3), 339-353.

Broekaert, W.F., Cammue, B.P., De Bolle, M.F., Thevissen, K., De Samblanx, G.W., Osborn, R.W. (1997). Antimicrobial peptides from plants. *Critical Reviews in Plant Sciences, 16*(3), 297-323.

Cao, L., Blekemolen, M.C., Tintor, N., Cornelissen, B.J.C., Takken, F.L.W. (2018). The *Fusarium oxysporum* Avr2-Six5 effector pair alters plasmodesmatal exclusion selectivity to facilitate cell to cell movement of Avr2. *Molecular Plant, 11*(5), 691-705.

Catanzariti, A.M., Do, H.T.T., Bru, P., de Sain, M., Thatcher, L.F., Rep, M., Jones, D.A. (2017). The tomato *I* gene for Fusarium wilt resistance encodes a typical leucine-rich repeat receptor-like protein whose function is nevertheless dependent on SOBIR1 and SERK3/BAK1. *The Plant Journal, 89*(6), 1195-1209.

Catanzariti, A.M., Lim, G.T.T., Jones, D.A. (2015). The tomato *I-3* gene: a novel gene for resistance to Fusarium wilt disease. *New Phytologist, 207*(1), 106-118.

Chakrabarti, A., Rep, M., Wang, B., Ashton, A., Dodds, P., Ellis, J. (2011). Variation in potential effector genes distinguishing Australian and non-Australian isolates of the cotton wilt pathogen *Fusarium oxysporum* f. sp. *vasinfectum*. *Plant Pathology, 60*(2), 232-243.

Chen, L.Q., Hou, B.H., Lalonde, S., Takanaga, H., Hartung, M.L., Qu, X.Q., Guo, W.J., Kim, J.G., Underwood, W., Chaudhuri, B., Frommer, W.B. (2010). Sugar transporters for intercellular exchange and nutrition of pathogens. *Nature*, *468*(7323), 527-532.

Choi, H.W., & Klessig, D.F. (2016). DAMPs, MAMPs, and NAMPs in plant innate immunity. *BMC Plant Biology, 16*(1), 232.

Couto, D., & Zipfel, C. (2016). Regulation of pattern recognition receptor signalling in plants. *Nature Reviews Immunology, 16*(9), 537-552.

Czislowski, E., Smith, S.F., Zander, M., O'Neill, W.T., Meldrum, R.A., Tran-Nguyen, L.T.T., Batley, J., Aitken, E.A.B. (2018). Investigation of the diversity of effector genes in the banana pathogen, *Fusarium oxysporum* f. sp. *cubense*, reveals evidence of horizontal gene transfer. *Molecular Plant Pathology, 19*(5), 1155-1171.

Dagvadorj, B., Outram, M.A., Williams, S.J., Solomon, P.S. (2022). The necrotrophic effector ToxA from *Parastagonospora nodorum* interacts with wheat NHL proteins to facilitate *Tsn1*-mediated necrosis. *The Plant Journal*, *110*(2), 407-418.

Davis, R.M., Colyer, P.D., Rothrock, C.S., Kochman, J.K. (2006). Fusarium wilt of cotton: population diversity implications and management. *Plant Disease, 90,* 692-703.

de Jonge, R., Peter van Esse, H., Kombrink, A., Shinya, T., Desaki, Y., Bours, R., Van Der Krol, S., Shibuya, N., Joosten, M.H., Thomma, B.P. (2010). Conserved fungal LysM effector Ecp6 prevents chitin-triggered immunity in plants. *Science*, *329*(5994), 953-955.

de Jonge, R., van Esse, H.P., Maruthachalam, K., Bolton, M.D., Santhanam, P., Saber, M.K., Zhang, Z., Usami, T., Lievens, B., Subbarao, K.V., Thomma, B.P.H.J. (2012). Tomato immune receptor Ve1 recognises effector of multiple fungal pathogens uncovered by genome and RNA sequencing. *Proceedings of the National Academy of Sciences, 109*(13) 5110-5115.

De Sain, M., & Rep, M. (2015). Review: The role of pathogen-secreted proteins in fungal vascular wilt diseases. *International Journal of Molecular Sciences, 16*(10), 23970-23993.

Dean, R., Van Kan, J.A., Pretorius, Z.A., Hammond-Kosack, K.E., Di Pietro, A., Spanu, P.D., Rudd, J.J., Dickman, M., Kahmann, R., Ellis, J., Foster, G.D. (2012). The Top 10 fungal pathogens in molecular plant pathology. *Molecular Plant Pathology, 13*(4), 414-430.

Deslandes, L., Olivier, J., Peeters, N., Feng, D.X., Khounlotham, M., Boucher, C., Somssich, I., Genin, S., Marco, Y. (2003). Physical interaction between RRS1-R, a protein conferring resistance to bacterial wilt, and PopP2, a type III effector targeted to the plant nucleus. *Proceedings of the National Academy of Sciences*, *100*(13), 8024-8029.

Di Pietro, A., Madrid, M.P., Caracuel, Z., Delgado-Jarana, J., Roncero, M.I. (2003). *Fusarium oxysporum*: exploring the molecular arsenal of a vascular wilt fungus. *Molecular Plant Pathology, 4*(5), 315-325.

Djamei, A., Schipper, K., Rabe, F., Ghosh, A., Vincon, V., Kahnt, J., Osorio, S., Tohge, T., Fernie, A.R., Feussner, I., Feussner, K., Meinicke, P., Stierhof, Y.D., Schwarz, H., Macek, B., Mann, M., Kahmann, R. (2011). Metabolic priming by a secreted fungal effector. *Nature*, *478*(7369), 395-398.

Dongus, J.A., & Parker, J.E. (2021). EDS1 signalling: At the nexus of intracellular and surface receptor immunity. *Current opinion in plant biology*, *62*, 102039.

Dou, D., & Zhou, J.M. (2012). Phytopathogen effectors subverting host immunity: different foes, similar battleground. *Cell Host & Microbe, 12*(4), 484-495.

Dunkle, L.D., & Macko, V. (1995). Peritoxins and their effects on sorghum. *Canadian journal of botany*, *73*(S1), 444-452.

Egel, D.S., & Martyn, R.D. (2007). Fusarium wilt of watermelon and other cucurbits. The plant health instructor. The American Phytopathological Society (APS). https://www.apsnet.org/edcenter/pdlessons/Pages/FusariumWatermelon.aspx.

Elias, K.S., & Schneider, R.W. (1991). Vegetative compatibility groups in *Fusarium oxysporum* f. sp. *lycopersici*. *Phytopathology, 81*(2), 159-162.

Faris, J.D., & Friesen, T.L. (2020). Plant genes hijacked by necrotrophic fungal pathogens. *Current Opinion in Plant Biology*, *56*, 74-80.

Faris, J.D., Zhang, Z., Lu, H., Lu, S., Reddy, L., Cloutier, S., Fellers, J.P., Meinhardt, S.W., Rasmussen, J.B., Xu, S.S., Friesen, T.L. (2010). A unique wheat disease resistance-like gene governs effector-triggered susceptibility to necrotrophic pathogens. *Proceedings of the National Academy of Sciences*, *107*(30), 13544-13549.

Flor, H.H. (1971). Current status of gene for gene concept. *Annual Review of Phytopathology, 9*(1), 275-296.

Fonseca, J.P., & Mysore, K.S. (2019). Genes involved in nonhost disease resistance as a key to engineer durable resistance in crops. *Plant Science, 279*, 108-116.

Frías, M., González, C., Brito, N. (2011). BcSpl1, a cerato-platanin family protein, contributes to Botrytis cinerea virulence and elicits the hypersensitive response in the host. *New Phytologist, 192*(2), 483-495.

Gabriels, S.H., Vossen, J.H., Ekengren, S.K., van Ooijen, G., Abd-El-Haliem, A.M., van den Berg, G.C., Rainey, D.Y., Martin, G.B., Takken, F.L.W., Wit, P.J.D. (2007). An NB-LRR protein required for HR signalling mediated by both extra- and intracellular resistance proteins. *The Plant Journal*, *50*(1), 14–28.

Gao, M., Wang, X., Wang, D., Xu, F., Ding, X., Zhang, Z., Bi, D., Cheng, Y.T., Chen, S., Li, X., Zhang, Y. (2009). Regulation of cell death and innate immunity by two receptor-like kinases in *Arabidopsis*. *Cell host & microbe*, *6*(1), 34-44.

Gawehns, F., Houterman, P.M., Ichou, F.A., Michielse, C.B., Hijdra, M., Cornelissen, B.J.C., Rep, M., Takken, F.L.W. (2014). The *Fusarium oxysporum* effector Six6 contributes to virulence and suppresses I-2-mediated cell death. *Molecular Plant-Microbe Interactions*, *27*(4), 336-348.

Gawehns, F., Ma, L., Bruning, O., Houterman, P.M., Boeren, S., Cornelissen, B.J.C., Rep, M., Takken, F.L.W. (2015). The effector repertoire of *Fusarium oxysporum* determines the tomato xylem proteome composition following infection. *Frontiers in Plant Science*, *6*, 967.

Geiser, D.M., Aoki, T., Bacon, C.W., Baker, S.E., Bhattacharyya, M.K., Brandt, M.E., Brown, D.W., Burgess, L.W., Chulze, S., Coleman, J.J., Correll, J.C., Covert, S.F., Crous,

P.W., Cuomo, C.A., De Hoog, G.S., Di Pietro, A., Elmer, W.H., Epstein, L., Frandsen, R.J., Freeman, S., Gagkaeva, T., Glenn, A.E., Gordon, T.R., Gregory, N.F., Hammond-Kosack, K.E., Hanson, L.E., Jímenez-Gasco M. del M., Kang, S., Kistler, H.C., Kuldau, G.A., Leslie, J.F., Logrieco, A., Lu, G., Lysøe, E., Ma, L.J., McCormick, S.P., Migheli, Q., Moretti, A., Munaut, F., O'Donnell, K., Pfenning, L., Ploetz, R.C., Proctor, R.H., Rehner, S.A., Robert, V.A., Rooney, A.P., bin Salleh, B., Scandiani, M.M., Scauflaire, J., Short, D.P., Steenkamp, E., Suga, H., Summerell, B.A., Sutton, D.A,. Thrane, U., Trail, F., Van Diepeningen, A., VanEtten, H.D., Viljoen, A., Waalwijk, C., Ward, T.J., Wingfield, M.J., Xu, J.R., Yang, X.B., Yli-Mattila, T., Zhang, N. (2013). One fungus, one name: defining the genus *Fusarium* in a scientifically robust way that preserves longstanding use. *Phytopathology, 103*(5), 400-408.

Gijzen, M., & Nürnberger, T. (2006). Nep1-like proteins from plant pathogens: Recruitment and diversification of the NPP1 domain across taxa. *Phytochemistry, 67*(16), 1800-1807.

Glass, N.L., Jacobson, D.J., Shiu, P.K. (2000). The genetics of hyphal fusion and vegetative incompatibility in filamentous ascomycete fungi. *Annual Review of Genetics, 34*(1), 165-186.

Gordon, T.R. (2017). *Fusarium oxysporum* and the Fusarium wilt syndrome. *Annual Review of Phytopathology, 4*(55), 23-39.

Grattidge, R., & O'Brien, R.G. (1982). Occurrence of a third race of Fusarium wilt of tomatoes in Queensland. *Plant Disease, 66,* 65-166.

Griffiths, D.A. (1973). Fine structure of chlamydospore germination in *Fusarium oxysporum*. *Transactions of the British Mycological Society, 61*(1), 7-12.

Guerreiro, J., & Marhavy, P. (2023). Unveiling the intricate mechanisms of plant defense. *Frontiers in Plant Physiology*, *1*, 1285373.

Heath, M.C. (2000). Nonhost resistance and nonspecific plant defences. *Current Opinion in Plant Biology, 3*(4), 315-319.

Hemetsberger, C., Herrberger, C., Zechmann, B., Hillmer, M., Doehlemann, G. (2012). The *Ustilago maydis* effector Pep1 suppresses plant immunity by inhibition of host peroxidase activity. *PLoS pathogens*, *8*(5), e1002684.

Herold, L., Ordon, J., Hua, C., Kohorn, B.D., Nürnberger, T., DeFalco, T.A., Zipfel, C. (2024). Arabidopsis wall-associated kinases are not required for oligogalacturonide-induced signaling and immunity. *Plant Cell, 37*(1), koae317.

Houterman, P.M., Cornelissen, B.J.C., Rep, M. (2008). Suppression of plant resistance gene-based immunity by a fungal effector. *PLoS Pathogens, 4*(5), e1000061.

Houterman, P.M., Ma, L., van Ooijen, G., de Vroomen, M.J., Cornelissen, B.J.C., Takken, F.L.W., Rep, M., (2009). The effector protein Avr2 of the xylem-colonizing fungus *Fusarium oxysporum* activates the tomato resistance protein I-2 intracellularly. *Plant Journal, 58*(6), 970-978.

Houterman, P.M., Speijer, D., Dekker, H.L., Koster, C.G.D., Cornelissen, B.J.C., Rep, M. (2007). The mixed xylem sap proteome of *Fusarium oxysporum*-infected tomato plants. *Molecular Plant Pathology, 2*(8), 215-221.

Hu, G., DeHart, A.K., Li, Y., Ustach, C., Handley, V., Navarre, R., Hwang, C.F., Aegerter, B.J., Williamson, V.M., Baker, B. (2005). EDS1 in tomato is required for resistance mediated by TIR-class R genes and the receptor-like R gene Ve. *The Plant Journal*, *42*(3), 376-391.

Huang, W.R., Braam, C., Kretschmer, C., Villanueva, S.L., Liu, H., Ferik, F., van der Burgh, A.M., Boeren, S., Wu, J., Zhang, L., Joosten, M.H. (2024). Receptor-like cytoplasmic kinases of different subfamilies differentially regulate SOBIR1/BAK1-mediated immune responses in *Nicotiana benthamiana*. *Nature Communications*, *15*(1), 4339.

Jashni, M.K., Dols, I.H., Iida, Y., Boeren, S., Beenen, H.G., Mehrabi, R., Collemare, J., de Wit, P.J. (2015). Synergistic action of a metalloprotease and a serine protease from *Fusarium oxysporum* f. sp. *lycopersici* cleaves chitin-binding tomato chitinases, reduces their antifungal activity, and enhances fungal virulence. *Molecular Plant-Microbe Interactions, 28*(9), 996-1008.

Ji, H.M., Mao, H.Y., Li, S.J., Feng, T., Zhang, Z.Y., Cheng, L., Luo, S.J., Borkovich, K.A., Ouyang, S.Q. (2021). *Fol-milR1*, a pathogenicity factor of *Fusarium oxysporum*, confers tomato wilt disease resistance by impairing host immune responses. *New Phytologist,* 232(2), 705-718.

Jones, J.D.G., & Dangl, J.L. (2006). The plant immune system. *Nature, 444*(7117), 323-329.

Joosten, M.H., Cozijnsen, T.J., De Wit, P.J. (1994). Host resistance to a fungal tomato pathogen lost by a single base-pair change in an avirulence gene. *Nature*, *367*(6461), 384-386.

Kourelis, J., & Adachi, H. (2022). Activation and regulation of NLR immune receptor networks. *Plant and Cell Physiology*, *63*(10), 1366-1377.

Lanubile, A., Ellis, M.L., Marocco, A., Munkvold, G.P. (2016). Association of effector *Six6* with vascular wilt symptoms caused by *Fusarium oxysporum* on soybean. *Phytopathology, 106*(11), 1404-1412.

Larkan, N.J., Ma, L., Haddadi, P., Buchwaldt, M., Parkin, I.A., Djavaheri, M., Borhan, M.H. (2020). The *Brassica napus* wall-associated kinase-like (WAKL) gene Rlm9 confers race-specific blackleg resistance. *The Plant Journal*, *104*(4), 892-900.

Laurence, M.H., Summerell, B.A., Liew, E.C.Y. (2015). *Fusarium oxysporum* f. sp. *canariensis*: evidence for horizontal gene transfer of putative pathogenicity genes. *Plant Pathology, 64*(5), 1068-1075.

Lee, H.A., Lee, H.Y., Seo, E., Lee, J., Kim, S.B., Oh, S., Choi, E., Choi, E., Lee, S.E., Choi, D. (2017). Current understandings of plant nonhost resistance. *Molecular Plant-Microbe Interactions, 30*(1), 5-15.

Lee, S.J., & Rose, J.K. (2010). Mediation of the transition from biotrophy to necrotrophy in hemibiotrophic plant pathogens by secreted effector proteins. *Plant signaling & behavior*, *5*(6), 769-772.

Li, B., Meng, X., Shan, L., He, P. (2016). Transcriptional regulation of pattern-triggered immunity in plants. *Cell Host & Microbe, 19*(5), 641-650.

Li, J., Fokkens, L., van Dam, P., Rep, M. (2020). Related mobile pathogenicity chromosomes in *Fusarium oxysporum* determine host range on cucurbits. *Molecular Plant Pathology*, *21*(6), 761-776.

Li, J., Ma, X., Wang, C., Liu, S., Yu, G., Gao, M., Qian, H., Liu, M., Luisi, B.F., Gabriel, D.W., Liang, W. (2022). Acetylation of a fungal effector that translocates host PR1 facilitates virulence. *Elife, 11*, e82628.

Liebrand, T.W., van den Berg, G.C., Zhang, Z., Smit, P., Cordewener, J.H., America, A.H., Sklenar, J., Jones, A.M., Tameling, W.I., Robatzek, S., Joosten, M.H. (2013). Receptor-like kinase SOBIR1/EVR interacts with receptor-like proteins in plant immunity against fungal infection. *Proceedings of the National Academy of Sciences*, *110*(24), 10010-10015.

Lievens, B., Houterman, P.M., Rep, M. (2009). Effector gene screening allows unambiguous identification of *Fusarium oxysporum* f. sp. *lycopersici* races and discrimination from other *formae speciales*. *FEMS Microbiology Letters, 300*(2), 201-215.

Lim, G.T.T., Wang, G.P., Hemming, M.N., Basuki, S., McGrath, D.J., Carroll, B.J., Jones, D.A. (2006). Mapping the *I-3* gene for resistance to Fusarium wilt in tomato: application of an *I-3* marker in tomato improvement and progress towards the cloning of *I-3*. *Australasian Plant Pathology, 35*(6), 671-680.

Liu, S., Wu, Bo., Lv, S., Shen, Z., Li, R., Yi, G., Li, C., Guo, X. (2019). Genetic diversity in *FUB* genes of *Fusarium oxysporum* f. sp. *cubense* suggests horizontal gene transfer. *Frontiers in Plant Science, 4*(10), 1069.

Liu, Y., Huang, X., Li, M., He, P., Zhang, Y. (2016). Loss-of-function of *Arabidopsis* receptor-like kinase BIR 1 activates cell death and defense responses mediated by BAK 1 and SOBIR 1. *New Phytologist*, *212*(3), 637-645.

Lorang, J., Kidarsa, T., Bradford, C.S., Gilbert, B., Curtis, M., Tzeng, S.C., Maier, C.S., Wolpert, T.J. (2012). Tricking the guard: exploiting plant defense for disease susceptibility. *Science*, *338*(6107), 659-662.

Lorang, J.M., Sweat, T.A., Wolpert, T.J. (2007). Plant disease susceptibility conferred by a "resistance" gene. *Proceedings of the National Academy of Sciences*, *104*(37), 14861-14866.

Ma, L., Houterman, P.M., Gawehns, F., Cao, L., Sillo, F., Richter, H., Clavijo-Ortiz, M.J., Schmidt, S.M., Boeren, S., Vervoort, J., Cornelissen, B.J.C., Rep, M., Takken, F.L.W. (2015). The *AVR2-SIX5* gene pair is required to activate *I-2* -mediated immunity in tomato. *New Phytologist, 208*(2), 507-518.

Ma, L.J., Geiser, D.M., Proctor, R.H., Rooney, A.P., O'Donnell, K., Trail, F., Gardiner, D.M., Manners, J.M., Kazan, K. (2013). *Fusarium* pathogenomics. *Annual Review of Microbiology, 67*, 399-416.

Ma, L.J., van der Does, H.C., Borkovich, K.A., Coleman, J.J., Daboussi, M.J., Di Pietro, A., Dufresne, M., Freitag, M., Grabherr, M., Henrissat, B., Houterman, P.M., Kang, S., Shim, W.B., Woloshuk, C., Xie, X., Xu, J.-R., Antoniw, J., Baker, S.E., Bluhm, B.H., Breakspear, A., Brown, D.W., Butchko, R.A.E., Chapman, S., Coulson, R., Coutinho, P.M., Danchin, E.G.J., Diener, A., Gale, L.R., Gardiner, D.M., Goff, S., Hammond-Kosack, K.E., Hilburn, K., Hua-Van, A., Jonkers, W., Kazan, K., Kodira, C.D., Koehrsen, M., Kumar, L., Lee, Y.H., Li, L., Manners, J.M., Miranda-Saavedra, D., Mukherjee, M., Park, G., Park, J., Park, S.Y., Proctor, R.H., Regev, A., Ruiz-Roldan, M.C., Sain, D., Sakthikumar, S., Sykes, S., Schwartz, D.C., Turgeon, B.G., Wapinski, I., Yoder, O., Young, S., Zeng, Q., Zhou, S., Galagan, J., Cuomo, C.A., Kistler, H.C., Rep, M. (2010). Comparative genomics reveals mobile pathogenicity chromosomes in *Fusarium*. *Nature, 464*(7287), 367-373.

Macho, A.P., & Zipfel, C. (2014). Plant PRRs and the activation of innate immune signaling. *Molecular cell, 54*(2), 263-272.

Mayer, A.M., Staples, R.C., Gil-ad, N.L. (2001). Mechanisms of survival of necrotrophic fungal plant pathogens in hosts expressing the hypersensitive response. *Phytochemistry, 58*(1), 33-41.

McCombe, C.L., Greenwood, J.R., Solomon, P.S., Williams, S.J. (2022). Molecular plant immunity against biotrophic, hemibiotrophic, and necrotrophic fungi. *Essays in Biochemistry*, *66*(5), 581-593.

McGrath, D.J., Gillespie, D., Vawdrey, L. (1987). Inheritance of resistance to *Fusarium oxysporum* f. sp. *lycopersici* races 2 and 3 in *Lycopersicon pennellii*. *Australian Journal of Agricultural Research, 38*(4), 729-733.

Mentlak, T.A., Kombrink, A., Shinya, T., Ryder, L.S., Otomo, I., Saitoh, H., Terauchi, R., Nishizawa, Y., Shibuya, N., Thomma, B.P., Talbot, N.J. (2012). Effector-mediated suppression of chitin-triggered immunity by *Magnaporthe oryzae* is necessary for rice blast disease. *The Plant Cell*, *24*(1), 322-335.

Michielse, C.B., & Rep, M. (2009). Pathogen profile update: *Fusarium oxysporum*. *Molecular Plant Pathology, 10*(3), 311-324.

Miya, A., Albert, P., Shinya, T., Desaki, Y., Ichimura, K., Shirasu, K., Nakagawa, T. (2007). CERK1, a LysM receptor kinase, is essential for chitin elicitor signaling in *Arabidopsis*. *Proceedings of the National Academy of Sciences*, *104*(47), 19613-19618.

Nagy, E.D., & Bennetzen, J.L. (2008). Pathogen corruption and site-directed recombination at a plant disease resistance gene cluster. *Genome research*, *18*(12), 1918-1923.

Ngou, B.P.M., Ahn, H.K., Ding, P., Jones, J.D.G. (2021). Mutual potentiation of plant immunity by cell-surface and intracellular receptors. *Nature*, *592*(7853), 105-109.

Ngou, B.P.M., Jones, J.D.G., Ding, P. (2021). Plant immune networks. *Trends in Plant Science*, *26*(4), 255-273.

Niu, X., Zhao, X., Ling, K. S., Levi, A., Sun, Y., Fan, M. (2016). The *FonSIX6* gene acts as an avirulence effector in the *Fusarium oxysporum* f. sp. *niveum*-watermelon pathosystem. *Scientific reports*, *6*(1), 28146.

Nürnberger, T., & Lipka, V. (2005). Non-host resistance in plants: new insights into an old phenomenon. *Molecular Plant Pathology, 6*(3), 335-345.

O'Donnell, K., Ward, T.J., Robert, V.A., Crous, P.W., Geiser, D.M., Kang, S. (2015). DNA sequence-based identification of *Fusarium*: Current status and future directions. *Phytoparasitica, 43*(5), 583-595.

Osbourn, A.E. (1996). Preformed antimicrobial compounds and plant defence against fungal attack. *The Plant Cell, 8*(10), 1821-1831.

Pareja-Jaime, Y., Roncero, M.I.G., Ruiz-Roldán, M.C. (2008). Tomatinase from *Fusarium oxysporum* f. sp. *lycopersici* is required for full virulence on tomato plants. *Molecular Plant-Microbe Interactions, 21*(6), 728-736.

Park, C.H., Chen, S., Shirsekar, G., Zhou, B., Khang, C.H., Songkumarn, P., Afzal, A.J., Ning, Y., Wang, R., Bellizzi, M., Wang, G.L. (2012). The *Magnaporthe oryzae* effector *AvrPiz-t* targets the RING E3 ubiquitin ligase APIP6 to suppress pathogen-associated molecular pattern–triggered immunity in rice. *The plant cell*, *24*(11), 4748-4762.

Pegg, K.G., Coates, L.M., Wayne, T., O'Neill W.T., Turner, D.W. (2019). The epidemiology of Fusarium wilt of banana. *Frontiers in Plant Science 10*, 1395.

Perincherry, L., Ajmi, C., Oueslati, S., Waśkiewicz, A., Stępień, L. (2020). Induction of *Fusarium* lytic enzymes by extracts from resistant and susceptible cultivars of pea (*Pisum sativum* L.). *Pathogens, 9*(11), 976.

Qian, H., Wang, L., Wang, B., Liang, W. (2022). The secreted ribonuclease T2 protein FoRnt2 contributes to *Fusarium oxysporum* virulence. *Molecular Plant Pathology, 23*(9), 1346-1360.

Reis, A., Costa, H., Boiteux, L.S., Lopes, C.A. (2005). First report of *Fusarium oxysporum* f. sp. *lycopersici* race 3 on tomato in Brazil. *Fitopatologia Brasileira, 30,* 426-428.

Rep, M., van der Does, H.C., Meijer, M., van Wijk, R., Houterman, P.M., Dekker, H.L., de Koster, C.G., Cornelissen, B.J.C. (2004). A small, cysteine-rich protein secreted by *Fusarium oxysporum* during colonisation of xylem vessels is required for *I-3*-mediated resistance in tomato. *Molecular Microbiology, 53*(5), 1373-1383.

Saintenac, C., Lee, W.S., Cambon, F., Rudd, J.J., King, R.C., Marande, W., Powers, S.J., Bergès, H., Phillips, A.L., Uauy, C., Kanyuka, K. (2018). Wheat receptor-kinase-like protein Stb6 controls gene-for-gene resistance to fungal pathogen *Zymoseptoria tritici*. *Nature Genetics*, *50*(3), 368-374.

Santamaria, M.E., Martínez, M., Cambra, I., Grbic, V., Diaz, I. (2013). Understanding plant defence responses against herbivore attacks: an essential first step towards the development of sustainable resistance against pests. *Transgenic Research, 22*(4), 697-708.

Schmidt, S.M., Houterman, P.M., Schreiver, I., Ma, L., Amyotte, S., Chellappan, B., Boeren, S., Takken, F.L.W., Rep, M. (2013). MITEs in the promoters of effector genes allow prediction of novel virulence genes in *Fusarium oxysporum*. *BMC genomics, 22*(14), 119.

Schouten, A., van Baarlen, P., van Kan, J.A. (2008). Phytotoxic Nep1-like proteins from the necrotrophic fungus *Botrytis cinerea* associate with membranes and the nucleus of plant cells. *New Phytologist, 177*(2), 493-505.

Scott, J.W., & Jones, J.P. (1989). Monogenic resistance in tomato to *Fusarium oxysporum* f. sp. *lycopersici* race 3. *Euphytica*, *40*(1), 49-53.

Senthil-Kumar, M., & Mysore, K.S. (2013). Non-host resistance against bacterial pathogens: Retrospectives and prospects. *Annual Review of Phytopathology, 519*(1), 407-427.

Shi, G., Zhang, Z., Friesen, T.L., Raats, D., Fahima, T., Brueggeman, R.S., Lu, S., Trick, H.N., Liu, Z., Chao, W., Faris, J.D. (2016). The hijacking of a receptor kinase–driven pathway by a wheat fungal pathogen leads to disease. *Science advances*, *2*(10), e1600822.

Simbaqueba, J., Catanzariti, A.M., González, C., Jones, D.A. (2018). Evidence for horizontal gene transfer and separation of effector recognition from effector function revealed by analysis of effector genes shared between cape gooseberry and tomato-infecting *formae speciales* of *Fusarium oxysporum*. *Molecular Plant Pathology, 19*(10), 2302-2318.

Simons, G., Groenendijk, J., Wijbrandi, J., Reijans, M., Groenen, J., Diergaarde, P., van der Lee, T., Bleeker, M., Onstenk, J., de Both, M., Haring, M., Mes, J., Cornelissen, B.J.C., Zabeau, M., Vos, P. (1998). Dissection of the Fusarium *12* gene cluster in tomato reveals six homologs and one active gene copy. *The Plant Cell, 10*(6), 1055-1068.

Stall, R.E., & Walter, J.M. (1965). Selection and inheritance of resistance in tomato to isolates of races 1 and 2 of the Fusarium wilt organism. *Phytopathology, 55*(11), 1213-1215.

Stergiopoulos, I., & de Wit, P.J.G.M. (2009). Fungal effector proteins. *Annual Review of Phytopathology, 47*(1), 233-263.

Stotz, H.U., Thomson, J.G., Wang, Y. (2009). Plant defensins: defence, development and application. *Plant Signaling & Behavior, 4*(11), 1010-1012.

Summerell, B.A. (2019). Resolving *Fusarium*: Current status of the genus. *Annual Review of Phytopathology, 57*(25), 323-339.

Sun, X., Fang, X., Wang, D., Jones, D.A., Ma, L. (2022). Transcriptome analysis of *Fusarium*–tomato interaction based on an updated genome annotation of *Fusarium oxysporum* f. sp. *lycopersici* identifies novel effector candidates that suppress or induce cell death in *Nicotiana benthamiana*. *Journal of Fungi, 8*(7), 672.

Sun, X., Wang, Y., Wang, J., Liu, Y., Song, D., Fu, J., Jones, D., Wang, D., Liu, M., Ma, L. (2025). Comparative genomic analysis of *Fusarium oxysporum* f. sp. *lycopersici* reveals telomeric duplications of a lineage-specific region carrying *SIX8* and *PSL1* and genome-wide expansion of *Foxy* transposable elements. *International Journal of Biological Macromolecules, 297*, 139636.

Sweat, T.A., & Wolpert, T.J. (2007). Thioredoxin h5 is required for victorin sensitivity mediated by a CC-NBS-LRR gene in *Arabidopsis*. *The Plant Cell*, *19*(2), 673-687.

Takayama, S., & Isogai, A. (2005). Self-incompatibility in plants. *Annual Review of Plant Biology*, *56*(1), 467-489.

Takken, F.L.W., & Rep, M. (2010). The arms race between tomato and *Fusarium oxysporum*. *Molecular Plant Pathology, 11*(2), 309-314.

Thatcher, L.F., Gardiner, D.M., Kazan, K., Manners, J.M. (2012). A highly conserved effector in *Fusarium oxysporum* is required for full virulence on Arabidopsis. *Molecular Plant-Microbe Interactions, 25*(2),180-190.

Thomas, C.M., Jones, D.A., Parniske, M., Harrison, K., Balint-Kurti, P.J., Hatzixanthis, K., Jones, J.D. (1997). Characterisation of the tomato *Cf-4* gene for resistance to

Cladosporium fulvum identifies sequences that determine recognitional specificity in Cf-4 and Cf-9. *The Plant Cell, 9*(12), 2209-2224.

Thynne, E., Saur, I.M.L., Simbaqueba, J., Ogilvie, H.A., Gonzalez-Cendales, Y., Mead, O., Taranto, A., Catanzariti, A.M., McDonald, M.C., Schwessinger, B., Jones, D.A., Rathjen, J.P., Solomon, P.S. (2017). Fungal phytopathogens encode functional homologues of plant rapid alkalinization factor (RALF) peptides. *Molecular Plant Pathology, 18*(6), 811-824.

Tintor, N., Paauw, M., Rep, M., Takken, F.L.W. (2020). The root-invading pathogen *Fusarium oxysporum* targets pattern-triggered immunity using both cytoplasmic and apoplastic effectors. *New Phytologist, 227*(5), 1479-1492.

Underwood, W. (2012). The plant cell wall: a dynamic barrier against pathogen invasion. *Frontiers in Plant Science, 3*, 85.

Valenzuela-Ureta, J.G., Lawn, D.A., Heisey, R.F., Zamudionaloa, V. (1996). First report of *Fusarium* wilt race 3, caused by *Fusarium oxysporum* f. sp. *lycopersici*, of tomato in Mexico. *Plant Disease 80,* 105.

van Dam, P., & Rep, M. (2017). The distribution of *miniature impala* elements and *SIX* genes in the *Fusarium* genus is suggestive of horizontal gene transfer. *Journal of Molecular Evolution, 85*(1), 14-25.

van Dam, P., Fokkens, L., Ayukawa, Y., van der Gragt, M., Ter Horst, A., Brankovics, B., Houterman, P.M., Arie, T., Rep, M. (2017). A mobile pathogenicity chromosome in *Fusarium oxysporum* for infection of multiple cucurbit species. *Scientific reports*, *7*(1), 9042.

van den Burg, H.A., Harrison, S.J., Joosten, M.H., Vervoort, J., de Wit, P.J. (2006). *Cladosporium fulvum Avr4* protects fungal cell walls against hydrolysis by plant chitinases accumulating during infection. *Molecular Plant-Microbe Interactions*, *19*(12), 1420-1430.

Van der Burgh, A.M., & Joosten, M.H. (2019). Plant immunity: thinking outside and inside the box. *Trends in plant science*, *24*(7), 587-601.

van der Does, H.C., Duyvesteijn, R.G., Goltstein, P.M., van Schie, C.C., Manders, E.M., Cornelissen, B.J.C., Rep, M. (2008). Expression of effector gene SIX1 of *Fusarium oxysporum* requires living plant cells. *Fungal Genetics and Biology*, *45*(9), 1257-1264.

van der Does, H.C., Lievens, B., Claes, L., Houterman, P.M., Cornelissen, B.J.C., Rep, M. (2008). The presence of a virulence locus discriminates *Fusarium oxysporum* isolates causing tomato wilt from other isolates. *Environmental Microbiology, 10*(6), 1475-1485.

van Esse, H.P., Van't Klooster, J.W., Bolton, M.D., Yadeta, K.A., van Baarlen, P., Boeren, S., Vervoort, J., de Wit, P.J., Thomma, B.P. (2008). The *Cladosporium fulvum* virulence protein Avr2 inhibits host proteases required for basal defense. *Plant Cell, 20*(7),1948-1963.

VanEtten, H.D., Mansfield, J.W., Bailey, J.A., Farmer, E.E. (1994). Two classes of plant antibiotics: phytoalexins versus "phytoanticipins". *The Plant Cell, 6*(9), 1191-1192.

Vlaardingerbroek, I., Beerens, B., Schmidt, S.M., Cornelissen, B.J.C., Rep, M. (2016). Dispensable chromosomes in *Fusarium oxysporum* f. sp. *lycopersici*. *Molecular Plant Pathology*, *17*(9), 1455-1466.

Volin, R.B., & Jones, J.P. (1982). A new race of Fusarium wilt of tomato in Florida and sources of resistance. *Proceedings of the Florida State Horticultural Society, 95,* 268-270.

Wang, X., Xu, Y., Fan, H., Cui, N., Meng, X., He, J., Ran, N., Yu, Y. (2023). Research progress of plant nucleotide-binding leucine-rich repeat protein. *Horticulturae*, *9*(1), 122.

Weiberg, A., Wang, M., Lin, F.M., Zhao, H., Zhang, Z., Kaloshian, I., Huang, H.D., Jin, H. (2013). Fungal small RNAs suppress plant immunity by hijacking host RNA interference pathways. *Science, 342*(6154), 118-123.

Yadeta, K.A., & Thomma, B.P. (2013). The xylem as battleground for plant hosts and vascular wilt pathogens. *Frontiers in Plant Science, 4*, 97.

Yu, X.Q., Niu, H. Q., Liu, C., Wang, HL., Yin, W., Xia, X. (2024). PTI-ETI synergistic signal mechanisms in plant immunity. *Plant biotechnology journal*, *22*(8), 2113-2128.

Yuan, M., Ngou, B.P.M., Ding, P., Xin, X. F. (2021). PTI-ETI crosstalk: an integrative view of plant immunity. *Current Opinion in Plant Biology*, *62*, 102030.

Zipfel, C. (2014). Plant pattern-recognition receptors. *Trends in Immunology, 35*(7), 345-351.

Zipfel, C., Kunze, G., Chinchilla, D., Caniard, A., Jones, J.D., Boller, T., Felix, G. (2006). Perception of the bacterial PAMP EF-Tu by the receptor EFR restricts *Agrobacterium*-mediated transformation. *Cell, 125*(4), 749-760.

Zhang, S., Li, C., Si, J., Han, Z., Chen, D. (2022). Action mechanisms of effectors in plant-pathogen interaction. *International Journal of Molecular Sciences*, *23*(12), 6758.

Chapter 2: Attempts to identify the *Avr7* effector gene from *Fusarium oxysporum* f. sp. *lycopersici* enable the identification of *SIX6* as an inducer of plant cell death

2.1 Introduction

Many plant pathogens secrete small proteins known as effector proteins that facilitate colonisation of the host plant and interfere with its defence mechanisms (Gurlebeck et al., 2006; Kamoun, 2006, 2007; Hogenhout et al., 2009; Mitchum et al., 2013). Most fungal effectors are secreted proteins of less than 300 amino acids and many are cysteine-rich (De Wit et al., 2009). New tools have been developed in recent years based on machine learning to predict fungal effectors with a high accuracy, including EffectorP 1.0, 2.0, and 3.0 with 73%, 89% and 91.7% accuracy, respectively (Sperschneider et al., 2016, 2018; Sperschneider and Dodds, 2022).

The comparative genomic studies by Ma et al (2010) with *Fol*, *Fg* and *Fv* genomes have identified lineage-specific (LS) regions rich in transposable elements found only in the *Fol* genome and not in the *Fg* or *Fv* genomes. Further analysis revealed that these LS regions are primarily located on chromosome 14, which was designated as a pathogenicity chromosome due to its essential role in *Fol* virulence. This chromosome harbours several Secreted In Xylem (SIX) genes, which were first discovered by Rep et al. (2004) through proteomic analysis of xylem sap from *Fol*-infected tomato plants. Initially, only a few SIX proteins were identified, but subsequent studies by Houterman et al. (2007) and Schmidt et al. (2013) expanded this repertoire to 14 SIX proteins (SIX 1-14). These SIX proteins function as effectors that either promote fungal virulence or trigger resistance responses in tomato plants carrying the corresponding resistance genes, highlighting the critical role of chromosome 14 in host-pathogen interactions.

Among these 14 SIX genes, three were found to correspond to avirulence (*Avr*) genes *Avr1*, *Avr2* and *Avr3,* which are recognised by their corresponding resistance (*R*) genes *I*, *I-2* and *I-3* in tomato (Simons et al., 1998; Rep et al., 2004; Houterman et al., 2008, 2009; Catanzariti et al., 2015, 2017). An additional resistance gene designated *I-7,* encoding a leucine-rich repeat receptor protein (LRR-RP), has also been identified in tomato by Gonzalez-Cendales et al. (2016), but the corresponding *Fol Avr7* gene has not. The main purpose of the work described in this chapter was to try to identify *Avr7*. Previous to this work, Ann Maree Catanzariti and Pierrick Bru in the Jones Lab had screened *SIX1*(*Avr3*)*, SIX3*(*Avr2*)*, SIX4*(*Avr1*)*, SIX5, SIX8, SIX8H, SIX9, SIX10* and *SIX14* as *Avr7* candidates and concluded that none of them was *Avr7* (Catanzariti, unpublished; Bru, 2017). S*IX2, SIX6, SIX7, SIX11, SIX12* and *SIX13* remained to be tested and RNAseq data generated from RNA extracted from *Fol* infected tomato roots at 2 days post-inoculation had enabled the identification of several novel effector candidates (Jones,

unpublished) that could also be tested. This chapter reports the screening of the remaining *SIX* genes and two novel effector candidate genes because of their location on a pathogenicity chromosome 14 as *Avr*7 candidates by *Agrobacterium*-mediated co-expression with *I-7* in *Nicotiana benthamiana* and looking for cell death induction indicative of effector recognition.

2.2 Materials and Methods

2.2.1 Plant growth conditions

For all agroinfiltration experiments, *Nicotiana benthamiana* plants were cultivated in 10 cm pots containing Martin's potting mix (Martins Fertilizers, Australia). Plants were maintained at 21°C under a controlled light cycle of 16 hours of light and 8 hours of darkness in a growth chamber with 60-65% relative humidity.

2.2.2 Testing of *Avr7* candidates

Candidate genes were amplified by PCR (Polymerase Chain Reaction) and then ligated into a binary vector (pSL or pSLG) (Vector maps are shown in Appendices 2.1 and 2.2) for the transformation.

2.2.3 *Fol* genomic DNA extraction protocol

Fungal biomass was produced by growing cultures in potato dextrose broth (PDB). The resulting mycelia were harvested by passing the culture through four sheets of Miracloth and subsequently allowed to dry in air. Approximately 200 mg of the dried fungal tissue was flash-frozen with liquid nitrogen and promptly crushed using a mortar and pestle. The ground material was combined with 1 ml of extraction buffer (containing 200 mM Tris-Cl [pH 8.0], 50 mM EDTA [pH 8.0], 200 mM NaCl, 2% w/v sodium N-laurylsarcosinate, and 0.1% v/v 2-mercaptoethanol) and gently homogenised. This mixture was transferred to 1.5 ml microcentrifuge tubes and incubated at 65°C for 30 minutes. After cooling to ambient temperature, the samples were mixed with an equivalent volume of phenol:chloroform:isoamyl alcohol (25:24:1) until homogenised, followed by centrifugation at 6,000 g for 10 minutes. The upper aqueous phase was carefully collected and subjected to a second extraction with an equal volume of chloroform:isoamyl alcohol (24:1). After gentle mixing and centrifugation under identical conditions (6,000 g, 10 minutes), the resulting DNA precipitation was initiated by adding an equal volume of isopropanol to the collected supernatant. To maximise DNA

recovery, the solution was stored at 20°C for 1 hour. The high molecular weight DNA, visible as a white precipitate, was collected by centrifugation at 6,000 g for 10 minutes. The supernatant was discarded, and the DNA pellet was purified through multiple washes with 70% (v/v) ethanol. Finally, the DNA was air dried to remove residual ethanol and reconstituted in sterile, deionised water (Jaime Simbaqueba, PhD thesis, The Australian National University, Australia, 2017).

2.2.4 Total RNA extraction and cDNA synthesis

Total RNA was extracted from *Fusarium oxysporum*-infected tomato roots using the ISOLATE II RNA Plant Kit (Bioline, Cat # BIO-52077), following the manufacturer's instructions. Complementary DNA (cDNA) was synthesised from the extracted RNA using the SensiFAST™ cDNA Synthesis Kit (Bioline, Cat # BIO-65054), according to the protocol provided by the manufacturer.

2.2.5 Ligation Independent Cloning (LIC)

A summary of the LIC procedure is shown in Figure 2.1 and described in detail in sections 2.2.5.1 to 2.2.5.4.

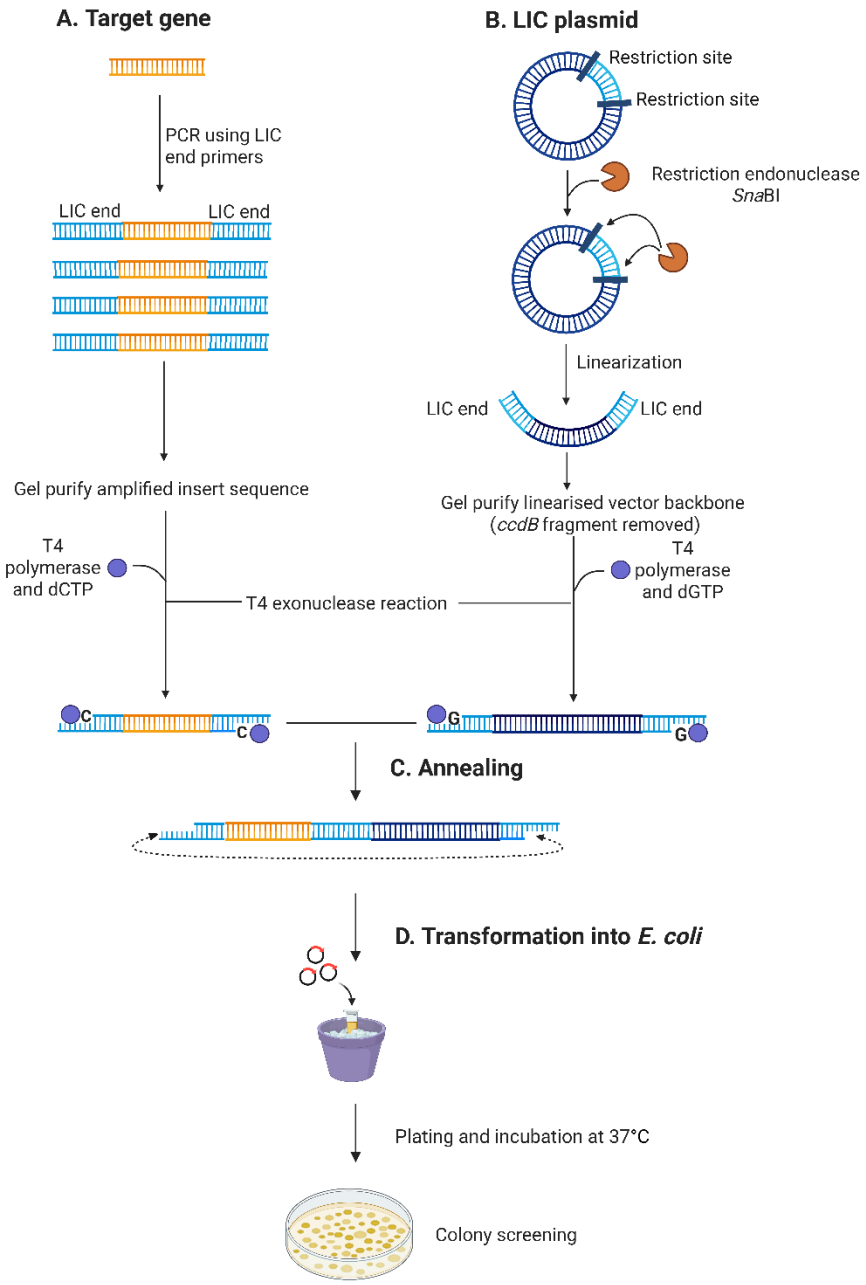

Figure 2.1 Graphic representation of Ligation Independent Cloning (LIC).

(A) PCR amplification and gel purification of desired insert DNA fragments, followed by T4 DNA polymerase treatment in the presence of dCTP to generate a 15-nucleotide vector-complementary overhang. **(B)** *Sna*BI digestion and gel purification of vector, followed by T4 DNA polymerase treatment in the presence of dGTP to generate a 15-nucleotide overhang. **(C)** Annealing of complementary insert and vector overhangs. **(D)** Transformation of the annealed vector and insert into *E. coli*. The illustration was generated using BioRender (https://app.biorender.com).

2.2.5.1 Amplification of target sequences

Genomic DNA (gDNA) or complementary DNA (cDNA) was used to amplify target DNA sequences. Genomic DNA was utilised for target sequences lacking introns, whereas cDNA, synthesised from RNA extracted from *Fol*-infected tomato roots, was used for targets containing introns. PCR was carried out using 8 µl of 5X Phusion HF buffer (NEB, Cat # M0530S), 2 µl of cDNA or gDNA (10 ng), 8 µl 2 mM dNTPs, 1 µl each of 10 µM forward and reverse insert-specific LIC primer (Appendix 2.3), 0.4 µl of Phusion High-Fidelity DNA Polymerase (NEB, Cat # M0530S), in a final volume of 40 µl made up using nuclease-free water. PCRs were heated to 98°C for 30 s, followed by 30 cycles of template denaturation at 98°C for 10 s, primer annealing at 56°C for 20 s and product extension at 72°C for 10 s and followed by a final extension of 72°C for 10 min before holding at 4°C. The entire reaction was then analysed by electrophoresis on a 1.2% (w/v) agarose gel containing RedSafe Nucleic Acid Stain (iNtRON Biotechnology, Cat # 21141). Desired PCR products were purified from gels using a Zymoclean Gel DNA recovery kit (Zymo Research, Cat # D40001). Purified PCR products were then used in LIC as described in sections 2.2.5.3 and 2.2.5.4 and shown in Figure 2.1A and C.

2.2.5.2 Preparation of the LIC Vector

The LIC vector (pSL or pSLG) was cut with *Sna*BI to remove the *ccd*B gene and generate a linearised plasmid with blunt ends. The digestion reaction was performed in a 15 µl volume containing 1 µg vector, 1.5 µl of 10X CutSmart buffer (NEB), and 1 µl of *Sna*BI (NEB, Cat # R0130S) and incubated for 1 h at 37°C. The digestion reaction was analysed by electrophoresis on a 0.8% (w/v) agarose gel and the linearised vector was purified from the gel using a Zymoclean Gel DNA Recovery Kit (Zymo Research Cat # D40001). The purified linearised vector was then used in LIC as described in sections 2.2.5.3 and 2.2.5.4 and shown in Figures 2.1B and C.

2.2.5.3 T4 DNA polymerase treatment

T4 DNA polymerase treatment allows the formation of 15 nucleotide overlaps between the vector and the insert owing to its 3' to 5' exonuclease activity and the inclusion of deoxyguanosine triphosphate (dGTP) to the vector reaction or deoxycytidine triphosphate (dCTP) to the insert reaction to prevent the removal of more than 15 nucleotides (Figure 2.1). Reactions were performed using 200 ng of vector or 50 ng of insert, 0.5 µl of T4 DNA

polymerase (NEB, Cat # M0203S), 1 µl of 10X NEB buffer 2.1 (NEB, Cat # M0203S), 1 µl of 10X BSA (NEB, Cat # B9000), 1 µl of 25 mM of dGTP (NEB, Cat # N0442S for vector reactions or dCTP (NEB, Cat # N0356S) for insert reactions in a final volume of 10 µl made up using nuclease-free water. Reactions were incubated at 22°C for 30 minutes and then incubated at 75°C for 20 min to inactivate the enzyme.

2.2.5.4 Annealing

Annealing of vector and insert overlaps was performed in a 10 µl reaction volume with a molar ratio of 3:1 of insert to vector (Figure 2.1C). The reaction was incubated at 22°C for 30 min and then either stored at 4°C or used immediately for transformation into *E. coli*.

2.2.6 *E. coli* transformation

Competent cells of *E. coli* strain DH5α were made in-house using the protocol of Behle (2018). The LIC annealing reaction was added to 50 µl of competent cells which were then incubated on ice for 30 min, heat shocked at 42°C for 30 sec in a water bath and incubated on ice for 2 min. Then, 500 µl of Lysogeny Broth (LB; 10 g tryptone, 5 g yeast extract, 5 g NaCl per 1000 ml media) was added and the cells were incubated at 37°C for 1 h with shaking at 200 rpm. Finally, 200 µl of the transformed cells were plated on LBA (LB with 15 g/L agar), supplemented with 50 µg/ml of Kanamycin and incubated overnight at 37°C (Figure 2.1D).

2.2.7 Colony screening

Colonies of putative transformants were screened for the presence of the desired insert using PCR with insert-specific primers (Appendix 2.3). Cells from each colony were suspended in 40 µl nuclease-free water. PCR was performed using 2 µl of 5X MyTaq Red Reaction Buffer (Bioline, Cat # BIO-21108), 0.5 µl of 10 µM forward and reverse insert-specific primer (Appendix 2.3), 3 µl of the cell suspension and 0.5 µl of MyTaq DNA Polymerase (Bioline, Cat # BIO-21108) in a final volume of 10 µl made up using nuclease-free water. Cycling conditions were as per the manufacturer's recommendation. The conditions include heating at 95°C for 2 min, followed by 30 cycles at 95°C for 15 sec for denaturation, 54°C for 15 sec for primer annealing and 72°C for 10 sec before holding at 4°C. The remaining colony suspension, which produced a band of the right size, was used to inoculate LB with Kanamycin (50 µg/ml) and grown overnight in a 37°C shaking incubator. FavorPrep Plasmid DNA Extraction Mini Kit (Favorgen, Cat # FAPDE300) was then used to isolate the plasmid DNA from the bacterial

culture. The concentration of the plasmid DNA was then measured with a SpectraMax QuickDrop Spectrophotometer (Molecular Devices, LLC, USA).

2.2.8 DNA sequencing

For DNA sequencing, 15 µl of plasmid (100 ng/µl) along with 15 µl of each forward and reverse primer (1.6 pmol/µl) were sent to the ANU Biomolecular Resource Facility (BRF) for sequencing. All binary vector constructs were checked to ensure that no PCR errors had occurred and, for pSLG vectors, that the inserted gene was in frame with the GFP tag.

2.2.9 Transformation of *Agrobacterium*

Transformation of plasmid DNA into *Agrobacterium* was done using electrocompetent cells of *Agrobacterium* strain GV3101 (containing pMP90 and the pSOUP helper plasmid) that were prepared in-house using the protocol described by Weise (2013). Electrocompetent cells were taken from the -80°C freezer and thawed on ice, and 20 µl of electrocompetent cells were added to a pre-cooled microcentrifuge tube containing 100 ng of plasmid in 40 µl of nuclease-free water. The entire reaction mixture was then transferred to a pre-cooled electroporation cuvette with a 0.2 cm gap (Bio-Rad) and electroporated using a MicroPulser Electroporator (Bio-Rad) with 2.5 kV electromotive force, 200 Ω resistance and 25 µF capacitance. Immediately after electroporation, 500 µl LB was added to the cuvette and the entire reaction mixture was then transferred to a microcentrifuge tube and incubated at 28°C with shaking at 250 rpm for 2 h. Aliquots of 50 to 100 µl were then plated on LBA with Kanamycin (50 µg/ml), Gentamycin (25 µg/ml) and Rifampicin (50 µg/ml), and incubated at 28°C for 2 days. Colonies that appeared after 2 days were screened by colony PCR as described in section 2.2.7.

2.2.10 *Agrobacterium*-mediated gene expression

Binary vector constructs in *Agrobacterium* strain GV3101 (containing pMP90 and the pSOUP helper plasmid) were used for expression of proteins in *N. benthamiana* leaves as described by Ma et al. (2012). A single transformed colony was re-streaked on LB agar containing Kanamycin (50 µg/ml), Gentamycin (25 µg/ml) and Rifampicin (50 µg/ml) and grown for 1 to 2 days at 28°C. Cells were then scraped from the LB agar and resuspended in infiltration medium (10 mM MES pH 5.6, 10 mM $MgCl_2$ and 200 µM acetosyringone) to an OD at 600 nm of 1.0 and kept at room temperature in the dark for 2 hours before infiltrating into *N. benthamiana* leaves. Four to five-week-old *N. benthamiana* plants were used for agroinfiltration. Two to three leaves per plant and four spots on each leaf were infiltrated with

Agrobacterium. A needle was used to prick the abaxial side of the leaf, and then a 1 ml syringe without a needle was used to infiltrate the *Agrobacterium* suspension. Single strains of *Agrobacterium*, such as the *Avr7* candidate and *MLA10-CC,* were infiltrated without further dilution. For co-infiltration experiments, strains of *Agrobacterium,* such as *I-7* and *Avr7* candidate or *I* and *Avr1*, were mixed in a 1:1 ratio. Infiltrated plants were kept at 25°C in a growth room with a 16-hour photoperiod at a light intensity of 250 µmol m^{-2} s^{-1} and relative humidity of 60-65% for 8 to 10 days.

2.3. Results

2.3.1 Co-expression of candidate *Avr7* genes with *I-7* in *N. benthamiana* leaves

The genes *SIX2*, *SIX6*, *SIX7*, *SIX11*, *SIX12* and *SIX13* were selected for analysis based on their characteristic properties as secreted in xylem (SIX) proteins. These proteins are distinguished by their cysteine-rich composition and relatively compact structure, with each comprising fewer than 300 amino acid residues. While the genes *FOXG_22509* and *FOXG_17276* were incorporated into the analysis based on their genomic localisation to chromosome 14, which has been characterised as a pathogenicity chromosome. All *Avr7* candidate genes were PCR amplified from *Fol* gDNA (*SIX2*, *SIX11, SIX12, FOXG_22509* and *FOXG_17276*) or cDNA (*SIX6, SIX7* and *SIX13*) and cloned into pSL (Appendix 2.1) and pSLG (Appendix 2.2) binary vectors via LIC as described in section 2.2.5 (Figure 2.1). DNA sequencing of the genes in these constructs (Figure 2.2) showed there were no PCR errors and that the coding sequences cloned into pSLG constructs were in-frame with the coding sequence of the C-terminal GFP tag. The binary vectors were then transformed into *Agrobacterium tumefaciens* strain GV3101 (containing pMP90 and the pSOUP helper plasmid) as described in section 2.2.9. *Agrobacterium* transformants were then used for *in planta* expression of the *Avr7* candidates either alone or together with *I-7* via agroinfiltration as described in section 2.2.10. The pL-*I-7* binary vector constructed by Gonzalez-Cendales et al. (2016) was used for expression of *I-7* (Figure 2.2).

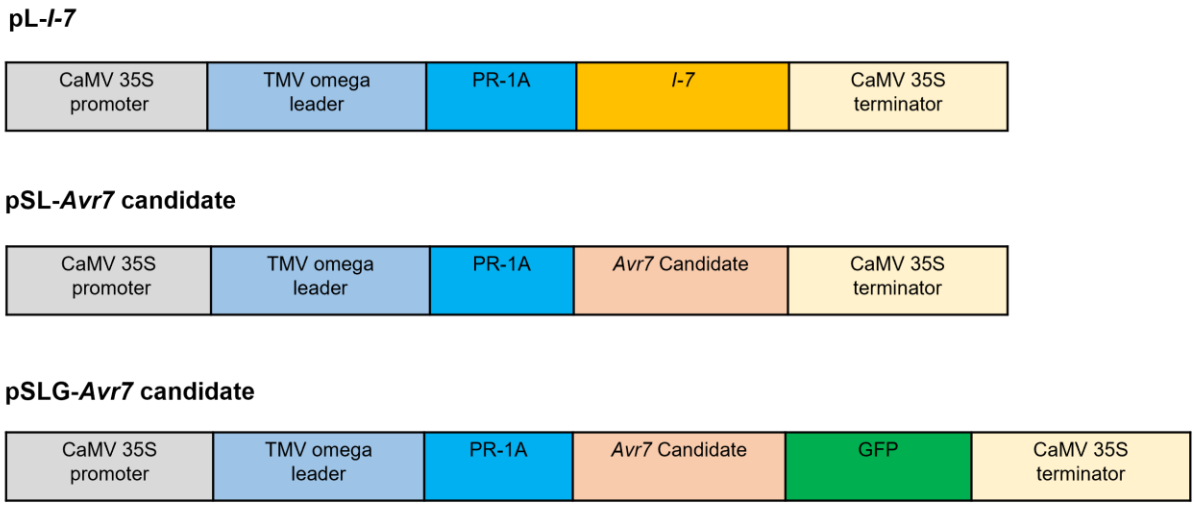

Figure 2.2 Schematic representation of the pL-*I-7* vector and *Avr7*-candidate constructs in pSL and pSLG.

Two positive controls for *R*-gene-related cell-death induction were used in these experiments. A binary vector plasmid enabling *in planta* expression of the autoactive MLA10 CC domain was used as one positive control for cell death induction (Bai et al., 2012). Binary vector plasmids pL-*I* and pL-*Avr1* were used in co-agroinfiltration experiments as a positive control for cell death induced by the co-expression of I and Avr1 (Catanzariti et al., 2017).

Two to three leaves per plant and four spots on each leaf were infiltrated as follows. 1) infiltrated with *Agrobacterium* containing the pSL or pSLG construct, 2) co-infiltrated with equal amounts of *Agrobacterium* containing the pSL or pSLG construct and *Agrobacterium* containing the *I-7* construct, 3) infiltrated with *Agrobacterium* containing the *MLA10-CC* construct, 4) co-infiltrated with equal amounts of *Agrobacterium* containing the *Avr1* construct and *Agrobacterium* containing the *I* construct. Infiltrations were carried out in two different patterns A and B to help avoid position effects. Whilst the positions of the *MLA10* and *I/Avr1* control infiltrations remained the same, the positions of the *Avr7* candidate infiltration and the *Avr7* candidate/*I-7* co-infiltration were interchanged (Figure 2.3).

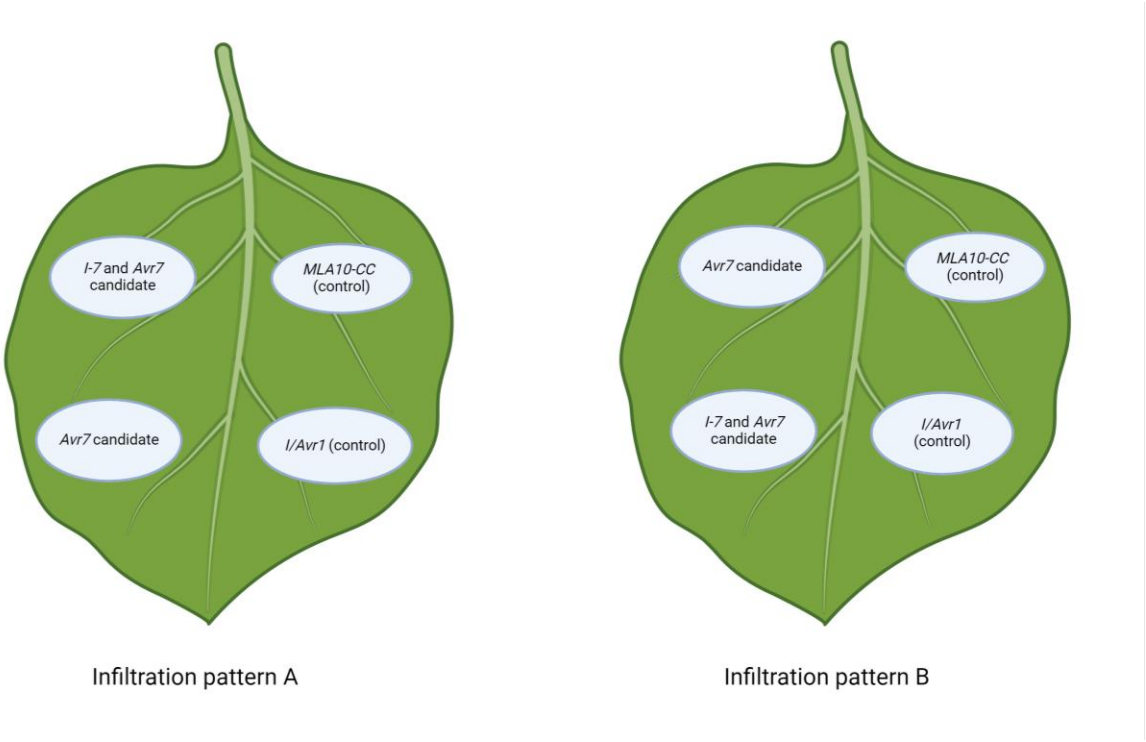

Figure 2.3 Patterns of agroinfiltration used in *N. benthamiana* leaves.

To help avoid any position effects, two different patterns (A and B) were used in agroinfiltration experiments testing *Avr7* candidates for possible cell-death induction in the presence of *I-7*. The illustration was generated using BioRender (https://app.biorender.com).

Representative results of these infiltration experiments are shown in Figure 2.4 and results from replicate experiments are shown in Appendix 2.4. Whilst the *MLA10-CC* and *I/Avr1* positive controls consistently showed cell death, no cell death was observed when *SIX2, SIX7, SIX11, SIX12, SIX13, FOXG_22509* or *FOXG_17276* were expressed either alone or together with *I-7* (Figure 2.4 and Appendix 2.4). These results suggest that none of these candidates was *Avr7.*

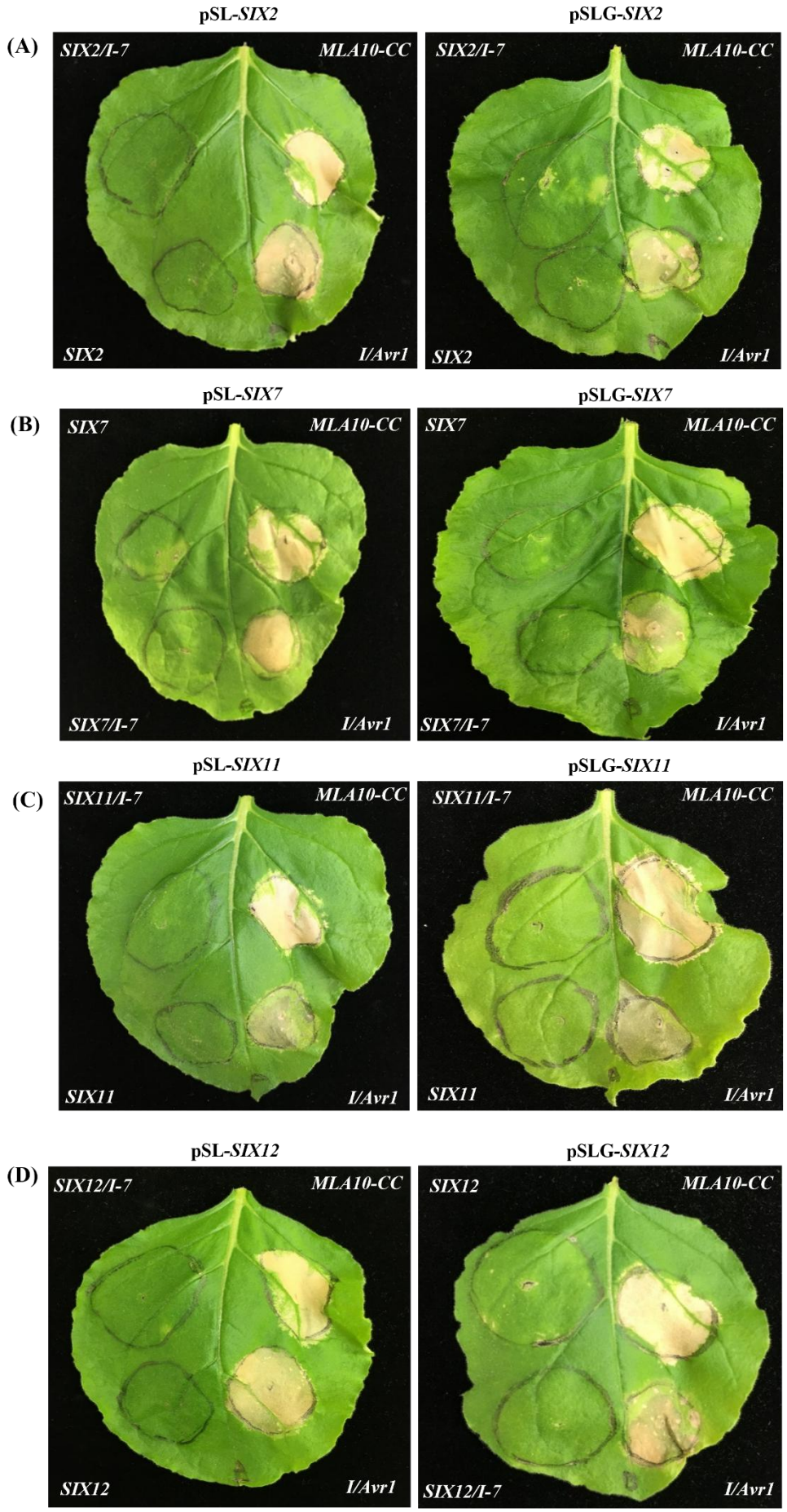
pSL-SIX2
pSLG-SIX2
(A)
SIX2/I-7
MLA10-CC
SIX2
I/Avr1
SIX2/I-7
MLA10-CC
SIX2
I/Avr1
pSL-SIX7
pSLG-SIX7
(B)
SIX7
MLA10-CC
SIX7/I-7
I/Avr1
SIX7
MLA10-CC
SIX7/I-7
I/Avr1
pSL-SIX11
pSLG-SIX11
(C)
SIX11/I-7
MLA10-CC
SIX11
I/Avr1
SIX11/I-7
MLA10-CC
SIX11
I/Avr1
pSL-SIX12
pSLG-SIX12
(D)
SIX12/I-7
MLA10-CC
SIX12
I/Avr1
SIX12
MLA10-CC
SIX12/I-7
I/Avr1

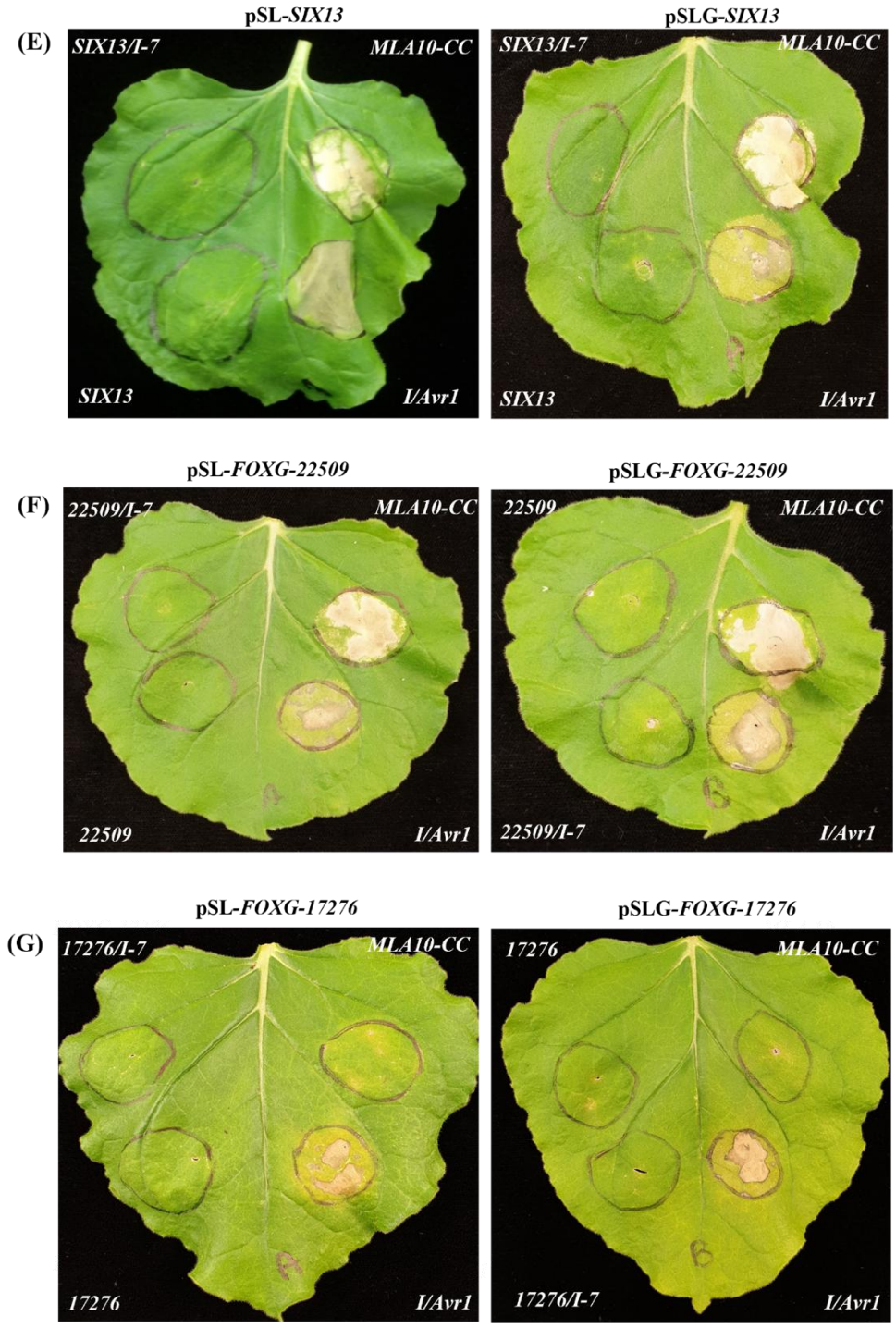

Figure 2.4 Co-agroinfiltration of *Avr7* candidates and *I-7* in *N. benthamiana* leaves.

Co-agroinfiltration of pSL-*I-7* and *Avr7* candidate genes in pSL or pSLG constructs in *N. benthamiana* leaves. Leaves of each plant were also agroinfiltrated with *Avr7* candidate gene constructs alone as a negative control and a *MLA10-CC* construct as a positive control. Leaves were also co-agroinfiltrated with pL-*I* and pL-*Avr1* as an additional positive control. **(A)** *SIX2*, **(B)** *SIX7*, **(C)** *SIX11*, **(D)** *SIX12*, **(E)** *SIX13*, **(F)** *FOXG_22509* and **(G)** *FOXG_17276* Photographs were taken 8 days after infiltration.

Although none of the above-mentioned *Avr7* candidates showed cell death when agroinfiltrated alone or co-agroinfiltrated with *I-7*, *SIX6* showed cell death when agroinfiltrated alone and when it was co-agroinfiltrated with *I-7* (Figure 2.5 and Appendix 2.5). This surprising result does not exclude *Fol SIX6* as a candidate for *Avr7* but suggests there is a pathogenicity target or receptor in *N. benthamiana* that is targeted by or recognises *Fol SIX6* to trigger a cell death response.

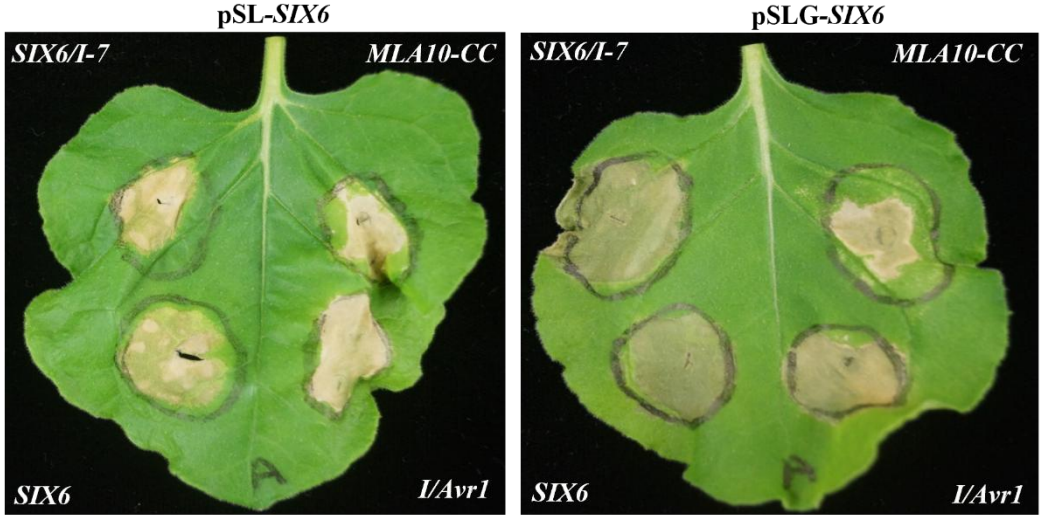

Figure 2.5 Agroinfiltration of *I-7* and *Fol SIX6* in *Nicotiana benthamiana* leaves.

Co-agroinfiltration of *I-7* with pSL- *SIX6* or pSLG-*SIX6* gene in *N. benthamiana* leaves. Leaves of each plant were also agroinfiltrated with pSL-*SIX6* or pSLG-*SIX6* alone as a negative control and *MLA10-CC* as a positive control. Leaves were also co-agroinfiltrated with pL-*I* and pL-*Avr1* as an additional positive control. Photographs were taken eight days after infiltration.

2.4 Discussion

2.4.1 Testing of seven *Avr7* candidates has not enabled the identification of *Avr7*

The *I-7* resistance gene from tomato was identified by Gonzalez-Cendales et al. (2016), and according to Flor's gene-for-gene hypothesis (Flor, 1971), there should be a corresponding *Avr7* gene in the pathogen. Previous work by Ann-Maree Catanzariti and Pierrick Bru in the Jones Lab showed that *SIX1* (*Avr3*), *SIX3* (*Avr2*), *SIX4* (*Avr1*), *SIX5, SIX8, SIX8H, SIX9, SIX10* and *SIX14* were not *Avr7* (Catanzariti, unpublished; Bru, 2017). In the work reported here, seven additional *Avr7* candidate genes comprising *SIX2, SIX7, SIX11, SIX12, SIX13*, *FOXG_22509* and *FOXG_17276* were found not to induce cell death in *N. benthamiana* leaves when co-agroinfiltrated with *I-7*. These results suggest that none of these genes corresponds to *Avr7*. However, no tests were carried out to determine whether these *I-7* or the candidate *Avr7*

genes were transcribed or translated following agroinfiltration. Originally, RT-PCR experiments were planned to check for transcript production following agroinfiltration, and protein gel blot experiments were planned with anti-GFP antibodies to test for protein production following agroinfiltration with pSLG constructs. However, the findings with *Fol SIX6,* discussed below, resulted in a change in project direction and these tests were never carried out. In the absence of results from these tests, the finding that none of the candidate genes tested correspond to *Avr7* cannot be regarded as conclusive.

Many other effectors and effector candidates have been identified in *Fol* that could be tested as *Avr7* candidates, including *Fol Ave1*, *RALF-B*, and *PSE1,* described in section 1.3.3. In a recent study, Sun et al (2022) used deep RNA sequencing of tomato infected with a *Fol* race 2 isolate to identify 40 candidate effector genes that were highly upregulated during *Fol* infection, including 14 that had already been tested as *Avr7* candidates, leaving 26 candidate effectors that could be tested in future including *PSL2*, *FOXGR_015522* and *FOXGR_015533* located on pathogenicity chromosome 14 (Table 2.1).

Table 2.1. List of effector candidates encoding small, secreted mostly cysteine-rich proteins, excluding those already tested as *Avr7* candidates, that had transcript per million values exceeding or equal to that of *SIX13* during *Fol* infection (Sun et al., 2022).

Gene Name	Lineage Specific	Protein Length	Cysteine Residues	Protein Domain/Homology
PSL1	YES	111	9	PSE1 homologue
PSL2	YES	106	9	PSE1 homologue
FOXGR_015522	YES	79	9	
FOXGR_015533	YES	114	3	
FOXG_10949	NO	107	8	Hydrophobin
FOXG_10950	NO	152	9	Hydrophobin
FOXG_11033	NO	226	0	
FOXG_05750	NO	265	12	LysM domain x2
FOXG_05755	NO	157	3	
FOXG_18699	NO	96	10	
FOXGR_007323	NO	86	0	
FOXG_10672	NO	198	13	PAN/Apple domain x2
FOXG_04863	NO	300	8	
FOXG_04805	NO	132	8	
FOXG_02829	NO	149	16	Glucanase
FOXGR_021626	NO	294	3	
FOXG_08899	NO	148	1	
FOXGR_010884	NO	264	0	
FOXG_11745	NO	183	4	
FOXG_10138	NO	261	2	Peptidase G1 family
FOXGR_025639	NO	61	2	
FOXG_16600	NO	164	0	
FOXG_13233	NO	131	4	Ribonuclease F1
FOXG_13248	NO	248	6	Trypsin
FOXG_14607	NO	275	7	Metalloprotease MEP1
FOXG_14684	NO	168	14	

Other approaches, such as chemical mutagenesis, could also be utilised to identify *Avr7*. Chemical mutagenesis could be used to induce deletion mutants of *Fol* that could be screened for pathogenicity on otherwise-resistant tomato plants carrying *I-7, i.e.* for loss of *Avr7*. Genome sequencing of independent mutants could then be used to identify candidate genes deleted or mutated in all or most mutants (excluding mutations in genes known to control effector gene expression). These candidates could then be tested for the ability to induce *I-7*-dependent cell death in *N. benthamiana* as described above. A similar approach was used by Li et al. (2020) to identify candidate avirulence genes in stripe rust (*Puccinia striiformis* f. sp. *tritici*).

2.4.2 *Fol SIX6* is an effector that causes cell death

The *Fol SIX6* gene induced cell death when co-agroinfiltrated with *I-7* but also induced cell death when agroinfiltrated alone (Figure 2.5). This was a surprising finding that, despite not excluding *SIX6* as an *Avr7* candidate, raised many questions about SIX6 function. Previous work on *Fol SIX6* showed that it contributed to pathogen virulence (Gawehns et al., 2014). However, the finding that SIX6 induces cell death makes a role in suppression of *Avr2*-induced cell death in *I-2* tomato plants, as proposed by Gawehns et al. (2014), untenable. Consequently, the role *SIX6* plays in pathogen virulence became unclear. The remainder of the work described in this thesis was aimed at obtaining a better understanding of *Fol* SIX6 function and the role, if any, that SIX6-induced cell death might play in *Fol* pathogenicity.

References

Bai, S., Liu, J., Chang, C., Zhang, L., Maekawa, T., Wang, Q., Xiao, W., Liu, Y., Chai, J., Takken, F.L.W., Schulze-Lefert, P., Shen, Q.H. (2012). Structure-function analysis of barley NLR immune receptor MLA10 reveals its cell compartment specific activity in cell death and disease resistance. *PLoS Pathogens, 8*(6), e1002752.

Behle, A. (2018). Preparation of chemically competent cells. *protocols.io* https://dx.doi.org/10.17504/protocols.io.n8mdhu6.

Bru, P. (2017). Identification of the *Avr7* effector from *Fusarium oxysporum* f. sp. *lycopersici* corresponding to the resistance gene *I-7* from the tomato and characterisation of the resistance gene *I* from tomato. (Master's thesis, The Australian National University, Australia).

Catanzariti, A.M., Do, H.T., Bru, P., de Sain, M., Thatcher, L.F., Rep, M., Jones, D.A. (2017). The tomato *I* gene for Fusarium wilt resistance encodes a typical leucine-rich repeat receptor-like protein whose function is nevertheless dependent on SOBIR1 and SERK3/BAK1. *Plant Journal, 89*(6), 1195-1209.

Catanzariti, A.M., Lim, G.T.T., Jones, D.A. (2015). The tomato *I-3* gene: a novel gene for resistance to Fusarium wilt disease. *New Phytologist, 207*(1), 106-118.

De Wit, P.J.G.M., Mehrabi, R., van den Burg, H.A., Stergiopoulos, I. (2009). Fungal effector proteins: past, present and future. *Molecular Plant Pathology, 10*(6), 735-747.

Flor, H.H. (1971). Current status of gene for gene concept. *Annual Review of Phytopathology, 9*, 275-296.

Gawehns, F., Houterman, P.M., Ichou, F.A., Michielse, C.B., Hijdra, M., Cornelissen, B.J., Rep, M., Takken, F.L.W. (2014). The *Fusarium oxysporum* effector Six6 contributes to virulence and suppresses I-2-mediated cell death. *Molecular Plant Microbe Interaction, 27*(4), 336-348.

Gonzalez-Cendales, Y., Catanzariti, A.M., Baker, B., McGrath, D.J., Jones, D.A. (2016). Identification of I-7 expands the repertoire of genes for resistance to Fusarium wilt in tomato to three resistance gene classes. *Molecular Plant Pathology, 17*(3), 448-463.

Gurlebeck, D., Thieme, F., Bonas, U. (2006). Type III effector proteins from the plant pathogen *Xanthomonas* and their role in the interaction with the host plant. *Journal of Plant Physiology, 163*(3), 233-255.

Hogenhout, S.A., van der Hoorn, R.A.L., Terauchi, R., Kamoun, S. (2009). Emerging concepts in effector biology of plant-associated organisms. *Molecular Plant-Microbe Interaction*, *22*(2), 115-122.

Houterman, P.M., Cornelissen, B.J., Rep, M. (2008). Suppression of plant resistance gene-based immunity by a fungal effector. *PLoS Pathogen, 4*(5), e1000061.

Houterman, P.M., Ma, L., van Ooijen, G., de Vroomen, M.J., Cornelissen, B.J., Takken, F.L. W., Rep, M. (2009). The effector protein Avr2 of the xylem-colonizing fungus *Fusarium oxysporum* activates the tomato resistance protein I-2 intracellularly. *Plant Journal, 58*(6), 970-978.

Houterman, P.M., Speijer, D., Dekker, H.L., de Koster, C.G. (2007). Cornelissen, B.J.C., Rep, M. The mixed xylem sap proteome of *Fusarium oxysporum*-infected tomato plants. *Molecular Plant Pathology, 8*(2), 215-221.

Kamoun, S. (2006). A catalogue of the effector secretome of plant pathogenic oomycetes. *Annual Review of Phytopathology, 44*(1), 41-60.

Kamoun, S. (2007). Groovy times: filamentous pathogen effectors revealed. *Current Opinion in Plant Biology, 10*(4), 358-365.

Li, Y., Xia, C., Wang, M., Yin, C., Chen, X. (2020). Whole-genome sequencing of *Puccinia striiformis* f. sp. *tritici* mutant isolates identifies avirulence gene candidates. *BMC Genomics, 21*(1), 247.

Ma, L.J., van der Does, H.C., Borkovich, K.A., Coleman, J.J., Daboussi, M.J., Di Pietro, A., Dufresne, M., Freitag, M., Grabherr, M., Henrissat, B., Houterman, P.M., Kang, S., Shim, W.B., Woloshuk, C., Xie, X., Xu, J.R., Antoniw, J., Baker, S.E., Bluhm, B.H., Breakspear, A., Brown, D.W., Butchko, R.A.E., Chapman, S., Coulson, R., Coutinho, P.M., Danchin, E.G.J., Diener, A., Gale, L.R., Gardiner, D.M., Goff, S., Hammond-Kosack, K.E., Hilburn, K., Hua-Van, A., Jonkers, W., Kazan, K., Kodira, C.D., Koehrsen, M., Kumar, L., Lee, Y.H., Li, L., Manners, J.M., Miranda-Saavedra, D.,

Mukherjee, M., Park, G., Park, J., Park, S.Y., Proctor, R.H., Regev, A., Ruiz-Roldan, M.C., Sain, D., Sakthikumar, S., Sykes, S., Schwartz, D.C., Turgeon, B.G., Wapinski, I., Yoder, O., Young, S., Zeng, Q., Zhou, S., Galagan, J., Cuomo, C.A., Kistler, H.C., Rep, M. (2010). Comparative genomics reveals mobile pathogenicity chromosomes in *Fusarium*. *Nature, 464*(7287), 367-373.

Mitchum, M.G., Hussey, R.S., Baum, T.J., Wang, X., Elling, A.A., Wubben, M., Davis, E.L. (2013). Nematode effector proteins: an emerging paradigm of parasitism. *New Phytologist, 199*(4), 879-894.

Rep, M., Van Der Does, H.C., Meijer, M., Van Wijk, R., Houterman, P.M., Dekker, H.L., De Koster, C.G., Cornelissen, B.J.C. (2004). A small, cysteine-rich protein secreted by *Fusarium oxysporum* during colonization of xylem vessels is required for I-3-mediated resistance in tomato. *Molecular Microbiology, 53*(5), 1373-1383.

Schmidt, S.M., Houterman, P.M., Schreiver, I., Ma, L., Amyotte, S., Chellappan, B., Boeren, S., Takken, F.L.W., Rep, M. (2013). MITEs in the promoters of effector genes allow prediction of novel virulence genes in *Fusarium oxysporum*. *BMC Genomics 14*, 119.

Simbaqueba, J. (2017). Analysis of *Fusarium oxysporum* effectors shared between strains that infect cape gooseberry and tomato. (PhD thesis, The Australian National University, Australia).

Simons, G., Groenendijk, J., Wijbrandi, J., Reijans, M., Groenen, J., Diergaarde, P., Van der Lee, T., Bleeker, M., Onstenk, J., de Both, M., Haring, M., Mes, J., Cornelissen, B., Zabeau, M., Vos, P. (1998). Dissection of the Fusarium *I2* gene cluster in tomato reveals six homologs and one active gene copy. *Plant Cell, 10*(6),1055-1068.

Sperschneider, J., & Dodds, P.N. (2022). EffectorP 3.0: prediction of apoplastic and cytoplasmic effectors in fungi and oomycetes. *Molecular Plant Microbe Interaction, 35*(2), 146-156.

Sperschneider, J., Dodds, P.N., Gardiner, D.M., Singh, K.B., Taylor, J.M. (2018). Improved prediction of fungal effector proteins from secretomes with EffectorP 2.0. *Molecular Plant Pathology, 19*(9), 2094-2110.

Sperschneider, J., Gardiner, D.M., Dodds, P.N., Tini, F., Covarelli, L., Singh, K.B., Manners, J.M., Taylor, J.M. (2016). EffectorP: predicting fungal effector proteins from secretomes using machine learning. *New Phytologist, 210*(2), 743-761.

Sun, X., Fang, X., Wang, D., Jones, D.A., Ma, L. (2022). Transcriptome analysis of *Fusarium*-tomato interaction based on an updated genome annotation of *Fusarium oxysporum* f. sp. *lycopersici* identifies novel effector candidates that suppress or induce cell death in *Nicotiana benthamiana*. *Journal of Fungi, 8*(7), 672.

Weise, S. (2013). *Agrobacterium* transformation and competent cell preparation. *Methods*, *Michigan State University*, 1-3.

Appendix 2.1 Map of pSL vector used in this study.

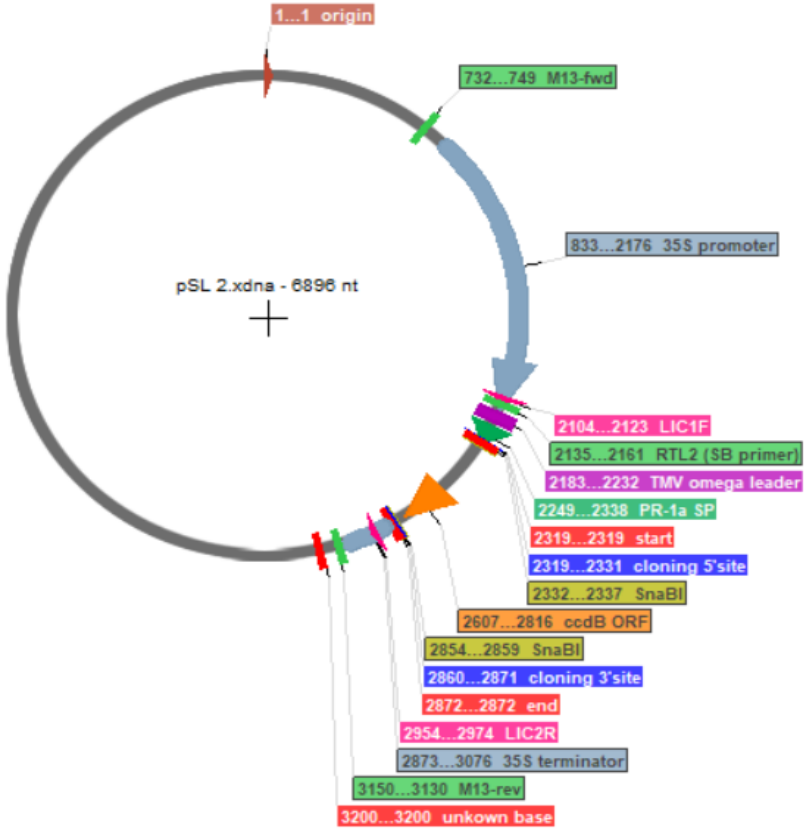

Appendix 2.2 Map of pSLG vector used in this study.

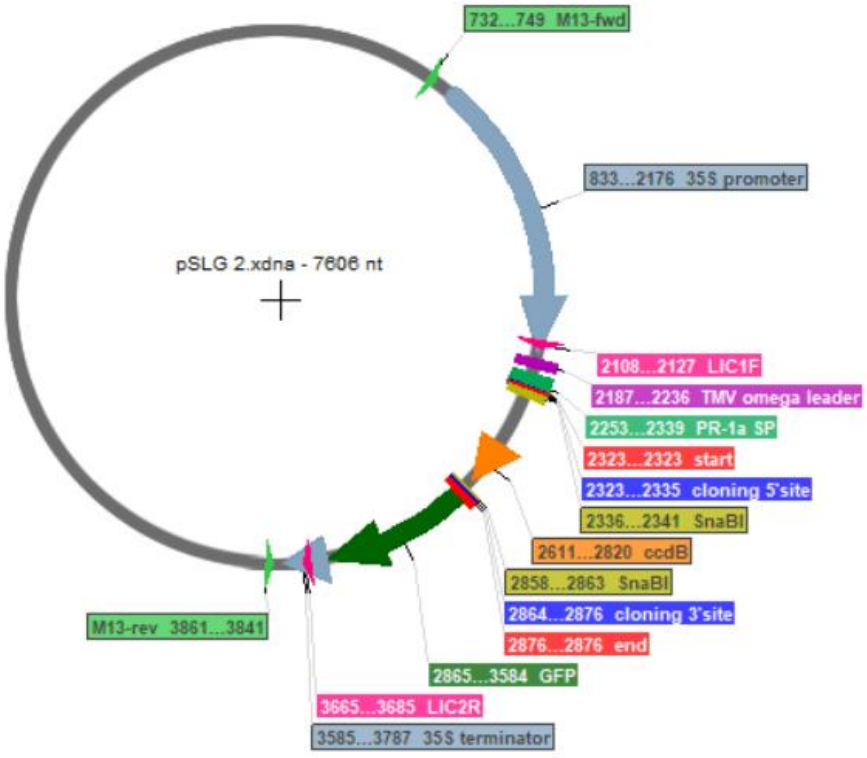

Appendix 2.3 Primers used for amplification of the target sequence (*Avr7* candidates).

Primer	Sequence 5'-3'
pSL-SIX2-Forward	ATCTTCTCACTCTACGAACCCGGCTGGGGATTCT
pSL-SIX2-Reverse	TCCTCTCCAAATTACGTCATGTACACCTTGACTGCGA
pSLG-SIX2-Reverse	CCTTTACTCATATACGTCCCTCCAGAGCCACCTGTACACCTTGACTGCGACGCA
pSL-SIX6-Forward	ATCTTCTCACTCTACGGGTCCCCTTGCTCAAACC
pSL-SIX6-Reverse	TCCTCTCCAAATTACGTTACTCCCAAGACCAGGTGT
pSLG-SIX6-Reverse	CCTTTACTCATATACGTCCCTCCAGAGCCACCCTCCCAAGACCAGGTGTAGGCA
pSL-SIX7-Forward	ATCTTCTCACTCTACGATACCTATGCTCGACCTATTT
pSL-SIX7-Reverse	TCCTCTCCAAATTACGTTAACTTTGAATCCGGAGC
pSLG-SIX7-Reverse	CCTTTACTCATATACGTCCCTCCAGAGCCACCACTTTGAATCCGGAGCCGAT
pSL-SIX11-Forward	ATCTTCTCACTCTACGATCAATATATGTTGCTCCTCCTTTG
pSL-SIX11-Reverse	TCCTCTCCAAATTACGTCAGATGCAGGGTCTATTGAG
pSLG-SIX11-Reverse	CCTTTACTCATATACGTCCCTCCAGAGCCACCGATGCAGGGTCTATTGAGAATGC
pSL-SIX12-Forward	ATCTTCTCACTCTACGTCCAGTTGTCTCAGCGTTGG
pSL-SIX12-Reverse	TCCTCTCCAAATTACGTCAGGAGTGGCATAGCTTGG
pSLG-SIX12-Reverse	CCTTTACTCATATACGTCCCTCCAGAGCCACCGGAGTGGCATAGCTTGGGCTTC
pSL-SIX13-Forward	ATCTTCTCACTCTACGGAGTTAGAGGTGTCTGATTTGTC
pSL-SIX13-Reverse	TCCTCTCCAAATTACGTTACTGTACAGTAGCCTCCCA
pSLG-SIX13-Reverse	CCTTTACTCATATACGTCCCTCCAGAGCCACCCTGTACAGTAGCCTCCCACTGT
pSL FOXG-17276-Forward	ATCTTCTCACTCTACGCTGCGCCGAGGATGCAAA
pSL FOXG-17276-Reverse	TCCTCTCCAAATTACGTTAGTTCCAGCTGCAGGGA
pSLG FOXG-17276-Reverse	CCTTTACTCATATACGTCCCTCCAGAGCCACCGTTCCAGCTGCAGGGAAC

Note: LIC adapter sequences are shown in green.

(A)

pSL-*SIX2*

pSLG-*SIX2*

(B)

pSL-*SIX7*

pSLG-*SIX7*

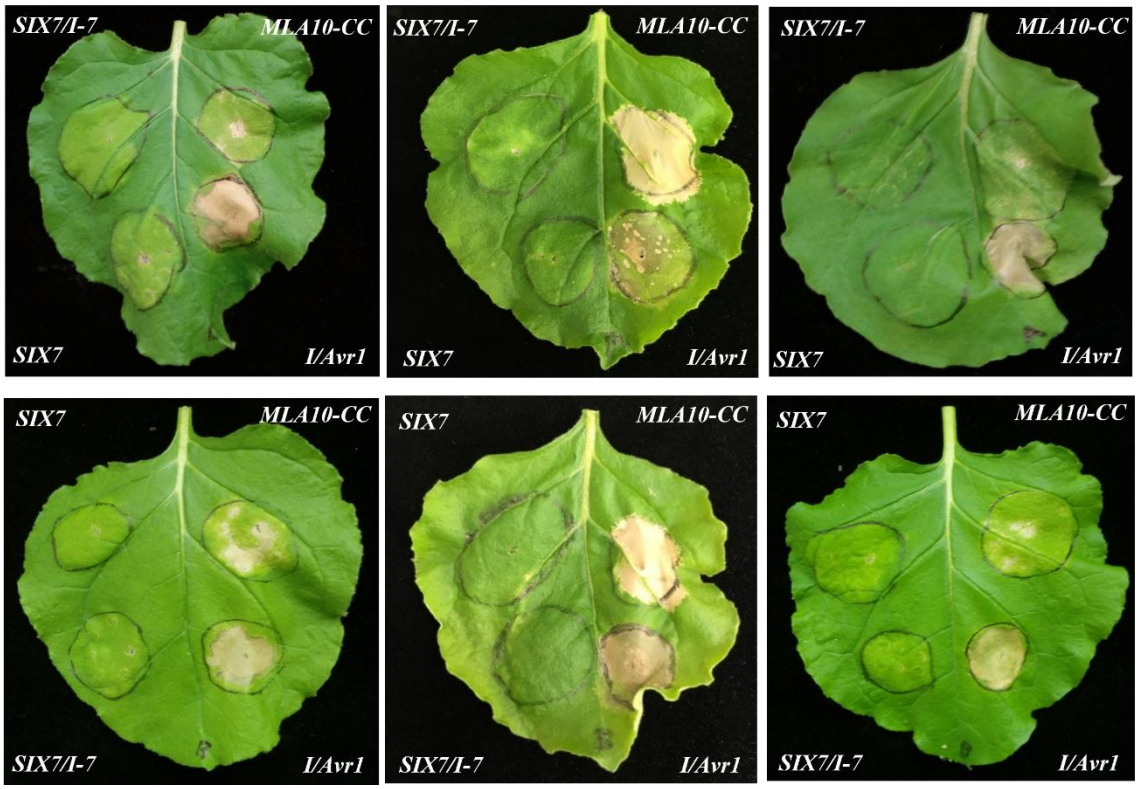

(C)

pSL-*SIX11*

pSLG-*SIX11*

(D)

pSL-*SIX12*

pSLG-*SIX12*

(E)

pSL-*SIX13*

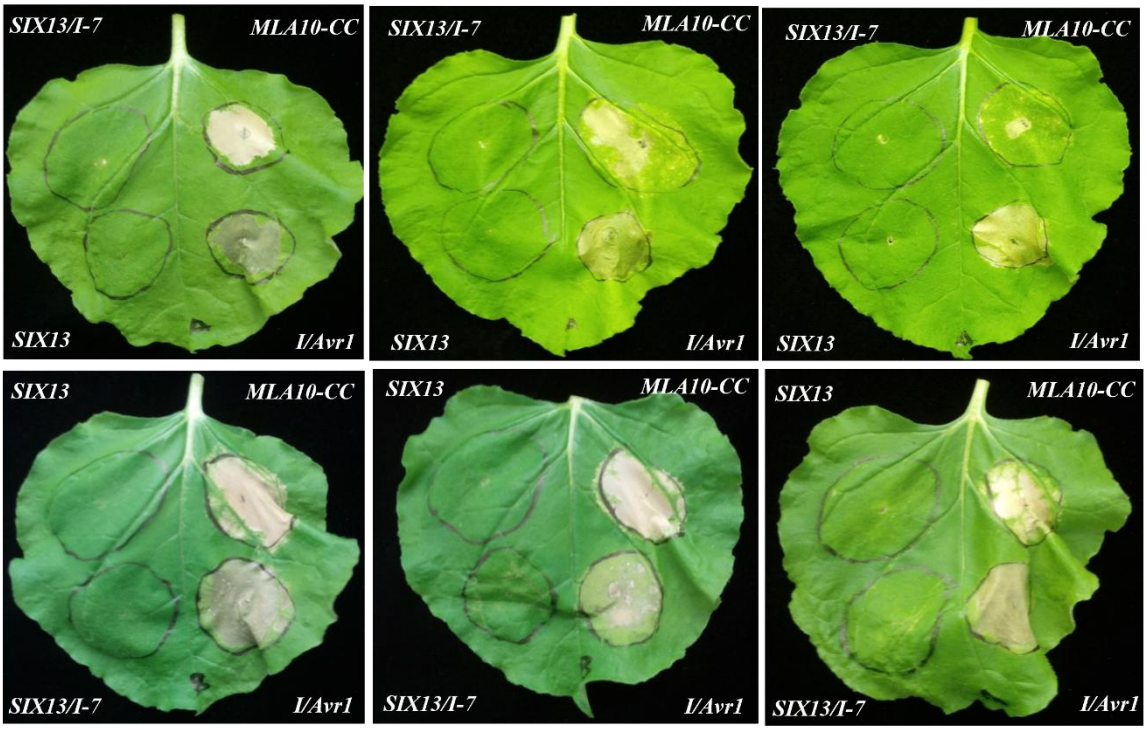

pSLG-*SIX13*

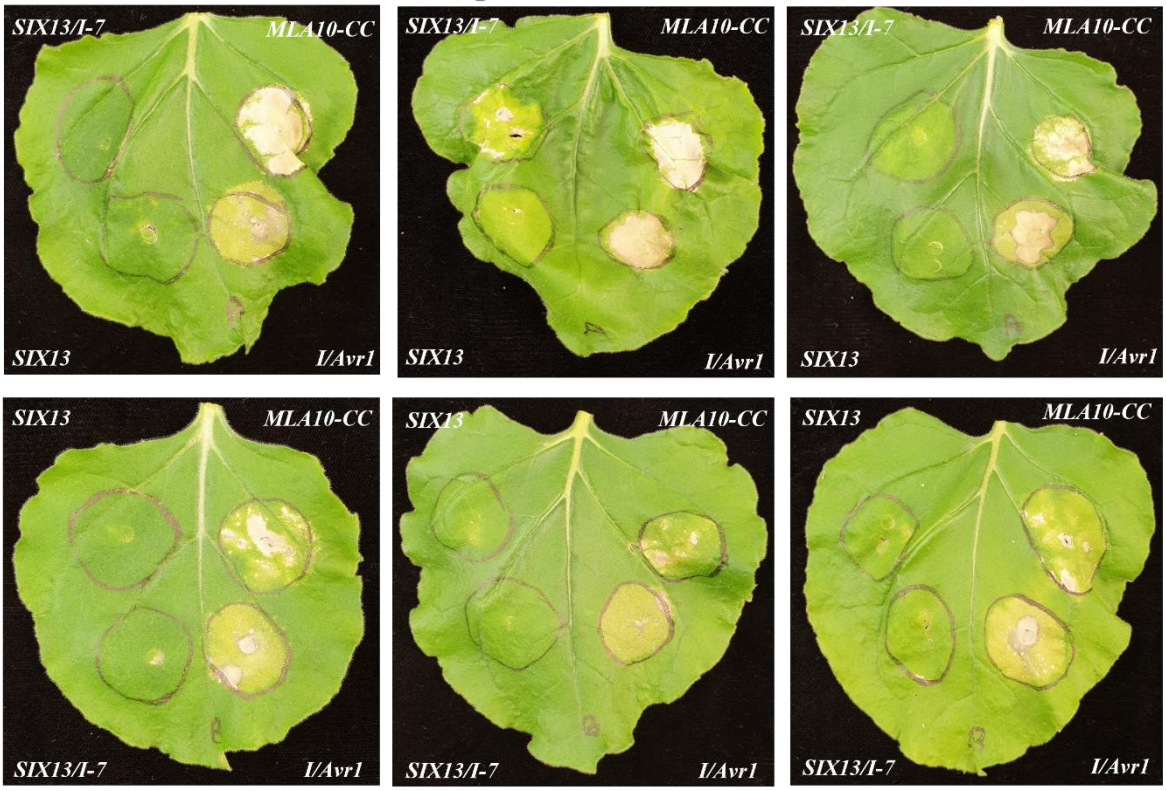

(F)

pSL-*FOXG_22509*

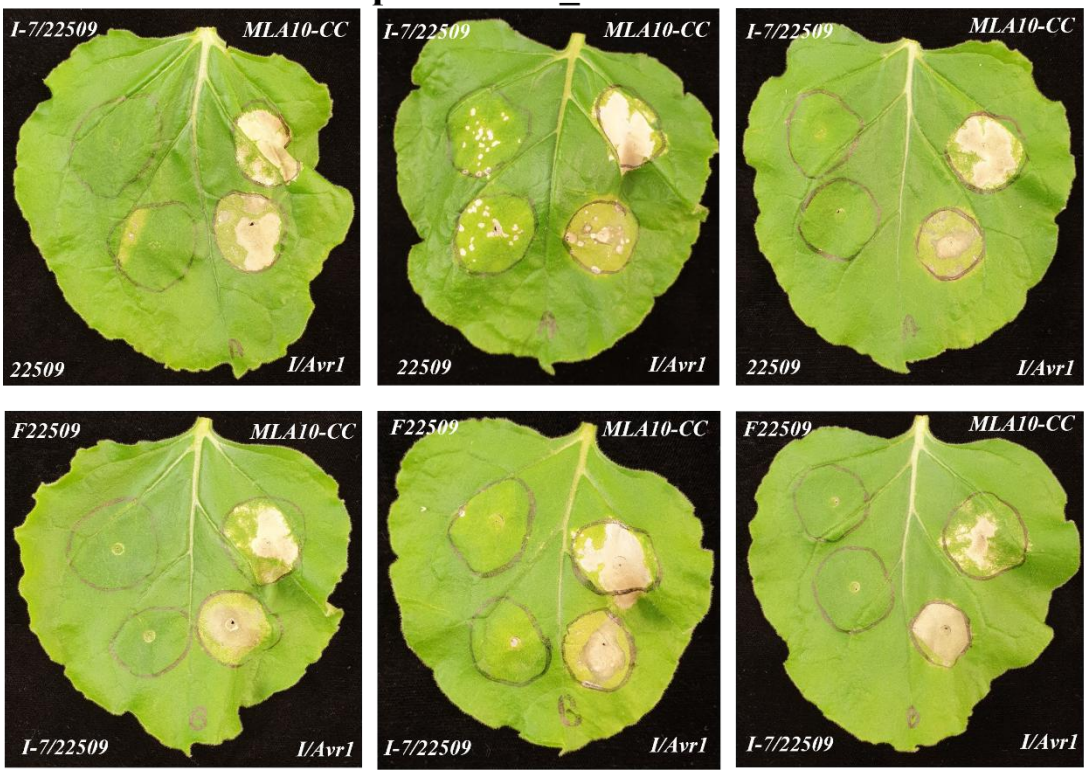

pSLG-*FOXG_22509*

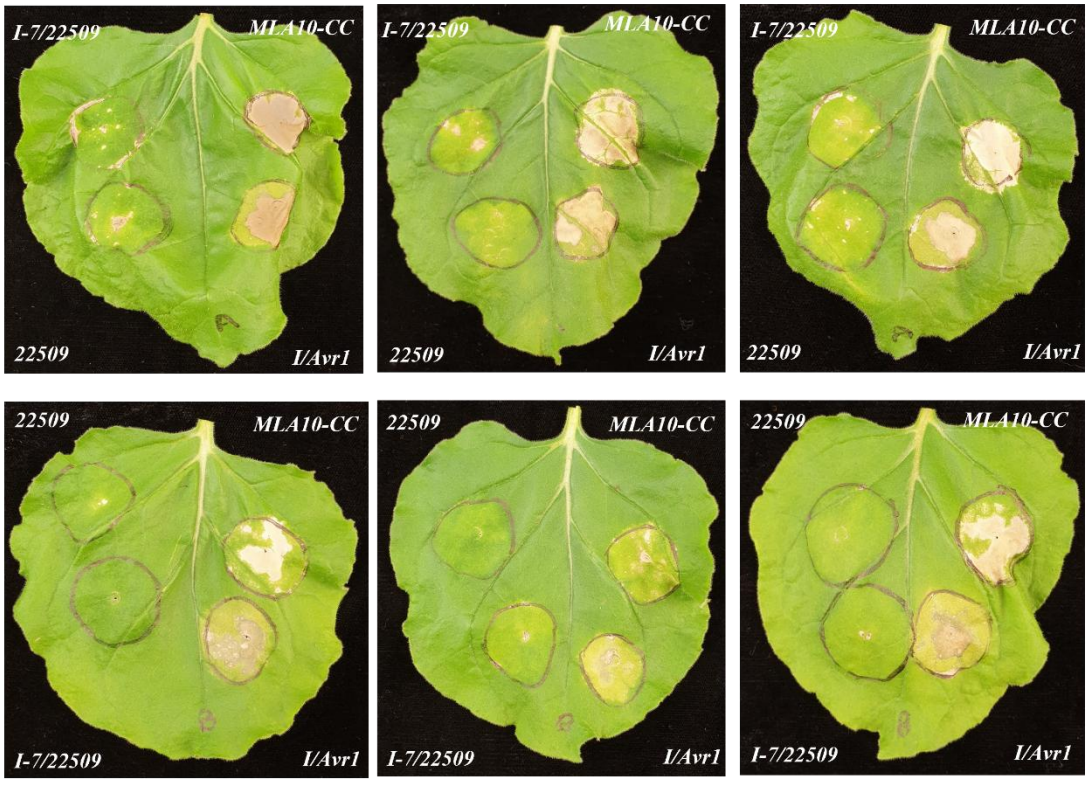

(G)

pSL-*FOXG_17276*

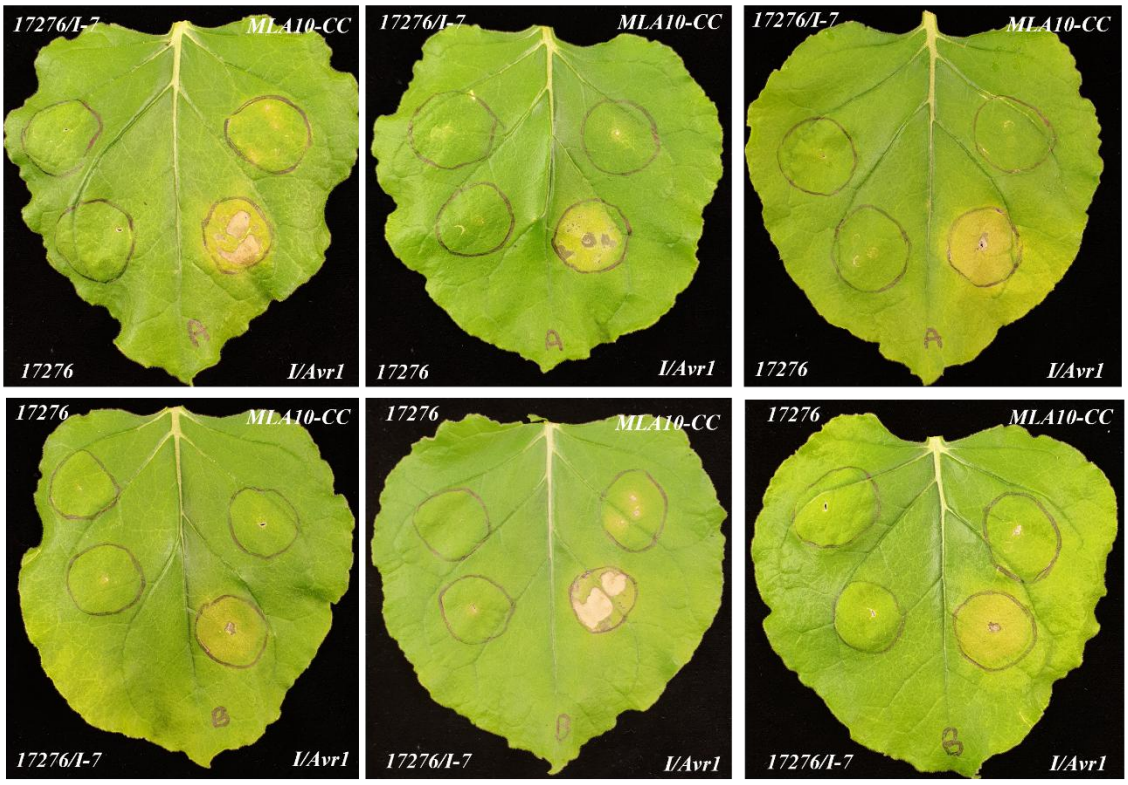

pSLG-*FOXG_17276*

Appendix 2.4 Co-agroinfiltration of *Avr7* candidates and *I-7* in *N. benthamiana* leaves.

Co-agroinfiltration of pSL-*I-7* and *Avr7* candidate genes in pSL or pSLG constructs in *N. benthamiana* leaves. Leaves of each plant were also agroinfiltrated with *Avr7* candidate gene constructs alone as a negative control and a *MLA10-CC* construct as a positive control. Leaves were also co-agroinfiltrated with pL-*I* and pL-*Avr1* as an additional positive control. **(A)** *SIX2*, **(B)** *SIX7*, **(C)** *SIX11*, **(D)** *SIX12*, **(E)** *SIX13*, **(F)** *FOXG_22509* and **(G)** *FOXG_17276*. Photographs were taken eight days after infiltration.

pSL-*SIX6*

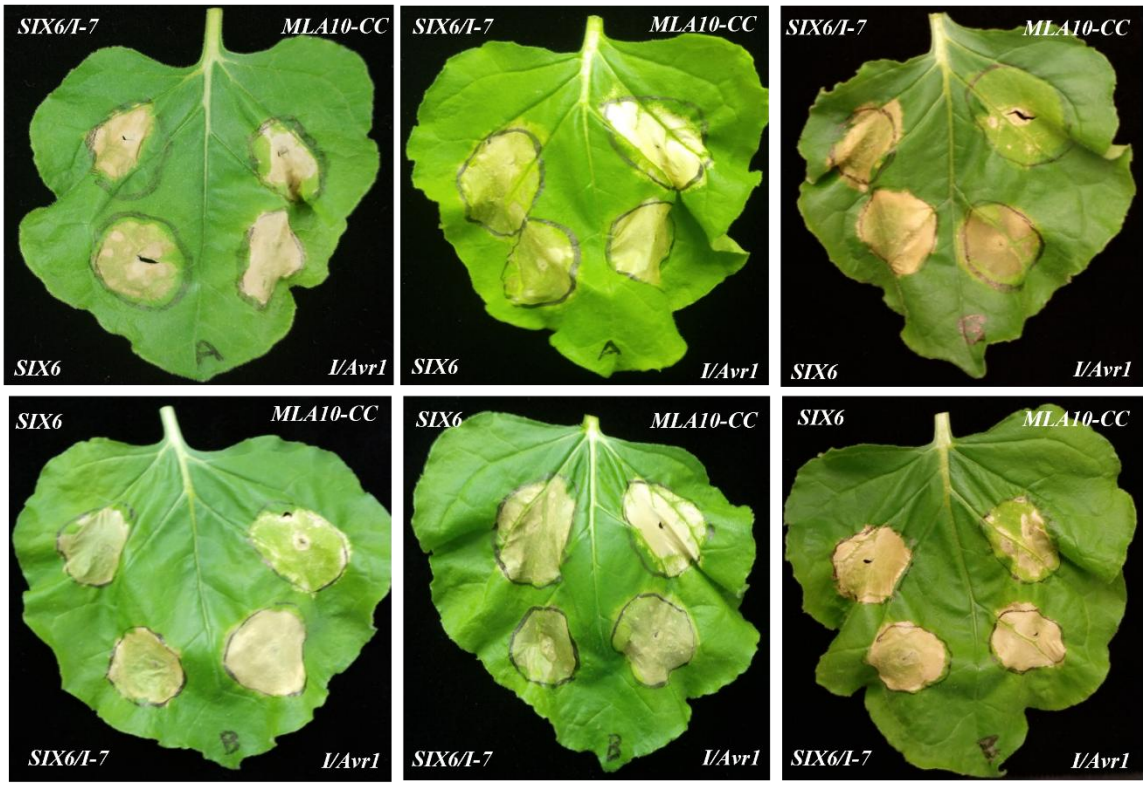

pSLG-*SIX6*

Appendix 2.5 Agroinfiltration of *I-7* and *Fol SIX6* in *Nicotiana benthamiana* leaves.

Co-agroinfiltration of *I-7* with pSL- *SIX6* or pSLG-*SIX6* gene in *N. benthamiana* leaves. Leaves of each plant were also agro-infiltrated with pSL-*SIX6* or pSLG-*SIX6* alone as a negative control and *MLA10-CC* as a positive control. Leaves were also co-agroinfiltrated with pL-*I* and pL-*Avr1* as an additional positive control. Photographs were taken eight days after infiltration.

Chapter 3: *Fol SIX6* is a cell death-inducing effector

3.1 Introduction

Interactions between plants and pathogens are studied using model systems that provide insights at the molecular level on how plant immunity protects plants from pathogen infection and how pathogens overcome plant immunity to attack plants (Jones and Dangl, 2006; Spoel and Dong, 2012; Han, 2019). The interaction between tomato and *Fol* is considered a model system to study plant-root pathogen interactions (Takken and Rep, 2010; Essarioui et al., 2016; Chitwood-Brown et al., 2021). While infecting tomato roots, *Fol* secretes a number of effectors to promote infection. These include the Secreted in Xylem (SIX) effectors, which are small (<300 amino acids), mostly cysteine-rich proteins that are secreted into the xylem during infection (Houterman et al., 2007).

The genome of *Fol* strain 4287 has been reported to consist of 15 chromosomes, of which 11 are considered core chromosomes and 4 are considered lineage-specific (LS) chromosomes (Ma et al., 2010). LS chromosome 14, which is required for pathogenicity, can convert non-pathogenic strains into pathogenic strains via horizontal transfer (Ma et al., 2010). Most of the SIX effectors are located on chromosome 14 (Ma et al., 2010; Vlaardingerbroek et al*.,* 2016; Sun et al., 2022). Proteomic studies of the xylem sap of *Fol*-infected tomato plants have enabled the identification of at least 14 different SIX proteins (Houterman et al., 2007; Lievens et al., 2009; Schmidt et al., 2013). Out of the 14 corresponding *SIX* genes, *SIX4 (Avr1)*, *SIX3 (Avr2)* and *SIX1 (Avr3)* have been identified as avirulence genes that encode effectors recognised by the tomato I, I-2 and I-3 resistance proteins, respectively (Houterman et al., 2008; Houterman et al., 2009; Rep et al., 2004). *Fol SIX2*, *SIX5* and *SIX8* have also been investigated to examine their roles in the pathogenicity (Schmidt et al., 2013; Ma et al., 2015; An et al., 2019; Cao et al., 2018; Blekemolen et al., 2022). Recently, 27 new candidate effector genes have been reported following transcriptome analysis of *Fol*-infected tomato plants, and of these, *Fol-EC19* was found to cause cell death while *Fol-EC14* and *Fol-EC20* were found to suppress *Bax*-induced cell death (Sun et al., 2022). However, most of these effector candidates and several *SIX* genes, including *SIX6*, have not been investigated in depth.

Fol SIX6 encodes a 225 amino acid protein containing a signal peptide and eight cysteine residues that form four disulphide bonds (Yu et al., 2024). The structure of *Fol* SIX6 reveals that it has two domains and is a founding member of the FOLD (*Fusarium oxysporum* f. sp. *lycopersici* dual domain) family (Yu et al., 2024). Homologues of *Fol SIX6* have been discovered in other *formae speciales* of *F. oxysporum,* including *F. oxysporum* f. sp. *cubense*

TR4 (*Foc*), which causes Panama disease in banana and plantains, *F. oxysporum* f. sp. *melonis* (*Fom*), which causes Fusarium wilt in melons, *F. oxysporum* f. sp. *vasinfectum* (*Fov*) which causes Fusarium wilt in cotton, and in many other, but not all, *formae speciales* of *F. oxysporum*. Homologues of *Fol SIX6* have also been found other fungal pathogens including *Colletotrichum orbiculare* (Gan et al., 2013) and *C. higginsianum* (Kleemann et al., 2012), and in arbuscular mycorrhizal fungi such as *Rhizophagus clarus* (Zeng et al., 2020) and *R. irregularis* (Zeng et al., 2020; Teulet et al., 2023).

Prior investigation of *Fol SIX6* showed that it was expressed during both early and late stages of infection and required a living host for expression (Gawehns et al., 2014). Gawehns et al. (2014) also showed that *Fol SIX6* contributed to *Fol* virulence, whereas another study showed that deletion of *SIX6* had no obvious effect on pathogen virulence (Vlaardingerbroek et al., 2016). However, the presence of a *SIX6* gene has been linked directly to the capacity of *F. oxysporum* f. sp. *phaseoli* to produce severe wilt symptoms in soybean (Lanubile et al., 2016). Another study indicates that deletion of *SIX6* in *F. oxysporum* f. sp. *cucumerinum* (*Forc*) reduces cucumber virulence, highlighting its contribution to virulence under specific conditions (Van Dam et al., 2017).

A *SIX6* gene, identical to that in *Forc,* has also been found in the watermelon pathogen *Fusarium oxysporum* f. sp. *niveum* (*Fon*). *Fon SIX6* is expressed during the early stages of infection and is present in races 0 and 1 but not race 2 (Niu et al., 2016). In the watermelon pathosystem, it is considered an avirulence gene with loss or mutation of the gene responsible for the emergence of *Fon* race 2. A knockout mutation of *Fon SIX6* in race 1 enhanced virulence in watermelon while restoration of wild-type *Fon SIX6* in *Fon* race 2 led to a reduction in its virulence, confirming that *Fon SIX6* acts as an avirulence gene in the watermelon pathosystem (Niu et al., 2016). Likewise, the *SIX6* gene from *F. oxysporum* f. sp. *fragariae* (*Fof*) has been identified as the gene causing avirulence on strawberry cultivars carrying the *FW1* gene for resistance to *Fof* (Dilla-Ermita et al., 2024). In a recent study, Li et al (2020) found that horizontal transfer of the *F. oxysporum* f. sp. *melonis* (*Fom*) chromosome containing a *SIX6* gene identical to that in *Forc* and *Fon* can convert a non-pathogenic *Fom* strain into a pathogenic strain able to cause disease on melon but not on cucumber or watermelon. However, strains of *Fom* carrying a deletion of *SIX6* showed no loss of virulence on melon plants compared to wild-type strains, suggesting that *Fom SIX6* does not play a role in virulence on melon plants (Li et al., 2020). The role of *SIX6* in virulence can vary depending on the *forma specialis* and the host plant being infected

Previous investigation of the role of *Fol SIX6* in the tomato/*Fol* pathosystem suggested that SIX6 behaved as a cytosolic effector able to suppress cell death induced by interaction between I-2 and Avr2 (Gawehns et al., 2014). Still, this conclusion must be considered suspect given the finding reported in Chapter 2 that SIX6 behaves as an extracellular effector able to induce plant cell death. The remainder of this thesis addresses the consequent lack of knowledge about *Fol SIX6* function and its role in pathogen virulence. For this purpose, proteins encoded by *Fol SIX6* and several of its homologues were expressed in *E. coli,* and this chapter reports the use of purified recombinant SIX6 proteins in tests for cell death induction in a range of plant species.

3.2 Materials and Methods

3.2.1 Plant material

For protein infiltration study, In-house or commercially obtained representatives of the Solanaceae, Cucurbitaceae, Brassicaceae, Leguminosae, Malvaceae, Asteraceae and Linaceae were used in this study (Appendix 3.1). All seeds were sown in pots with seed raising mix (Martins Fertilizers, Australia) and seedlings grown in a glasshouse under a 16 h 21°C light / 8 h 16°C dark cycle with ambient humidity. Tomato, *N. benthamiana* and tobacco plants were raised until they were 4 to 6 weeks old for infiltration experiments. All other seedlings were raised until they were 2 weeks old. Banana clones (provided by Professor Elizabeth Aitken, University of Queensland) were raised initially in Jiffy pots for root growth initiation and then transferred to soil. Banana plants were grown for 45-50 days for infiltration experiments**.**

3.2.2 Bacterial strains and vectors

E. coli strain DH5α was used for routine cloning work. *Agrobacterium* strain GV3101(pMP90) was used for *Agrobacterium*-mediated plant transformation. The SHuffle strain of *E. coli* (NEB) was used for recombinant protein expression. pSL and pSLG vectors (Appendices 2.1 and 2.2) were used for cloning and *Agrobacterium*-mediated expression of the *Fol SIX6*, *Fom SIX6*, *Foc SIX6* and *Fov SIX6* genes. For expression of *Fol* SIX6 and homologous proteins, a Golden-Gate-compatible derivative of the pOPIN expression vector was used (Bentham et al., 2021). Final protein expression constructs had an N-terminal 6xHis-GB1-tag followed by a 3C protease recognition site.

3.2.3 Purification of plasmid DNA

The plasmid isolation and purification from bacteria was done using a Plasmid DNA Extraction kit (Favorgen, Cat # FAPDE300) according to the manufacturer's protocol. For plasmid isolation, cultures were grown overnight from single colonies in 1-3 ml LB (lysogeny broth; tryptone 10 g/l, yeast extract 5 g/l, NaCl 5 g/l) with appropriate antibiotics at 37°C with shaking at 250 rpm. Bacterial cultures were then centrifuged at 11000 x g for 1 min, supernatants were discarded, and pellets were used for plasmid extraction. Plasmid DNA was then stored at -20 °C.

3.2.4 DNA gel electrophoresis

Gel electrophoresis was used to separate DNA fragments according to their sizes. Agarose (Scientifix, Cat # 9010E) gels were prepared based on expected DNA fragment sizes (0.8% w/v agarose gels for fragment sizes 0.8 to 12 kb, 1% w/v gels for fragment sizes 0.5 to 10 kb and 1.5% w/v gels for fragment sizes 0.1 to 2 kb). Gels were prepared in 1x TBE buffer (220 mM Tris, 180 mM boric acid, 5 mM EDTA, pH 8.3). Redsafe (iNtRON Biotechnology, Cat # 21141) was added, 5 µl for every 100 ml of gel solution to stain DNA fragments. DNA samples were mixed with 1 µl of blue loading buffer (Bioline, Cat # BIO-37045) for every 5 µl of DNA sample. Gels were run in 1x TBE buffer at a constant voltage of 80-120 V using a Powerpac 300 (Bio-Rad). DNA was visualised using a Molecular Imager Gel Doc XR+System (Bio-Rad) and images were taken using Image Lab Software 6.0 (Bio-Rad).

3.2.5 Purification of DNA from PCR samples

Gel electrophoresis was used to separate PCR products from template DNAs. Gels were prepared and run as described above, and gel pieces containing desired PCR products cut out with the assistance of a Dark Reader Transilluminator (Clare Chemical Research). DNA was eluted from gel pieces using a Zymoclean Gel DNA Recovery Kit (Zymo Research, Cat # D40001) as described in the manufacturer's protocol. Purified DNA was then stored at -20°C.

3.2.6 Transformation of *E. coli*

Heat-shock competent cells of DH5α (prepared in-house as described by Behle 2018) or SHuffle (NEB, Cat # C3028) were taken from -80°C freezer and thawed on ice for 10 min. For routine cloning, 5 µl or 100 ng of plasmid DNA were gently mixed with 30 µl of competent cells, which were then kept on ice for 30 minutes, heated at 45°C for 30 sec and transferred to ice for 10 min before adding 500 µl of LB and incubating at 37°C for 1 hour with shaking.

Finally, 200 µl aliquots of transformed cells were plated on LBA (LB with 15 g/l agar), supplemented with appropriate antibiotics and incubated overnight at 37°C. Colonies were then screened by colony PCR using specific primers as described in section 3.2.8.

3.2.7 Transformation of *Agrobacterium* (GV3101)

Electrocompetent cells of *Agrobacterium* strain GV3101(pMP90) (prepared in-house as described by Weise 2013) were taken from -80°C freezer and thawed on ice and kept on ice. In a pre-cooled microcentrifuge tube, 100 ng of plasmid, 40 µl of sterile water and 20 µl of electrocompetent cells were added. The entire reaction mixture was then added to a pre-cooled electroporation cuvette with a 0.2 cm gap (Bio-Rad) and electroporated using a MicroPulser Electroporator (Bio-Rad) with 2.5 kV electromotive force, 200 Ω resistance and 25 µF capacitance. Immediately after electroporation, 500 µl LB was added to the cuvette and the entire reaction mixture was then transferred to a microcentrifuge tube and kept in a 28°C incubator shaker at 250 rpm for 2 hours. Around 50 to 100 µl aliquots of transformed cells were plated on LBA with appropriate antibiotics and incubated at 28°C for 2 days. Colonies that appeared after 2 days were screened by colony PCR as described in section 3.2.8.

3.2.8 Colony PCR screening

Colonies were picked using sterile pipette tips and cells suspended in 40 µl sterilised deionised water. PCR was performed in 10 µl volumes using 2 µl of 1x MyTaq Reaction Buffer Red (Bioline Cat # Bio 37112), 0.5 µM of each of the primer (either LIC1F and LIC2R, or T7 Forward and Golden Gate-STOP Reverse primers; Appendix 3.4), 0.15 µl of MyTaq DNA polymerase (Bioline, Cat # 21105) and 3 µl of colony suspension using a T100 thermal cycler (Bio-Rad). Cycling conditions were as recommended by the manufacturer of MyTaq (Bioline). In brief, reactions were heated to 98°C for 2 minutes followed by 30 cycles at 95°C for 15 sec for denaturation, 54°C for 15 sec for primer annealing and 72°C for 10 sec for extension before holding at 4°C. PCR products were analysed by gel electrophoresis as described in section (3.2.4). The remainder of the colony suspensions that produced a band of the right size, were used to inoculate LB with appropriate antibiotics and grown overnight in a 37°C shaking incubator. Plasmid DNA was extracted as described in section 3.2.3. Concentrations of plasmid DNAs were measured using a Spectramax Quick Drop spectrophotometer (Molecular Devices).

3.2.9 SDS-PAGE (Sodium Dodecyl-Sulphate Polyacrylamide Gel Electrophoresis)

SDS-PAGE was used to separate and visualise the proteins according to their molecular size. Stacking (4% w/v) and resolving (8%, 10%, 13% or 15% w/v depending on the size of the protein being analysed) gels were prepared in batches of four and stored in wet paper towel at 4°C for later use. Stacking gels consisted of 0.67 ml 30% (w/v) Acrylamide/Bis (Bio-Rad, Cat #1610156), 1.25 ml 0.5 M Tris-HCl (pH 8.8), 50 µl 10% (w/v) SDS, 5 µl TEMED (Sigma Aldrich, Cat # T22500), 50 µl 10% (w/v) ammonium persulphate and deionised water to a final volume of 5 ml. A 13% (w/v) resolving gel consisted of 3.47 ml 30% (w/v) Acrylamide/Bis (Bio-Rad, Cat #1610156), 2 ml 1.5 M Tris-HCl (pH 6.8), 80 µl 10% (w/v) SDS, 8 µl TEMED (Sigma Aldrich, Cat # T22500), 80 µl 10% (w/v) ammonium persulphate and deionised water to a final volume of 8 ml. During the process of purifying recombinant *Fol* SIX6 protein and its homologues, all fractions (total protein, clarified lysate, flow through, wash and others) were collected in PCR tubes. For SDS PAGE, initial samples of 1 µl of total protein or clarified lysate were mixed with 11 µl of water and 4 µl of loading dye (NEB, Cat #B7703S). For all other fractions, initial samples of 5 µl were mixed with 7 µl of water and 4 µl of loading dye. All samples were boiled at 95°C for 5 min. SDS-PAGE was run in 1x SDS running buffer (10x SDS buffer: 30 g Tris base, 144 g glycine, 10 g SDS in 1000 ml deionised water) at 200 V (Bio-Rad, Powerpac 300) until the dye front ran out from the bottom of the gel. As a reference, Precision Plus Protein Dual Color Standards (Bio-Rad, Cat # 1610394) were run along with samples. Gels were then stained in Coomassie Brilliant Blue R250 (Bio-Rad, Cat # 1610400) staining solution (0.125% w/v Coomassie Brilliant Blue R250 in 10% v/v acetic acid, 50% v/v methanol in 400 ml of deionised water) for 15 minutes and then destained three times with deionised water for 10 minutes. Proteins were visualised by Molecular Imager Gel Doc (Bio-Rad) and Image Lab Software 6.0 (Bio-Rad) was used to analyse the image.

3.2.10 Generation of binary vector constructs by ligation independent cloning (LIC)

The *Fol SIX6* coding sequence was amplified by PCR using 0.5 µM pSL-SIX6 forward primer, 0.5 µM pSL-SIX6 reverse primer (Appendix 2.3) and cDNA made from *Fol*-infected tomato roots. Following gel electrophoresis, the *Fol SIX6* PCR product was recovered and purified as described in section 3.2.5. *Fom SIX6*, *Foc SIX6*, *Fov SIX6* sequences with desired LIC overhangs were obtained using gBlocks (Appendix 3.2) synthesised by IDT (Integrated DNA Technologies). PCR product/gBlock sequences were cloned into pSL and pSLG binary vectors by ligation independent cloning (LIC) as described in section 2.2.5. LIC reactions were

transformed into *E. coli* strain DH5α as described in section 3.2.6. Colonies of transformants growing on selective medium were then screened by colony PCR as described in section 3.2.8. Constructs from PCR positive colonies were sequence verified and then used to transform *Agrobacterium* strain GV3101 as described in section 3.2.7.

3.2.11 *Agrobacterium*-mediated gene expression

Binary vector constructs in *Agrobacterium* strain GV3101 were used for transient expression of proteins as described by Ma et al. (2012). Cultures were grown on LBA with appropriate antibiotics for 2 days at 28°C and cells suspended in infiltration media (10 mM MES (pH 5.6), 10 mM $MgCl_2$ and 200 µM acetosyringone) to an OD at 600 nm of 1.0 and kept in the dark for 2 hours before infiltrating in either *N. benthamiana*, *N. tabacum* or tomato leaves. A needle was used to prick the abaxial side of the leaf and then a 1 ml syringe without a needle was used to infiltrate the *Agrobacterium* suspension. Different panels of the same leaf were used for different infiltrations and controls in *N. benthamiana* and *N. tabacum*, but in tomato different leaflets of the same leaf were used. Infiltrated plants were kept at 25°C in a growth room with a 16-hour photoperiod at a light intensity of 250 µmol m^{-2} s^{-1} and relative humidity of 60-65% for 8 to 10 days.

3.2.12 Generation of protein expression constructs by Golden Gate cloning

PCR amplification of coding sequences was performed using Phusion DNA polymerase (NEB) with template DNA from IDT-synthesised Gene gBlocks (Appendix 3.2). Primers containing overhangs designed for compatibility with the pOPIN Golden Gate cloning system were utilised (primer sequences listed in Appendix 3.4). The PCR thermal cycling protocol consisted of an initial denaturation at 98°C for 30 sec, then 25 repetitive cycles each containing denaturation at 98°C for 10 sec, primer annealing at 60°C for 15 sec, and extension at 72°C for 15 sec, concluded with a final extension step at 72°C for 5 min. Golden Gate assembly reactions were performed in a total volume of 15 µl. Each reaction contained 25 ng of gene fragments with Golden Gate overhangs, 100 ng of the Golden Gate-compatible pOPIN backbone, 75 ng of an N-terminal solubility tag (6xHis-GB1), and 70 ng of a 3′ STOP sequence. To facilitate the digestion and ligation, 0.5 µl of *Bsa*I restriction enzyme (NEB, Cat # 3535), 0.5 µl of T4 DNA ligase (NEB, Cat # M0202S), 1.5 µl of 10x BSA (NEB, Cat # B9200), and 1.5 µl of 10x T4 ligase buffer (provided by the manufacturer) were also included in the reaction mix. The reactions were placed in a thermocycler (Bio-Rad) for 25 cycles, alternating between 37°C for 1.5 minutes and 16°C for 3 minutes. After cycling, the reactions were incubated at 50°C for 5

min and finally at 80°C for 10 min to inactivate the enzymes. The assembled Golden Gate constructs were then transformed into *E. coli* DH5α cells, as detailed in section 3.2.6. Transformants grown on selective media were initially identified based on red/white screening, which relies on disruption of the red fluorescent protein gene in the pOPIN vector by the inserted gene fragment. Positive colonies were further verified using colony PCR, employing the T7 Forward primer and the Golden Gate-STOP Reverse primer (Appendix 3.4), as described in section 3.2.8. Selected bacterial colonies were transferred to LB with appropriate antibiotics and grown at 37°C with shaking at 250 rpm for one day. Plasmid DNAs were extracted using a Plasmid DNA Extraction kit (Favorgen) as described in section 3.2.3, and constructs were verified by sequencing. The Golden Gate cloning procedures were performed under the guidance and technical support of Daniel Yu (Williams Laboratory, ANU).

3.2.13 Preparation and infiltration of recombinant SIX6 proteins

Recombinant SIX6 proteins were produced and purified as described previously by Yu et al., (2022 and 2024). Purified recombinant proteins were divided into 10 or 20 µl aliquots before rapidly freezing in liquid nitrogen and kept at -80°C for future applications. Thawed protein samples were diluted in either deionised water or gel filtration buffer (10 mM HEPES, 150 mM NaCl, pH 7.5) to a final concentration of 50 µg/ml or 100 µg/ml and maintained on ice. To create a wound, a needle was used to pierce the lower surface of leaves or cotyledons. The diluted protein solution was then infiltrated into the leaf through the wound site using a 1 ml syringe without a needle. As negative controls, water, buffer or buffer BSA (gel filtration buffer with BSA at equal concentration to the SIX6 protein used for each particular experiment) were infiltrated as appropriate in opposite cotyledons or in adjacent panels on the same leaf or in a different leaflet on the same leaf in the case of tomato. When comparing the response of two SIX6 homologues, both proteins were infiltrated into the same plant. SDS-PAGE was performed to confirm that all samples contained comparable levels of the SIX6 protein. Protein production and purification were carried out in collaboration with Daniel Yu, who supervised these aspects of the project. While we worked together on the broader project, he took the lead in the protein production and purification steps, providing critical support for obtaining purified protein. For banana plants where infiltration of protein was hard and efficiency needed to be verified or where responses to SIX6 were ambiguous, purified recombinant NLP (necrosis and ethylene-inducing peptide 1-like protein from *Pythium aphanidermatum*) provided by the Williams Lab, ANU, was used as a positive control for cell death induction. NLP was infiltrated

following the same procedures described above for SIX6 proteins, at a concentration of 100 µg/ml.

3.3 Results

3.3.1 *Agrobacterium*-mediated expression of *Fol SIX6* and its homologues induces cell death

The *Fol SIX6* coding-sequence with its signal-peptide coding-sequence replaced by a tobacco PR1 signal-peptide coding-sequence was expressed in leaves of *N. benthamiana* and *N. tabacum* via *Agrobacterium*-mediated transformation (agroinfiltration) as described in section 3.2.11. *Fol SIX4* with its signal-peptide coding-sequence likewise replaced by a tobacco PR1 signal-peptide was used as a negative control. *Fol SIX6* induced a strong cell-death response in the leaves of *N. benthamiana* (Figure 3.1A) and *N. tabacum* (Figure 3.1B), but *Fol SIX4* did not. When *Fol SIX6* was agroinfiltrated without a signal peptide coding sequence, it did not induce cell death in either *N. benthamiana* (Figure 3.1C) or in *N. tabacum* (Figure 3.1D), indicating that *Fol SIX6* needs to be secreted to cause plant cell death. Homologues of *Fol SIX6,* including *Foc*, *Fom* and *Fov SIX6* (Figure 3.2) were also tested for the ability to induce plant cell death by agroinfiltration, partly because these *ff. spp.* of *F. oxysporum* are important pathogens that infect banana, melon and cotton, respectively, but primarily because they were the only other *ff. spp.* for which full-length *SIX6* sequences were available at the time this work was initiated. *Foc SIX6* and *Fom SIX6* were found to cause strong cell-death responses and *Fov SIX6* caused a weak cell-death response in leaves of *N. benthamiana* (Figure 3.1E) and *N. tabacum* (Figure 3.1F).

To test whether *Fol SIX6* could induce cell death in tomato (the host for *Fol*), leaves of tomato cv. M82 were agroinfiltrated with *Fol SIX6* as described previously (section 3.2.11). Given that M82 carried the *I* gene conferring resistance to isolates of *Fol* carrying the *SIX4* (*Avr1*) gene, *SIX4* was used as a positive control for cell-death induction. No cell death was observed for either *Fol SIX6* or *SIX4* (Appendix 3.4). *Fol* SIX4 protein was known from previous work to cause cell death in tomato cv. M82 (Yu et al., 2022), suggesting that agroinfiltration was not working in tomato and that no conclusion could be drawn from the agroinfiltration experiment about the ability of *Fol SIX6* to cause cell death in tomato. To address this question further, recombinant *Fol* SIX6 protein was expressed in *E. coli* and purified for use in further studies.

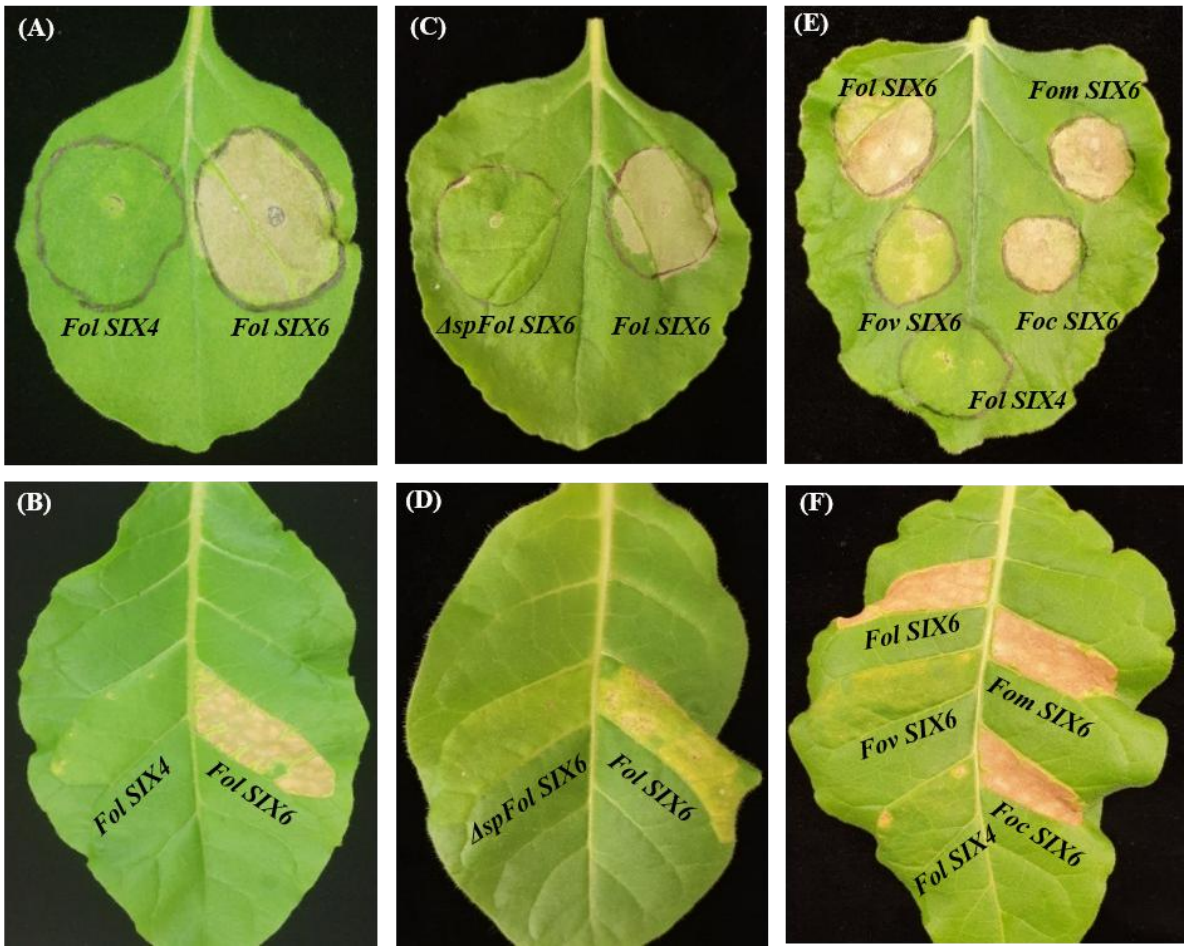

Figure 3.1 Cell death responses caused by *Agrobacterium*-mediated expression of *Fol SIX6* and its homologues.

(**A, B**) Cell death induced by agroinfiltration of *Fol SIX6* in leaves of (**A**) *N. benthamiana* and (**B**) *N. tabacum* with *Fol SIX4* used as a negative control. (**C, D**) Cell death responses following agroinfiltration of *Fol SIX6* with and without signal peptide (*ΔspFol SIX6*) in leaves of (**C**) *N. benthamiana* and (**D**) *N. tabacum.* (**E, F**) Cell death response caused by *Agrobacterium*-mediated expression of *SIX6* homologues in leaves of (**E**) *N. benthamiana* and (**F**) *N. tabacum*. Photographs were taken at 8 days post-agroinfiltration.

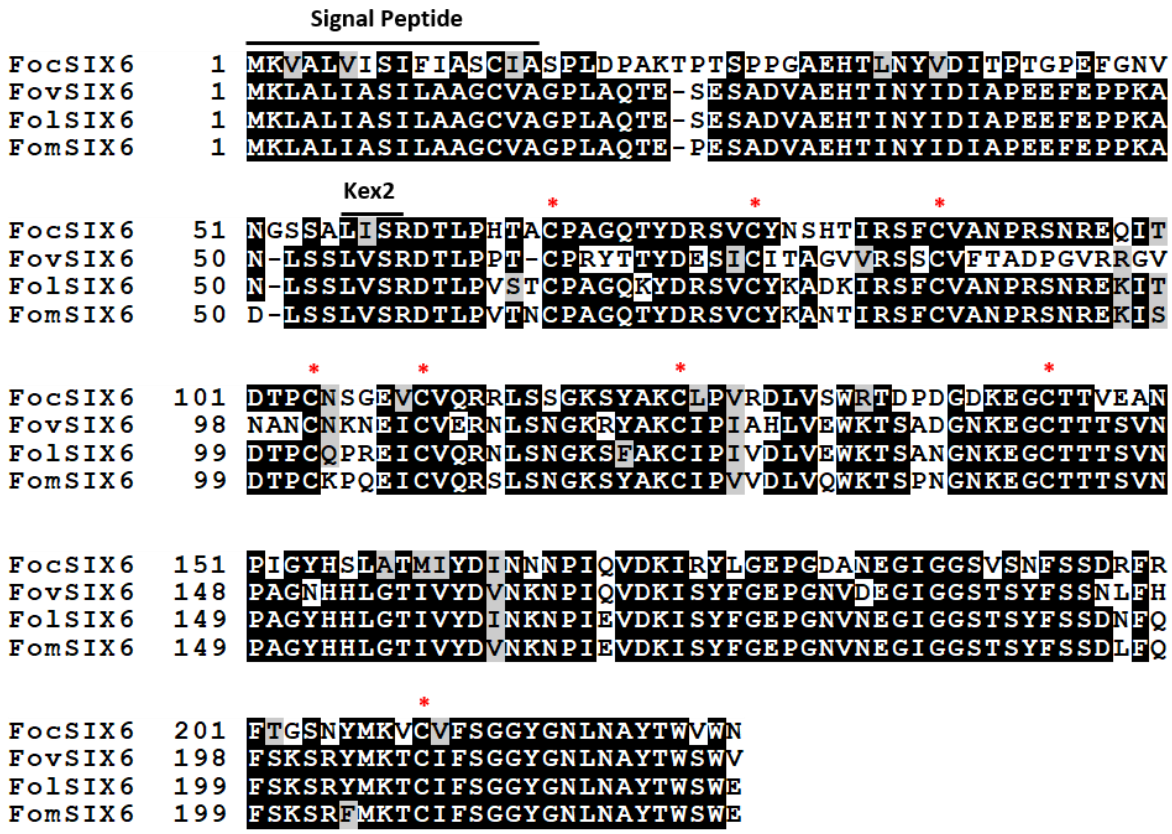

Figure 3.2 Multiple sequence alignment of *Fol SIX6* and homologues.

Sequences were aligned with MUSCLE (https://www.ebi.ac.uk/Tools/msa/muscle/). Amino acid identities are highlighted in black, while similarities are highlighted in grey. Conserved cysteine residues are indicated with red asterisks. Signal peptides and Kex2 cleavage sites (LxxR) are overlined. *Foc* = *F. oxysporum* f. sp. *cubense* Tropical Race 4, *Fov* = *F. oxysporum* f. sp. *vasinfectum*, *Fom* = *F. oxysporum* f. sp. *melonis.*

3.3.2 *Fol* SIX6 protein induces cell death in tomato

Fol SIX6 containing an N-terminal 6xHis-GB1 solubility tag was expressed in the SHuffle strain of *E. coli* (NEB). Clarified lysate was recovered after centrifugation of total protein (Figure 3.3A), and *Fol* SIX6 protein was purified by nickel affinity chromatography (Figure 3.3B). After tag cleavage and removal, SIX6 was further purified by size exclusion chromatography using fast protein liquid chromatography (FPLC, GE Healthcare AKTA pure) (Figure 3.3C) and concentrated by Amicon centrifugal concentrators (Figure 3.3D) for use in protein infiltration and other experiments. A similar process was used to produce *Foc* SIX6, *Fom* SIX6 and *Fov* SIX6 proteins (Figure 3.3E). Gel electrophoresis of the purified SIX6 proteins revealed multiple lower molecular weight contaminants (Figure 3.3D and 3.3E). Protein gel blot analysis of His-tagged *Fol* SIX6 during production showed the occurrence of

C-terminal truncations of *Fol* SIX6 proteins early during purification (Appendix 3.5). This suggests that in the case of *Fol* SIX6, at least some of the lower molecular weight bands were C-terminal truncation products. The entire protein purification and production procedures were performed in collaboration with Daniel Yu (Williams Laboratory, ANU).

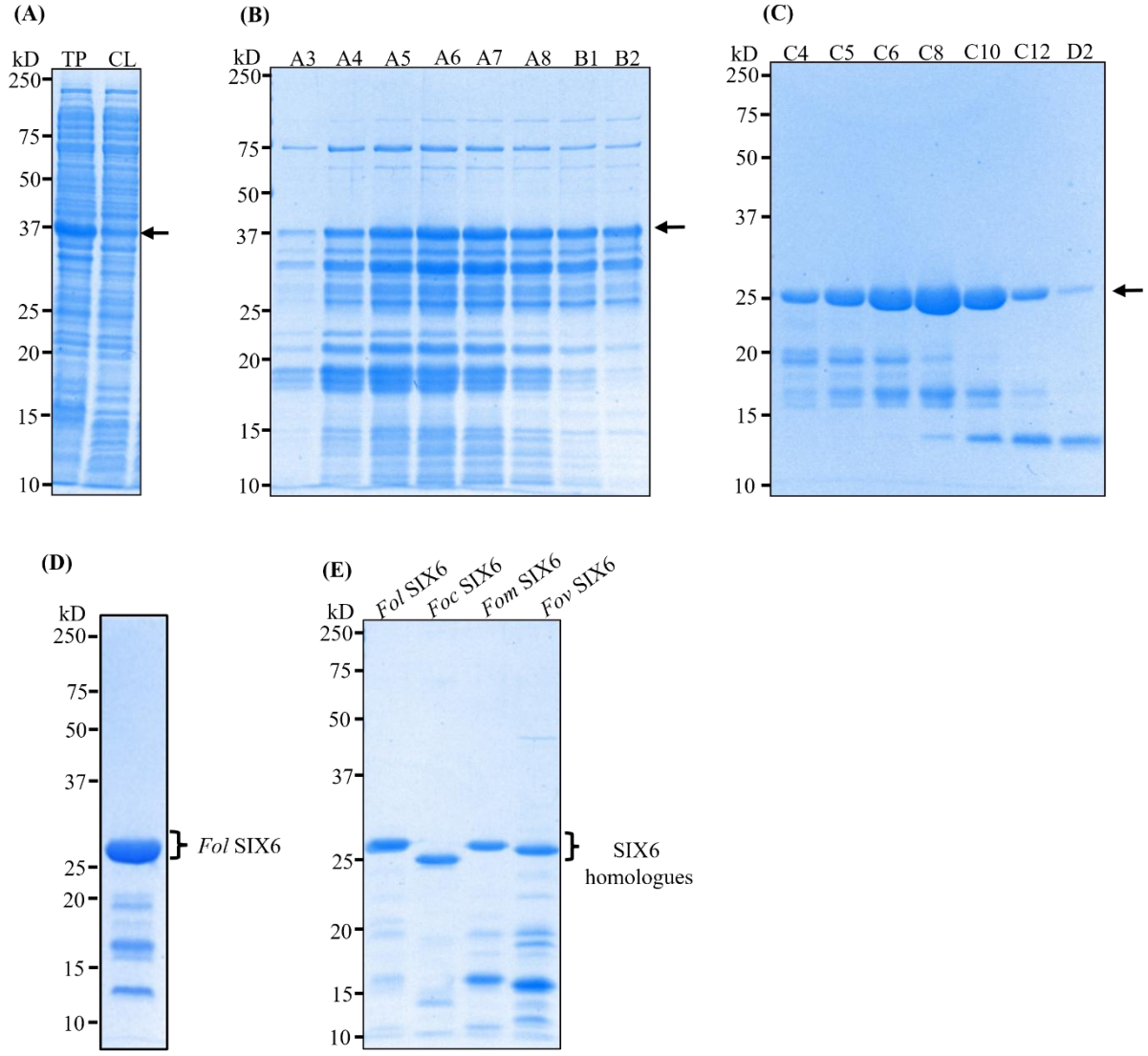

Figure 3.3 SDS-PAGE analysis of SIX6 proteins during and after purification.

(A) Clarified lysate (CL) of *Fol* SIX6 was separated from the total protein (TP) by centrifugation. **(B)** *Fol* SIX6 was purified using nickel affinity chromatography. Fractions corresponding to peaks of absorbance at 280 nm were collected and analysed by SDS-PAGE. **(C)** After tag cleavage and removal, SIX6 was further purified by size exclusion chromatography using fast protein liquid chromatography, and fractions corresponding to peaks of absorbance at 280 nm were collected and analysed by SDS-PAGE. **(D)** In the final step of purification, *Fol* SIX6 protein was concentrated by Amicon centrifugal concentrators. **(E)** The same general process was used to produce *Fol*, *Foc*, *Fom* and *Fov* SIX6 proteins. Letters with numbers, e.g. A3, indicate fractions collected. The work was conducted in

collaboration with Daniel Yu, and the image is sourced from Daniel Yu's Honours thesis at the Australian National University.

Purified *Fol* SIX6 was diluted in water to concentrations ranging from 10 µg/ml to 200 µg/ml and infiltrated into leaves of *N. benthamiana* as described previously (section 3.2.13) with water used as a negative control. A concentration of 20 µg/ml was sufficient for *Fol* SIX6 to cause cell death in *N. benthamiana* (Figure 3.4A). Protein purified from the vector-only control (100 µg/ml) did not cause any cell death (Appendix 3.6), indicating that cell death was specific to *Fol* SIX6. With biologically active *Fol* SIX6 now available, the possibility that *Fol* SIX6 could induce cell death in tomato was re-investigated. Purified recombinant *Fol* SIX6 protein was found to induce a strong cell death response in tomato (Figure 3.4B).

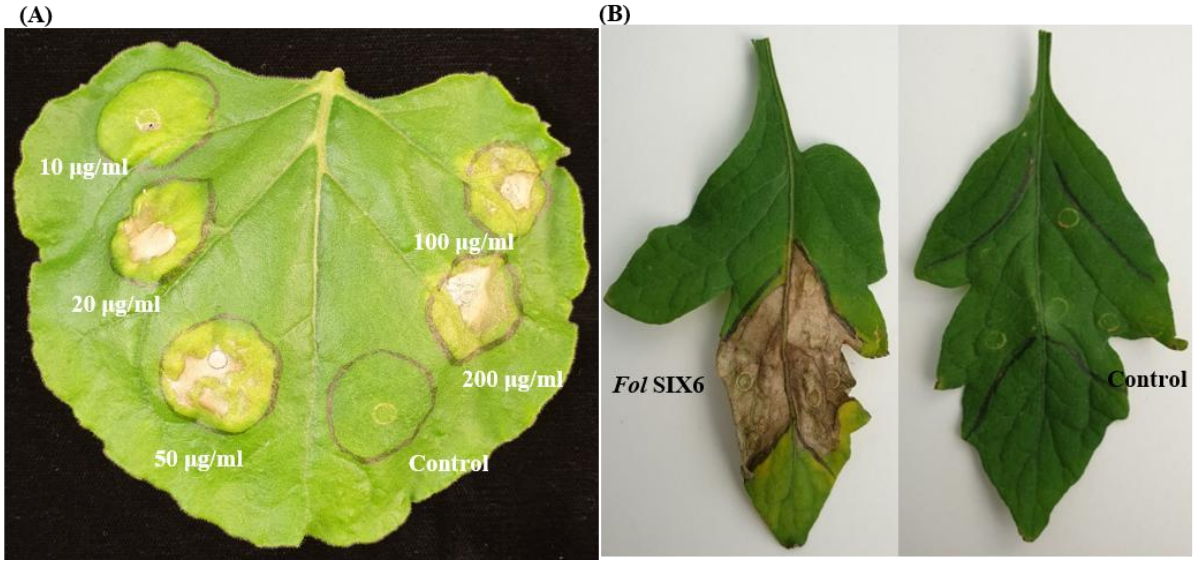

Figure 3.4 *Fol* SIX6 protein causes cell death in *N. benthamiana* and tomato.

(A) Leaves of *N. benthamiana* were infiltrated with various concentrations of recombinant *Fol* SIX6 protein diluted in water. **(B)** Cell death induced in tomato cv. M82 following infiltration with recombinant *Fol* SIX6 (100 µg/ml) protein diluted in water. Water was used as a negative control in (A) and (B). Photographs were taken 6 days after protein infiltration.

3.3.3 DTT treatment but not heat treatment affects the cell death-inducing activity of *Fol* SIX6 protein

Fol SIX6 contains eight cysteine residues that could potentially form four disulphide bonds (Figure 3.2). To find out whether heat treatment affected the ability of *Fol* SIX6 to induce cell death, the protein was heated at 95°C for 5 minutes and then infiltrated into leaves of *N. benthamiana* along with controls (untreated *Fol* SIX6 protein, heat-treated buffer). Heat treated

Fol SIX6 protein still caused cell death in *N. benthamiana,* indicating that it was resistant to heat denaturation (Figure 3.5A). To assess whether disulphide bonds were important for the ability of *Fol* SIX6 to cause cell death, the protein was heated at 95°C for 5 minutes with the disulphide reducing agent DTT and infiltrated into leaves of *N. benthamiana* along with controls (untreated *Fol* SIX6 protein, DTT-treated buffer). DTT-treated *Fol* SIX6 protein was unable to cause cell death (Figure 3.5B). When untreated, heat-treated and DTT-treated *Fol* SIX6 protein samples were analysed by SDS-PAGE, a band shift was visible in the DTT-treated protein sample relative to the untreated control, confirming that DTT treatment had reduced the disulphide bonds, whereas there was no band shift in the case of the heat-treated protein sample (Figure 3.5C). These findings indicate that disulphide bonds are not only required for the structural integrity of the *Fol* SIX6 protein but also for its ability to cause cell death in *N. benthamiana*.

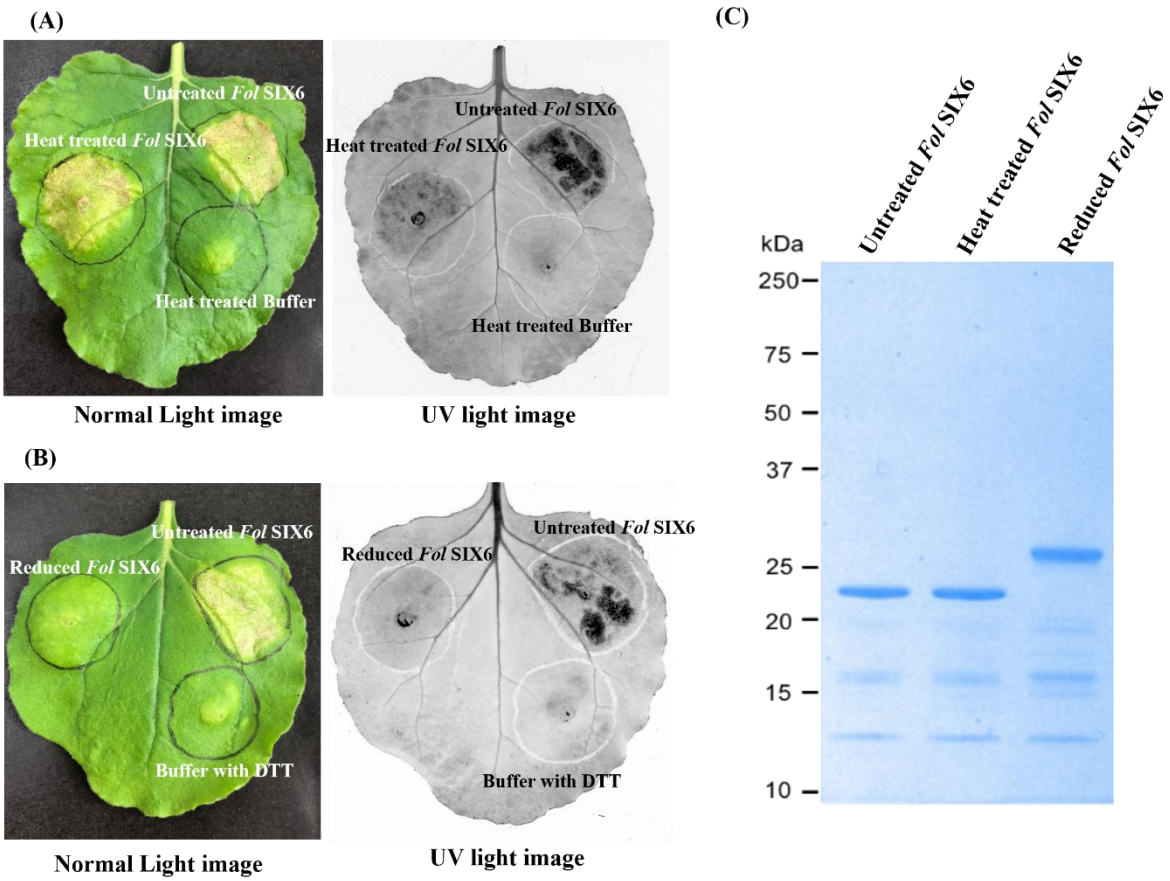

Figure 3.5 Effects of heat and DTT treatments on cell death induced by *Fol* SIX6 in *N. benthamiana.*

(A, B) *Fol* SIX6 protein (100 µg/ml) was **(A)** heat-treated at 95°C for 5 minutes or **(B)** reduced by the addition of 2 mM DTT (final concentration) and heating to 95°C for 5 minutes, then

cooled on ice and infiltrated into leaves of *N. benthamiana* alongside untreated *Fol* SIX6 (100 µg/ml) protein and heat or DTT-treated buffer. Visible light (left) and UV (right) images were photographed 6 days after infiltration. **(C)** SDS-PAGE analysis of untreated, heat-treated, and DTT-treated *Fol* SIX6 proteins used for infiltration into the leaves of *N. benthamiana*. The work was conducted in collaboration with Daniel Yu, and the image is sourced from Daniel Yu's Honours thesis at the Australian National University.

3.3.4 Homologues of *Fol* SIX6 induce cell death responses of different intensities

To test their relative abilities to cause cell death in *N. benthamiana*, *Fom*, *Foc* and *Fov* SIX6 proteins were expressed and purified as described above for *Fol* SIX6 and equal concentrations of *Fol*, *Fom*, *Foc* and *Fov* SIX6 were infiltrated into leaves of *N. benthamiana*. *Fol* and *Fom* SIX6 showed strong cell death responses, whereas *Foc* and *Fov* SIX6 showed chlorosis with spots of cell death (Figure 3.6A and 3.6B), indicating that homologues of *Fol* SIX6 are able to cause cell death in *N. benthamiana* but with different intensities. SDS-PAGE analysis showed the presence of SIX6 proteins of the expected size in the preparations used for infiltration (Figure 3.6C).

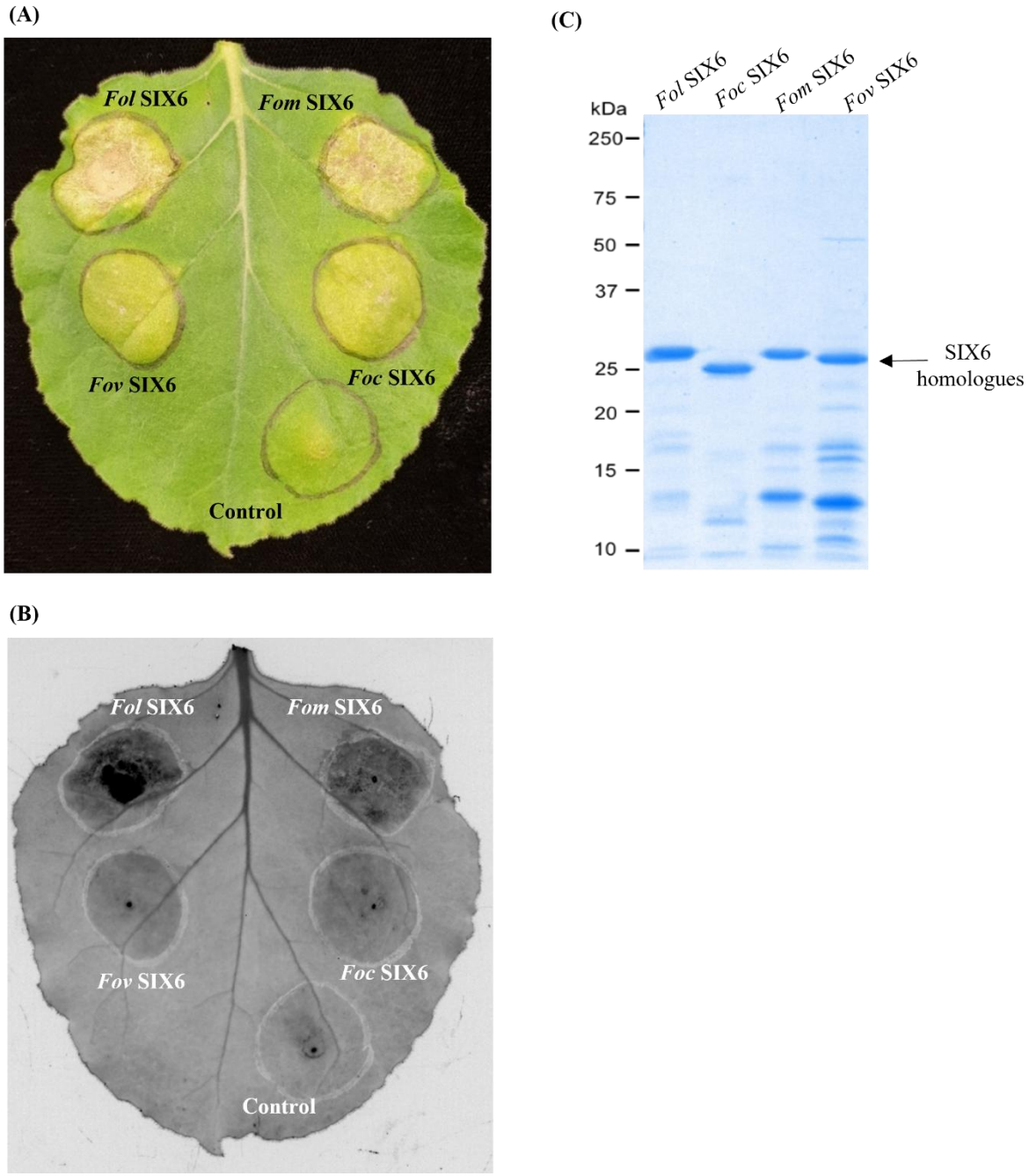

Figure 3.6 Cell death induced by recombinant SIX6 proteins in *N. benthamiana.*

(A, B) Recombinant SIX6 protein preparations were diluted in water to achieve equal SIX6 concentrations of 100 µg/ml and infiltrated into leaves of *N. benthamiana*. Visible light **(A)** and UV images **(B)** were photographed 6 days after infiltration. **(C)** SDS-PAGE analysis of the SIX6 proteins used for infiltration into leaves of *N. benthamiana*. The work was conducted in collaboration with Daniel Yu, and the image is sourced from Daniel Yu's Honours thesis at the Australian National University. I did the infiltration work while Daniel ran SDS-PAGE analysis.

3.3.5 *Fol* SIX6 induces a variety of responses in different plant species

To test whether *Fol* SIX6 could induce cell death in plants more broadly, *Fol* SIX6 protein was infiltrated into cotyledons or leaves of several crop or ornamental plants representing different plant families (Appendix 3.1). All members of the Solanaceae tested showed strong confluent cell death responses apart from *N. tabacum* which showed chlorosis with patches of cell death (Figure 3.7A). Interestingly, eggplant only showed cell death in the distal portions of cotyledons. In the Cucurbitaceae, watermelon likewise showed cell death in the distal portions of cotyledons. Cucumber showed curling and chlorosis and rockmelon just showed chlorosis, but squash, zucchini and pumpkin showed no response (Figure 3.7B). In the Brassicaceae, radish, cabbage, turnip and mustard showed no response, whereas Arabidopsis showed cell death at the tips of leaves (Figure 3.7C). In the Fabaceae, a strong confluent cell death response was observed in the infiltrated areas of dwarf bean leaves, whereas only tip death was found in broad bean leaves, and pea showed no response (Figure 3.7D). In the Malvaceae, *Fol* SIX6 caused wilting and curling in cotton cotyledons and patches of cell death. *Gossypium sturtianum* showed browning and patches of cell death, whereas okra and hollyhock were largely unaffected (Figure 3.7E). In the Amaranthaceae, spinach showed chlorosis (Figure 3.7F). Flax, the only member of the Linaceae included in the study, showed wilting and curling with no sign of chlorosis or cell death. (Figure 3.7G). In the Asteraceae, calendula showed a strong cell death response in distal parts of the cotyledons, whereas sunflower was unaffected (Figure 3.7H). *Fol* SIX6 protein was also infiltrated into wheat, but it did not show any response (Appendix 3.7). In summary, *Fol* SIX6 showed a range of phenotypic effects besides confluent cell death and it also showed an unexpected degree of specificity among the various family members tested, making *Fol* SIX6 a semi-specific cell-death-inducing protein.

(A) Solanaceae

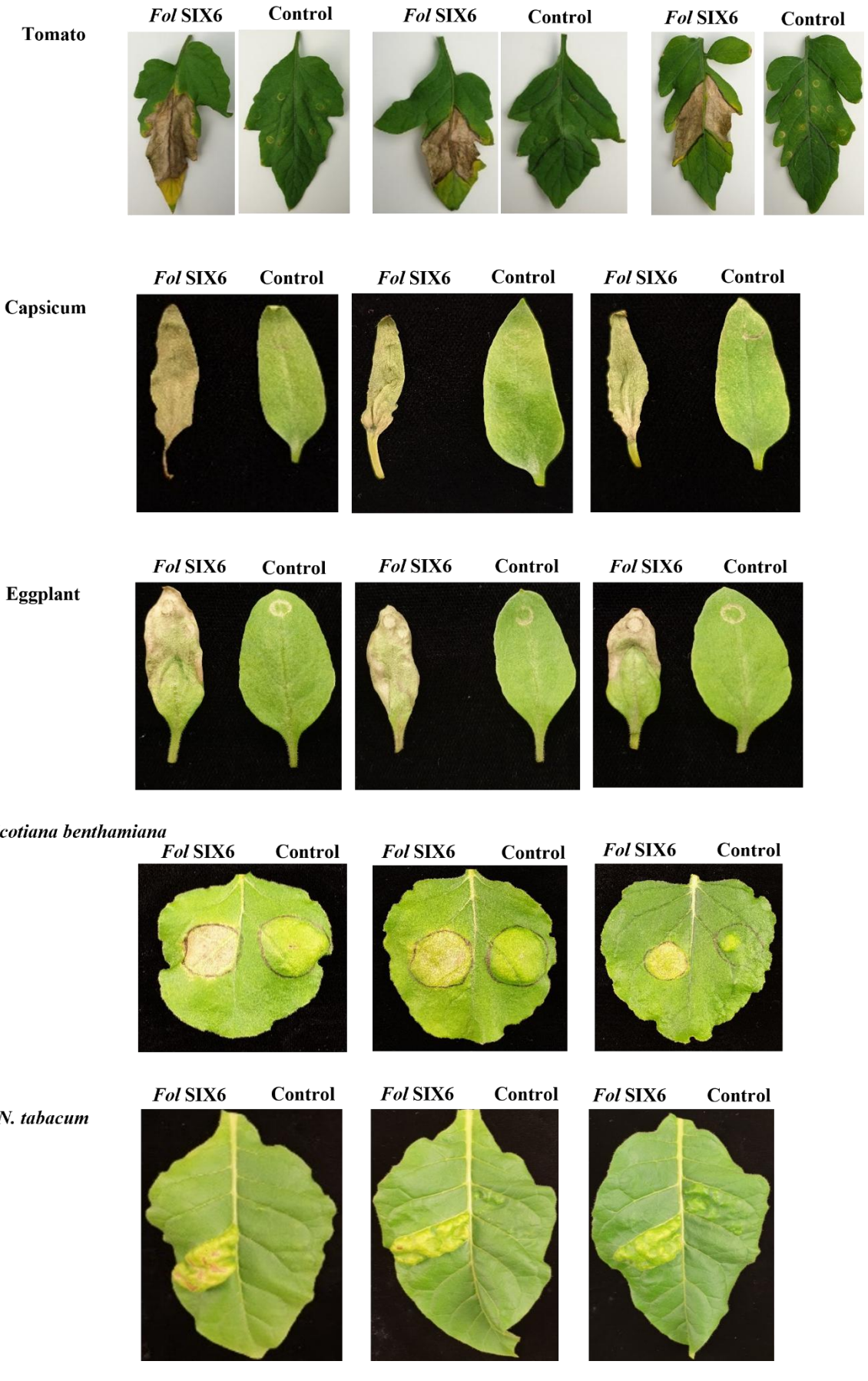

(B) Cucurbitaceae

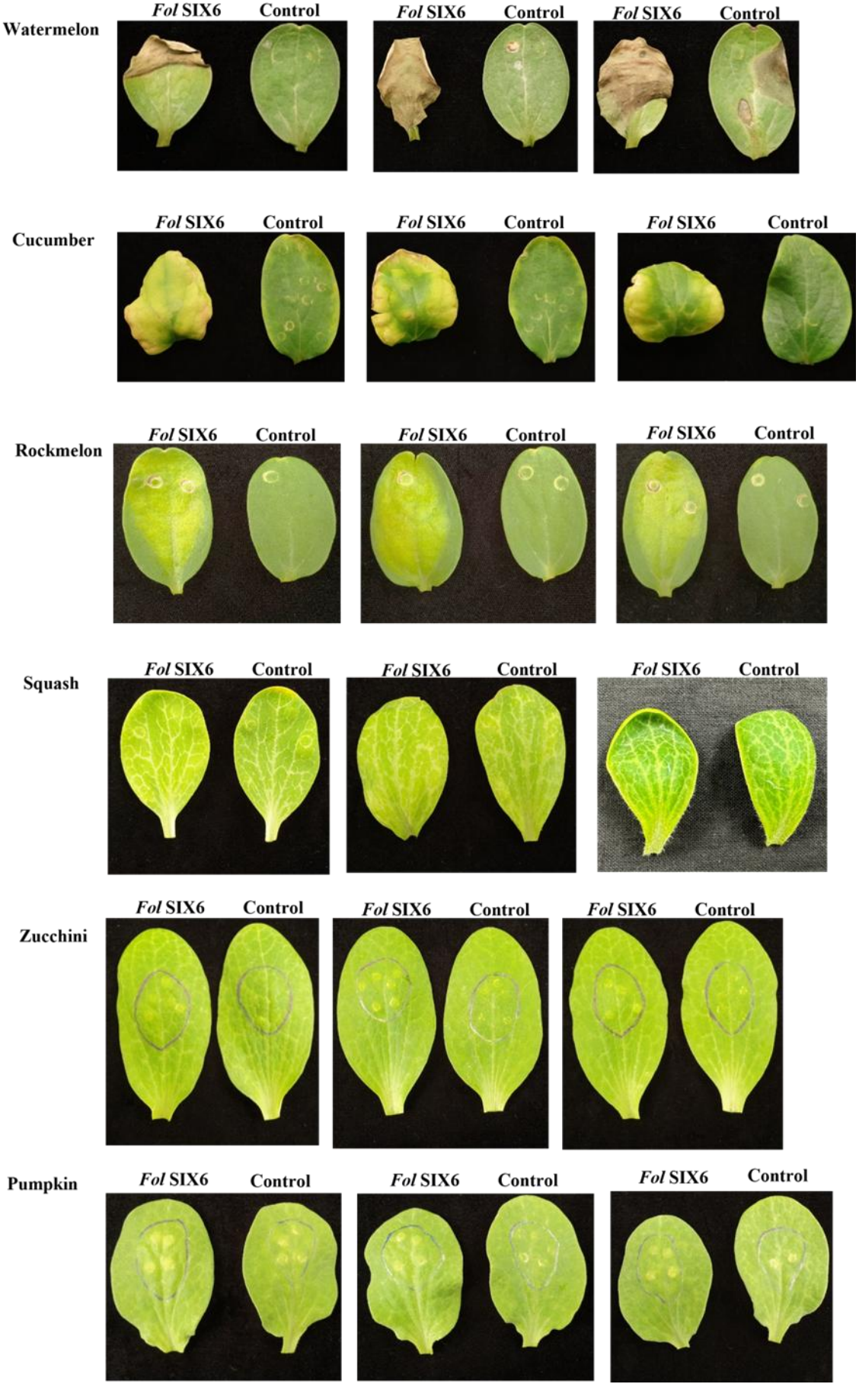

(C) Brassicaceae

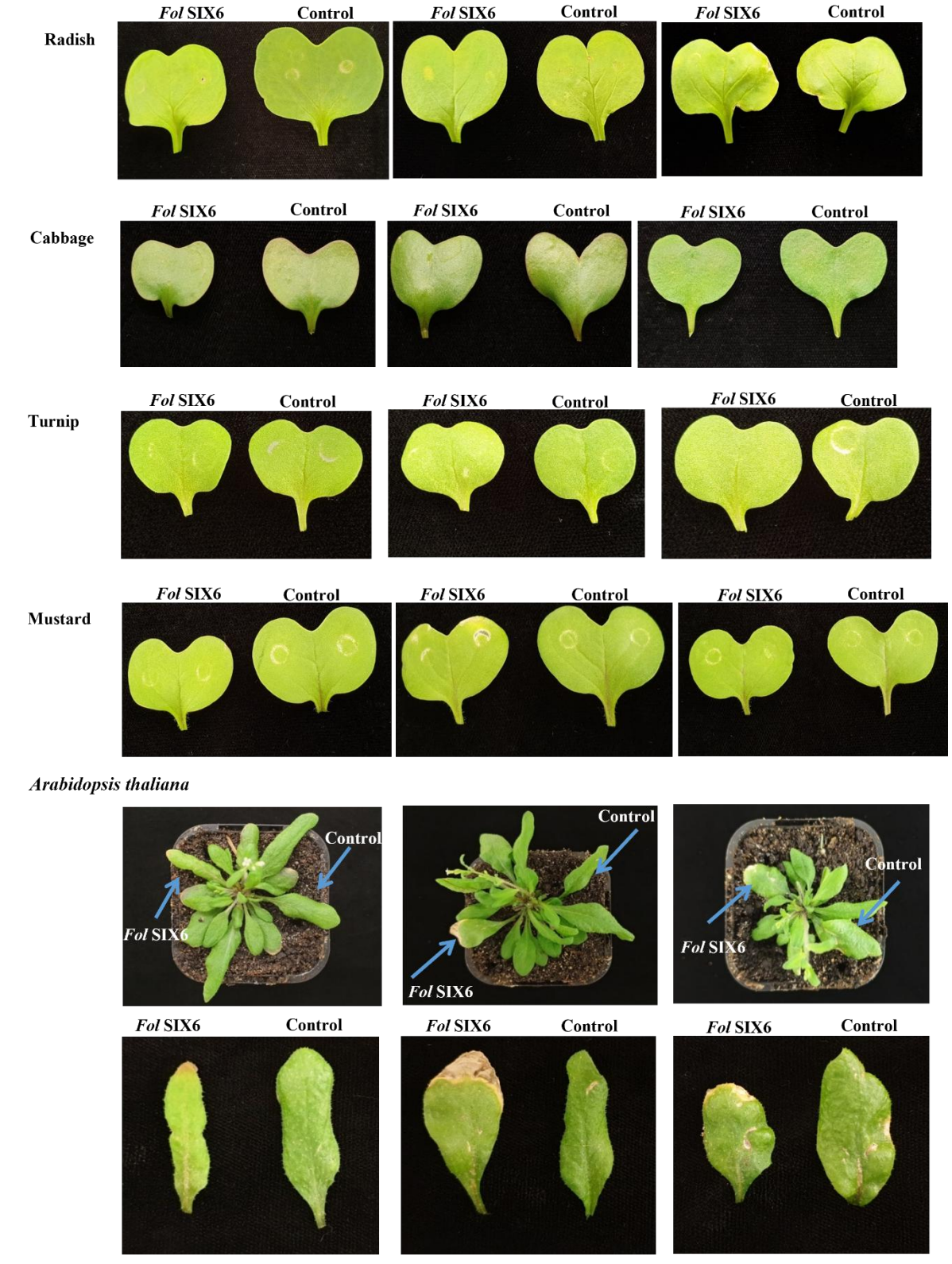

(D) Fabaceae

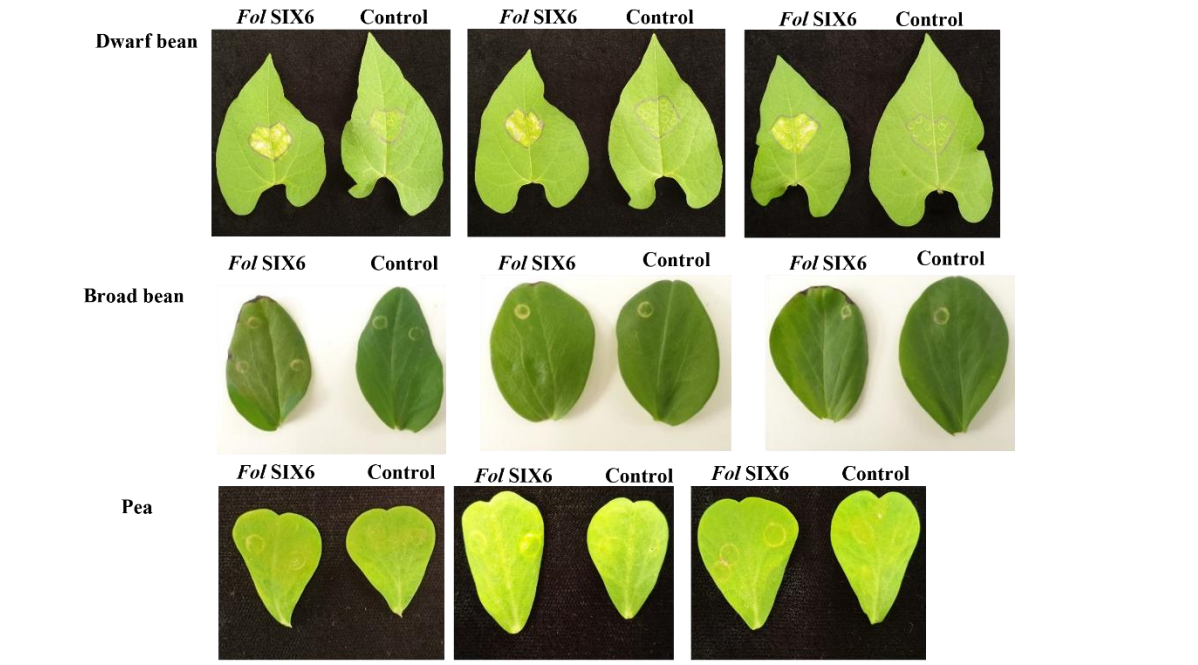

(E) Malvaceae

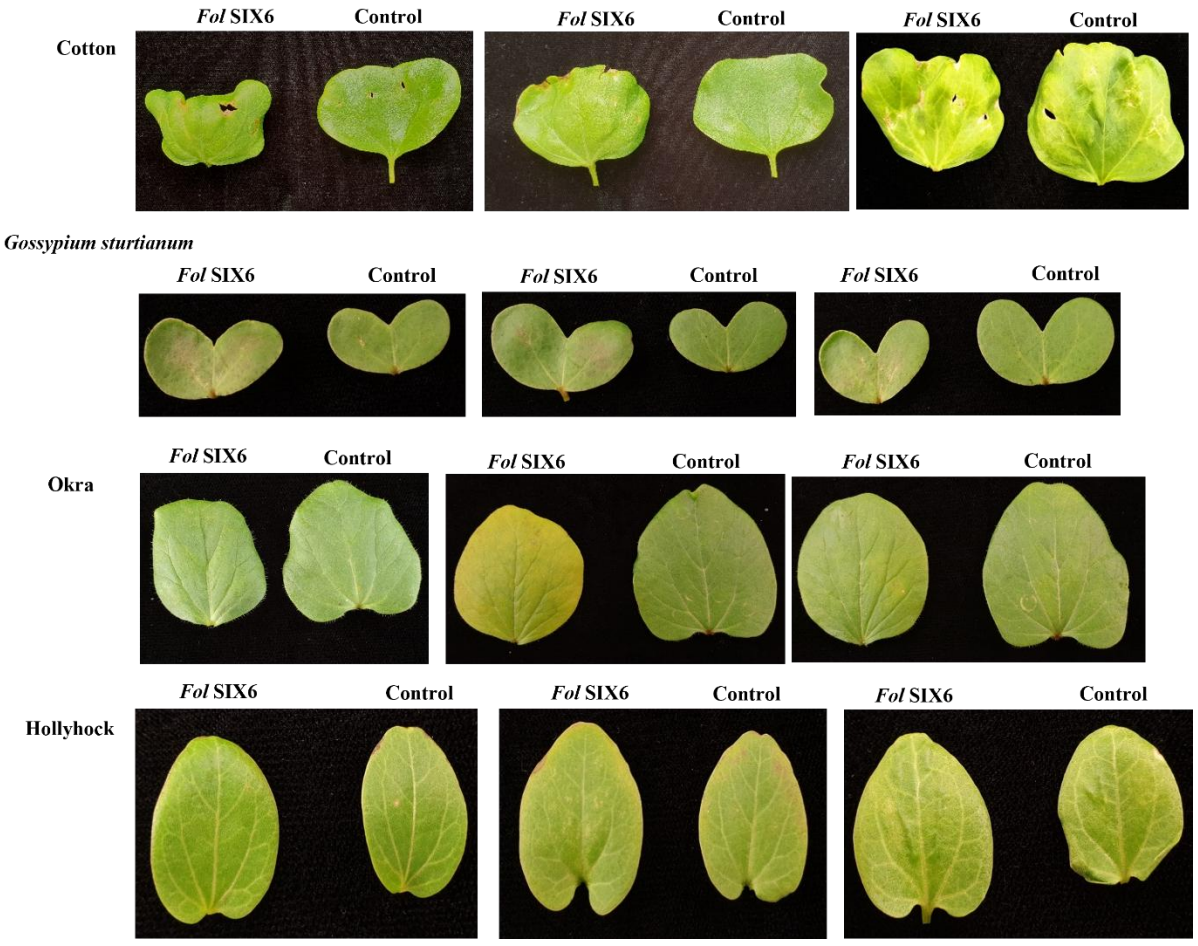

(F) Amaranthaceae

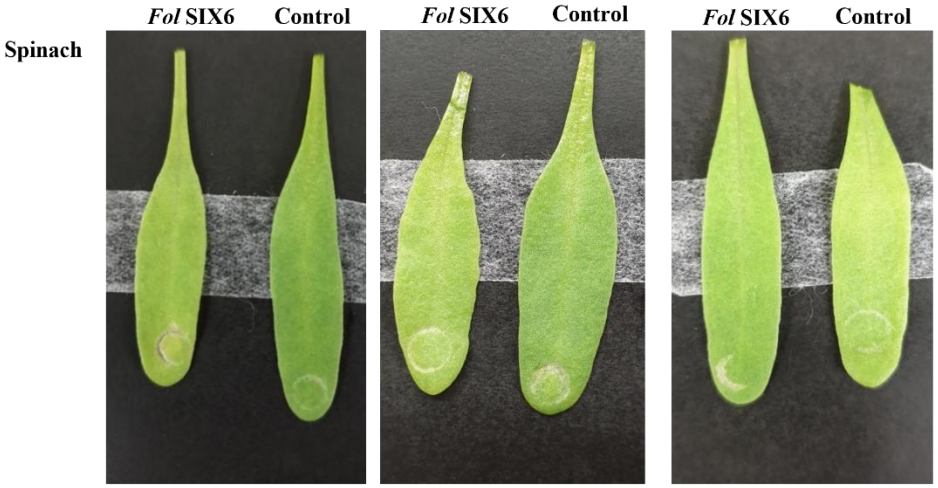

(G) Linaceae

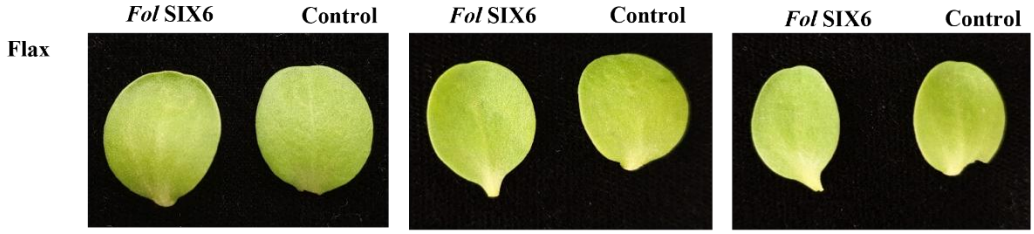

(H) Asteraceae

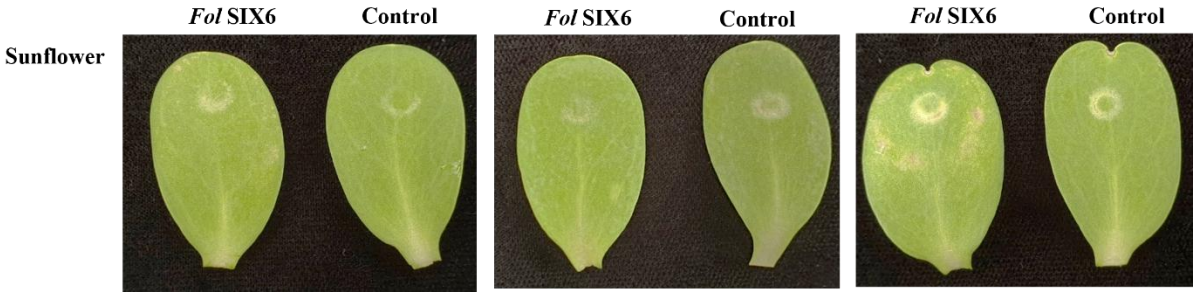

Figure 3.7 *Fol* SIX6 causes cell death in some plant species, but different responses or no response in other species.

Fol SIX6 protein at a concentration of 100 µg/ml and water (control) were infiltrated into leaves or cotyledons of representatives from the **(A)** Solanaceae, **(B)** Cucurbitaceae, **(C)** Brassicaceae, **(D)** Fabaceae, **(E)** Malvaceae **(F)** Amaranthaceae **(G)** Linaceae and **(H)** Asteraceae. Photographs were taken 6 days after protein infiltration.

3.3.6 *Fom* SIX6 and *Foc* SIX6 proteins induce similar responses compared to *Fol* SIX6 with some variations

To compare plant responses to SIX6 variants from other *formae speciales* of *F. oxysporum,* recombinant *Fom* SIX6 and *Foc* SIX6 proteins were tested on the same array of plant species used to test *Fol* SIX6. All members of the Solanaceae tested showed strong confluent cell death responses to *Fom* SIX6 except *N. benthamiana* which showed chlorosis with patches of cell death (Figure 3.8A). In the Cucurbitaceae, watermelon showed cell death in distal regions of the cotyledons, whereas rockmelon, cucumber, squash, zucchini and pumpkin showed little or no response (Figure 3.8B). None of the Brassicaceae tested showed any response to *Fom* SIX6 (Figure 3.8C). In the Fabaceae, patches of cell death were observed at infiltration sites in dwarf bean and tip death in broad bean, whereas pea leaves showed browning (Figure 3.8D). In the Malvaceae, *Fom* SIX6 caused wilting and curling in cotton cotyledons with chlorosis and patches of cell death, but had no effect in *Gossypium sturtianum*, okra or hollyhock (Figure 3.8E). In the Amaranthaceae, spinach did not show any response (Figure 3.8F). In the Linaceae, flax just showed chlorosis (Figure 3.8G). In the Asteraceae, calendula showed browning and sunflower remained unaffected (Figure 3.8H). Overall, *Fom* SIX6 showed a pattern of responses similar to that of *Fol* SIX6, with some quantitative differences e.g. in calendula and a few qualitative differences e.g. in cucumber.

(A) Solanaceae

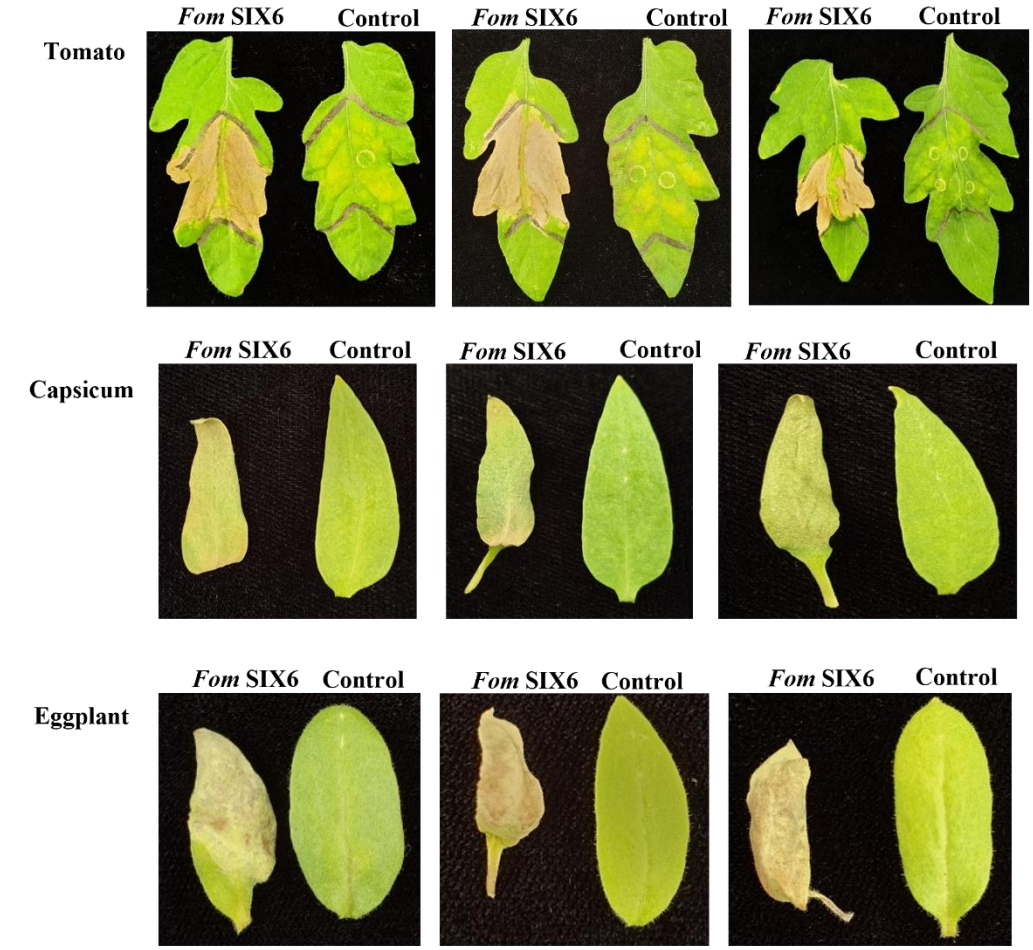

Nicotiana benthamiana

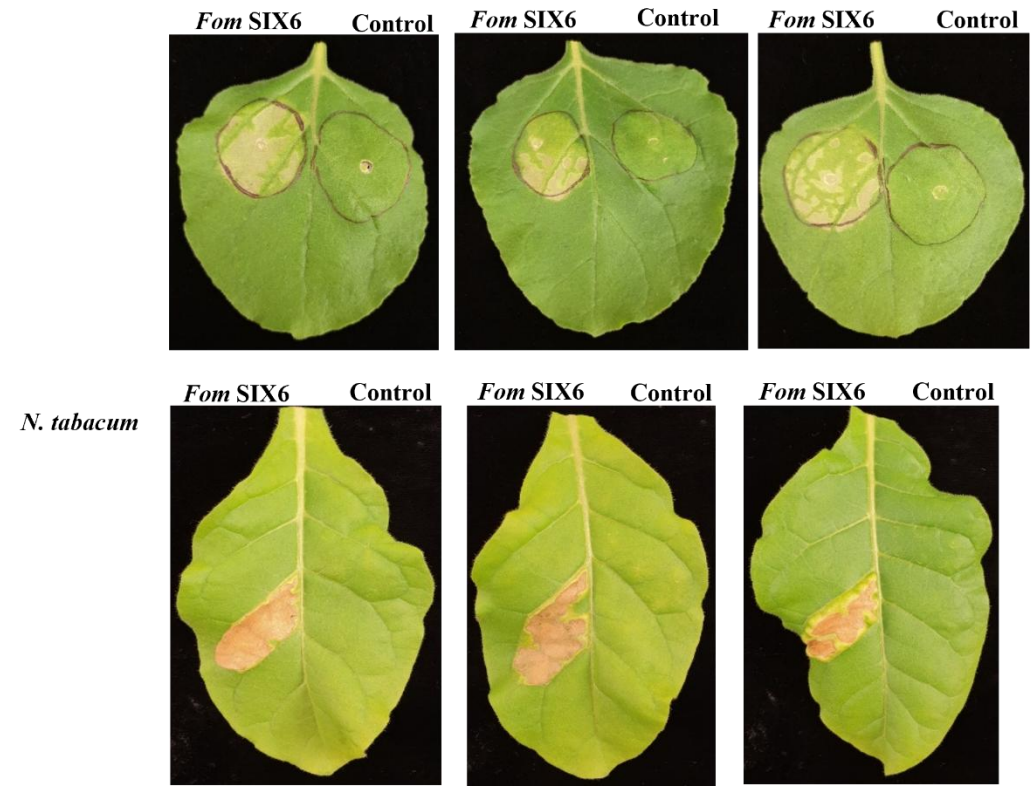

(B) Cucurbitaceae

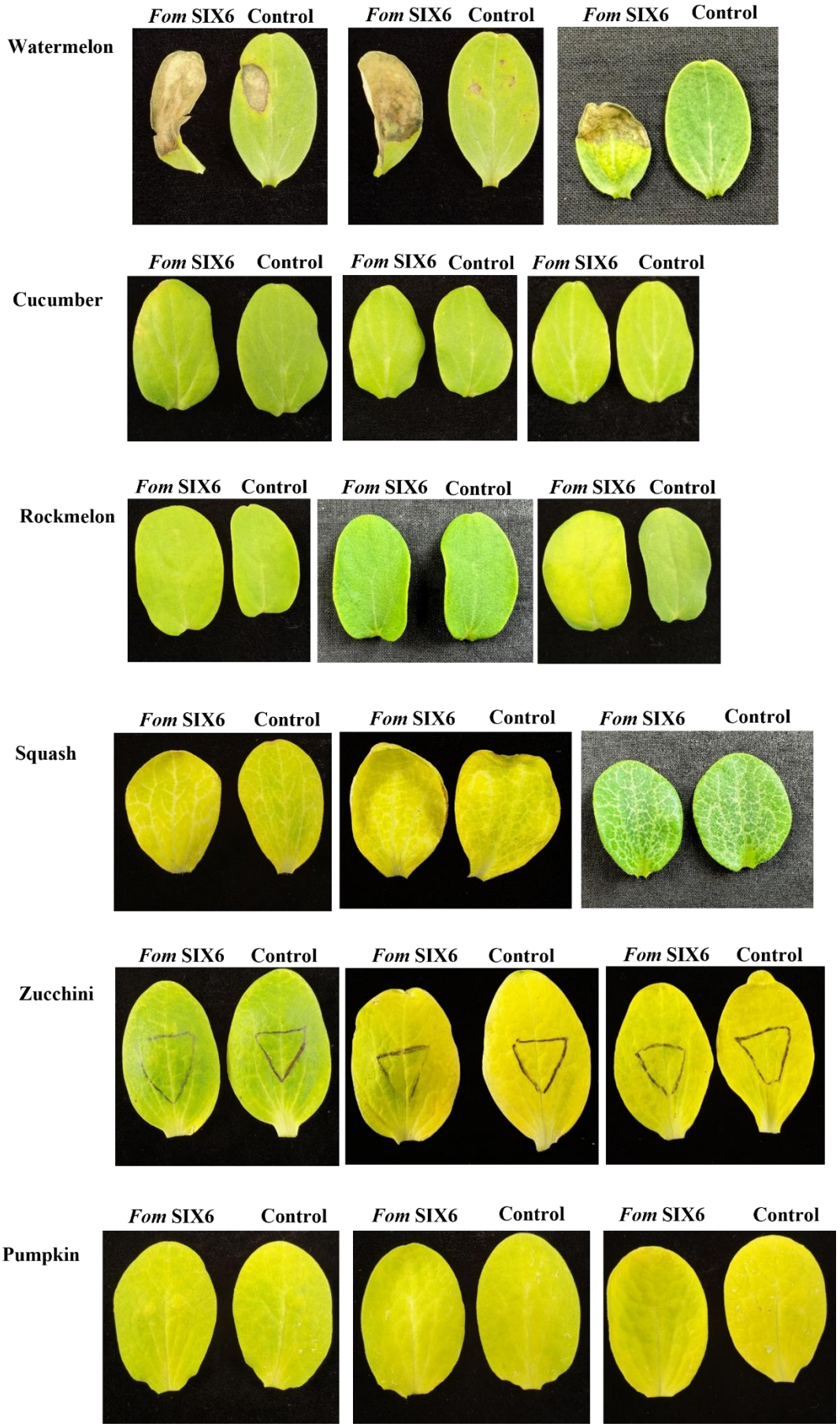

(C) Brassicaceae

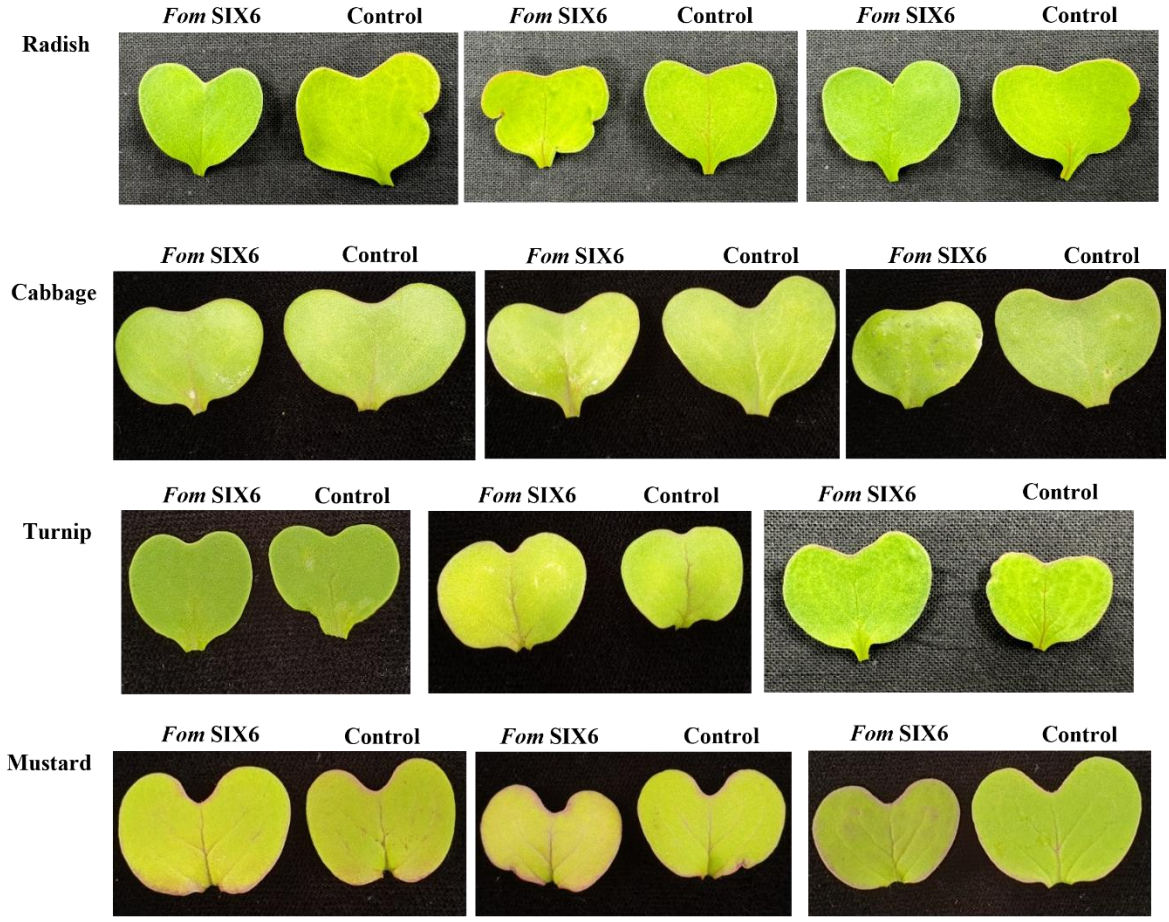

(D) Fabaceae

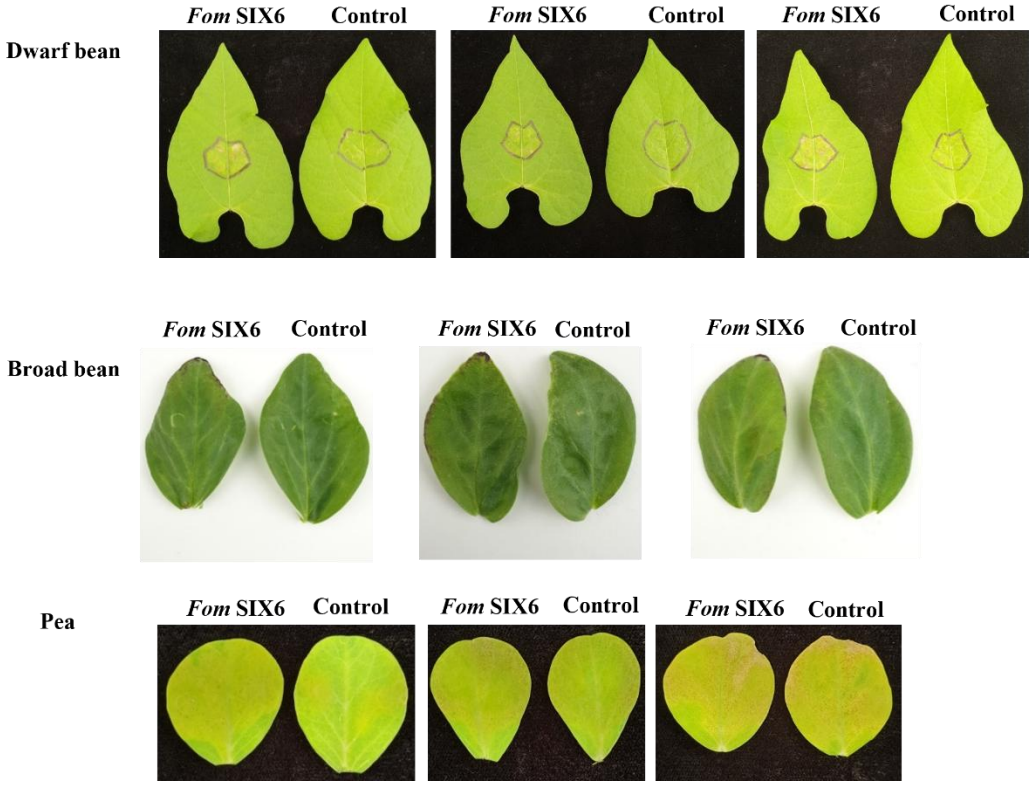

(E) Malvaceae

(F) Amaranthaceae

Figure 3.8 *Fom* SIX6 causes cell death in some plant species but different responses or no response in other species.

Fom SIX6 protein at a concentration of 100 µg/ml was infiltrated into the leaves or cotyledons of representatives from the **(A)** Solanaceae, **(B)** Cucurbitaceae, **(C)** Brassicaceae, **(D)** Fabaceae, **(E)** Malvaceae **(F)** Amaranthaceae **(G)** Linaceae and **(H)** Asteraceae. Photographs were taken 6 days after protein infiltration.

In the Solanaceae, *Foc* SIX6 caused chlorosis and patches of cell death in tomato and *N. benthamiana*, and chlorosis in *N. tabacum,* while capsicum showed a strong cell death response and eggplant showed no cell death (Figure 3.9A). In the Cucurbitaceae, watermelon and cucumber showed tip death, and cucumber and rockmelon showed chlorosis, but squash, zucchini and pumpkin showed no response (Figure 3.9B). In the Brassicaceae, cabbage showed flecks of chlorosis and cell death while radish, turnip and mustard showed no response (Figure

3.9C). In the Fabaceae, a strong cell death response was observed in dwarf bean, and tip death in broad bean, but pea showed a mixed response that included curling, chlorosis and patches of cell death (Figure 3.9D). In the Malvaceae, *Foc* SIX6 caused curling, chlorosis and patches of cell death in cotton, a strong cell death response in *Gossypium sturtianum*, and curling and chlorosis in okra, but hollyhock was unaffected (Figure 3.9E). In the Amaranthaceae, spinach did not show any response to *Foc* SIX6 protein infiltration (Figure 3.9F). In the Linaceae, flax showed no sign of chlorosis or curling. (Figure 3.9G). In the Asteraceae, calendula showed chlorosis and patches of cell death and sunflower showed no response (Figure 3.9H). Overall, *Foc* SIX6 showed a pattern of responses that bore some similarity to that of *Fol* SIX6 but contained a few more quantitative and qualitative differences.

(A) Solanaceae

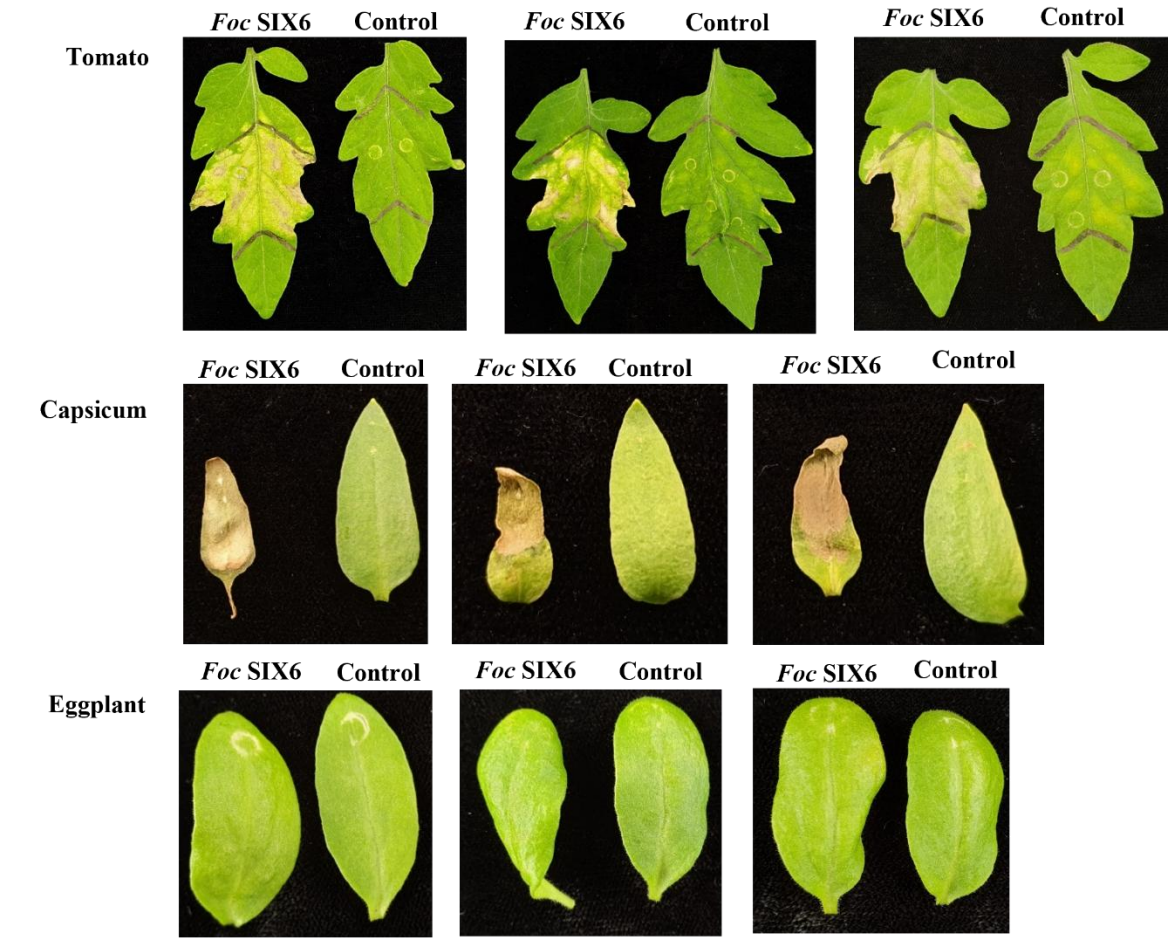

Nicotiana benthamiana

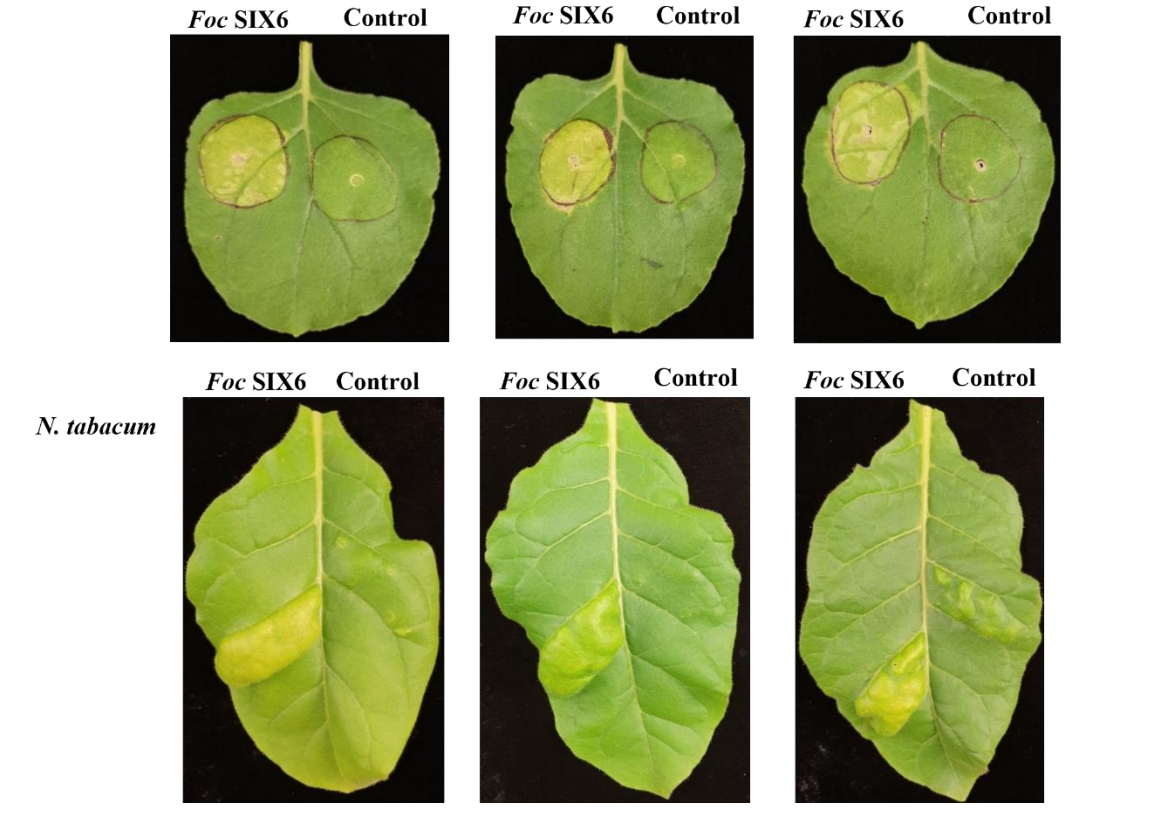

(B) Cucurbitaceae

(C) Brassicaceae

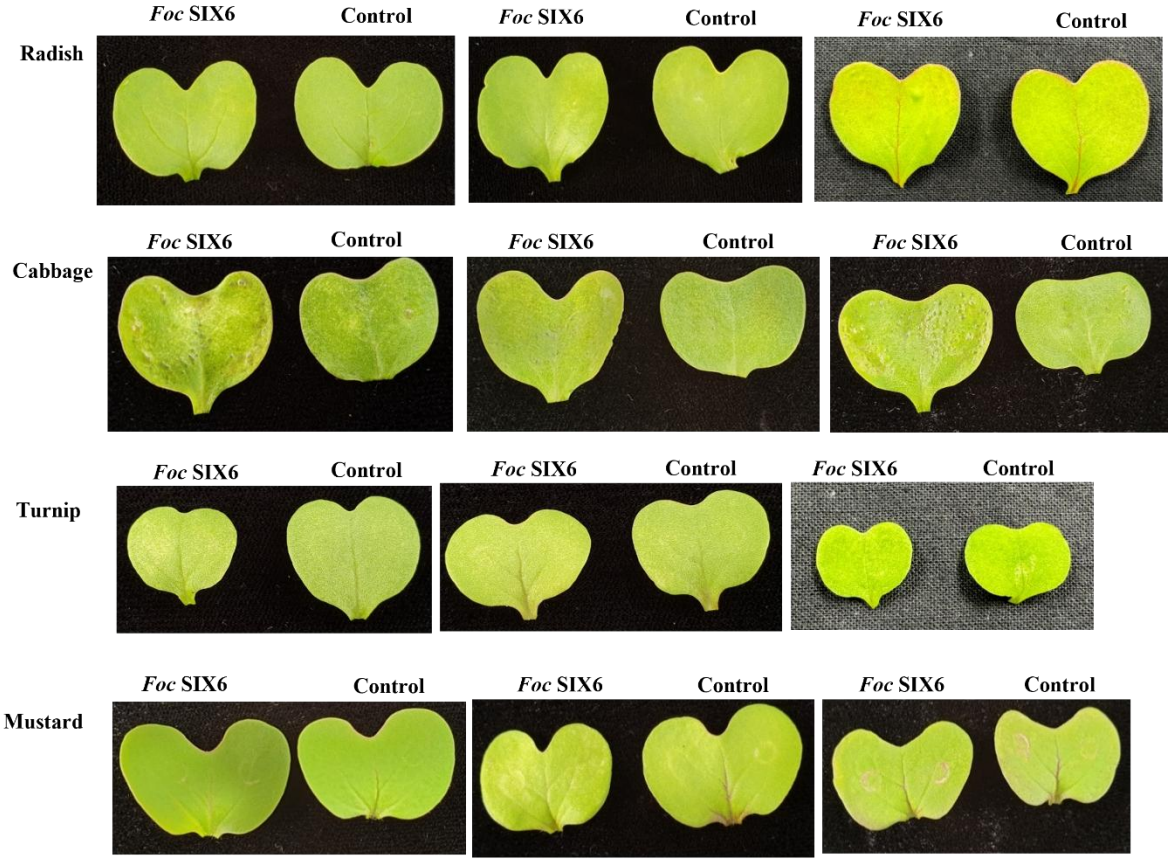

(D) Fabaceae

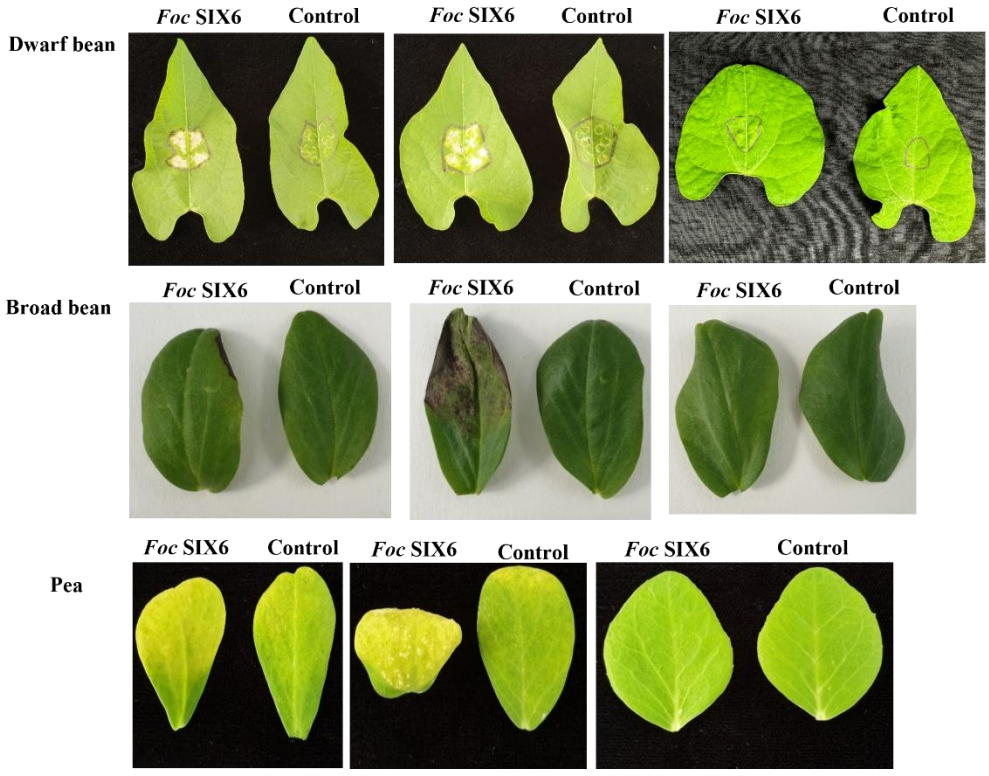

(E) Malvaceae

Cotton

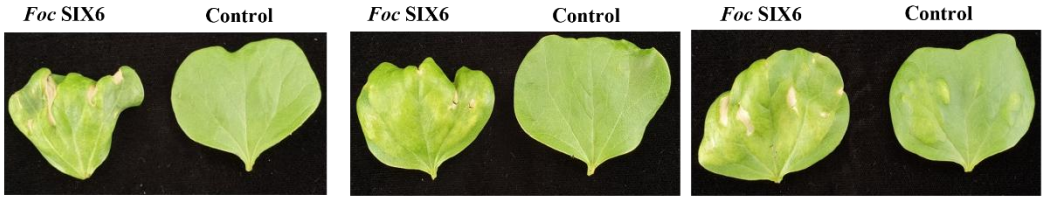

Gossypium sturtianum

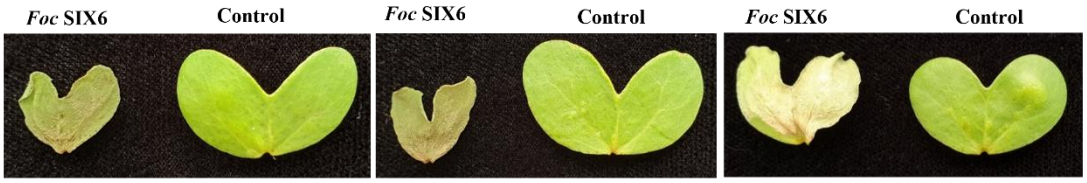

Okra

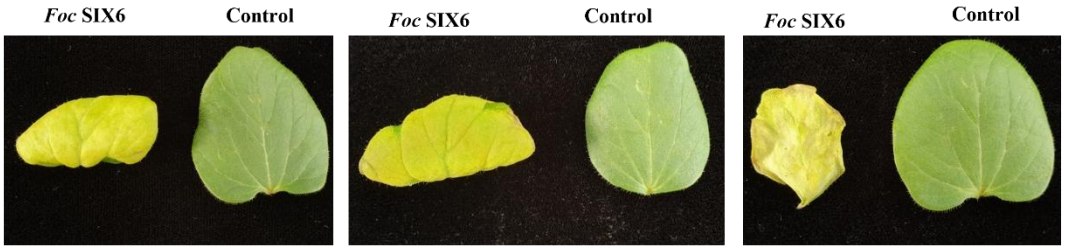

Hollyhock

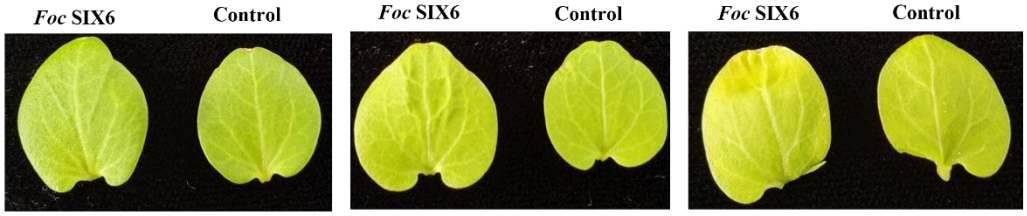

(F) Amaranthaceae

Spinach

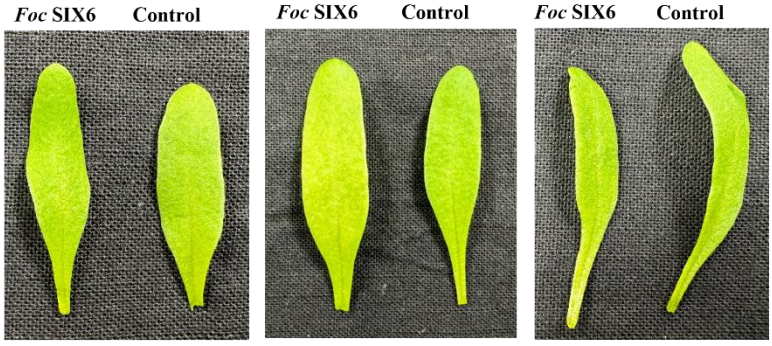

(G) Linaceae

Flax

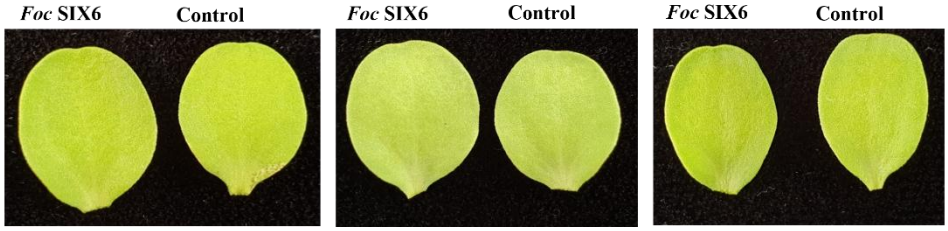

Figure 3.9 *Foc* SIX6 causes cell death in some plant species but a different response or no response in other species.

Foc SIX6 protein at a concentration of 100 µg/ml was infiltrated into the leaves or cotyledons of representatives from the **(A)** Solanaceae, **(B)** Cucurbitaceae, **(C)** Brassicaceae, **(D)** Fabaceae, **(E)** Malvaceae **(F)** Amaranthaceae **(G)** Linaceae, and **(H)** Asteraceae. Photographs were taken 6 days after protein infiltration.

SIX6 was found to cause other responses beside chlorosis and cell death in some plant species (Figures 3.7-3.9). For example, *Fol* SIX6 was found to cause cotyledon curling preceded by wilting in cotton and flax, whereas *Fom* SIX6 caused wilting and curling in flax but not cotton and vice versa for *Foc* SIX6 (Figure 3.10). *Fol* SIX6 was found to cause cotyledon curling and chlorosis without wilting in cucumber (Figure 3.10). *Foc* SIX6 was found to cause curling and chlorosis in okra (Figure 3.10).

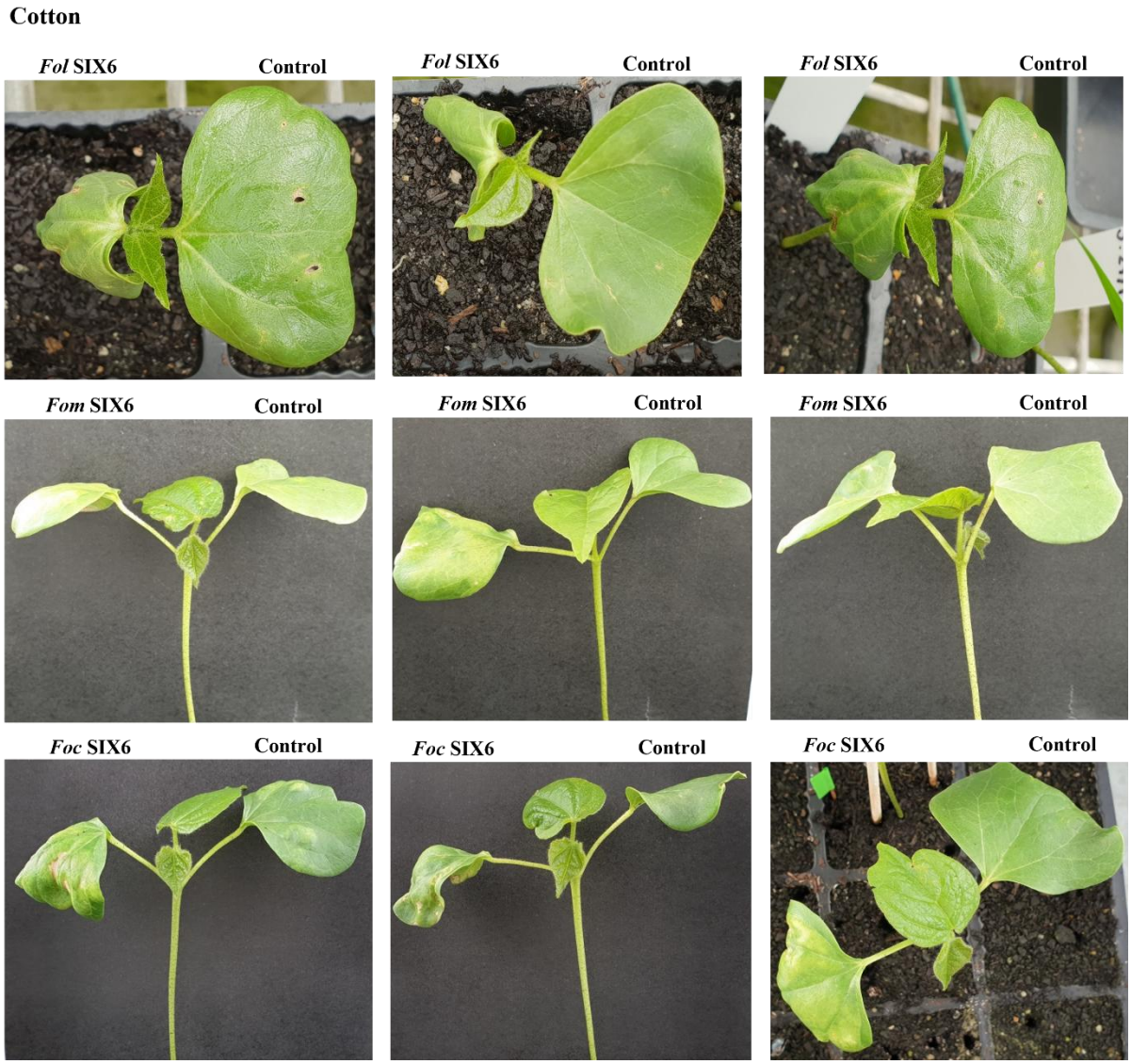

Flax

Fol SIX6
Control
Fol SIX6
Control
Fol SIX6
Control
Fom SIX6
Control
Fom SIX6
Control
Fom SIX6
Control
Foc SIX6
Control
Foc SIX6
Control
Foc SIX6
Control

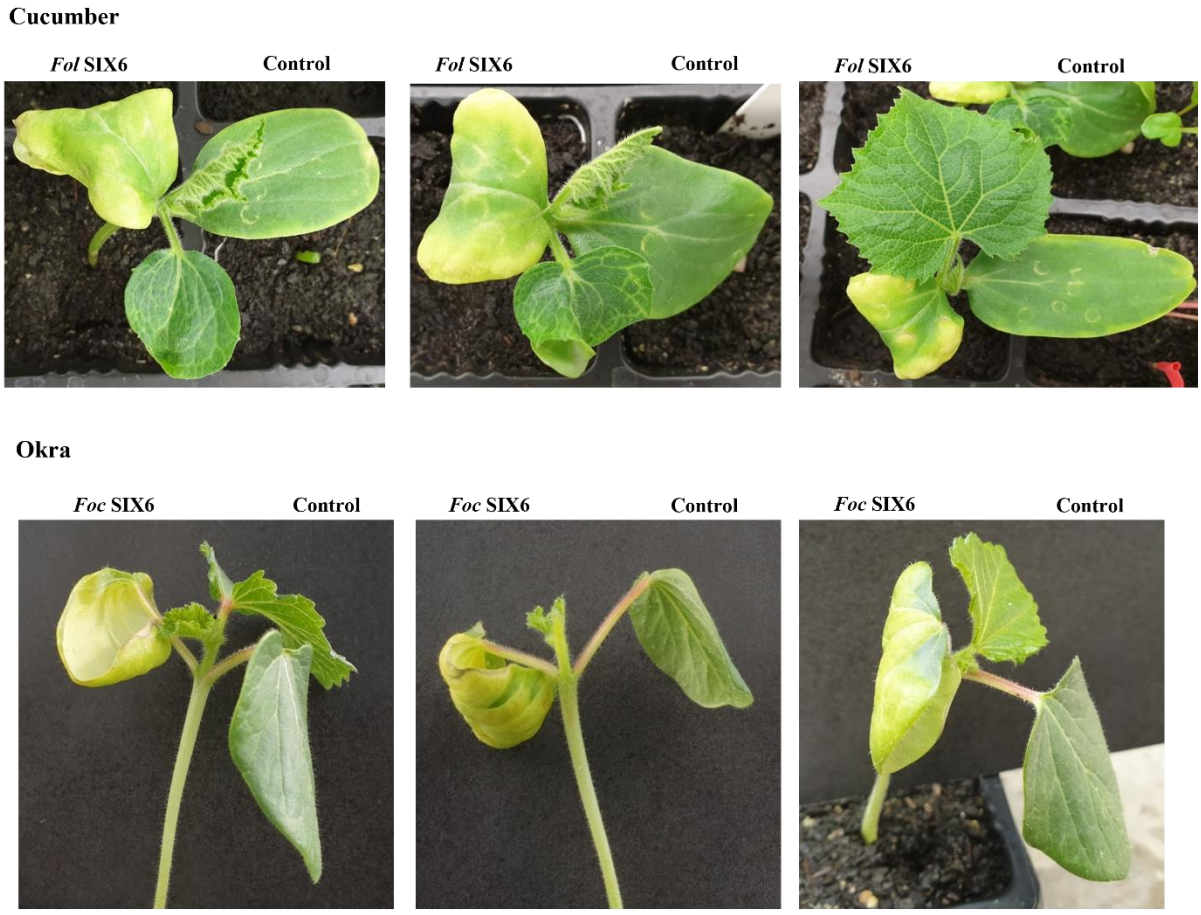

Figure 3.10 *SIX*6 causes wilting and curling of cotyledons in some plant species.

Fol, Fom and *Foc* SIX6 proteins at a concentration of 100 µg/ml and water (control) were infiltrated into cotyledons of cotton, cucumber and okra. White arrows in flax infiltration indicate *Fol*, *Fom* or *Foc* SIX6 protein infiltrated cotyledon.

Figure 3.11 summarises the data from Figures 3.7, 3.8 and 3.9 in a graphic side-by-side comparison. Collectively, these data suggest that the three SIX6 proteins tested showed a similar underlying pattern of responses among the members of the plant families tested. Most members of the Solanaceae showed strong cell death responses to all three SIX6 proteins (Figure 3.11). Most members of the Brassicaceae and Cucurbitaceae, apart from watermelon, showed no response (Figure 3.11). In the Fabaceae, dwarf bean consistently showed a strong cell death response and broad bean consistently showed tip death. In the Malvaceae, cotton consistently showed chlorosis and patches of cell death while hollyhock did not show any response (Figure 3.11). Interestingly, eggplant, pea, flax and okra showed qualitatively distinct responses to *Foc* SIX6 compared to *Fol* SIX6 and *Fom* SIX6. Overall, responses to *Fol* SIX6 showed more similarity with *Fom* SIX6 than *Foc* SIX6 (Figure 3.11), which could be a consequence of their greater (97% versus 67%) sequence similarity (Figure 3.2).

Family	Name	*Fol* SIX6			*Fom* SIX6			*Foc* SIX6		
Solananceae	Tomato							• • •	• • •	• • •
	Capsicum								•	•
	Eggplant									
	N. benthamiana					• • •	• • •	• • •	• • •	• • •
	N. tabacum	• • •	• • •							
Cucurbitaceae	Watermelon							(	(	
	Cucumber	((	((	(				(	(	
	Rockmelon									
	Squash									
	Zucchini									
	Pumpkin									
Brassicaceae	Radish									
	Cabbage							• • •	• • •	• • •
	Turnip									
	Mustard									
	A. thaliana	(	(	(	Not tested			Not tested		
Fabaceae	Dwarf bean				• • •	• • •	• • •			
	Broad bean	(	(	(	(	(	(	(		
	Pea							• • •	•(• •	
Malvaceae	Cotton	(•(•	(•(•	(• •	• • •	• • •	• • •	•(• •	•(• •	•(• •
	G. sturtianum									
	Okra							(	(	• • •
	Hollyhock									
Amaranthaceae	Spinach									
Linaceae	Flax	(			(		(			
Asteraceae	Calendula							(• •	(• •	(• •
	Sunflower			• • •						

No cell death

Chlorosis

Cell death

Cell death in distal half

Chlorosis in distal half

(Wilting and/or downward curling

(Tip and/or lateral cell death

• • • Patches of cell death

Browning

Figure 3.11 A graphic comparison of the effects of *Fol*, *Fom* and *Foc* SIX6 on different plant species.

This figure was made using colours and symbols to summaries the protein infiltration data shown in Figures 3.7, 3.8 and 3.9.

3.3.7 SIX6 proteins from different *ff. spp.* induce stronger cell death in their corresponding host plants than in non-host plants

From the SIX6 protein infiltration experiments shown in sections 3.3.5 and 3.3.6 and summarised in section 3.3.7, it was evident that the *Fol* and *Fom* SIX6 proteins induced strong cell death in their corresponding host plants (Figure 3.12). Cell death induced by *Foc* SIX6 could not be investigated in banana because infiltration of banana leaves was too difficult owing to their highly vascularised architecture, although the NLP protein (Lenarcic et al., 2017) used as a positive control showed cell death (Appendix 3.8). The yield of *Fov* SIX6 was too low to check its activity in a range of different plant species, but sufficient protein was obtained for testing in cotton (the host of *Fov*), which showed a strong cell death response (Figure 3.12).

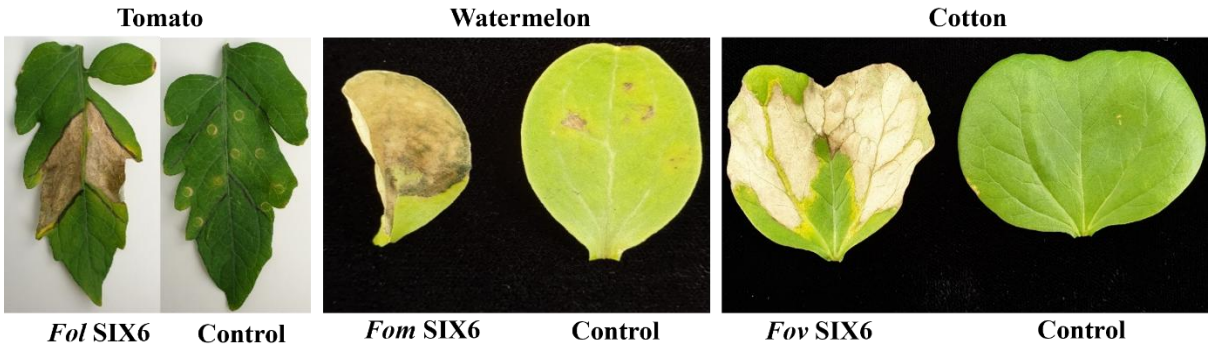

Figure 3.12 Recombinant *Fol*, *Fom* and *Fov* SIX6 proteins induce strong cell death responses in their respective plant hosts.

Fol, Fom and *Fov* SIX6 proteins were infiltrated at a concentration of 100 µg/ml into leaflets of tomato, watermelon cotyledons and cotton cotyledons, respectively. The tomato and watermelon images were taken from Figures 3.7 and 3.8 for comparison purposes. Water was used as a negative control on the opposite leaflet or cotyledon from the same plant or seedling. Photographs were taken 6 days after infiltration.

To investigate whether there was any host specificity in these responses, equal concentrations of *Fol* SIX6 and *Fov* SIX6 were infiltrated into leaflets of tomato and cotyledons of cotton. *Fol* SIX6 produced a strong cell death response in tomato, whereas *Fov* SIX6 induced a much weaker response (Figure 3.13A). Conversely, *Fov* SIX6 produced a strong cell death response in cotton, whereas *Fol* SIX6 induced a much weaker response (Figure 3.13B). These results suggest that there is a degree of host specificity in the cell death response caused by the various SIX6 homologues in different plant species.

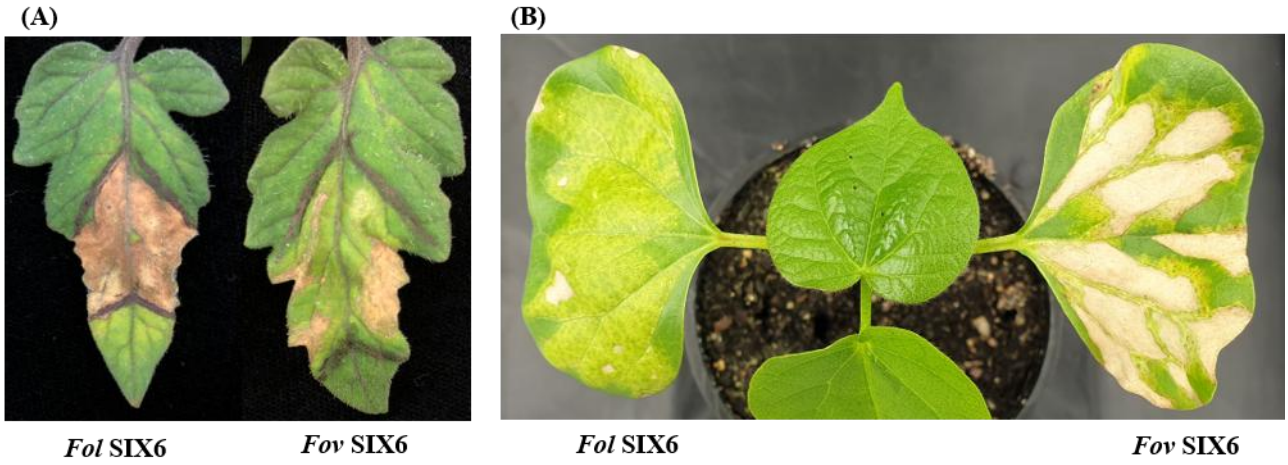

Figure 3.13 Cell death responses induced by *Fol* SIX6 and *Fov* SIX6 proteins in tomato and cotton.

Recombinant *Fol* SIX6 and *Fov* SIX6 proteins at a concentration of 50 µg/ml were infiltrated into opposite leaflets on the same tomato leaf and cotyledons of the same cotton seedling. Photographs were taken 4 days after infiltration. The work was conducted in collaboration with Daniel Yu, and the image is sourced from Daniel Yu's Honours thesis at the Australian National University.

3.4 Discussion

3.4.1 *Fol* SIX6 is a semi-specific cell death-inducing protein

Fol SIX6 is an effector secreted in the xylem sap of tomato by *Fol* during the infection. Gawehns et al. (2014) reported that *Fol* SIX6 suppressed I-2 mediated cell death when expressed in planta, however, the sequence used in their study was incomplete and expressed without a signal peptide, thereby directing it to the plant cytosol rather than the apoplast (Figure 3.14). The incomplete sequence used by Gawehns et al. (2014) replaced 19 amino acids encoded by exon 2 of *SIX6* with either nine amino acids encoded by the intron between exons 1 and 2 (assuming the splice-donor site was non-functional in the absence of the splice-acceptor site) or an unknown vector-encoded sequence (assuming the splice-donor site functioned in conjunction with a substitute vector-encoded splice-acceptor site). In addition to the resulting loss of a cysteine residue required for disulphide bond formation, cytosolic expression of SIX6 would have prevented disulphide bond formation altogether. The lack of four disulphide bonds that would otherwise have formed would be expected to have a major negative impact on the structure and function of SIX6.

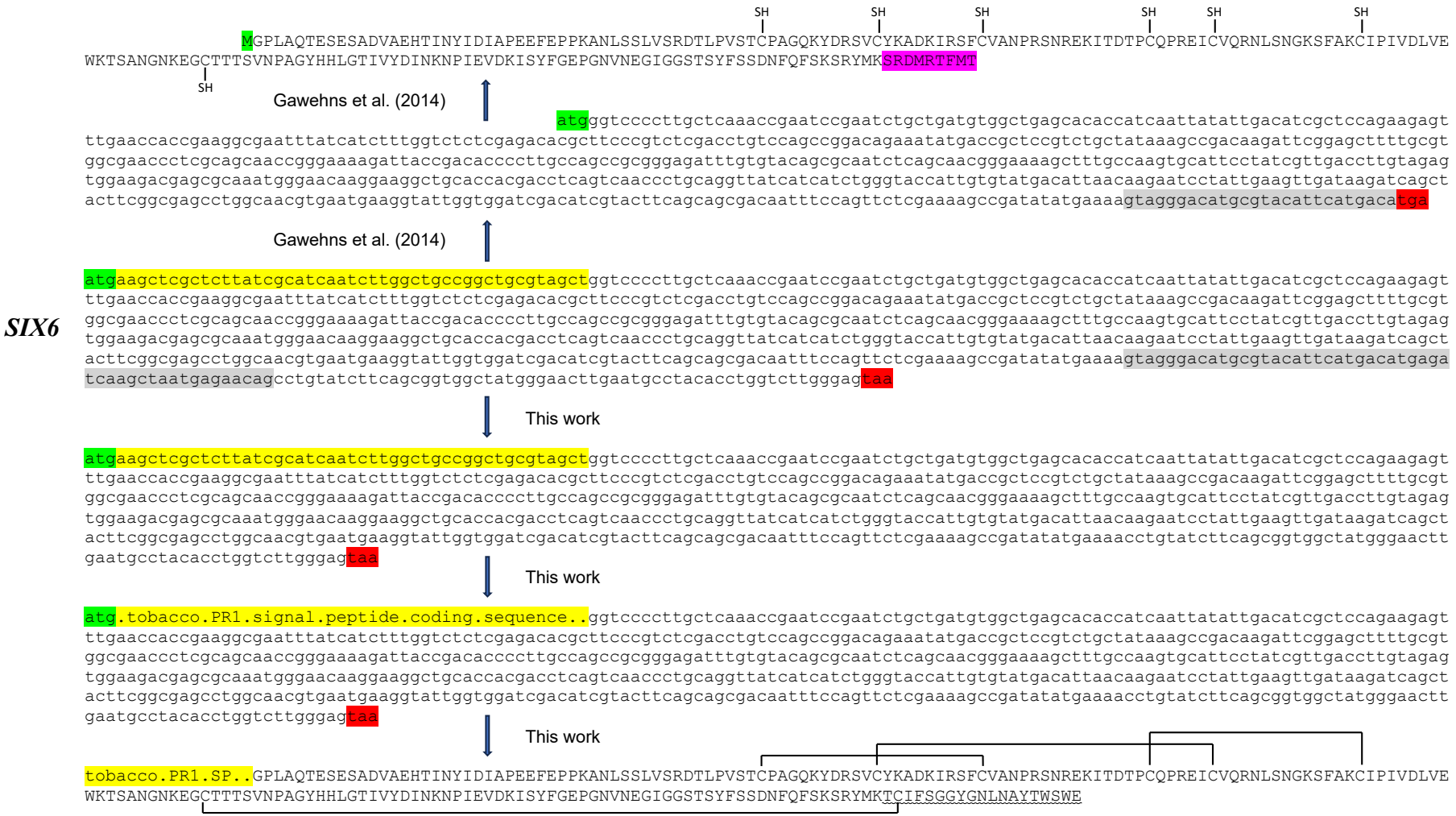

Figure 3.14 Comparison of SIX6 sequences expressed by Gawehns et al. (2014) and in this study.

Gawehns et al. (2014) expressed a truncated version of SIX6 lacking its signal-peptide coding sequence (yellow) and truncated at a stop codon (red) in the intron (grey), resulting in a protein with exon-2-encoded amino-acids replaced by intron-encoded amino-acids (magenta) and unable to form disulphide bonds. By comparison, a secreted, complete version of SIX6 able to form disulphide bonds was used in this study.

In this study, a complete *Fol SIX6* sequence with a tobacco PR1 signal-peptide coding sequence in place of its own signal-peptide coding sequence (Figure 3.14) was tested via agroinfiltration for ability to induce *I-7*-mediated cell death in the leaves of *N. benthamiana* and *N. tabacum* (Chapter 2). Surprisingly, agroinfiltration with *Fol SIX6* alone was found to induce a strong cell death response in the leaves of *N. benthamiana* and *N. tabacum* (Figure 3.1A and Figure 3.1B). However, when *Fol SIX6* was agroinfiltrated into tomato leaves, no cell death was observed (Appendix 3.4). Agroinfiltration of *Avr1* in *I* tomato plants also failed to induce cell death indicating that agroinfiltration was not working in tomato. To overcome this problem, *Fol SIX6* was expressed in *E. coli* and SIX6 protein extracted and purified using nickel affinity chromatography, size exclusion chromatography. Purified *Fol* SIX6 protein was found to cause cell death in tomato (Figure 3.4). *Fol* SIX6 is demonstrated by its ability to induce cell death responses across multiple plant families (Solanaceae, Cucurbitaceae, Fabaceae, Malvaceae, and Asteraceae) while showing no effect in others (most Brassicaceae members, some Cucurbitaceae, and monocots like wheat) (Figure 3.7). Furthermore, the protein exhibited marked selectivity even within plant families, as evidenced by strong responses in some species (dwarf bean, eggplant) while closely related species (pea, other Cucurbitaceae members) remained unaffected. This pattern of selective activity across diverse plant taxa, combined with intra-family specificity, indicates semi-specific nature of *Fol* SIX6 protein.

Effector proteins able to trigger plant cell death have also been identified in other pathosystems. Notable examples include SnToxA, SnTox1, SnTox2, and SnTox3 from *Stagonospora nodorum*, but unlike SIX6 they are highly specific and only able to cause cell death in wheat lines carrying the corresponding susceptibility genes *Tsn1*, *Snn1*, *Snn2* and *Snn3* respectively (Liu et al., 2006; Liu et al., 2009). Other cell-death inducing effectors are less specific. *CbNip1* encodes a necrosis-inducing effector produced by the hemibiotrophic fungus *Cercospora beticola* which causes leaf spot disease in sugar beet (Ebert et al., 2021). The CbNip1 protein was found to induced chlorosis followed by cell death in both it sugar beet host and in *N. benthamiana.* Expression of *CbNip1* is up regulated when the fungus switches from a biotrophic to necrotrophic lifestyle and gene knockout studies showed that it plays a critical role in *C. beticola* virulence (Ebert et al., 2021). *Fol* is also a hemibiotrophic fungus but unlike *CbNip1, Fol* SIX6 was expressed at both early and late stages of host infection. Understanding the contrasting expression patterns suggests that CbNip1 role is more tightly linked to the necrotrophic phase, and its function is possibly more specialised. This stage-specific expression could mean that targeting CbNip1 might disrupt the transition to necrosis,

potentially providing a strategic intervention point. Conversely, SIX6's persistent expression indicates it might be involved in maintaining infection throughout the pathogen's lifecycle, requiring different management strategies. Overall, the comparison underscores the diversity in infection strategies among hemibiotrophic fungi and emphasises the importance of understanding the timing and regulation of effector genes to develop effective disease control methods.

RsSCR10 is another cysteine-rich effector from *Rhizoctonia solani* that can cause cell death in *N. benthamiana* as well as Arabidopsis and plays a significant role in the virulence of *Rhizoctonia solani* (Niu et al., 2021). *RsSCR10* induced cell death creates a conducive environment for fungal growth and nutrition by decomposing host tissue and the functionality of *RsSCR10* relies on specific cysteine residues, which are essential for its ability to trigger cell death (Niu et al., 2021). The contrasting functions of *Fol* SIX6 and *RsSCR10* illustrate how effector proteins have evolved to support distinct pathogenic strategies. *RsSCR10'*s rapid cell death induction, coupled with immune suppression, directly facilitates *R. solani's* necrotrophic lifestyle by quickly creating the nutrient-rich dead tissue environment required for saprotrophic growth. In contrast, *Fol* SIX6's constitutive expression and semi-specific cell death activity reflects the complex requirements of hemibiotrophy, where the effector likely serves multiple functions across infection phases rather than immediate tissue destruction. Overall, SIX6 represents a novel effector that exhibits distinct differences compared to both host-specific and broad-host-range cell-death-inducing effectors. It also has other phenotypic impacts that make it unique.

3.4.2 *Fol* SIX6 homologues cause cell death and other phenotypes in different plant families

Purified recombinant SIX6 proteins were assessed for their potential to induce cell death across various plant species representing a range of plant orders across the core eudicots (Figure 3.15). The results demonstrated that infiltration of the SIX6 elicited a spectrum of responses ranging from confluent cell death, chlorosis and/or patches of cell death, tissue browning, apical cell death and wilting/leaf curling in some species, but no observable response in others (Figures 3.7 to 3.11). A degree of host specificity was observed in *Fol* SIX6 and *Fov* SIX6 proteins, where they were infiltrated into their respective host plants and vice versa (Figure 3.12). Infiltration with SIX6 protein consistently resulted in strong cell death responses in the Solanaceae, while none of the Brassicaceae exhibited any response apart from leaf tip death in

A. thaliana. Other plant families showed a mixture of cell death and other responses. This suggests that SIX6 has a degree of specificity towards the Solanaceae, thereby classifying it as a semi-specific cell death-inducing protein.

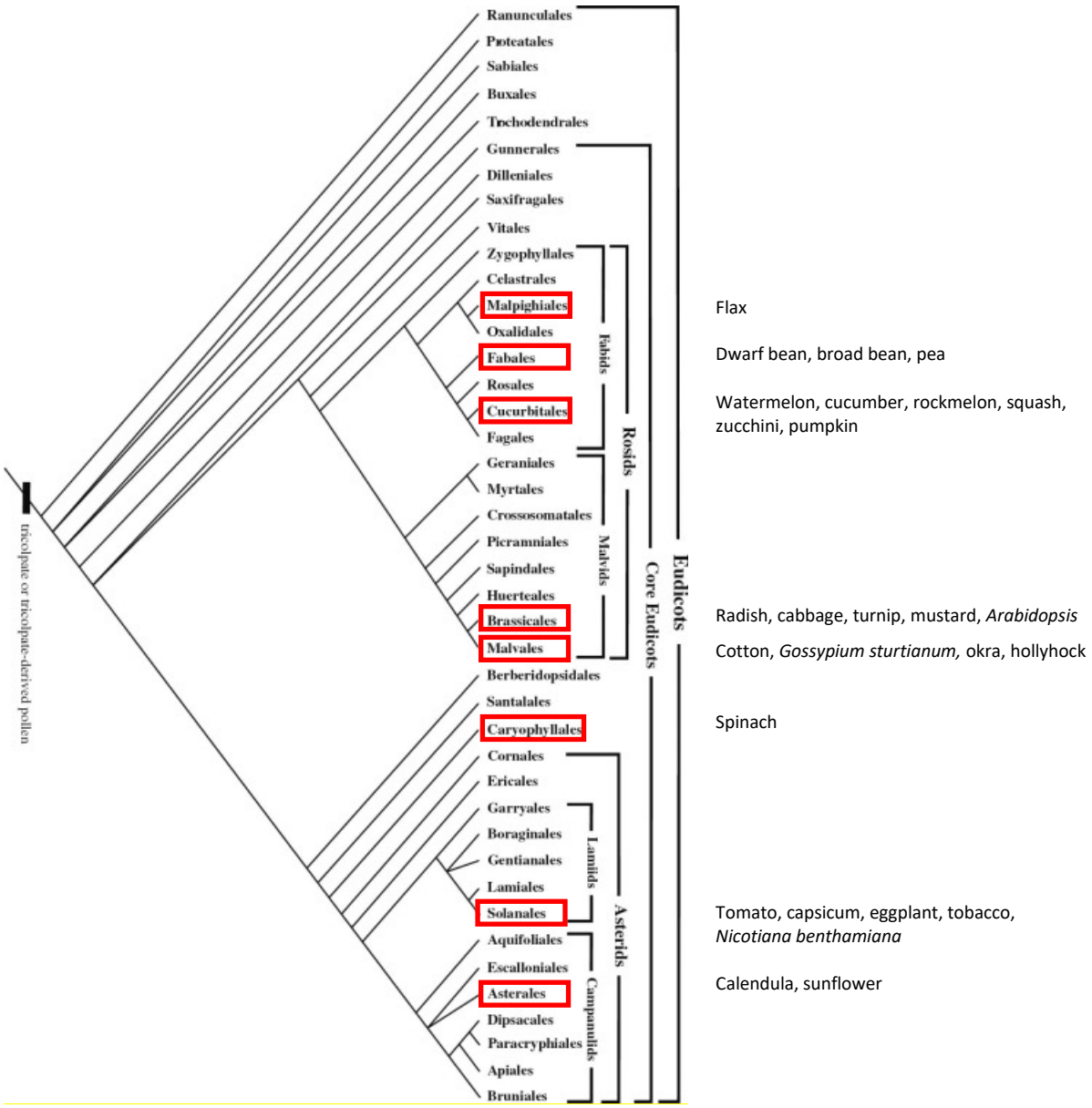

Figure 3.15 Phylogenetic distribution of plant species tested for responses to SIX6.

Plant species tested for their response to SIX6 are shown to the right of the phylogenetic tree taken from Simpson (2010). Their distribution across corresponding plant orders in the core dicots is highlighted in red.

The scope for SIX6 testing could be expanded beyond core dicots to provide broader evolutionary insights. Basal eudicots in the Ranunculales, including poppy, delphinium, ranunculus and anemone, would reveal whether SIX6 recognition is ancestral in eudicots or evolved specifically within core lineages. Additionally, testing other Zingiberales monocots beyond banana that may include ginger, turmeric, galangal and maranta could prove valuable. This would determine if SIX6 recognition is conserved across the Zingiberales order or represents a banana-specific adaptation. Such phylogenetically diverse testing would address fundamental questions about effector recognition evolution while remaining practically feasible through commercially available plant materials. Moreover, testing the effect of *Fol* SIX6 protein infiltration on strawberry plants is possible and could provide valuable insights into its role in triggering FW1-mediated resistance (Dilla-Ermita et al., 2024). This approach is commonly used in plant pathology to assess whether specific pathogen effectors can elicit defence responses, such as the hypersensitive response (HR) or other immune responses, when directly applied to plant tissue.

The assumption that all forms of plant cell death are uniform mechanisms has been increasingly challenged by mounting evidence for distinct cellular death pathways with unique characteristics and regulatory networks. This diversity has critical implications for understanding plant responses to pathogens, including the effects of effector proteins such as *Fol* SIX6. Current research recognises at least three major categories of plant cell death, each with distinct morphological and molecular features. Apoptotic-like programmed cell death (AL-PCD) serves as a crucial defence mechanism, particularly in the hypersensitive response to avirulent pathogens, where it functions to restrict pathogen spread through localised cell sacrifice. This pathway can also be triggered by various abiotic stresses, including heat shock, H_2O_2, and specific chemical treatments, suggesting a role in broader stress responses beyond pathogen defence (Reape and McCabe, 2008). In contrast, autophagic programmed cell death operates primarily during normal plant development, facilitating the controlled degradation and recycling of cellular components in tissues such as the tapetum, aerenchyma, and senescent leaves (Reape et al., 2008). A third distinct pathway, necrotic cell death, typically occurs under overwhelming stress conditions and is characterised by cell swelling and lysis, representing a more catastrophic cellular collapse (William and Dickman, 2008). The existence of these mechanistically distinct pathways creates significant challenges for researchers studying plant cell death, as different types often involve unique regulatory mechanisms and contribute distinctly to plant development, stress responses and pathogen interactions. Simple

measurements of cell viability cannot differentiate between AL-PCD and necrosis, potentially leading to misleading conclusions about the effects of specific treatments or gene functions on cellular death pathways. This limitation becomes particularly relevant when examining the effects of pathogen effectors like *Fol* SIX6, which induces a complex array of symptoms, including chlorosis, tissue browning, apical cell death, wilting, leaf curling, and confluent cell death. Without rigorous characterisation of the specific type of cell death occurring, it becomes impossible to make precise comparisons between different experimental conditions, identify the specific regulatory molecules involved, or develop a comprehensive understanding of how *Fol* SIX6 manipulates plant cellular processes during pathogen interactions. Future research must therefore prioritise the detailed characterisation of cell death mechanisms to move beyond superficial observations toward a mechanistic understanding of plant-pathogen dynamics.

The wilting (Figure 3.10) and leaf curling (Figure 3.10) phenotypes observed in SIX6 response studies represent an overlooked aspect that requires critical examination. These symptoms suggest that SIX6-induced responses extend beyond localised cell death to affect broader plant physiological processes, yet the mechanistic basis and functional significance of these systemic effects remain unexplored. The wilting phenotype implies disruption of water relations, potentially through interference with stomatal function, vascular integrity, or osmotic regulation (Buckley, 2019), while leaf curling suggests altered cell expansion or turgor pressure responses (Ali et al., 2023). These symptoms could indicate that SIX6 recognition triggers systemic defence responses that compromise normal plant function, or alternatively, that SIX6 itself has direct effects on plant water homeostasis independent of cell death induction. Furthermore, the wilting/curling responses might serve as early diagnostic markers for SIX6 recognition in different plant species, potentially more sensitive than waiting for cell death development. Future direction should focus on understanding the mechanistic basis of these systemic symptoms and finding out how effector recognition affects whole-plant physiology and the broader trade-offs involved in plant immune responses.

Fol SIX6 contributes to virulence, as its deletion compromises pathogenicity (Li et al., 2020). *Fom*, *Foc* and *Fov* SIX6 homologs induce diverse responses in different plant species, ranging from strong confluent cell death to chlorosis, wilting, or no observable effect (Figure 3.7, 3.8, 3.9). Interestingly, *SIX6* proteins from different *ff. spp.* often induce stronger cell death in their corresponding host plants than in non-host plants. For example, *Fov* SIX6 (a cotton pathogen) elicits a strong cell death response in cotton, while *Fol* SIX6 (a tomato pathogen) induces a weaker response in cotton, and vice versa in tomato (Figure 3.13). *Forc* SIX6 from a cucurbit

pathogen contributes to virulence on cucumber, although this contribution can be temperature-dependent (Li et al., 2020). In soybean *SIX6* gene contributes to virulence in *F. oxysporum* by acting as an effector that likely facilitates the infection process and suppresses host defence responses (Lanubile et al., 2016). However, the absence of *SIX6* (by deleting or knocking out) in certain virulent *ff. spp.* (like *Fon* race 2 and *Fof* race 2) enhanced its virulence where SIX6 acts as an avirulence factor (Niu et al., 2016; Dilla Ermita et al., 2024). This indicates that the role of *SIX6* can vary, sometimes contributing to virulence, sometimes acting as an avirulence factor. Future research focuses on some key factors explaining the varied presence and absence of *SIX6* across *ff. spp.* is its frequent location on mobile, lineage-specific pathogenicity chromosomes. It will be crucial to investigate whether SIX6 homologs found in other plant pathogens are also required for full pathogenicity in their respective pathosystems.

The observed differences in SIX6 responses between *Fol*, *Fom*, *Fov* and *Foc* represent a significant gap in our understanding that deserves critical examination. These *formae speciales* have evolved distinct SIX6 variants that elicit different responses in their respective hosts (tomato, melon, cotton, and banana), yet the functional and evolutionary significance of these differences remains unexplored. Notably, *Fom* SIX6, *Fov* SIX6 and *Foc* SIX6 share considerable amino acid similarity with *Fol* SIX6 (97%, 73% and 67%, respectively), and taken together with their similar patterns of cell death induction, it can be hypothesised that they will have a functional role similar to that of *Fol* SIX6. However, despite this sequence conservation and similar cell death responses, the mechanistic basis for the observed differences requires investigation. The variations could reflect different recognition mechanisms in each host and potentially using distinct immune receptors or downstream signalling pathways to detect SIX6 variants.

References

Ali, O., Cheddadi, I., Landrein, B., Long, Y. (2023). Revisiting the relationship between turgor pressure and plant cell growth. *New Phytologist, 238*(1), 62-69.

An, B., Hou X., Guo, Y., Zhao, S., Luo, H., He, C., Wang, Q. (2019). The effector SIX8 is required for virulence of *Fusarium oxysporum* f. sp. *cubense* tropical race 4 to Cavendish banana. *Fungal Biology 123*(5), 423-430.

Behle, A. (2018). Preparation of chemically competent cells. *protocols.io* (doi: https://dx.doi.org/10.17504/protocols.io.n8mdhu6).

Bentham, A.R., Youles, M., Mendel, M.N., Varden, F.A., De la Concepcion, J.C., Banfield, M.J. (2021). pOPIN-GG: A resource for modular assembly in protein expression vectors. *BioRxiv,* (doi: https://doi.org/10.1101/2021.08.10.455798).

Blekemolen, M.C., Cao, L., Tintor, N., Tamara, G., Papp, D., Faulkner, C., Takken, F.L.W. (2022). The primary function of Six5 of *Fusarium oxysporum* is to facilitate Avr2 activity by together manipulating the size exclusion limit of plasmodesmata. *Frontiers in Plant Science, 13,* 910594. (doi: https://doi.org/10.3389/fpls.2022.910594).

Buckley, T.N. (2019). How do stomata respond to water status? *New Phytologist*, *224*(1), 21-36.

Cao, L., Blekemolen, M.C., Tintor, N., Cornelissen B.J.C., Takken, F.L.W. (2018). The *Fusarium oxysporum* Avr2-Six5 effector pair alters plasmodesmatal exclusion selectivity to facilitate cell-to-cell movement of Avr2. *Molecular Plant, 11*(5), 691-705.

Chitwood-Brown, J., Vallad, G.E., Lee, T.G., Hutton, S.F. (2021). Breeding for resistance to Fusarium wilt of tomato: A Review. *Genes, 12*(11), 1673.

Dilla-Ermita, C.J., Goldman, P., Anchieta, A., Feldmann, M.J., Pincot, D.D.A., Famula, R.A., Vachev, M., Cole, G.S., Knapp, S.J., Klosterman, S.J., Henry, P.M. (2024). Secreted in xylem 6 (SIX6) mediates *Fusarium oxysporum* f. sp. *fragariae* race 1 avirulence on *FW1*-resistant strawberry cultivars. *Molecular Plant-Microbe Interactions, 37*(6), 530-541.

Ebert, M.K., Rangel, L.I., Spanner, R.E., Taliadoros, D., Wang, X., Friesen, T.L., de Jonge, R., Neubauer, J.D., Secor, G.A., Thomma, P.H.J., Stukenbrock, E.H., Bolton, M.D. (2021). Identification and characterization of *Cercospora beticola* necrosis-inducing effector CbNip1. *Molecular Plant Pathology, 22*(3), 301-316.

Essarioui, A., Mokrini, F., Afechtal, M. (2016). Molecular interactions between tomato and its wilt pathogen *Fusarium oxysporum* f. sp. *lycopersici. Revue Marocaine des Sciences Agronomiques et Vétérinaires, 4*(1), 66-74.

Gan, P., Ikeda, K., Irieda, H., Narusaka, M., O'Connell, R. J., Narusaka, Y., Takano, Y., Kubo, Y. and Shirasu, K. (2013). Comparative genomic and transcriptomic analyses reveal the hemibiotrophic stage shift of *Colletotrichum* fungi. *New Phytologist, 197*(4), 1236-1249.

Gawehns, F., Houterman, P. M., Ichou, F. A., Michielse, C. B., Hijdra, M., Cornelissen, B. J., Rep, M., Takken, F. L. W. (2014). The *Fusarium oxysporum* effector Six6 contributes to virulence and suppresses I-2-mediated cell death. *Molecular Plant Microbe Interaction, 27*(4), 336-348.

Han, G.Z. (2019). Origin and evolution of the plant immune system. *New Phytologist, 222*(1), 70-83.

Houterman, P.M., Cornelissen, B.J.C., Rep, M. (2008). Suppression of plant resistance gene-based immunity by a fungal effector. *PLoS Pathogens, 4*(5), e1000061.

Houterman, P.M., Ma, L., van Ooijen, G., de Vroomen, M.J., Cornelissen, B.J., Takken, F.L. W., Rep, M. (2009). The effector protein Avr2 of the xylem-colonizing fungus *Fusarium oxysporum* activates the tomato resistance protein I-2 intracellularly. *Plant Journal, 58*(6), 970-978.

Houterman, P.M., Speijer, D., Dekker, H.L., de Koster, C.G. (2007). Cornelissen, B.J.C., Rep, M. The mixed xylem sap proteome of *Fusarium oxysporum*-infected tomato plants. *Molecular Plant Pathology, 8*(2), 215-221.

Jones, J.D.G., & Dangl, J.L. (2006). The plant immune system. *Nature, 444*, 323-329.

Kleemann, J., Rincon-Rivera, L.J., Takahara, H., Neumann, U., van Themaat, E.V.L., van der Does, H.C., Hacquard, S., Stüber, K., Will, I., Schmalenbach, W., Schmelzer, E., O'Connell, R.J. (2012). Sequential delivery of host-induced virulence effectors by

appressoria and intracellular hyphae of the phytopathogen *Colletotrichum higginsianum*. *PLoS Pathogens, 8*(4), e1002643.

Lanubile, A., Ellis, M.L., Marocco, A., Munkvold, G.P. (2016). Association of effector Six6 with vascular wilt symptoms caused by *Fusarium oxysporum* on soybean. *Phytopathology, 106*(11), 1404-1412.

Lenarcic, T., Albert, I., Bohm, H., Hodnik, V., Pirc, K., Zavec, A., Podobnik, M., Pahovnik, D., Zagar, E., Pruitt, R., Greimel, P., Yamaji-Hasegawa, A., Kobayashi, T., Zienkiewicz, A., Gömann, J., Mortimer, J., Fang, L., Mamode-Cassim, A., Deleu, M., Lins, L., Oecking, C., Feussner, I., Mongrand, S., Anderluh, G., Nürnberger, T. (2017). Eudicot plant-specific sphingolipids determine host selectivity of microbial NLP cytolysins. *Science, 358*(6369), 1431-1434.

Li, J., Fokkens, L., Van Dam, P., Rep, M., (2020). Related mobile pathogenicity chromosomes in *Fusarium oxysporum* determine host range on cucurbits. *Molecular Plant Pathology 21*(6), 761-776.

Lievens, B., Houterman, P.M., Rep, M. (2009). Effector gene screening allows unambiguous identification of *Fusarium oxysporum* f. sp. *lycopersici* races and discrimination from other *formae speciales*. *FEMS Microbiology Letters, 300*(2), 201-215.

Liu, Z., Faris, J.D., Oliver, R.P., Tan, K.C., Solomon, P.S., McDonald, M.C., McDonald, B.A., Nunez, A., Lu, S., Rasmussen, J.B., Friesen, T.L. (2009). SnTox3 acts in effector triggered susceptibility to induce disease on wheat carrying the *Snn3* gene. *PLoS Pathogens, 5*(9), e1000581.

Liu, Z.H., Friesen, T.L., Ling, H., Meinhardt, S.W., Oliver, R.P., Rasmussen, J.B., Faris, J.D. (2006). The Tsn1-ToxA interaction in the wheat-*Stagonospora nodorum* pathosystem parallels that of the wheat-tan spot system. *Genome 49*(10),1265-1273.

Ma, L., Houterman, P.M., Gawehns, F., Cao, L., Sillo, F., Richter, H., Clavijo-Ortiz, M.J., Schmidt, S.M., Boeren, S., Vervoort, J., Cornelissen, B.J.C., Rep, M. and Takken, F.L.W. (2015). The *AVR2–SIX5* gene pair is required to activate I-2-mediated immunity in tomato. *New Phytologist, 208*(2), 507-518.

Ma, L.J., van der Does, H.C., Borkovich, K.A., Coleman, J.J., Daboussi, M.J., Di Pietro, A., Dufresne, M., Freitag, M., Grabherr, M., Henrissat, B., Houterman, P.M., Kang, S.,

Shim, W. B., Woloshuk, C., Xie, X., Xu, J.R., Antoniw, J., Baker, S.E., Bluhm, B.H., Breakspear, A., Brown, D.W., Butchko, R.A.E., Chapman, S., Coulson, R., Coutinho, P.M., Danchin, E.G.J., Diener, A., Gale, L.R., Gardiner, D.M., Goff, S., Hammond-Kosack, K.E., Hilburn, K., Hua-Van, A., Jonkers, W., Kazan, K., Kodira, C.D., Koehrsen, M., Kumar, L., Lee, Y.H., Li, L., Manners, J.M., Miranda-Saavedra, D., Mukherjee, M., Park, G., Park, J., Park, S.Y., Proctor, R.H., Regev, A., Ruiz-Roldan, M.C., Sain, D., Sakthikumar, S., Sykes, S., Schwartz, D.C., Turgeon, B.G., Wapinski, I., Yoder, O., Young, S., Zeng, Q., Zhou, S., Galagan, J., Cuomo, C.A., Kistler, H.C., Rep, M. (2010). Comparative genomics reveals mobile pathogenicity chromosomes in *Fusarium*. *Nature, 464*(7287), 367-373.

Niu, X., Yang, G., Lin, H., Liu, Y., Li, P., Zheng, A. (2021). A novel, small cysteine-rich effector, RsSCR10 in *Rhizoctonia solani* is sufficient to trigger plant cell death. *Frontiers in Microbiology, 12,* 684923.

Niu, X., Zhao, X., Ling, K.S., Levi, A., Sun, Y., Fan, M. (2016). The *FonSIX6* gene acts as an avirulence effector in the *Fusarium oxysporum* f. sp. *niveum* - watermelon pathosystem *Scientific Reports, 6*(1), 28146.

Reape, T.J., & McCabe, P.F. (2008). Apoptotic-like programmed cell death in plants. *New Phytologist, 180*(1), 13-26.

Reape, T.J., Molony, E.M., McCabe, P.F. (2008). Programmed cell death in plants: distinguishing between different modes. *Journal of Experimental Botany, 59*(3), 435-44.

Rep, M., Van Der Does, H.C., Meijer, M., Van Wijk, R., Houterman, P.M., Dekker, H.L., De Koster, C.G., Cornelissen, B.J.C. (2004). A small, cysteine-rich protein secreted by *Fusarium oxysporum* during colonization of xylem vessels is required for I-3-mediated resistance in tomato. *Molecular Microbiology, 53*(5), 1373-1383.

Schmidt, S.M., Houterman, P.M., Schreiver, I., Ma, L., Amyotte, S., Chellappan, B., Boeren, S., Takken, F.L.W., Rep, M. (2013). MITEs in the promoters of effector genes allow prediction of novel virulence genes in *Fusarium oxysporum*. *BMC Genomics 14*, 119.

Simpson, M.G. (2010). Diversity and classification of flowering plants: eudicots, Plant Systematics (Second Edition). *Academic Press,* 275-448, (doi: https://doi.org/10.1016/B978-0-12-374380-0.50008-7).

Spoel, S., & Dong, X. (2012). How do plants achieve immunity? Defence without specialized immune cells. *Nature Review Immunology, 12*(2), 89-100.

Sun, X., Fang, X., Wang, D., Jones, D.A., Ma, L. (2022). Transcriptome analysis of *Fusarium*–tomato interaction based on an updated genome annotation of *Fusarium oxysporum* f. sp. *lycopersici* identifies novel effector candidates that suppress or induce cell death in *Nicotiana benthamiana*. *Journal of Fungi 8*(7), 672.

Takken, F.L.W., & Rep, M. (2010). The arms race between tomato and *Fusarium oxysporum*. *Molecular Plant Pathology, 11*(2), 309-314.

Teulet, A., Quan, C., Evangelisti, E., Wanke, A., Yang, W., Schornack, S. (2023). A pathogen effector FOLD diversified in symbiotic fungi. *New Phytologist, 239*(3),1127-1139.

van Dam, P., Fokkens, L., Ayukawa, Y., van der Gragt, M., Ter Horst, A., Brankovics, B., Houterman, P.M., Arie, T., Rep, M. (2017). A mobile pathogenicity chromosome in *Fusarium oxysporum* for infection of multiple cucurbit species. *Scientific Reports, 22*(7), 9042.

Vlaardingerbroek, I., Beerens, B., Schmidt, S.M., Cornelissen, B.J.C., Rep, M. (2016). Dispensable chromosomes in *Fusarium oxysporum* f. sp. *lycopersici*. *Molecular Plant Pathology, 17*(9), 1455-1466.

Weise, S. (2013). Agrobacterium transformation and competent cell preparation. Michigan State University, 1-3.

Williams, B., & Dickman, M. (2008). Plant programmed cell death: can't live with it; can't live without it. *Molecular Plant Pathology, 9*(4), 531-544.

Yu, D. (2019). Structural and functional characterisation of SIX6: A cell death-inducing effector. (Honours thesis, The Australian National University, Australia).

Yu, D.S., Outram, M.A., Crean, E., Smith, A., Sung, Y.C., Darma, R., Sun, X., Ma, L., Jones, D.A., Solomon, P.S., Williams, S.J. (2022). Optimized production of disulfide-bonded

fungal effectors in *Escherichia coli* using CyDisCo and FunCyDisCo coexpression approaches. *Molecular Plant Microbe Interaction, 35*(2),109-118.

Yu, D.S., Outram, M.A., Smith, A., McCombe, C.L., Khambalkar, P.B., Rima, S.A., Sun, X., Ma, L., Ericsson, D.J., Jones, D.A., Williams, S.J. (2024). The structural repertoire of *Fusarium oxysporum* f. sp. *lycopersici* effectors revealed by experimental and computational studies. *eLife, 12*, RP89280.

Zeng, T., Rodriguez-Moreno, L., Mansurkhodzaev, A., Wang, P., van den Berg, W., Gasciolli, V., Cottaz, S., Fort, S., Thomma, B.P.H.J., Bono, J.J., Bisseling, T., Limpens, E. (2020). A lysin motif effector subverts chitin-triggered immunity to facilitate arbuscular mycorrhizal symbiosis. *New Phytologist, 225*(1), 448-460.

Appendix 3.1 Plant species used in the study.

Common Name	Species	Family	Age of the plant	Part of plant used for infiltration	Variety	Supplier
Tomato	*Solanum lycopersicum*	Solanaceae	50 days	Leaf	M82	Jones lab, RSB
Nicotiana benthamiana	*Nicotiana benthamiana*	Solanaceae	45 days	Leaf	Wild type	Plant services, RSB
Tobacco	*Nicotiana tabacum*	Solanaceae	50 days	Leaf	Wild type	Plant services, RSB
Capsicum	*Capsicum annuum*	Solanaceae	17 days	Cotyledon	Giant Bell	Mr. Fothergill's
Eggplant	*Solanum melongena*	Solanaceae	17 days	Cotyledon	Black Beauty	Mr. Fothergill's
Pumpkin	*Cucurbita moschata*	Cucurbitaceae	14 days	Cotyledon	Butternut	Mr. Fothergill's
Cucumber	*Cucumis sativus*	Cucurbitaceae	14 days	Cotyledon	Marketmore	Mr. Fothergill's
Rock melon	*Cucumis melo var. cantalupensis*	Cucurbitaceae	14 days	Cotyledon	Hales Best	Mr. Fothergill's
Squash	*Cucurbita pepo*	Cucurbitaceae	17 days	Cotyledon	Yellow Scallop	Mr. Fothergill's
Watermelon	*Citrullus lanatus*	Cucurbitaceae	14 days	Cotyledon	Sugar baby	Mr. Fothergill's
Zucchini	*Cucurbita pepo*	Cucurbitaceae	14 days	Cotyledon	Blackjack	Mr. Fothergill's
Cabbage	*Brassica oleracea*	Brassicaeae	14 days	Cotyledon	Golden Acre	Mr. Fothergill's
Mustard	*Sinapis alba*	Brassicaeae	14 days	Cotyledon	White	Mr. Fothergill's
Radish	*Rhaphanus rhaphanistrum*	Brassicaeae	14 days	Cotyledon	Scarlet Globe	Mr. Fothergill's
Turnip	*Brassica rapa*	Brassicaeae	14 days	Cotyledon	Early Purple	Mr. Fothergill's
Broad Bean	*Vicia faba*	Fabaceae	14 days	Cotyledon	Early Long Pod	Mr. Fothergill's
Dwarf Bean	*Phaseolus vulgaris*	Fabaceae	14 days	Leaf	Tender green	Mr. Fothergill's
Pea	*Pisum sativum*	Fabaceae	14 days	Cotyledon	Percy	Mathesius lab, RSB
Spinach	*Spinacia oleracea*	Amaranthaceae	14 days	Cotyledon	Perpetual Leaf	Mr. Fothergill's
Cotton	*Gossypium hirsutum*	Malvaceae	14 days	Cotyledon	Coker 315	Jones lab, RSB
Okra	*Abelmoschus esculentus*	Malvaceae	14 days	Cotyledon	Clemson's Spineless	Mr. Fothergill's
Hollyhock	*Alcea rosea*	Malvaceae	14 days	Cotyledon	Chaters Double Mixed	Mr. Fothergill's
Sturt's desert rose	*Gossypium sturtianum*	Malvaceae	14 days	Cotyledon	Sturtianum	Jones lab, RSB
Common marigold	*Calendula officinalis*	Asteraceae	14 days	Cotyledon	Pacific Beauty	Mr. Fothergill's
Sunflower	*Helianthus annuus*	Asteraceae	14 days	Cotyledon	Giant Russian	Mr. Fothergill's
Flax	*Linum usitatissimum*	Linaceae	14 days	Cotyledon	Ward	Jones lab, RSB
Banana	*Musa Sp.*	Musaceae	50 days	Leaf	2150, 2154	University of Queensland

Appendix 3.2 Gene blocks used in the study.

***Fol* SIX6**

GGTCCCTTAGCCCAAACAGAATCCGAGTCGGCAGACGTCGCTGAACATACAATCA
ATTATATCGACATTGCCCCTGAAGAATTTGAACCGCCCAAAGCTAATTTGTCATCTC
TGGTGAGTCGTGACACGCTTCCTGTCAGTACCTGTCCTGCGGGTCAGAAATACGA
TCGTTCCGTGTGTTACAAGGCAGACAAAATTCGTAGCTTTTGTGTCGCAAACCCTC
GTAGCAACCGTGAGAAGATTACCGACACACCGTGTCAGCCCCGTGAAATCTGTGT
GCAACGCAATCTTTCCAACGGCAAGAGTTTCGCTAAGTGTATCCCCATTGTAGACC
TGGTGGAATGGAAGACATCCGCAAATGGGAATAAAGAAGGCTGTACTACAACGTC
CGTGAATCCGGCTGGGTACCATCACCTTGGTACTATTGTTTACGATATCAATAAGAA
TCCTATCGAAGTTGATAAAATCTCGTACTTCGGCGAGCCGGGAAATGTAAACGAG
GGCATTGGTGGCAGCACAAGCTATTTTAGTAGTGACAACTTTCAATTTTCTAAGTC
CCGCTACATGAAAACTTGTATTTTCAGTGGTGGGTACGGGAATCTTAACGCCTATA
CGTGGAGCTGGGAA

***Foc* SIX6**

AGTCCTCTTGATCCGGCCAAGACGCCGACTTCCCCACCGGGAGCTGAGCACACGT
TAAACTATGTCGATATCACTCCAACGGGACCCGAATTTGGAAACGTCAACGGCTCT
AGTGCTTTGATTTCTCGCGACACTTTGCCACATACAGCTTGCCCTGCCGGCCAGAC
ATATGATCGTTCTGTGTGCTACAATTCGCATACCATTCGCAGTTTCTGCGTTGCTAA
CCCTCGTTCAAACCGTGAGCAAATCACCGATACTCCGTGCAACTCAGGGGAGGTC
TGCGTTCAACGCCGCTTATCGAGTGGCAAATCATATGCGAAGTGTCTTCCCGTTCG
TGACCTTGTATCGTGGCGTACAGACCCGGACGGCGACAAGGAGGGTTGCACGAC
GGTGGAAGCGAACCCTATCGGGTATCACAGCTTGGCCACGATGATTTATGATATCA
ACAACAACCCAATTCAAGTGGACAAGATTCGTTATTTGGGAGAACCAGGGGATGC
AAACGAGGGCATTGGCGGATCTGTATCTAACTTCTCTTCAGACCGCTTCCGCTTCA
CTGGGTCGAACTACATGAAGGTCTGTGTTTTTTCGGGAGGATACGGAAATTTAAAC
GCTTATACATGGGTATGGAAC

***Fom* SIX6**

GGGCCACTGGCACAGACTGAGCCTGAGTCAGCCGATGTGGCGGAGCATACCATTA
ACTATATCGATATTGCCCCAGAAGAATTTGAGCCTCCGAAGGCAGACCTTAGCTCC
TTGGTATCTCGTGACACTTTACCAGTTACAAATTGCCCTGCGGGCCAGACGTATGA
CCGCTCCGTGTGCTATAAAGCAAACACGATCCGTAGTTTTTGTGTTGCAAACCCAC
GCTCCAACCGTGAGAAAATTAGTGATACTCCTTGTAAACCGCAGGAAATCTGCGT
CCAACGCTCATTATCAAACGGGAAGTCGTATGCCAAGTGTATCCCAGTGGTTGATC
TGGTGCAATGGAAGACGAGCCCCAATGGTAACAAAGAAGGGTGCACAACTACGT
CTGTCAATCCCGCAGGTTATCATCACTTGGGAACAATCGTATATGACGTCAATAAG
AACCCAATTGAAGTTGACAAGATTAGCTATTTCGGAGAGCCGGGTAACGTCAACG
AAGGAATTGGTGGTTCTACGTCGTACTTTTCAAGCGATCTGTTTCAGTTTAGTAAG
TCACGCTTTATGAAAACCTGCATTTTTAGCGGAGGATACGGTAATTTAAACGCATA
CACCTGGTCTTGGGAG

***Fov* SIX6**

TAGGTCTCCAATGGGTCCGTTAGCTCAAACCGAGTCGGAATCGGCGGATGTAGCT
GAGCATACCATCAATTACATTGACATTGCGCCCGAGGAGTTTGAACCACCTAAGGC
AAACTTGTCGTCATTAGTGAGTCGCGACACATTACCTCCCACCTGCCCGCGCTACA
CGACATACGATGAGTCCATTTGTATCACGGCAGGCGTAGTACGCTCTTCTTGCGTT
TTCACTGCAGATCCAGGAGTACGTCGTGGGGTCAACGCGAATTGTAATAAGAACG
AGATTTGCGTTGAACGCAACTTGTCTAACGGTAAACGCTATGCGAAGTGTATTCCC
ATCGCGCACTTGGTGGAATGGAAAACAAGTGCCGATGGCAACAAGGAGGGCTGC
ACGACGACGAGCGTGAATCCAGCCGGTAATCATCATTTAGGCACGATCGTTTACGA
TGTTAACAAGAACCCGATTCAGGTTGATAAAATTTCATACTTTGGAGAACCCGGAA
ATGTGGACGAGGGAATTGGTGGGTCTACCTCATACTTTTCTTCTAATTTGTTCCACT
TCAGCAAGTCCCGTTACATGAAAACGTGTATTTTCTCTGGAGGTTACGGGAACTTA
AACGCTTATACGTGGTCCTGGGTTTCTTGGAGACCGT

Appendix 3.3 Primers used in this study.

Primer name	**Sequence (5'-3')**
Fol SIX6	F: TAGGTCTCCAATGGGTCCCTTAGCCCAAACAGAATCCG R: ACGGTCTCCAAGATTCCCAGCTCCACGTATAGGCGTTAAG
Foc SIX6	F: TAGGTCTCCAATGAGTCCTCTTGATCCGGCCAAGACG R: ACGGTCTCCAAGAGTTCCATACCCATGTATAAGCGTTTAAATTTCCG
Fom SIX6	F: TAGGTCTCCAATGGGGCCACTGGCACAGACTGAG R: ACGGTCTCCAAGACTCCCAAGACCAGGTGTATGCGTTTAAAT
Fov SIX6	F: TAGGTCTCCAATGTAGGTCTCCAATGGGTCCG R: ACGGTCTCCAAGAACGGTCTCCAAGAAACCCAGGACCA
T7 Promoter (Colony PCR)	F: TAATACGACTCACTATAGGG
Golden Gate-STOP (Colony PCR)	R: TGGATCCCTAGAAAGCGATCGTT
LIC	1F: CACTATCCTTCGCAAGACCC 2R: CCTATAAGAACCCTAATTCCC

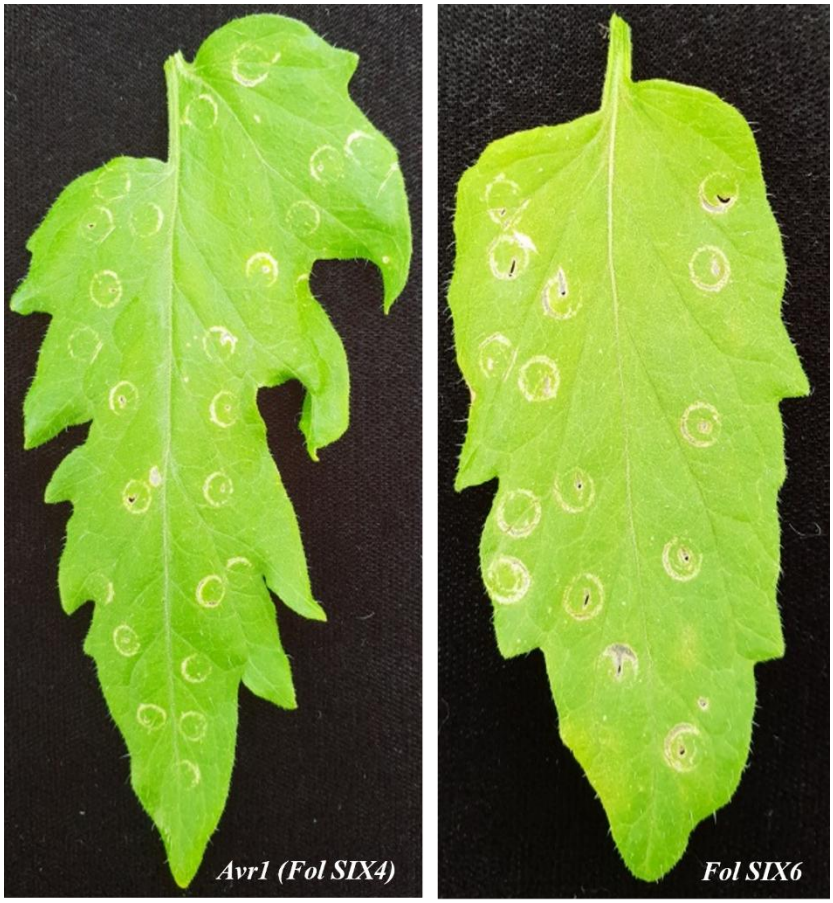

Appendix 3.4 Agroinfiltration of *Fol SIX6* and *Avr1* (*Fol SIX4* used as a positive control) into leaves of tomato cv. M82 (which carried the *I* gene) did not induce a cell death response. Leaves were photographed 8 days after agroinfiltration.

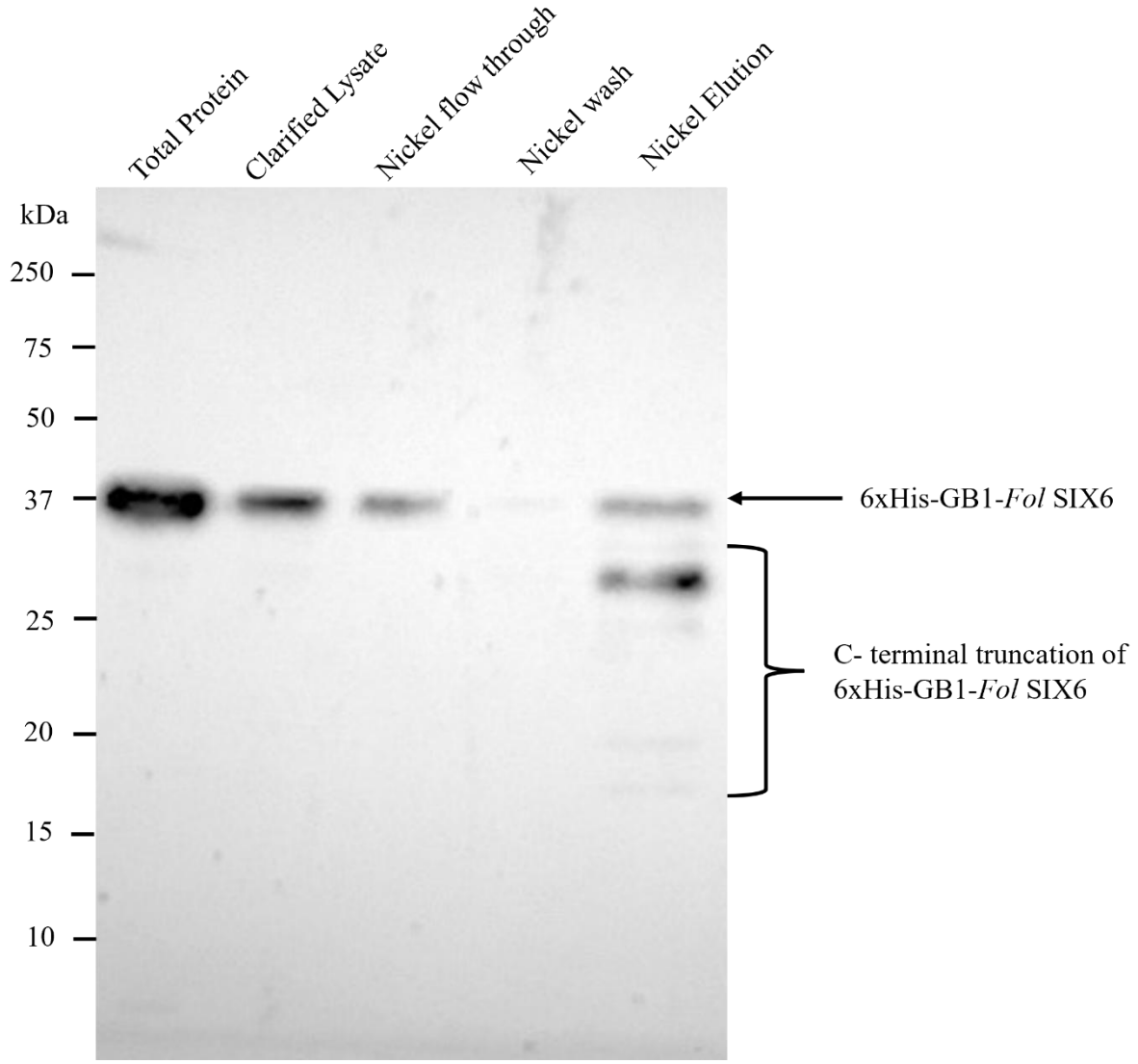

Appendix 3.5 Protein gel blot of 6xHis-GB1-*Fol*SIX6 protein at various steps during its purification, probed using HRP-conjugated anti-His antibodies.

Samples include 1 µl each of total protein, clarified lysate, nickel column flow through, nickel column wash, and 10 µl of nickel column elution. Chemiluminescence was imaged using an Image Quant LAS 4000 chemiluminescence imager. This gel blot has been taken from Daniel Yu's Honours thesis, ANU.

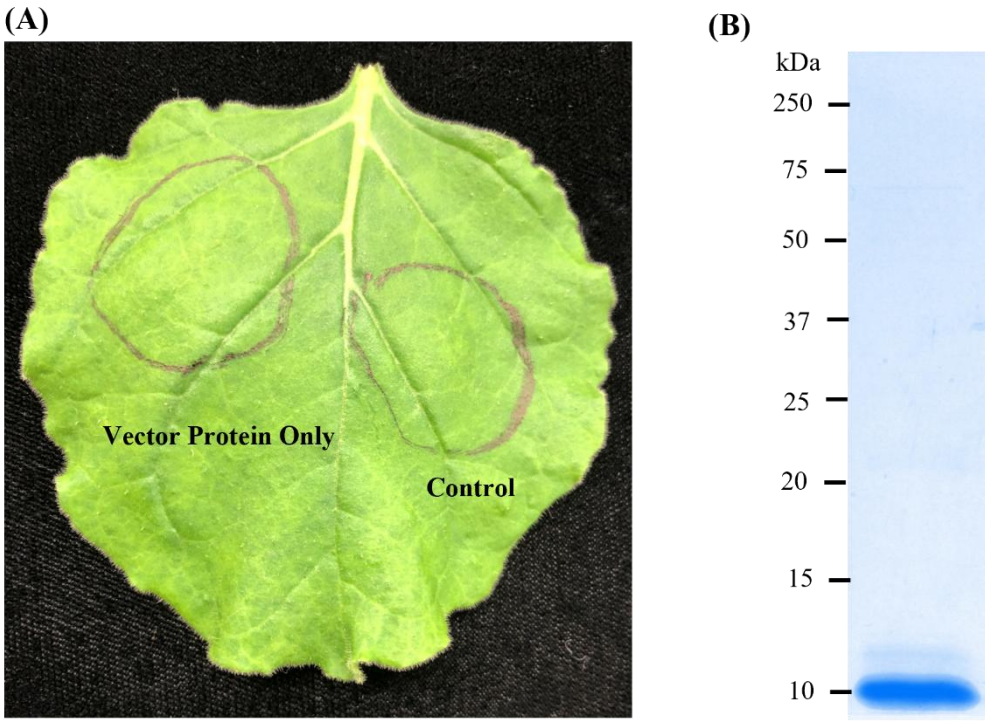

Appendix 3.6 Agroinfiltration of protein extracted from a vector-only control into leaves of *N. benthamiana* tomato did not induce a cell death response.

(A) Leaf of *N. benthamiana* infiltrated with water (control) or protein extracted from a vector-only control and purified by nickel affinity chromatography. Photographed 6 days post-infiltration. **(B)** SDS-PAGE analysis of the protein infiltration. The major band represents the GB1 solubility tag.

Wheat

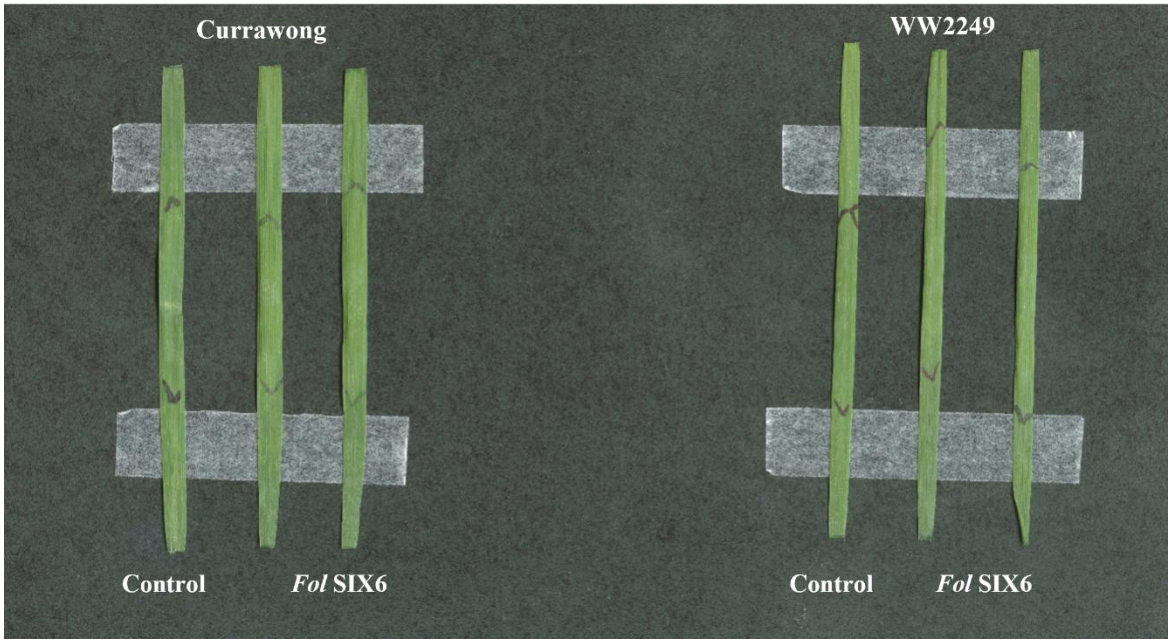

Appendix 3.7 *Fol* SIX6 protein 100 µg/ml and water (control) infiltration in wheat varieties Currawong and WW2249. Photographed 6 days post-infiltration.

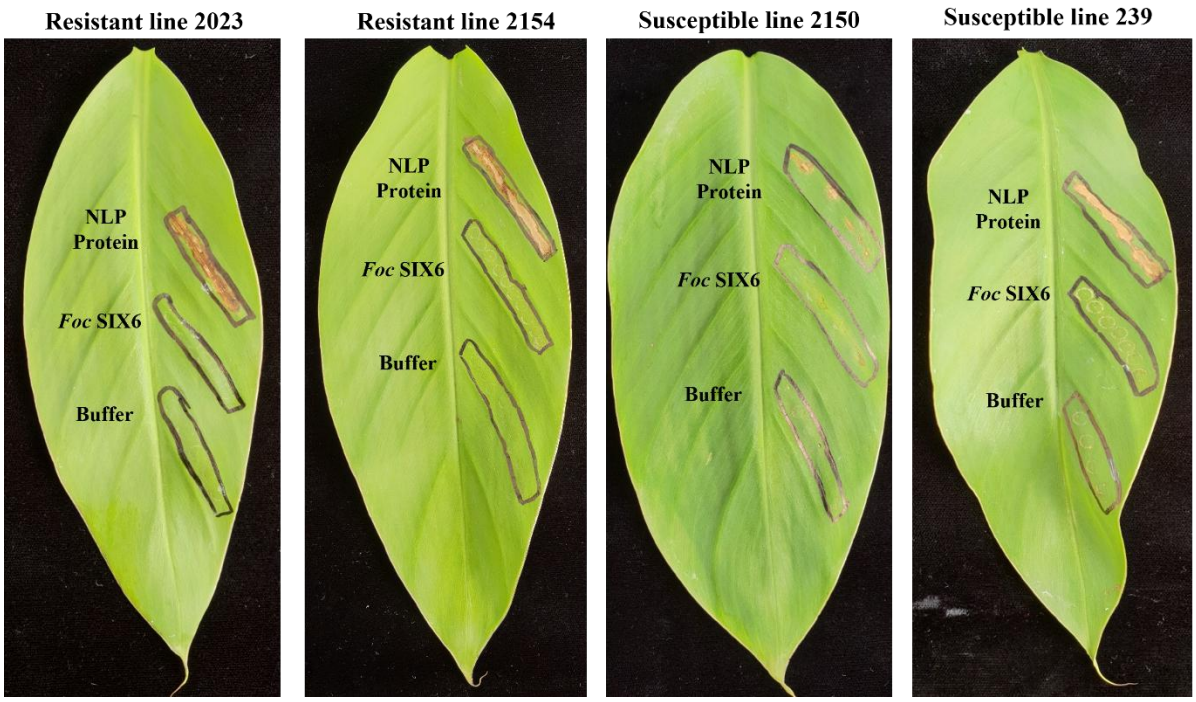

Appendix 3.8 Leaves of banana lines resistant or susceptible to *Foc* TR4 were infiltrated with *Foc* SIX protein (100 µg/ml), NLP protein (100 µg/ml) (Lenarcic et al., 2017) or buffer.

Photographed 6 days post-infiltration. Banana lines were provided by Professor Elizabeth Aitken, University of Queensland.

Chapter 4: Is *Fol*-SIX6-induced cell death a plant-defence response?

4.1 Introduction

Plant-pathogen interactions involve complex molecular dialogues in which pathogen-derived effector proteins are perceived by host immune receptors, triggering diverse cellular responses that range from coordinated defence signalling to programmed cell death. The specificity and molecular mechanisms underlying these responses vary considerably depending on the nature of both the effector and its receptor, as well as the downstream signalling networks they engage. Understanding whether a given effector-induced phenotype represents immune recognition or an alternative mode of action requires systematic dissection of the canonical defence pathways known to transduce resistance signals. In this context, the cell death phenotype induced by the *Fusarium oxysporum* f. sp. *lycopersici* (*Fol*) effector SIX6 presents an intriguing case for investigation, as its lack of host specificity and requirement for high expression levels suggest a mechanism distinct from classical effector-triggered immunity. This chapter investigates whether SIX6-induced cell death operates through established plant defence signalling pathways by examining the genetic requirements for key immune components in both *Nicotiana benthamiana* and tomato.

The interaction between *R* and *Avr* genes is often confirmed by co-agroinfiltration in *N. benthamiana* or *N. tabacum* and assessing the induction of cell death, for example, cell death induced by co-expression of tomato *Cf-4* and *Cf-9* genes with the *Cladosporium fulvum Avr4* and *Avr9* genes, respectively (Thomas et al., 2000; van der Hoorn et al., 2000) or the tomato *I* and *I-2* genes with the *Fol Avr1* and *Avr2* genes, respectively (Catanzariti et al., 2017; Houterman et al., 2009). Purified recombinant Avr1 protein has been shown to trigger cell death in tomato plants that carry the *I* gene but not in those lacking the *I* gene, indicating a specific interaction between the Avr1 effector and the I resistance protein from host plant resistance (Yu et al., 2022). Although co-agroinfiltration of *I-3* and *Avr3* did not cause cell death in *N. benthamiana* (Catanzariti et al., 2015), purified recombinant Avr3 protein is able to induce cell death in tomato plants carrying the *I-3* gene (Rima et al., unpublished). *R/Avr* cell-death responses are typically highly specific, as seen with the *Cf-4/Avr4*, *Cf-9/Avr9, I/Avr1*, *I-2/Avr2* and *I-3/Avr3* interactions (Thomas et al., 2000; van der Hoorn et al., 2000; Houterman et al., 2009; Catanzariti et al., 2017; Rima et al., unpublished).

On the other hand, agroinfiltration of *Fol SIX6* alone induces cell death in *N. benthamiana* (Chapter 3). Moreover, infiltration of purified *Fol* SIX6 protein induced cell death and a variety of other responses in various plant species, including tomato (Chapter 3). unlike the examples

above, SIX6 protein induced cell death without the specificity normally associated with recognition by a resistance protein. This suggests that the cell death associated with SIX6 is unlikely to be directly mediated by a specific R protein. However, it could still involve a signalling pathway associated with R protein-mediated cell death responses. Potentially, SIX6 might act as an extracellular effector that targets signalling components activated by extracellular perception, including components like BAK1/SERK3 (BRI1-associated kinase 1/somatic embryogenesis receptor kinase 1) or SOBIR1 (suppressor of *BIR1-1*), which would in turn affect responses by downstream signalling components, including the MAP kinases (mitogen-activated protein kinases) WIPK (wound-inducible protein kinase) and SIPK (salicylic acid-induced protein kinase) (Liu et al., 2003; Zhou et al., 2014; Peng et al., 2015; Seifbarghi et al., 2020), EDS1 (enhanced disease susceptibility 1) (Hu et al., 2005; Wierme et al., 2005) or ethylene (de Jong et al., 2002; Trobacher, 2009). The work described in this chapter aimed to examine the possible role of these plant defence signalling components in the induction of cell death by *Fol* SIX6.

Plant defence has been well studied in Arabidopsis, which is considered a model system for studying plant defence mechanisms at the molecular level (Thatcher et al., 2005) and several key components involved in defence responses (Figure 4.1) are conserved between Arabidopsis and solanaceous plants, such as tomato and tobacco. When a pathogen attacks the host plant it is perceived by PRRs (pattern recognition receptors) that detect PAMPs (pathogen-associated molecular patterns) or DAMPS (damage-associated molecular patterns). After PAMP or DAMP perception, cell surface LRR-RKs (leucine-rich-repeat receptor kinases) interact with BAK1 to activate PTI (pattern-triggered immunity), initiating broad-spectrum responses including callose deposition at infection sites, reactive oxygen species production, and upregulation of defence-related genes. PTI focuses on pathogen containment while maintaining host cell viability, creating an inhospitable environment for invading microorganisms without sacrificing the plant's own tissues through programmed cell death (Zhang et al., 2018; Yu et al., 2024; Nabi et al., 2024).

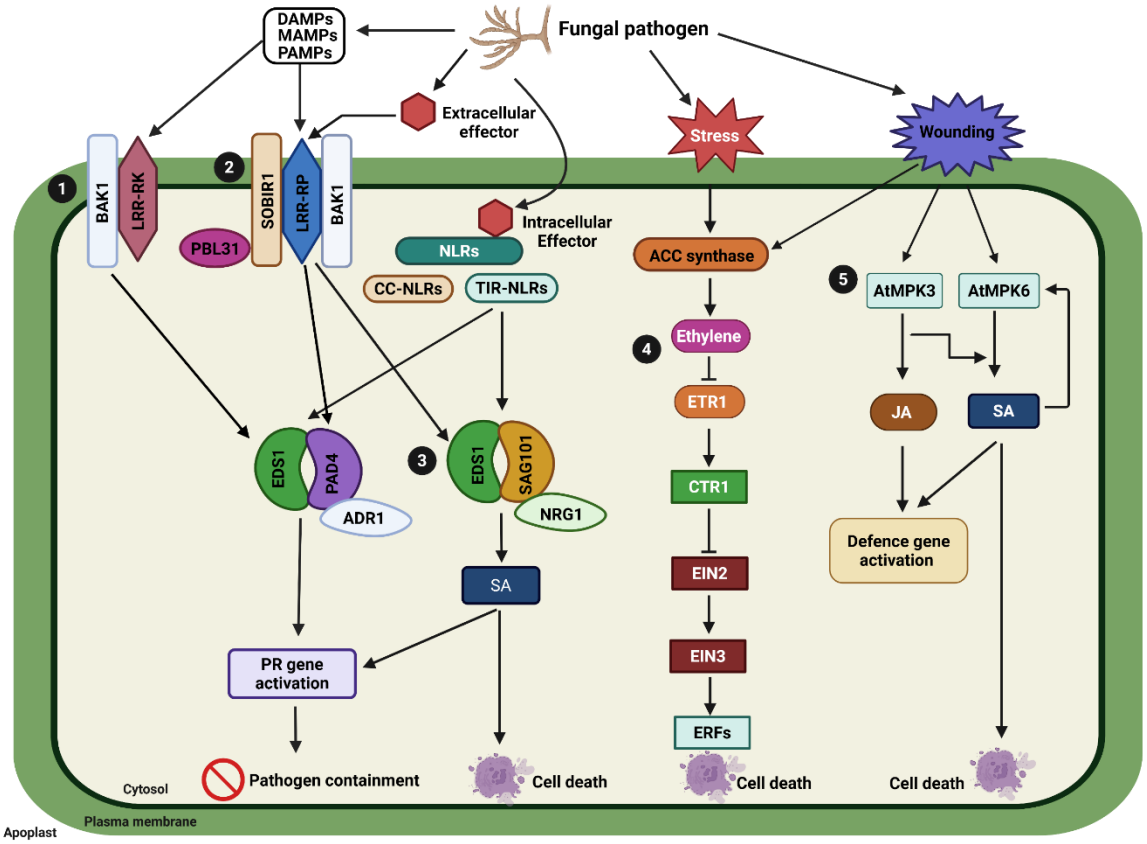

Figure 4.1 Simplified diagram showing where 1) BAK1, 2) SOBIR1, 3) EDS1, 4) ethylene and 5) Arabidopsis orthologues of tobacco WIPK and SIPK act in Arabidopsis defence-signalling pathways leading to cell death.

DAMPs: damage-associated molecular patterns; MAMPs: microbe-associated molecular patterns; PAMPs: pathogen-associated molecular patterns; BAK1: BRI1-associated receptor kinase; LRR-RK: leucine-rich repeat receptor kinase; LRR-RP: leucine-rich repeat receptor protein; SOBIR1: suppressor of bir1-1 1; PBL31: PBS1-like 31; EDS1: enhanced disease susceptibility 1; PAD4: phytoalexin deficient 4; NLRs: nucleotide-binding leucine-rich repeat proteins; CC-NLRs: coiled-coil domain NLRs; TIR-NLRs: Toll/interleukin-1 receptor cytosolic domain NLRs; SAG101: senescence-associated gene 101; NRG1: N requirement gene 1; ADR1: activated disease resistance 1; SA: salicylic acid; ACC synthase: 1-aminocyclopropane-1-carboxylic acid synthase; ETR1: ethylene receptor 1; ERFs: ethylene response factors; CTR1: constitutive triple response 1; EIN2: ethylene insensitive 2; EIN3: ethylene insensitive 3; AtMPK3: *Arabidopsis thaliana* mitogen-activated kinase 3 (orthologous to SIPK); AtMPK6: *A. thaliana* mitogen-activated kinase 6 (orthologous to WIPK); JA: jasmonic acid. The illustration was based on information provided in the text and generated using BioRender (https://app.biorender.com).

BAK1 is a co-receptor of LRR-RKs and LRR-RPs and has a role in a number of defence responses, including localised cell death in Arabidopsis (Kemmerling and Nurnberger 2008; Liebrand et al., 2014; Fan et al., 2016). BAK1 and SOBIR1 are co-receptors for LRR-RPs that

recognise DAMPs/MAMPs/PAMPs and extracellular effectors to initiate a resistance response, causing cell death in Arabidopsis (Liebrand et al., 2013, 2014; Peng et al., 2015; van der Burgh et al., 2019). *BAK1* and *SOBIR1* have also been found to play a role in cell death in tomato and tobacco mediated by LRR-RPs such as I, Cf-4, and Cf-9 following recognition of their corresponding effectors Avr1, Avr4, and Avr9, respectively (Catanzariti et al., 2017; Postma et al., 2016; van der Hoorn et al., 2000). Recently, Rima et al. (unpublished) found that *BAK1* and *SOBIR1* are also required for cell death induced by recognition of purified Avr3 protein by the I-3 resistance protein, which is a SRLK (self-incompatibility receptor-like kinase).

EDS1 is essential for plant defence against many plant diseases caused by bacteria, oomycetes, viruses and fungi (Lund et al., 1998; Wierme et al., 2005; Nambeesan et al., 2012) and plays a significant role in mediating cell death associated with resistance responses (Li et al., 2019). Moreover, *EDS1* is essential for regulating SA (salicylic acid) levels during cell death related to plant defence (Figure 4.1) (Straus et al., 2010). In Arabidopsis, EDS1 forms heterodimers with the related lipase-like proteins PAD4 (phytoalexin-deficient 4) and SAG101 (senescence-associated gene 101), which interact with helper NLRs ADR1 (activated disease resistance 1) and NRG1 (N requirement gene 1), respectively, to regulate plant immunity, including the cell death response (Figure 4.1) (Feys et al., 2001; Lipka et al., 2005; Wagner et al., 2013; Lapin et al., 2020; Pruitt et al., 2021).

LRR-RK-dependent responses are dependent on the EDS1-PAD4-ADR1 signalling node for their function (Kourelis, 2023). Cell surface LRR-RPs (leucine-rich repeat receptor proteins), such as Arabidopsis RLP23, that interact with complexes containing BAK1 and SOBIR1 to initiate defence responses through the EDS1-PAD4-ADR1 and EDS1-SAG101-NRG1 signalling nodes, leading to PTI and cell death (Figure 4.1) (Liebrand et al., 2013, 2014; Albert et al., 2015; Ma and Borhan, 2015; Lapin et al.,2019; Pruitt et al., 2021; Maruta et al., 2025). EDS1 and SAG101b induce a cell death response in *Nicotiana benthamiana,* but EDS1 and PAD4 do not (Gantner et al., 2019).

EDS1 is required for *Fol* resistance mediated by the tomato *I* and *I-7* genes (Hu et al., 2005; Gonzalez-Cendales et al., 2016), which encode LRR-RPs (Catanzariti et al., 2017; Gonzalez-Cendales et al., 2016). In tomato, using the *sun1-1* (*eds1*) mutant of tomato, Hu et al. (2005) showed that *EDS1* was required for *I*-mediated *Fol* resistance and *Ve*-mediated resistance to *Verticillium dahliae* (I and Ve are both LRR-RPs) as well as *Bs4*-mediated resistance to *Xanthomonas campestris* pv. *vesicatoria* (Bs4 is a TNR) (Hu et al., 2005). Cell death was

reduced and SA signalling was impaired in *sun1-1* plants. Even with exogenous application of SA, *sun1-1* plants were unable to induce an HR in response to TMV infection, indicating that *EDS1* is essential for the proper execution of the cell death pathway associated with plant defence (Hu et al., 2005).

In plants, ethylene signalling has a role during biotic interactions with microbial pathogens and herbivorous insects (Broekgaarden et al., 2015). It regulates SA and JA responses to promote plant defence or promote pathogenicity depending on the plant-pathogen interaction (van der Ent and Pieterse, 2012; Broekgaarden et al., 2015). It is considered an important hormone for cross-talk between different hormone responses, including SA, JA and ABA (abscisic acid), which work mainly against biotrophic pathogens, necrotrophic pathogens and chewing insects, respectively (Broekgaarden et al., 2015). Ethylene serves as a key regulator of PCD (programmed cell death) in plants, influencing various physiological processes and interacting with other signalling pathways to ensure proper development and response to environmental stresses, and plays a role in defence-related cell death in tomato (de Jong et al., 2002; Trobacher, 2009). In tomato, ethylene also promotes the ripening of tomato fruit (Oetiker and Yang 1995; Alexander and Grierson 2002; Huang et al., 2022). Pearson *Never ripe* (*Nr*) tomato plants carry a dominant negative mutation of the *LeETR3* (ethylene receptor 3) gene (an orthologue of the Arabidopsis *ETR1* gene), which significantly delays the process of tomato ripening and confers ethylene insensitivity (Lanahan et al., 1994; Tieman et al., 2000). Interestingly, *Nr* plants showed a considerable decrease in disease symptoms compared to wild-type plants following *Fol* race 3 inoculation (Lund et al., 1998).

Ethylene perception in Arabidopsis primarily involves a family of five receptors, ETR1 (ethylene receptor 1), ERS1 (ethylene response sensor 1), ERS2 and EIN4 (ethylene insensitive 4) (Klee, 2002), which act as repressors of ethylene signalling in the absence of ethylene, and downstream components like CTR1, EIN2 and EIN3 (Kieber et al., 1993; Yanagisawa et al., 2003; Yang et al., 2008; Trobacher 2009). When an Arabidopsis plant experiences biotic or abiotic stress, it triggers the production of ethylene (Druege, 2006; Fatma et al., 2022). This process begins with ACC synthase catalysing the conversion of S-adenosylmethionine into 1-aminocyclopropane-1-carboxylic acid (ACC), the immediate precursor of ethylene (Druege, 2006). Upon ethylene production, the hormone binds and inactivates ethylene receptors, notably ETR1, and repression of the ethylene signalling cascade is relieved. This cascade leads to the modulation of key regulatory proteins, including deactivation of the negative regulator

CTR1 (constitutive triple response 1) and reactivation of the positive regulators EIN2 and EIN3. ETR1, in the absence of ethylene, activates CTR1, which represses EIN2. ET represses ETR1, which no longer activates CTR1, and this depresses EIN2, allowing it to activate EIN3, which in turn activates ERF transcription. This binding enhances the expression of these genes and triggers a variety of defence mechanisms, including programmed cell death (Huang et al., 2016) (Figure 4.1).

While tomato utilises a similar ethylene receptor system, some of the specific interactions and downstream signalling components differ (Binder, 2020). Tomato have been shown to have a more complex hormonal interplay, particularly with gibberellic acid (GA) and abscisic acid (ABA), which can influence the ethylene response and PCD (Alexander and Grierson 2002; Yakimova et al., 2006; Binder, 2020).

Ethylene also serves as a key regulator of defence and cell death responses triggered by various biotic and abiotic stresses in tomato. Ethylene is implicated in the regulation of PCD and interacts with other phytohormones, such as jasmonic acid (JA) and salicylic acid (SA), to coordinate defence responses (Broekgaarden et al., 2015; Yang et al., 2015). Ethylene influences the production of reactive oxygen species, which are signalling molecules that can trigger defence responses and PCD (Czekus et al., 2022). Unlike Arabidopsis, tomato has a larger family of ethylene receptors, with six identified members (LeETR1, LeETR2, LeETR3, LeETR4, LeETR5, LeETR6), including the ethylene response during fruit ripening (Klee 2002). Similar to Arabidopsis, tomato receptors also act as negative regulators for ethylene signalling (Klee 2002).

Wounding by an herbivorous insect or plant pathogen activates WIPK and SIPK in tobacco (de Bruxelles and Roberts, 2001; Hettenhausen et al., 2001; Sun et al., 2024; Maruta et al., 2025). In Arabidopsis, the MAPKs (mitogen-activated protein kinases) AtMPK3 (orthologous to WIPK) and AtMPK6 (orthologous to SIPK**)** are activated by upstream MAPKKs in response to similar stresses (Mishra et al., 2006; Sharma et al., 2020; Kumar et al., 2020). MPK3 regulates the production of jasmonic acid which helps to activate JA-inducible defence-related genes such as PDF1.2 (plant defensin), VSP1 (vegetative storage protein), LOX2 (lipoxygenase) and genes involved in secondary metabolite biosynthesis, while MPK6 promotes salicylic acid biosynthesis which helps to activate SA-responsive genes including PR (pathogenesis-related) genes such as PR1, PR2 and PR5, and induce cell death (van Verk et al., 2009) (Figure 4.1).

WIPK and SIPK and their orthologues have been found to play important roles in causing cell death in tobacco and tomato and are involved in signalling and cell death arising from effector recognition by extracellular R proteins (Zhang et al., 2000; Zhang and Liu, 2001; Stulemeijer et al., 2007; Melech-Bonfil and Sessa, 2010; Ogata et al., 2015; Stulemeijer et al., 2007). For example, Avr9/Cf-9 recognition rapidly activates WIPK and SIPK, leading to their participation in transducing the recognition signal into a downstream defence response and cell death (Stulemeijer et al., 2007). WIPK orthologue LeMPK3 and SIPK orthologues LeMPK1 and LeMPK2 are crucial components of the defence system in tomato, involving both basal defence responses as well as *R*-gene-mediated resistance and cell death (Pedley and Martin, 2004; Stulemeijer et al., 2007; Melech-Bonfil and Sessa, 2010).

To investigate whether cell death caused by *Fol SIX6* is a plant defence response or not, VIGS (virus-induced gene silencing) was used to silence defence-related genes involved in cell death as described in Figure 4.1 and analyse the effect on *Fol-SIX6*-induced cell death in leaves of *N. benthamiana*. Four genes *BAK1, SOBIR1, WIPK* and *SIPK* were targeted for silencing as they play important roles in cell death induction (Yang et al., 2011; Liebrand et al., 2013, 2014; Seo et al., 2007). In addition, sun*1-1* and *Never ripe* mutant tomato lines with impaired EDS1 and ethylene signalling pathways, respectively, were used to test the role of these signalling molecules in cell death induced by *Fol* SIX6.

4.2 Materials and Methods

4.2.1 Plant material

Seeds of *N. benthamiana* and M82, Pearson *Never ripe* (Lanahan et al., 1994) and *sun1-1* (Hu et al., 2005) tomato lines were sown in pots with seed-raising mix (Martins Fertilizers, Australia) and grown at 25°C in a growth room with a 16-hour photoperiod, light intensity of 250 µmol m^{-2} s^{-1} and relative humidity of 60-65% for 4 to 6 weeks before protein infiltration. Infiltrated seedlings were then allowed to grow in the same conditions for another 8 days. Two-week-old *N. benthamiana* seedlings were used for VIGS as described in section 4.2.4.

4.2.2 *Fol* SIX6 protein infiltration in tomato and *N. benthamiana*

Recombinant *Fol* SIX6 protein was produced and purified as described in Chapter 3. An aliquot of purified recombinant protein was taken out from the -80°C freezer and the thawed protein was diluted in gel filtration buffer (10 mM HEPES, 150 mM NaCl, pH 7.5) to a final

concentration of 100 µg/ml and kept on ice. A needle was used to prick the underside of the leaves of *N. benthamiana* and tomato to introduce a wound. Diluted protein was then infiltrated through the wound into the leaf using a 1 ml syringe without a needle. As a negative control, gel filtration buffer was infiltrated into the same leaf in *N. benthamiana* or into a different leaflet on the same leaf in tomato.

4.2.3 VIGS constructs used in *N. benthamiana*

Tobacco rattle virus (TRV) VIGS constructs targeting *NbBAK1*, *NbSOBIR1* and *NbCITRX* were prepared by Della Rinarta (Rinarta 2017, Master's thesis, ANU) using the TRV2-LIC binary vector plasmid pYYI3, which contains a *ccdB* gene (lethal for *E. coli* carrying wild-type DNA gyrase gene) flanked by ligation-independent cloning (LIC) sites (Dong et al., 2007). LIC is explained in Chapter 2. Primers containing LIC adapters were used to amplify and clone fragments of target genes of interest from *N. benthamiana* as described by Della Rinarta (Rinarta 2017, Master's thesis, ANU). Daigo Takemoto, Nagoya University, provided the TRV:RNA2 construct pTV00-S/W (here designated TRV:RNA2:*NbWIPK/SIPK*) targeting both *NbSIPK* and *NbWIPK* (Ohtsu et al., 2014).

4.2.4 VIGS assay in *N. benthmiana*

Tobacco Rattle Virus (TRV) construct carrying *A. tumefaciens* GV3101 (pMP90) cultures carrying TRV:RNA1, TRV:RNA2:*GFP* (negative control), TRV:RNA2:*NbCITRX* (positive control for silencing), TRV:RNA2:*NbBAK1*, TRV:RNA2:*NbSOBIR1* or TRV:RNA2:*NbWIPK/SIPK* constructs were grown on fresh LB agar plates supplemented with suitable antibiotics for 2 days at 28°C and cells resuspended in freshly prepared infiltration media (10 mM MES pH 5.3, 10 mM $MgCl_2$, 0.2 mM acetosyringone). Cell suspensions were then adjusted to an OD600 and equal volumes of 1.0. TRV:RNA1 and TRV:RNA2 cultures were mixed together and incubated at room temperature in the dark for 2 hours. Two-week-old *N. benthamiana* seedlings were infiltrated with *A. tumefaciens* cultures carrying TRV:RNA1 and TRV:RNA2 constructs and kept in a growth chamber with a constant temperature of 21°C, a photoperiod of 16 hours of light per day with an intensity of 250 µmol m^{-2} s^{-1} and a relative humidity ranging between 60-65% for 3 to 4 weeks, when the target genes were expected to be silenced. A needle was used to wound the abaxial side of the leaf and then a 1 ml syringe without a needle was used to infiltrate the *Agrobacterium* suspension through the wound. Different areas of the same leaf were used for different infiltrations and controls. Infiltrated

plants were kept in the growth room and grown under the same conditions as described above for 8 days before taking photographs of the responses. An overview of the VIGS assay is shown in Figure 4.2.

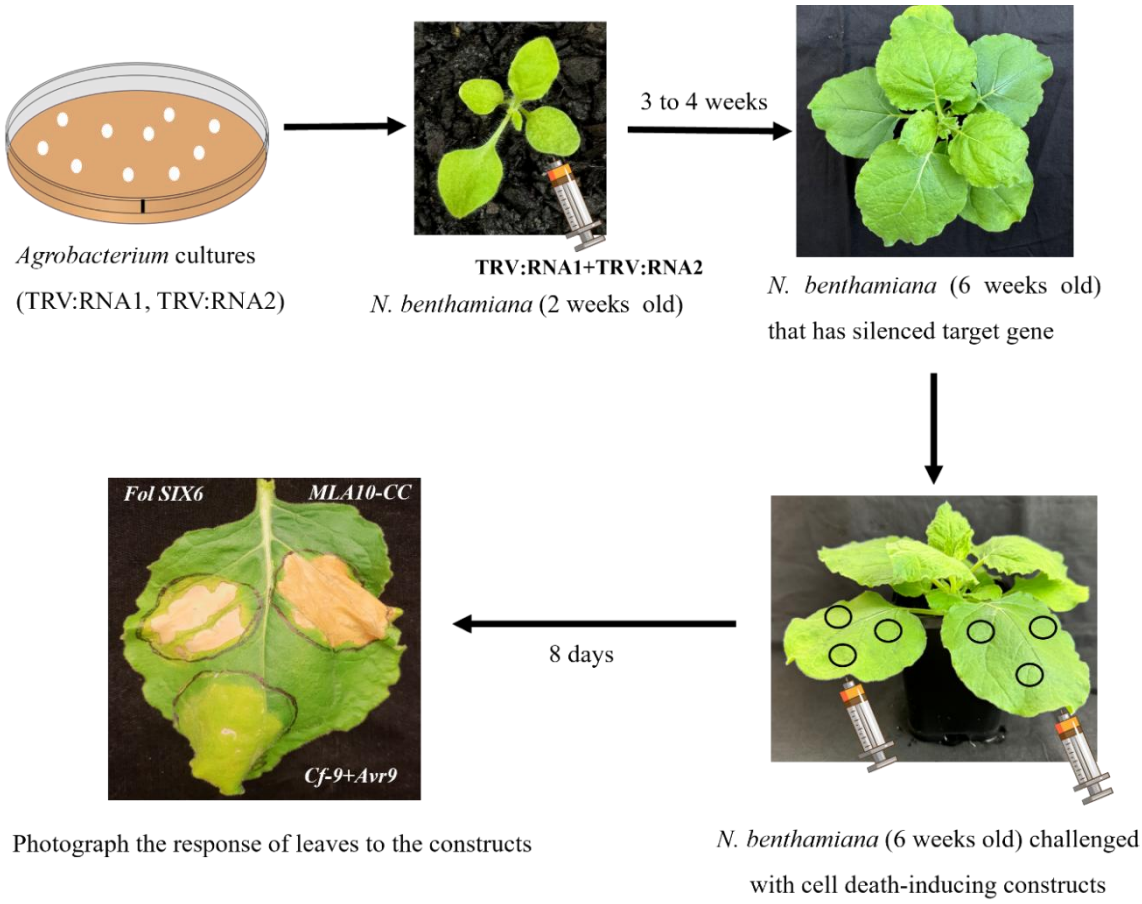

Figure 4.2 An overview of the VIGS study in *N. benthamiana* used to test the requirement for defence-related genes in *Fol-SIX6*-mediated cell death.

TRV:RNA1 and TRV:RNA2:target-sequence cultures of *Agrobacterium* were infiltrated into two-week-old *N. benthamiana* seedlings. Three to four weeks after the initial infiltration, *Fol SIX6* and other cell death-inducing constructs were agroinfiltrated into the leaves of the VIGS plants and the effect of VIGS on cell death induction was assessed and photographed 8 days later.

4.3 Results

4.3.1 Virus-induced gene silencing of *BAK1, SOBIR1* or *WIPK* and *SIPK* does not reduce the cell death response induced by expression of *Fol SIX6* in *N. benthamiana*

Before conducting the VIGS experiment, a trial was conducted with VIGS of *CITRX* in combination with VIGS of *BAK1* or *SOBIR1*. Silencing of *CITRX* can be used as a reporter to examine the establishment of the VIGS because it causes chlorosis in leaves of silenced plants (Della Rinarta, 2017, Masters thesis, ANU). Leaves with chlorosis were observed in plants silenced for *CITRX* and *BAK1* as well as those silenced for *CITRX* and *SOBIR1* indicating VIGS was working as expected in *N. benthamiana* (Figure 4.3). Moreover, *BAK1* silencing causes leaf curling (Catanzariti et al., 2017) and this effect was also observed in the *BAK1+CITRX* silenced plants. *Fol SIX6*, *MLA10-CC* and *Cf9/Avr9* constructs were tested for cell death induction in leaves of the VIGS plants silenced for *BAK1*, *SOBIR1* or *WIPK* and *SIPK* using agroinfiltration (Figure 4.4). Co-agroinfiltration of tomato *Cf-9* and *Cladosporium fulvum Avr9* was used as a positive control for suppression of cell death (van der Hoorn et al., 2000) by silencing of *BAK1, SOBIR1* or *SIPK* and *WIPK,* and barley *MLA10-CC* was used as a negative control (Bai et al., 2012). Co-agroinfiltration of *Cf-9* and *Avr9* induced cell death in GFP-silenced plants, but not in *SOBIR1*, *BAK1* or *WIPK* and *SIPK* silenced plants, whereas agroinfiltration of *MLA10-CC* and *Fol SIX6* caused cell death in leaves of all VIGS plants (Figure 4.4). These results suggest cell death induced by *Fol* SIX6 is not a plant defence response because silencing of *BAK1*, *SOBIR1* or *WIPK* and *SIPK* (which encode proteins in defence responses triggered by extracellular effectors) had no effect on cell death triggered by *Fol SIX6*.

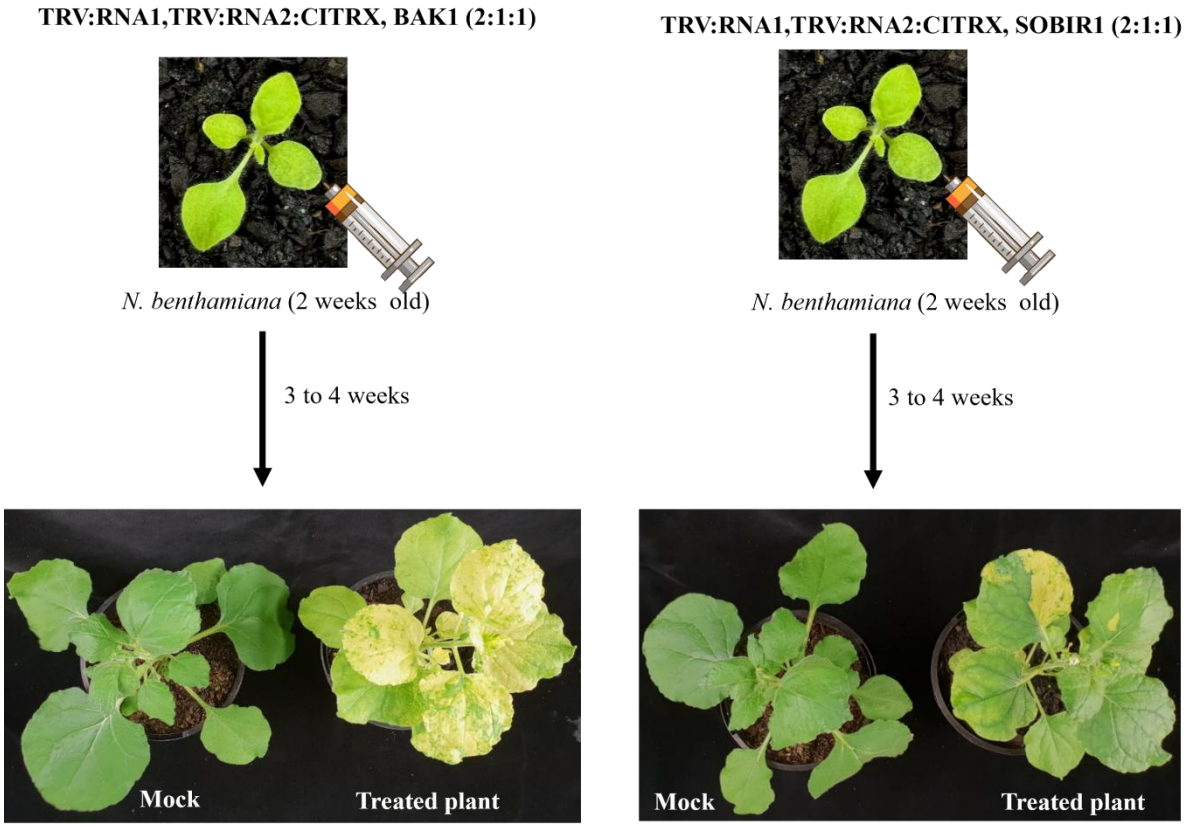

Figure 4.3 Virus-Induced Gene Silencing (VIGS) with CITRX to examine the establishment of VIGS in *N. benthamiana*.

VIGS was established using *Agrobacterium tumefaciens*-mediated tobacco rattle virus (TRV) expression in *N. benthamiana* seedlings. TRV:RNA1 and either TRV:RNA2 constructs carrying *CITRX* or *BAK1* gene fragments, or TRV:RNA2 constructs carrying *CITRX* or *SOBIR1* gene fragments were infiltrated in two-week-old *N. benthamiana* plants. The ratios of *A. tumefaciens* cultures used are shown in parentheses. Photographs were taken 21 days after infiltration.

Figure 4.4 Virus-Induced Gene Silencing (VIGS) testing for a requirement for *BAK1*, *SOBIR1* or *WIPK* and *SIPK* in *Fol-SIX6*-mediated cell death in *N. benthamiana*.

TRV:RNA1 and TRV:RNA2 constructs targeting *GFP*, *BAK1*, *SOBIR1* or *WIPK* and *SIPK* were infiltrated into two-week-old *N. benthamiana* plants. Three weeks after the initial infiltration, *Fol* SIX6 was agroinfiltrated into uppermost fully-expanded leaves along with a positive cell-death control expected to be affected by silencing (co-agroinfiltration of *Cf-9* and *Avr9*) and a negative cell-death control expected not to be affected by silencing (*MLA10-CC*). Infiltrated leaves were photographed 8 days later.

4.3.2 Mutations affecting *EDS1* and ethylene perception do not reduce the cell death response induced by *Fol* SIX6 in tomato

Mutant tomato plants carrying a loss-of-function mutation of the tomato *EDS1* gene called *sun1-1* (Hu et al., 2005) were used to investigate whether *EDS1* has any role in cell death induced by *Fol SIX6*. Leaves of *sun1-1* plants were infiltrated with *Fol* SIX6 protein as described in section 4.2.2 and strong cell death was observed in *sun1-1* plants compared to M82 (control) plants (Figure 4.5), suggesting that *EDS1* does not play a major role in cell death triggered by *Fol* SIX6. To determine whether ethylene plays a role in the cell-death response to *Fol* SIX6, leaves of *Nr* tomato plants were infiltrated with *Fol* SIX6 protein. The response of *Nr* tomato plants to *Fol* SIX6 protein infiltration was no different from that of M82 tomato plants (Figure 4.5). This result suggests ethylene has little or no role in the cell death-inducing function of *Fol* SIX6.

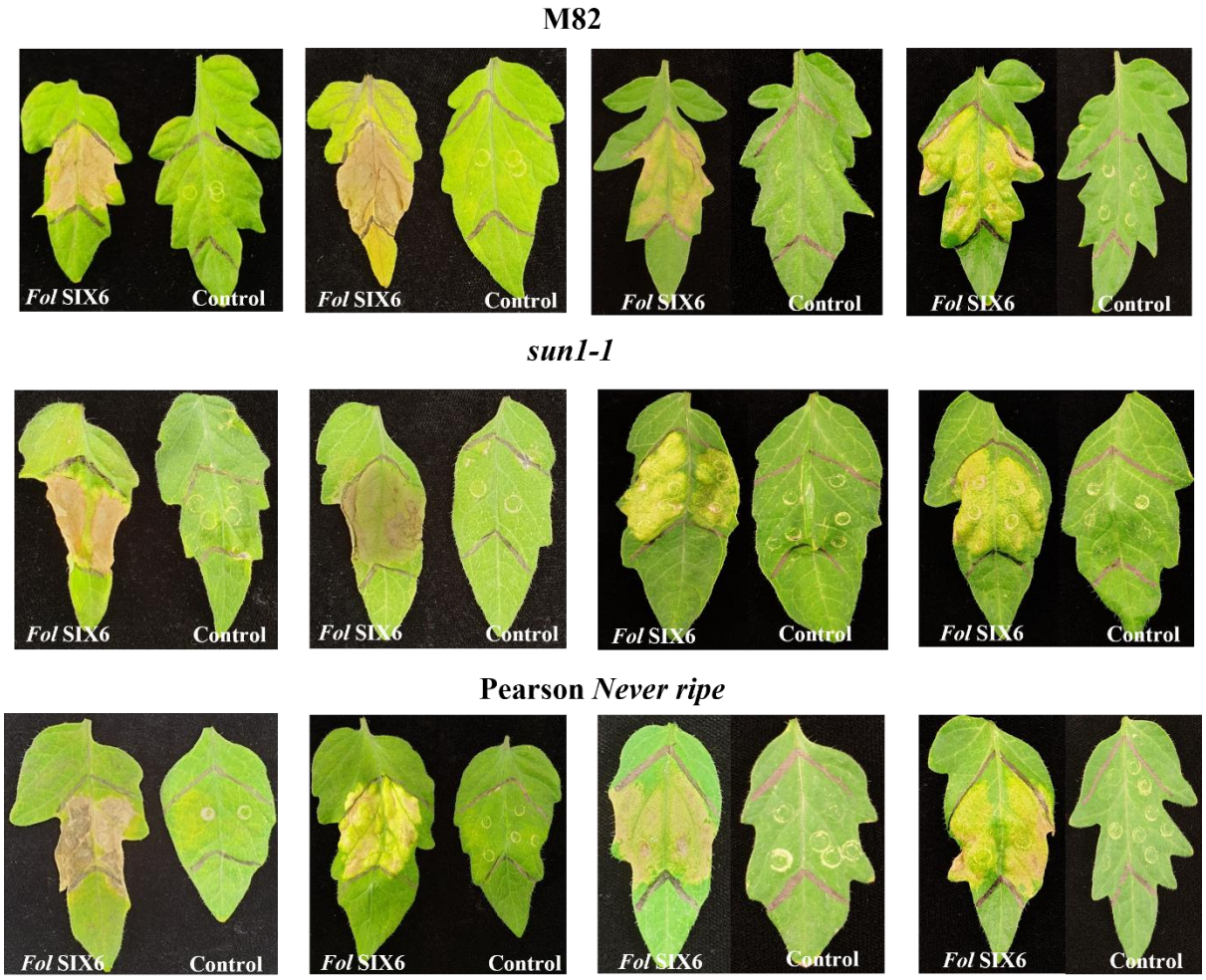

Figure 4.5 Cell death response induced by *Fol* SIX6 protein infiltrations in mutant tomato lines.

Fol SIX6 protein diluted in gel filtration buffer to a concentration of 100 µg/ml and buffer (control) infiltrated in M82 (control), Pearson *Never ripe* (Lanahan et al., 1994) and *sun1-1* (Hu et al., 2005) tomato plants. Photographs were taken 6 days after protein infiltration under normal light.

4.4 Discussion

4.4.1 *Fol* SIX6-mediated cell death is not dependent on defence signalling

Potentially, SIX6 could act as an extracellular effector that targets signalling pathways activated by extracellular receptors with the co-receptors BAK1 and SOBIR1 and their downstream intracellular signalling component EDS1. However, VIGS experiments targeting *BAK1* and *SOBIR1,* and experiments with the *sun1-1* (*EDS1*) mutant of tomato showed that they are not required for cell death induced by *Fol* SIX6 (Figures 4.4 and 4.5). Together, these experiments suggest that neither LRR-RKs (which require BAK1 and EDS1) nor LRR-RPs (which require BAK1, SOBIR1 and EDS1) nor TIR-NLRs (which require EDS1) play a role in *Fol* SIX6-induced cell death. It is possible that SIX6 recognition may involve a different class of extracellular receptor that functions independently of the BAK1 and SOBIR1 co-receptors. For example, WAK1 that detects DAMP, or CERK1, LYK5 (PAMP detectors), which detect chitin (Miya et al., 2007; Brutus et al., 2010; Cao et al., 2014). It is also possible that SIX6 may involve cell death induced by a sensor CC-NLR rather than a TIR-NLR. EDS1 functions in conjunction with the helper CC-NLRs ADR1 and NRG1, but in solanaceous plants, there is also another resistance pathway that does not function through EDS1 and uses NRCs (NB-LRR protein required for HR-associated cell death) rather than ADR1 and NRG1 as helper CC-NLRs. Tomato and *N. benthamiana* have multiple NRC genes (e.g. *NRC1*, *NRC2*, *NRC3* and *NRC4* in tomato) that encode helper NLRs for the LRR-RPs Cf-4, Cf-9, LeEix and Ve1, and various sensor CC-NLRs including Rx, Mi and Prf (Gabriels et al., 2007; Fradin et al., 2009; Wu et al., 2016; 2017; Goh et al., 2024). VIGS or CRISPR-Cas9-mediated mutations of *NRC* genes could be used to test whether they are required for SIX6-induced cell death. However, *NRC* genes are present in the Asterids, which include the Solanaceae, but not in the Rosids (Wu et al., 2017). Whilst SIX6 induced cell death in almost all of the Asterids tested (members of the Solanaceae and Asteraceae), it also induced cell death in a number of the Rosids tested (watermelon in the Cucurbitaceae, dwarf bean in the Fabaceae and *Gossypium sturtianum* in the Malvaceae) as well as a number of other responses such as wilting and curling (Chapter 3). Assuming the mechanism of cell death is the same in the Asterids and Rosid species tested, this would suggest that *NRC* genes do not play a role in SIX6-induced cell death.

Potentially, SIX6 could induce a cell-surface change that is transmitted to the interior of the cell and detected by a sensor CC-NLR. Sensor CC-NLRs are often dependent on the

chaperones SGT1 (Suppressor of G-two allele of Skp1), RAR1 (Required for Mla12 resistance) and HSP90 (Heat shock protein 90) required for their correct folding in functional proteins (Azevedo et al., 2002; Liu et al., 2004). Mutations of one or more of these proteins can abolish the function of various CC-NLRs (Takahashi et al., 2003). For example, *rar1* mutants lose RPM1, RPS2, and RPS5 function (Hubert et al., 2009), HSP90 mutations compromise RPM1 and RPS2 resistance (Hubert et al., 2003; Takahashi et al., 2003), and SGT1 mutations affect resistance protein levels (Takahashi et al., 2007), demonstrating the critical roles of these chaperones in CC-NLR function. VIGs or CRISPR-Cas9-mediated mutations of tomato *SGT1, RAR1* or *HSP90* genes could be used to test whether they are required for SIX6-induced cell death.

WIPK and SIPK have been identified as downstream signalling components able to cause cell death in tomato defence against herbivorous insects or pathogens (Melech-Bonfil and Sessa 2010). *WIPK* and *SIPK* have also been found to play an important role in causing cell death in *N. benthamiana* and tobacco (Zhang et al., 2000; Ogata et al., 2015). Activation of WIPK and SIPK (the tobacco orthologues of Arabidopsis MPK6 and MPK3, respectively) leads to the production of defence hormones, including JA acid and SA, respectively (Hettenhausen et al., 2015). SA and JA are involved in the induction and regulation of cell death in Arabidopsis and *N. benthamiana*, with SA primarily promoting localised cell death to contain pathogens, while JA induces the expression of defence related proteins such as PDF1.2 and enhances defence through chemical and physical barriers without inducing cell death (Penninckx et al., 1996; Devadas et al., 2002; Mur et al., 2006). Potentially, SIX6 could have activated WIPK and SIPK via a BAK1/SOBIR1-independent defence signalling pathway, but VIGS experiments showed that *WIPK* and *SIPK* were not involved in SIX6-induced cell death. On the other hand, they do not provide evidence for a lack of SA or JA production and involvement in cell death induction by SIX6. *NahG* and *def1* tomato lines could be employed to determine the roles of SA and JA, respectively, in SIX6-induced cell death. Transgenic *NahG* tomato lines expresses the bacterial enzyme salicylate hydroxylase, which converts SA into the inactive molecule catechol and leads to reduced SA accumulation and abolition of Avr9-induced cell death in *Cf-9* tomato plants (Brading et al. 2000). Similarly, the *def1* tomato mutant shows reduced JA accumulation owing to a defect in JA biosynthesis (Li et al. 2002; Thaler et al. 2004).

The *Never ripe* (*Nr*) mutant of tomato was used to investigate the role of ethylene signalling in cell death induced by SIX6. Cell death induction was found to be unaffected in *Nr* tomato

plants. However, the *Nr* mutant is not entirely insensitive to ethylene but rather has reduced sensitivity (Aloni et al., 1998; Clark et al., 1999; Diaz et al., 2002). The *Nr-2* mutant of tomato, which is completely insensitive to ethylene (Barry et al., 2005), could be used to further test the role of ethylene signalling in SIX6-induced cell death.

The overall results of the VIGS experiments targeting *BAK1*, *SOBIR1*, *SIPK* and *WIPK* and experiments with *sun1-1* and *Nr* mutant tomato lines, although not conclusive, suggest that the cell death response induced by SIX6 is unlikely to be a defence response. Rather, SIX6 seems more likely to have a role in pathogen virulence, with cell death likely arising as a consequence of overexpression of SIX6. The following chapters report experiments investigating the physiological effects underpinning SIX6-induced cell death, which provide some clues about SIX6 function *in planta*.

References

Albert, I., Bohm, H., Albert, M., Feilar, C.E., Imkampe, J., Wallmeroth, N., Raaymakers, T.M., Oome, S., Zhang, H., Krol, E. (2015). An RLP23–SOBIR1–BAK1 complex mediates NLP-triggered immunity. *Nature Plants, 5*(1), 15140.

Alexander, L., & Grierson, D. (2002). Ethylene biosynthesis and action in tomato: a model for climacteric fruit ripening. *Journal of Experimental Botany, 53*(377), 2039-2055.

Aloni, R., Wolf, A., Feigenbaum, P., Avni, A., Klee, H.J. (1998). The Never ripe mutant provides evidence that tumor-induced ethylene controls the morphogenesis of *Agrobacterium tumefaciens*-induced crown galls in tomato stems. *Plant Physiology, 117*(3), 841-849.

Azevedo, C., Sadanandom, A., Kitagawa, K., Freialdenhoven, A., Shirasu, K., Schulze-Lefert, P. (2002). The RAR1 interactor SGT1, an essential component of R gene-triggered disease resistance. *Science*, *295*(5562), 2073-2076.

Bai, S., Liu, J., Chang, C., Zhang, L., Maekawa, T., Wang, Q., Xiao, W., Liu, Y., Chai, J., Takken, F.L.W., Schulze-Lefert, P., Shen, Q.H. (2012). Structure-function analysis of barley NLR immune receptor MLA10 reveals its cell compartment specific activity in cell death and disease resistance. *PLoS Pathogens, 8*(6), e1002752.

Barry, C.S., McQuinn, R.P., Thompson, A.J., Seymour, G.B., Grierson, D., Giovannoni, J.J. (2005). Ethylene insensitivity conferred by the *Green-ripe* and *Never-ripe 2* ripening mutants of tomato. *Plant Physiology, 138*(1), 267-275.

Binder, B.M. (2020). Ethylene signaling in plants. *Journal of Biological Chemistry, 295*(22), 7710-7725.

Brading, P.A., Hammond-Kosack, K.E., Parr, A., Jones, J.D. (2000). Salicylic acid is not required for *Cf-2* and *Cf-9*-dependent resistance of tomato to *Cladosporium fulvum*. *The Plant Journal*, *23*(3), 305-318.

Broekgaarden, C., Caarls, L., Vos, I.A., Pieterse, C.M., Van Wees, S.C. (2015). Ethylene: traffic controller on hormonal crossroads to defense. *Plant Physiology, 169*(4), 2371-2379.

Brutus, A., Sicilia, F., Macone, A., Cervone, F., De Lorenzo, G. (2010). A domain swap approach reveals a role of the plant wall-associated kinase 1 (WAK1) as a receptor of

oligogalacturonides. *Proceedings of the National Academy of Sciences*, *107*(20), 9452-9457.

Cao, Y., Liang, Y., Tanaka, K., Nguyen, C.T., Jedrzejczak, R.P., Joachimiak, A., Stacey, G. (2014). The kinase LYK5 is a major chitin receptor in Arabidopsis and forms a chitin-induced complex with related kinase CERK1. *elife*, *3*, e03766.

Catanzariti, A.M., Do, H.T.T., Bru, P., de Sain, M., Thatcher, L.F., Rep, M., Jones, D.A. (2017). The tomato *I* gene for Fusarium wilt resistance encodes an atypical leucine-rich repeat receptor-like protein whose function is nevertheless dependent on SOBIR1 and SERK3/BAK1. *The Plant Journal, 89*(6), 1195-1209.

Catanzariti, A.M., Lim, G.T.T., Jones, D.A. (2015). The tomato *I-3* gene: a novel gene for resistance to Fusarium wilt disease. *New Phytologist, 207*(1), 106-118.

Clark, D.G., Gubrium, E.K., Barrett, J.E., Nell, T.A., Klee, H.J. (1999). Root formation in ethylene-insensitive plants. *Plant Physiology, 121*(1), 53-60.

Czekus, Z., Szalai, G., Tari, I., Khan, M.I.R., Poor, P. (2022). Role of ethylene in ER stress and the unfolded protein response in tomato (*Solanum lycopersicum* L.) plants. *Plant Physiology and Biochemistry, 15*(181), 1-11.

de Bruxelles, G.L., & Roberts, M.R. (2001). Signals regulating multiple responses to wounding and herbivores. *Critical Reviews in Plant Sciences*, *20*(5), 487-521.

de Jong, A.J., Yakimova, E.T., Kapchina, V.M., Woltering, E.J. (2002). A critical role for ethylene in hydrogen peroxide release during programmed cell death in tomato suspension cells. *Planta, 214*(4), 537-545.

Devadas, S.K., Enyedi, A., Raina, R. (2002). The *Arabidopsis hrl1* mutation reveals novel overlapping roles for salicylic acid, jasmonic acid and ethylene signalling in cell death and defense against pathogens. *The Plant Journal, 30*(4), 467-480.

Díaz, J., ten Have, A., van Kan, J.A. (2002). The role of ethylene and wound signaling in resistance of tomato to *Botrytis cinerea*. *Plant Physiology, 129*(3), 1341-1351.

Dong, Y., Burch-Smith, T.M., Liu, Y., Mamillapalli, P., Dinesh-Kumar, S.P. (2007). A ligation-independent cloning tobacco rattle virus vector for high-throughput virus-

induced gene silencing identifies roles for NbMADS4-1 and -2 in floral development. *Plant Physiology, 145*(4), 1161-1170.

Druege, U. (2006). Ethylene and plant responses to abiotic stress. *Springer*, Berlin, Heidelberg. https://doi.org/10.1007/978-3-540-32846-9_5.

Fan, M., Wang, M., Bai, M.Y. (2016). Diverse roles of SERK family genes in plant growth, development and defense response. *Science China Life Science, 59*(9), 889-896.

Fatma, M., Asgher, M., Iqbal, N., Rasheed, F., Sehar, Z., Sofo, A., Khan, N.A. (2022). Ethylene signaling under stressful environments: analyzing collaborative knowledge. *Plants, 11*(17), 2211.

Feys, B.J., Moisan, L.J., Newman, M.A., Parker, J.E. (2001). Direct interaction between the Arabidopsis disease resistance signaling proteins, EDS1 and PAD4. *The EMBO Journal, 20*(19), 5400-5411.

Fradin, E.F., Zhang, Z., Juarez Ayala, J.C., Castroverde, C.D., Nazar, R.N., Robb, J., Chun-Ming Liu, Thomma, B.P. (2009). Genetic dissection of *Verticillium* wilt resistance mediated by tomato Ve1. *Plant physiology*, *150*(1), 320-332.

Gabriëls, S.H., Takken, F.L., Vossen, J.H., de Jong, C.F., Liu, Q., Turk, S.C., Wachowski, L.K., Peters, J., Witsenboer, H.M., de Wit, P.J., Joosten, M.H. (2006). cDNA-AFLP combined with functional analysis reveals novel genes involved in the hypersensitive response. *Molecular Plant-Microbe Interactions*, *19*(6), 567-576.

Gantner, J., Ordon, J., Kretschmer, C., Guerois, R., Stuttmann, J. (2019). An EDS1-SAG101 complex is essential for TNL-mediated immunity in *Nicotiana benthamiana*. *The Plant Cell*, *31*(10), 2456-2474.

Goh, F.J., Huang, C.Y., Derevnina, L., Wu, C.H. (2024). NRC Immune receptor networks show diversified hierarchical genetic architecture across plant lineages. *Plant Cell, 36*(9), 3399-3418.

Gonzalez-Cendales, Y., Catanzariti, A.M., Baker, B., McGrath, D.J., Jones, D.A. (2016). Identification of I-7 expands the repertoire of genes for resistance to Fusarium wilt in tomato to three resistance gene classes. *Molecular Plant Pathology, 17*(3), 448-463.

Hettenhausen, C., Schuman, M.C., Wu, J. (2015). MAPK signaling: a key element in plant defense response to insects. *Insect Science, 22*(2),157-164.

Houterman, P.M., Ma, L., van Ooijen, G., de Vroomen, M. J., Cornelissen, B. J., Takken, F. L. W., Rep, M. (2009). The effector protein Avr2 of the xylem-colonizing fungus *Fusarium oxysporum* activates the tomato resistance protein I-2 intracellularly. *Plant Journal, 58*(6), 970-978.

Hu, G., DeHart, A.K., Li, Y., Ustach, C., Handley, V., Navarre, R., Hwang, C.F., Aegerter, B.J., Williamson, V.M. Baker, B. (2005). *EDS1* in tomato is required for resistance mediated by TIR-class *R* genes and the receptor-like *R* gene *Ve*. *The Plant Journal, 42*(3), 376-391.

Huang, P.Y., Catinot, J., Zimmerli, L. (2016). Ethylene response factors in Arabidopsis immunity. *Journal of Experimental Botany, 67*(5), 1231-1241.

Huang, W., Hu, N., Xiao, Z., Qiu, Y., Yang, Y., Yang, J., Mao, X., Wang, Y., Li, Z., Guo, H. (2022). A molecular framework of ethylene-mediated fruit growth and ripening processes in tomato, *The Plant Cell*, *34*(9), 3280-3300.

Hubert, D.A., Tornero, P., Belkhadir, Y., Krishna, P., Takahashi, A., Shirasu, K., Dangl, J.L. (2003). Cytosolic HSP90 associates with and modulates the Arabidopsis RPM1 disease resistance protein. *The EMBO journal*, *22*(21),5679-5689.

Hubert, D.A., He, Y., McNulty, B.C., Tornero, P., Dangl, J.L. (2009). Specific Arabidopsis HSP90.2 alleles recapitulate RAR1 cochaperone function in plant NB-LRR disease resistance protein regulation. *Proceedings of the National Academy of Sciences*, *106*(24), 9556-9563.

Kemmerling, B., & Nurnberger, T. (2008). Brassinosteroid-independent functions of the BRI1-associated kinase BAK1/SERK3. *Plant Signaling & Behavior, 3*(2), 116-118.

Kieber, J.J., Rothenberg, M., Roman, G., Feldmann, K.A., Ecker, J.R. (1993). *CTR1*, a negative regulator of the ethylene response pathway in Arabidopsis, encodes a member of the Raf family of protein kinases. *Cell, 72*(3), 427-441.

Klee, H.J. (2002). Control of ethylene-mediated processes in tomato at the level of receptors. *Journal of Experimental Botany, 53*(377), 2057-2063.

Kourelis, J. (2023). Interplay between cell-surface receptor and intracellular NLR-mediated immune responses. *New Phytologist*, *240*(6), 2218-2226.

Kumar, K., Raina, S.K. Sultan, S.M. (2020). Arabidopsis MAPK signalling pathways and their cross-talks in abiotic stress response. *Journal of Plant Biochemistry and Biotechnology, 29*(4), 700-714.

Lanahan, M.B., Yen, H.C., Giovannoni, J.J., Klee, H.J. (1994). The *Never Ripe* mutation blocks ethylene perception in tomato. *The Plant Cell, 6*(4), 521-530.

Lapin, D., Bhandari, D.D., Parker, J.E. (2020). Origins and immunity networking functions of EDS1 family proteins. *Annual Review of Phytopathology, 25*(58), 253-276.

Lapin, D., Kovacova, V., Sun, X., Dongus, J.A., Bhandari, D., Von Born, P., Bautor, J., Guarneri, N., Rzemieniewski, J., Stuttmann, J., Beyer, A., Parker, J.E. (2019). A coevolved EDS1-SAG101-NRG1 module mediates cell death signaling by TIR-domain immune receptors. *The Plant Cell*, *31*(10), 2430-2455.

Li, N., Han, X., Feng, D., Yuan, D., Huang, L.J. (2019). Signalling Crosstalk between Salicylic Acid and Ethylene/Jasmonate in plant defense: do we understand what they are whispering? *International Journal of Molecular Science, 20*(3), 671.

Li., S, Zhao, J., Zhai, Y., Yuan, Q., Zhang, H., Wu, X., Lu, Y., Peng, J., Sun, Z., Lin, L., Zheng, H., Chen, J., Yan, F. (2019). The *hypersensitive induced reaction 3* (*HIR3*) gene contributes to plant basal resistance via an EDS1 and salicylic acid-dependent pathway. *The Plant Journal, 98*(5), 783-797.

Liebrand, T.W.H, van den Burg, H.A., Joosten, M.H. (2014). Two for all: receptor-associated kinases SOBIR1 and BAK1. *Trends Plant Science, 19*(2), 123-32.

Liebrand, T.W.H., van den Berg, G.C.M., Zhang, Z. Smit, P., Cordewener, J.H.G., America, A.H.P., Sklenar, J., Jones, A.M.E., Tameling, W.I.L., Robatzek. S. (2013). Receptor-like kinase SOBIR1/EVR interacts with receptor-like proteins in plant immunity against fungal infection. *Proceedings of the National Academy of Sciences, 110*(24), 10010-10015.

Lipka, V., Dittgen, J., Bednarek, P., Bhat, R., Wiermer, M., Stein, M., Landtag, J., Brandt, W., Rosahl, S., Scheel, D., Llorente, F., Molina, A., Parker, J., Somerville, S., Schulze-Lefert, P. (2005). Pre and post invasion defenses both contribute to nonhost resistance in Arabidopsis. *Science, 18*(310),1180-1183.

Liu, Y., Burch-Smith, T., Schiff, M., Feng, S., Dinesh-Kumar, S.P. (2004). Molecular chaperone Hsp90 associates with resistance protein N and its signaling proteins SGT1 and Rar1 to modulate an innate immune response in plants. *Journal of Biological Chemistry*, *279*(3), 2101-2108.

Liu, Y., Jin, H., Yang, K.Y., Kim, C.Y., Baker, B., Zhang, S. (2003). Interaction between two mitogen-activated protein kinases during tobacco defense signaling. *Plant Journal, 34*(2), 149-160.

Lund, S.T., Stall, R.E., Kleea, H.J. (1998). Ethylene regulates the susceptible response to pathogen infection in tomato. *The Plant Cell, 10*, 371-382.

Ma, L., & Borhan, M.H. (2015). The receptor-like kinase SOBIR1 interacts with *Brassica napus* LepR3 and is required for *Leptosphaeria maculans* AvrLm1-triggered immunity. *Frontiers in Plant Science, 29*(6), 933.

Maruta, N., Sorbello, M., Kobe, B. (2025). TIR-mediated immune signaling through the EDS1: PAD4: ADR1 node is conserved in monocots and dicots. *Molecular Plant*, *18*(2), 192-194.

Melech-Bonfil, S., & Sessa, G. (2010). Tomato MAPKKKε is a positive regulator of cell-death signaling networks associated with plant immunity. *The Plant Journal, 64*(3), 379-391.

Mishra, N.S., Tuteja, R., Tuteja, N. (2006). Signalling through MAP kinase networks in plants. *Archives of Biochemistry and Biophysics, 452*(1), 55-68.

Miya, A., Albert, P., Shinya, T., Desaki, Y., Ichimura, K., Shirasu, K., Narusaka, Y., Kawakami, N., Kaku, H., Shibuya, N. (2007). CERK1, a LysM receptor kinase, is essential for chitin elicitor signaling in Arabidopsis. *Proceedings of the National Academy of Sciences*, *104*(49), 19613-19618.

Mur, L.A., Kenton, P., Atzorn, R., Miersch, O., Wasternack, C. (2006). The outcomes of concentration-specific interactions between salicylate and jasmonate signaling include synergy, antagonism, and oxidative stress leading to cell death. *Plant Physiology, 140*(1), 249-262.

Nabi, Z., Manzoor, S., Nabi, S.U., Wani, T.A., Gulzar, H., Farooq, M., Arya, V.M., Baloch, F.S., Vladulescu, C., Popescu, S.M., Mansoor, S. (2024). Pattern-triggered immunity and effector-triggered immunity: crosstalk and cooperation of PRR and NLR-mediated plant defense pathways during host–pathogen interactions. *Physiology Molecular Biology of Plants, 30*(4), 587-604.

Nambeesan, S., Qamar, S.A., Laluk, K., Mattoo, A.K., Mickelbart, M.V., Ferruzzi, M.G., Mengiste, T., Handa, A.K. (2012). Polyamines attenuate ethylene-mediate defense responses to abrogate resistance to *Botrytis cinerea* in tomato. *Plant Physiology, 158*(2), 1034-1045.

Oetiker, J.H., & Yang, S.F. (1995). The role of ethylene in fruit ripening. *Acta Horticulture, 398*, 167-178.

Ogata, T., Okada, H., Kawaide, H., Takahashi, H., Seo, S., Mitsuhara, I., Matsushita, Y. (2015). Involvement of NtERF3 in the cell death signalling pathway mediated by SIPK/WIPK and WRKY1 in tobacco plants. *Plant Biolgy, 17*(5), 962-972.

Ohtsu, M., Shibata, Y., Ojika, M., Tamura, K., Hara-Nishimura, I., Mori, H., Kawakita, K., Takemoto, D. (2014). Nucleoporin 75 is involved in the ethylene-mediated production of phytoalexin for the resistance of *Nicotiana benthamiana* to *Phytophthora infestans*. *Molecular Plant-Microbe Interactions*, *27*(12), 1318-1330.

Pedley, K.F., Martin, G.B. (2004). Identification of MAPKs and their possible MAPK kinase activators involved in the Pto-mediated defense response of tomato. *Journal of Biological Chemistry, 279*(47), 49229-49235.

Peng, K.C., Wang, C.W., Wu, C.H., Huang, C.T., Liou, R.F. (2015). Tomato SOBIR1/EVR homologs are involved in elicitin perception and plant defense against the oomycete pathogen *Phytophthora parasitica*. *Molecular Plant-Microbe Interaction, 28*(8), 913-926.

Penninckx, I.A., Thomma, B.P., Buchala, A., Métraux, J.P., Broekaert, W.F. (1998). Concomitant activation of jasmonate and ethylene response pathways is required for induction of a plant defensin gene in Arabidopsis. *The Plant Cell*, *10*(12), 2103-2113.

Postma, J., Liebrand, T.W., Bi, G., Evrard, A., Bye, R.R., Mbengue, M., Kuhn, H., Joosten, M.H., Robatzek, S. (2016). Avr4 promotes Cf-4 receptor-like protein association with

the BAK1/SERK3 receptor-like kinase to initiate receptor endocytosis and plant immunity. *New Phytologist, 210*(2), 627-642.

Pruitt, R.N., Locci, F., Wanke, F., Zhang, L., Saile, S.C., Joe, A., Karelina, D., Hua, C., Fröhlich, K., Wan, W.L., Hu, M., Rao, S., Stolze, S.C., Harzen, A., Gust, A.A., Harter, K., Joosten, M.H.A.J., Thomma, B.P.H.J., Zhou, J.M., Dangl, J.L., Weigel, D., Nakagami, H., Oecking, C., Kasmi, F.E., Parker, J.E., Nürnberger, T. (2021). The EDS1-PAD4-ADR1 node mediates Arabidopsis pattern-triggered immunity. *Nature, 598*(7881), 495-499.

Rinarta, D. (2017). Engineering the tomato *I* gene and identification of signalling partners. Master thesis submitted to the Australian National University (ANU), Canberra, Australia.

Seifbarghi, S., Borhan, M.H., Wei, Y., Ma, L., Coutu, C., Bekkaoui, D., Hegedus, D.D. (2020). Receptor-like kinases BAK1 and SOBIR1 are required for necrotising activity of a novel group of *Sclerotinia sclerotiorum* necrosis-inducing effectors. *Frontiers in Plant Science, 10*(11), 1021.

Seo, S., Katou, S., Seto, H., Gomi, K., Ohashi, Y. (2007). The mitogen-activated protein kinases WIPK and SIPK regulate the levels of jasmonic and salicylic acids in wounded tobacco plants. *The Plant Journal, 49*(5), 899-909.

Sharma, D., Verma, N., Pandey, C., Verma, D., Bhagat, P.K., Noryang, S., Singh, K., Tayyeba, S., Banerjee, G. and Sinha, A.K. (2020). MAP kinases as regulators for stress responses in plants. *Protein Kinases and Stress Signalling in Plants,* 369-392.

Straus, M.R., Rietz, S., Ver Loren van Themaat, E., Bartsch, M., Parker, J.E. (2010). Salicylic acid antagonism of EDS1-driven cell death is important for immune and oxidative stress responses in Arabidopsis. *Plant Journal, 62*(4), 628-640.

Stulemeijer, I.J., Stratmann, J.W., Joosten, M.H. (2007). Tomato mitogen-activated protein kinases LeMPK1, LeMPK2, and LeMPK3 are activated during the Cf-4/Avr4-induced hypersensitive response and have distinct phosphorylation specificities. *Plant Physiology, 144*(3),1481-1494.

Sun, G., Zhang, X., Liu, Y., Chai, L., Liu, D., Chen, Z., Lu, S. (2024). Plant chemical defenses against insect herbivores using the wild tobacco as a model. *Phyton-International Journal of Experimental Botany, 93*(4), 641-659.

Takahashi, A., Casais, C., Ichimura, K., Shirasu, K. (2003). HSP90 interacts with RAR1 and SGT1 and is essential for RPS2-mediated disease resistance in Arabidopsis. *Proceedings of the National Academy of Sciences*, *100*(20), 11777-11782.

Takahashi, A., Agrawal, G.K., Yamazaki, M., Onosato, K., Miyao, A., Kawasaki, T., Shimamoto, K., Hirochika, H. (2007). Rice Pti1a negatively regulates *RAR1*-dependent defense responses. *The Plant Cell*, *19*(9), 2940-2951.

Thaler, J.S., Owen, B., Higgins, V.J. (2004). The role of the jasmonate response in plant susceptibility to diverse pathogens with a range of lifestyles. *Plant Physiology, 135*(1), 530-538.

Thatcher, L.F., Anderson, J.P., Singh, K.B. (2005). Plant defense responses: what have we learnt from Arabidopsis? *Functional Plant Biology, 32*(1), 1-19.

Thomas, C.M., Tang, S., Hammond-Kosack, K., Jones, J.D. (2000). Comparison of the hypersensitive response induced by the tomato *Cf-4* and *Cf-9* genes in *Nicotiana* spp. *Molecular Plant Microbe Interaction, 13*(4), 465-469.

Tieman, D.M., Taylor, M.G., Ciardi, J.A., Klee, H.J. (2000). The tomato ethylene receptors NR and LeETR4 are negative regulators of ethylene response and exhibit functional compensation within a multigene family. *Proceedings of the National Academy of Sciences, 97*(10), 5663-5668.

Trobacher, C.P. (2009). Ethylene and programmed cell death in plants. *Botany, 87*(8), 757-769.

van der Burgh, A.M., Postma, J., Robatzek, S., Joosten, M. (2019). Kinase activity of SOBIR1 and BAK1 is required for immune signalling. *Molecular Plant Pathology, 20*(3), 410-422.

Van der Ent, S., & Pieterse, C.M. (2012). Ethylene: multi-tasker in plant–attacker interactions. *Annual Plant Reviews, 44,* 343-377.

Van der Hoorn, R.A., Laurent, F., Roth, R., De Wit, P.J. (2000). Agroinfiltration is a versatile tool that facilitates comparative analyses of Avr9/Cf-9-induced and Avr4/Cf-4-induced necrosis. *Molecular Plant Microbe Interaction, 13*(4),439-446.

van Verk, M.C., Gatz, C., Linthorst, H.J.M. (2009). Chapter 10. Transcriptional regulation of plant defense responses. *Advances in Botanical Research, Academic Press, 51*, 397-438.

Wagner, S., Stuttmann, J., Rietz, S., Guerois, R., Brunstein, E., Bautor, J., Niefind, K., Parker, J.E. (2013). Structural basis for signaling by exclusive EDS1 heteromeric complexes with SAG101 or PAD4 in plant innate immunity. *Cell Host Microbe, 14*(6), 619-630.

Wierme, M., Feys, B.J., Parker, J.E. (2005). Plant immunity: the EDS1 regulatory node. *Current Opinion in Plant Biology, 8*(4), 383-389.

Wu, C.H., Abd-El-Haliem, A., Bozkurt, T.O., Belhaj, K., Terauchi, R., Vossen, J.H., Kamoun, S. (2017). NLR network mediates immunity to diverse plant pathogens. *Proceedings of the National Academy of Sciences, 114*(30), 8113-8118.

Wu, C.H., Belhaj, K., Bozkurt, T.O., Birk, M.S., Kamoun, S. (2016). Helper NLR proteins NRC2a/b and NRC3 but not NRC1 are required for Pto-mediated cell death and resistance in *Nicotiana benthamiana*. *New Phytologist, 209*(4),1344-1352.

Yakimova, E.T., Kapchina-Toteva, V.M., Laarhoven, L.J., Harren, F.M., Woltering, E.J. (2006). Involvement of ethylene and lipid signalling in cadmium-induced programmed cell death in tomato suspension cells. *Plant Physiology and Biochemistry, 44(*10), 581-589.

Yanagisawa, S., Yoo, S.D., Sheen, J. (2003). Differential regulation of EIN3 stability by glucose and ethylene signalling in plants. *Nature, 2*(425), 521-525.

Yang, D., Hettenhausen, C., Baldwin, I.T., Wu, J. (2011). BAK1 regulates the accumulation of jasmonic acid and the levels of trypsin proteinase inhibitors in *Nicotiana attenuata*'s responses to herbivory. *Journal of Experimental Botany, 62*(2), 641-652.

Yang, T.F., Gonzalez-Carranza, Z.H., Maunders, M.J., Roberts, J.A. (2008). Ethylene and the regulation of senescence processes in transgenic *Nicotiana sylvestris* plants. *Annals of Botany, 101*(2), 301-310.

Yang, Y.X., Ahammed, G.J., Wu, C., Fan, S.Y., Zhou, Y.H. (2015). Crosstalk among jasmonate, salicylate and ethylene signaling pathways in plant disease and immune responses. *Current Protein Peptide Science, 16*(5), 450-461.

Yu, D.S., Outram, M.A., Crean, E., Smith, A., Sung, Y.C., Darma, R., Sun, X., Ma, L., Jones, D.A., Solomon, P.S., Williams, S.J. (2022). Optimized production of disulfide-bonded fungal effectors in *Escherichia coli* using CyDisCo and FunCyDisCo coexpression approaches. *Molecular Plant Microbe Interaction*, *35*(2),109-118.

Yu, X.Q., Niu, H.Q., Liu, C., Wang, H.L., Yin, W., Xia, X. (2024). PTI-ETI synergistic signal mechanisms in plant immunity. *Plant Biotechnology Journal, 22*(8), 2113-2128.

Zhang, S., & Liu, Y. (2001). Activation of salicylic acid-induced protein kinase, a mitogen-activated protein kinase, induces multiple defense responses in tobacco. *Plant Cell, 13*(8), 1877-1889.

Zhang, S., Liu, Y., Klessig, D.F. (2000). Multiple levels of tobacco WIPK activation during the induction of cell death by fungal elicitins. *The Plant Journal, 23*(3), 339-347.

Zhang, W., Zhao, F., Jiang, L., Chen, C., Wu, L., Liu, Z. (2018). Different pathogen defense strategies in *Arabidopsis*: more than pathogen recognition. *Cells*, *7*(12), 252.

Zhou, J., Wu, S., Chen, X., Liu, C., Sheen, J., Shan, L., He, P. (2014). The *Pseudomonas syringae* effector HopF2 suppresses *Arabidopsis* immunity by targeting BAK1. *The Plant Journal, 77*(2), 235-245.

Chapter 5: *Fol* SIX6 induces stomatal opening and increases leaf transpiration

5.1 Introduction

Stomata act as a gateway for controlling water and gas exchange between the plant and the environment (Hetherington and Woodward 2003; Lawson and Matthews 2020). Stomata are bordered by two guard cells which control stomatal aperture by regulating the opening and closing of stomata. Stomata are generally open during the day, allowing entry of the CO_2 required for photosynthesis, while during the night stomata are closed because photosynthesis cannot occur in the dark and there is no requirement for CO_2 entry. Stomata also play a critical role in plant defence against abiotic stresses, including drought, salinity, high light and high CO_2 and biotic stresses, including attack by pathogenic fungi, bacteria, viruses and nematodes. In response to pathogen attack, stomata often close as a strategy to limit pathogen entry and reduce the risk of infection (Ayres 1984; Melotto et al., 2008; Lim et al., 2015; Melotto et al., 2017), while during abiotic stress stomatal closure helps limit water loss (Agurla et al., 2018; Daszkowska-Golec and Szarejko, 2013).

Opening and closing of stomata is mediated by various ion channels and transporters including K^+, Cl^-, Ca^{+2}, Na^+, NO_3^- channels and malate transporters. Activation of K^+ channels leads to K^+ influx into guard cells, while anion influx (Cl^-, NO_3-, malate) occurs through H^+ symporters, both processes raising ion concentrations in the cytosol. The increased ion concentration draws water into guard cells, causing them to swell which leads to stomatal opening (Figure 5.1) (Dietrich et al., 2001; Daszkowska-Golec and Szarejko, 2013). An H^+-ATPase pump is essential for stomatal opening as it actively transports protons out of guard cells, leading to hyperpolarisation of the membrane (Figure 5.1). This process facilitates the uptake of K^+ ions, increases water uptake and turgor pressure, ultimately resulting in the opening of stomata (Figure 5.1) (Dietrich et al., 2001; Daszkowska-Golec and Szarejko, 2013). During stress conditions, an H^+ ATPase pump transports protons into to guard cells leading to the acidification of the cytosol and activation of ion channels that move K^+, Cl^-, Ca^{+2}, Na^+ and NO_3^- ions out of guard cells along with water. This causes a decrease in turgor pressure which leads to stomatal closure (Figure 5.1) (Dietrich et al., 2001; Daszkowska-Golec and Szarejko, 2013.

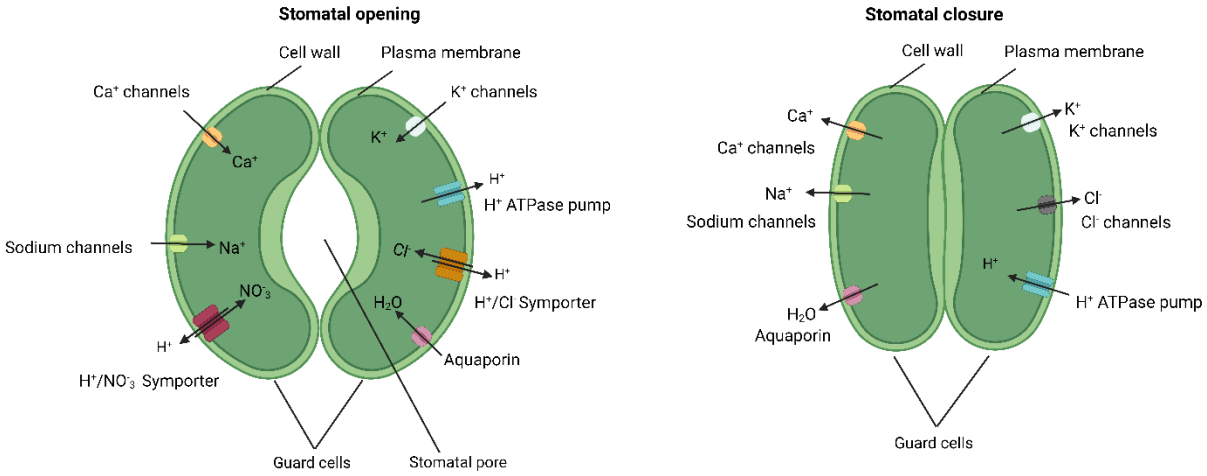

Figure 5.1 Simple illustration of various ion channels and transporters involved in the process of ion movement in guard cells, leading to stomatal opening and closure.

The illustration was generated using BioRender (https://app.biorender.com).

Previous research has identified vacuoles as essential components in regulating stomatal movement, highlighting the importance of understanding their structure and function (Li et al., 2022; Mirasole et al., 2023). Vacuoles are essential organelles in plant cells, playing a critical role in maintaining cellular homeostasis, storage and various metabolic processes (Maeshima et al., 2001). These large, membrane-bound compartments are primarily filled with a mixture of water, ions, sugars and other metabolites (Rogers, 2000). The central vacuole occupies a significant part of the cell, often accounting for up to 90% of the cell's volume (Taiz and Zeiger, 2010). It not only contributes to turgor pressure, which helps maintain cell rigidity, but also serves as a reservoir for nutrients and waste products (Cosgrove, 2005). One of the key features of vacuoles is their ability to regulate their volume in response to environmental conditions, a process that is intricately linked to the activity of water channels known as aquaporins (Maeshima et al., 2001). Aquaporins are membrane-spanning proteins that enable the swift movement of water molecules through cell membranes, including the tonoplast, the membrane enclosing the vacuole (Chaumont and Tyerman, 2014). These channels are crucial for maintaining water balance within the cell and enabling the dynamic changes in vacuolar volume that are necessary for various physiological processes (Gao et al., 2005; Boursiac et al., 2005).

Aquaporins are specialised membrane proteins in the major intrinsic protein (MIP) family. They mediate the selective transport of water molecules across biological membranes, playing a critical role in regulating cellular water homeostasis and maintaining osmotic balance (Maurel and Chrispeels, 2001. In plants, aquaporins are classified into subfamilies based on their localisation and function. PIPs (plasma membrane intrinsic proteins) are found on the plasma membrane and primarily facilitate water transport across the cell membrane. TIPs (tonoplast intrinsic proteins) are located in the vacuolar membrane (tonoplast) and regulate water movement between the cytoplasm and vacuole. NIPs (Nodulin-26-like intrinsic proteins) are found in root nodules and peri-bacteroid membranes, playing roles in symbiotic nitrogen fixation by facilitating the transport of water and other small molecules. SIPs (small basic intrinsic proteins) are found in the endoplasmic reticulum and other internal membranes, though their specific functions are less well characterised. XIPs (X intrinsic proteins) are present in dicotyledonous plants and some fungi, where they may transport water and other small solutes, though they are absent from monocots and most other plant groups (Maurel and Chrispeels, 2001; Johanson and Gustavsson, 2002; Danielson and Johanson, 2008; Sade et al., 2014).

In guard cells, the regulation of vacuolar volume is vital for controlling stomatal opening and closing, which in turn affects gas exchange and transpiration in plants (Gao et al., 2005). During stomatal opening, guard cells first take up water from the apoplast through plasma membrane aquaporins (PIPs), driven by the decreased water potential resulting from ion accumulation. This initial water influx increases cellular volume. Water then moves from the cytosol into the vacuole through tonoplast aquaporins TIP1;1 and TIP2;1, causing vacuolar expansion that further contributes to guard cell swelling and stomatal opening (Ding et al., 2024) (Figure 5.2). Conversely, during stomatal closure, ion efflux from guard cells (mediated by ion channels) and proton pumping by tonoplast H^+-ATPase reduce the osmotic potential of both the cytosol and vacuole. This drives water movement out of the vacuole through tonoplast aquaporins (TIP1;1 and TIP2;1) into the cytosol, followed by water export from the guard cell through plasma membrane aquaporins (PIPs) to the apoplast. The sequential loss of vacuolar and cellular water causes guard cells to shrink and stomata to close (Figure 5.2) (Tyerman et al., 2002; Schroeder et al., 2001; Ding et al., 2024).

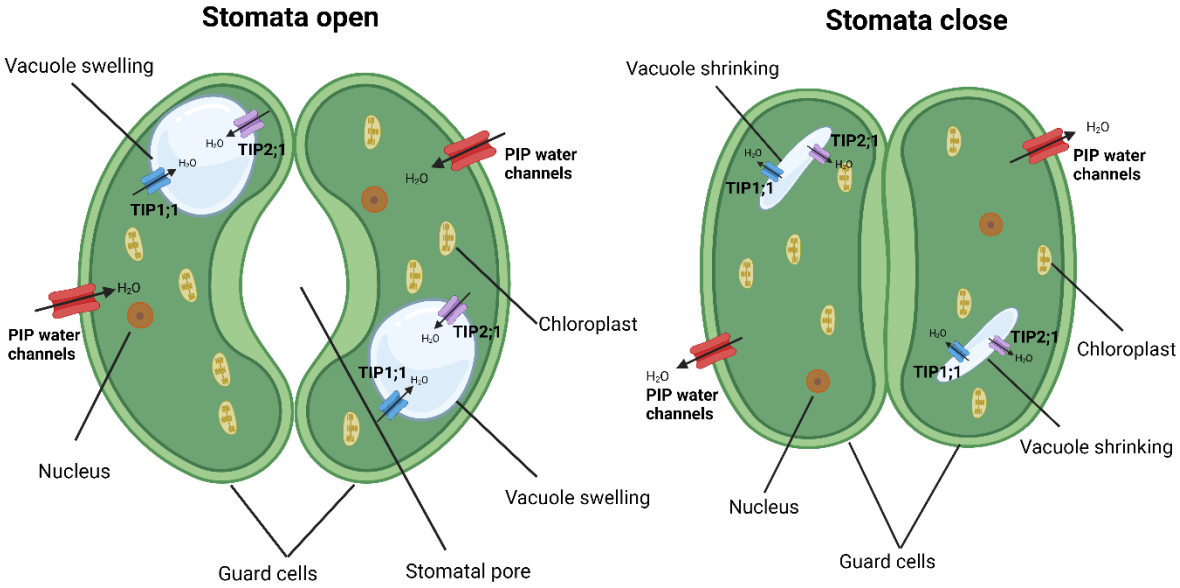

Figure 5.2 Simple illustration of aquaporin involvement in the process of stomatal opening and closing.

During stomatal opening (left), water enters guard cells through plasma membrane intrinsic protein (PIP) water channels and moves into vacuoles via tonoplast intrinsic proteins (TIP1;1 and TIP2;1), causing vacuole swelling and stomatal pore opening. During stomatal closing (right), water exits vacuoles through TIPs and leaves guard cells via PIP water channels, resulting in vacuole shrinkage and stomatal closure. Chloroplasts, nucleus, and other cellular organelles are shown for cellular context. The illustration was generated using BioRender (https://app.biorender.com).

Environmental stress leads to the synthesis of ABA in plant organs undergoing stress, which in turn leads to stomatal closure (to avoid excessive water loss) and activation of defence-related genes (Swamy and Smith, 1999; Seo and Koshiba, 2002; Tuteja, 2007; Lim et al., 2015). ABA plays a crucial role in the regulation of stomatal closure, particularly under water-deficit conditions (Hetherington and Quatrano, 1991; Leung and Giraudat, 1998; Hsu et al., 2021; Bharath et al., 2021). When plants experience drought stress, ABA is synthesised and released, leading to several physiological responses in guard cells, which control the opening and closing of stomata (Hetherington and Quatrano, 1991; Leung and Giraudat, 1998; Hsu et al., 2021; Bharath et al., 2021). Initially, ABA binds to receptors such as members of the PYR/PYL/RCAR family, which leads to inhibition of type 2C protein phosphatases (PP2Cs) (Figure 5.3) (Hsu et al., 2021). This inhibition activates SnRK2 protein kinases, such as OPEN

STOMATA 1 (OST1/SnRK2.6), which are essential for the signalling cascade that results in stomatal closure (Figure 5.3) (Hsu et al., 2021). Activated SnRK2s phosphorylate various target proteins, including the S-type anion channel SLAC1, and this phosphorylation promotes the efflux of ions (such as chloride and malate) from guard cells via anion channels. The loss of these osmotically active solutes reduces the osmotic potential of guard cells, which subsequently drives water efflux from the vacuoles through tonoplast intrinsic proteins (TIPs) and out of the cells through plasma membrane intrinsic proteins (PIPs), leading to a decrease in turgor pressure within these cells (Figure 5.3) (Hsu et al., 2021). As a result, the decreased osmotic potential drives water efflux from the vacuoles through TIPs and out of the guard cells through PIPs, causing them to shrink and the stomata to close and the closure of stomata reduces water loss through transpiration, helping the plant conserve water during periods of drought (Hsu et al., 2021).

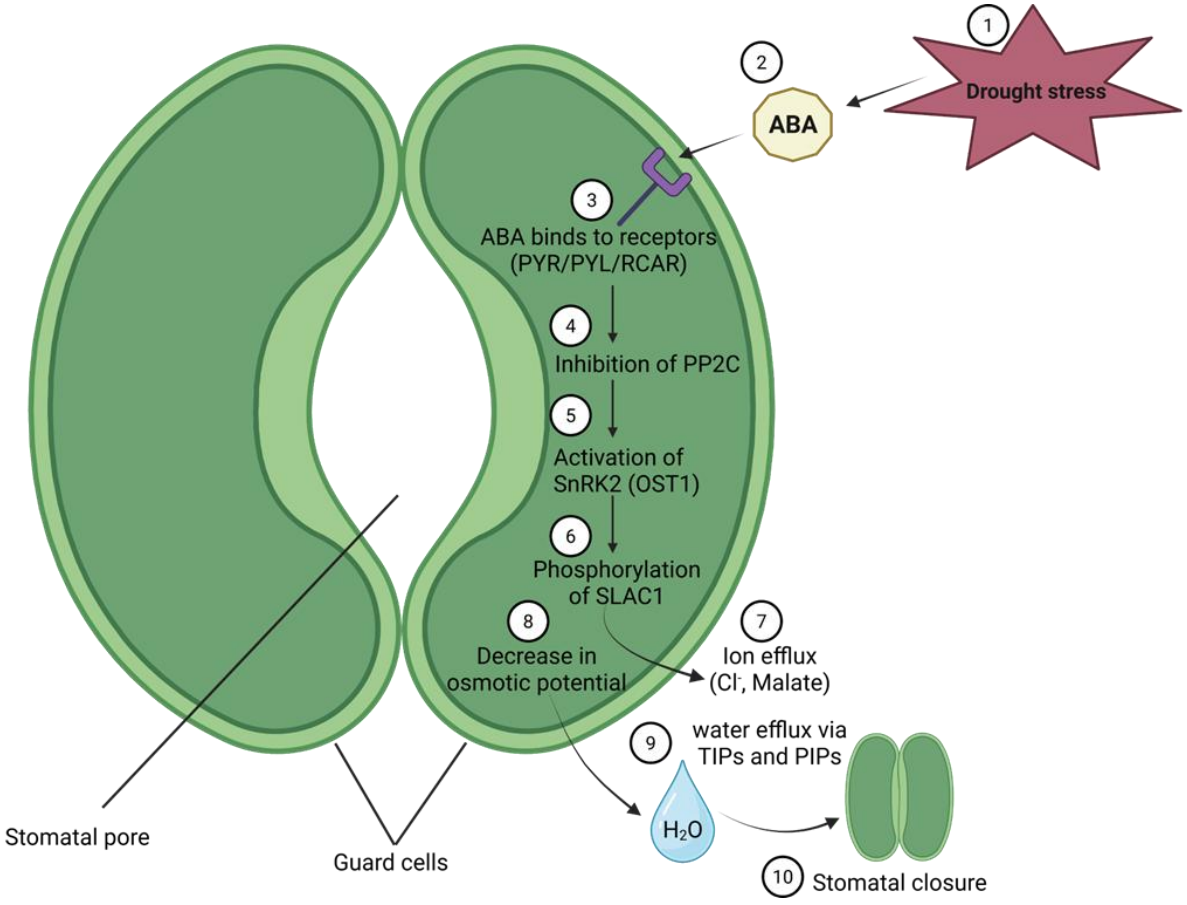

Figure 5.3 Simple illustration of the role of ABA in stomatal closure.

(1) Drought stress triggers (2) ABA synthesis. (3) ABA binds to PYR/PYL/RCAR receptors, leading to (4) inhibition of PP2C phosphatases and (5) activation of SnRK2 kinases (OST1). (6) SnRK2 phosphorylates SLAC1 anion channels, promoting (7) ion efflux (Cl^-, malate). (8) Loss of osmotic solutes decreases osmotic potential, driving (9) water efflux through tonoplast

and plasma membrane aquaporins, resulting in (10) stomatal closure. The illustration was generated using BioRender (https://app.biorender.com).

After finding that *Fol* SIX6 could induce plant cell death (Chapter 3) and that this was unlikely to be defence-related (Chapter 4), the initial objective of the research described in this chapter was to look at what was happening at the microscopic level. This led to the discovery that SIX6 induced stomatal opening. The next step was to further investigate SIX6-induced stomatal opening and the mechanism behind it.

5.2 Materials and Methods

5.2.1 Plant Materials

Seeds of *N. benthamiana* and M82 tomato (*Solanum lycopersicum*) were sown in pots with seed-raising mix (Martins Fertilizers, Australia) and grown at 25°C in a growth room with a 16-hour photoperiod, light intensity of 250 μmol m^{-2} s^{-1} and relative humidity 60-65% for 4 to 6 weeks before protein infiltration. Infiltrated seedlings were then allowed to grow in the same conditions for different periods depending on the experiment.

5.2.2 Preparation of epidermal peels and measurements of stomatal length and aperture

Leaf epidermal peels were prepared from the abaxial side of the leaf area where the protein of interest or control was infiltrated using round bent forceps. They were mounted in water on a microscope slide and viewed under water immersion using a Leica DM5500 Compound Microscope with 40X magnification. Photographic images of stomata (arrowed) were assessed using ImageJ software (https://imagej.net/software). Stomatal pore length and widths were measured using the line tool option from ImageJ to obtain length values, which were then converted into μm using the 50 μm scale bar as a reference. The procedure is outlined in Figure 5.4.

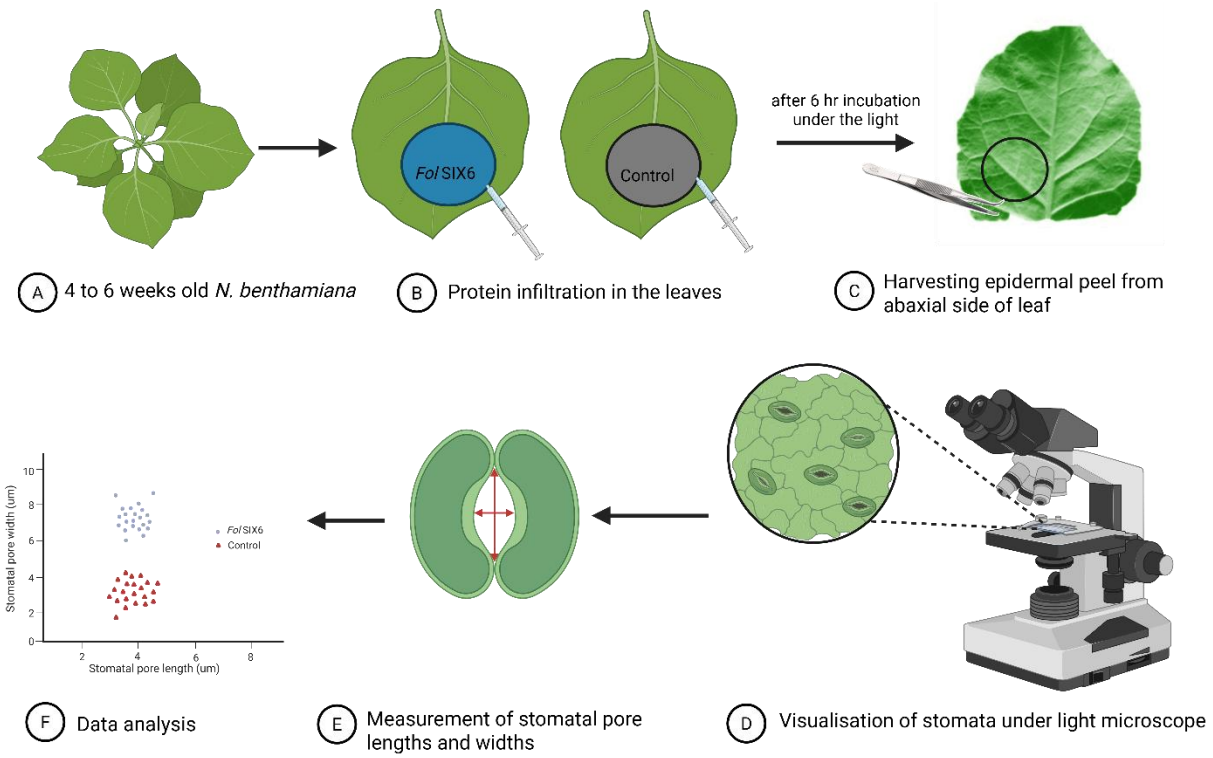

Figure 5.4 Stomatal pore length and width measurements from leaves of *Nicotiana benthamiana* infiltrated with *Fol* SIX6 protein.

(A) *N. benthamiana* plants were allowed to grow for 4 to 6 weeks. **(B)** Leaves were then infiltrated with recombinant *Fol* SIX6 protein (100 µg/ml) or water (control) and kept in the light for 6 hours. **(C)** Epidermal peels were harvested from the abaxial side of the infiltrated leaf area using round, bent forceps. **(D)** Stomata were visualised and photographed using a Leica DM5500 compound microscope with a 40X water-immersion objective. **(E)** Stomatal pore lengths and widths were measured using ImageJ software (https://imagej.net/software). **(F)** Data were plotted and statistically analysed for all stomatal measurements.

5.2.3 Gas exchange measurements

All gas exchange measurements were performed using a LI-6800 Portable Photosynthesis System (LI-COR Biosciences) fitted with a 6800-01A Multiphase Flash Fluorometer (LI-COR Biosciences). Two different leaves of each *N. benthamiana* plant used in these experiments were infiltrated in normal light conditions, one with 100 µg/ml of *Fol* SIX6 protein (treatment) and the other with water (control). When light was the initial treatment, plants were exposed to light (250 µmol m^{-2} s^{-1}) for 1 hour prior to leaves (still attached) being clamped in the leaf chamber of the LI-6800. Conversely, they were kept in darkness for 1 hour prior to clamping when the initial treatment was dark. For all experiments, chamber conditions were controlled

to an ambient CO_2 concentration of 400 µmol mol^{-1} and a leaf-to-air vapour pressure difference of 1 kPa. The leaf temperature was maintained at 25°C and the flow rate was 500 µmol air s^{-1}. For gas exchange measurements taken on plants when exposed to light, the photosynthetically active radiation was set to 500 or 1000 µmol photons m^{-2} s^{-1}. Gas exchange measurements were logged every two minutes. The procedure is explained in Figure 5.5.

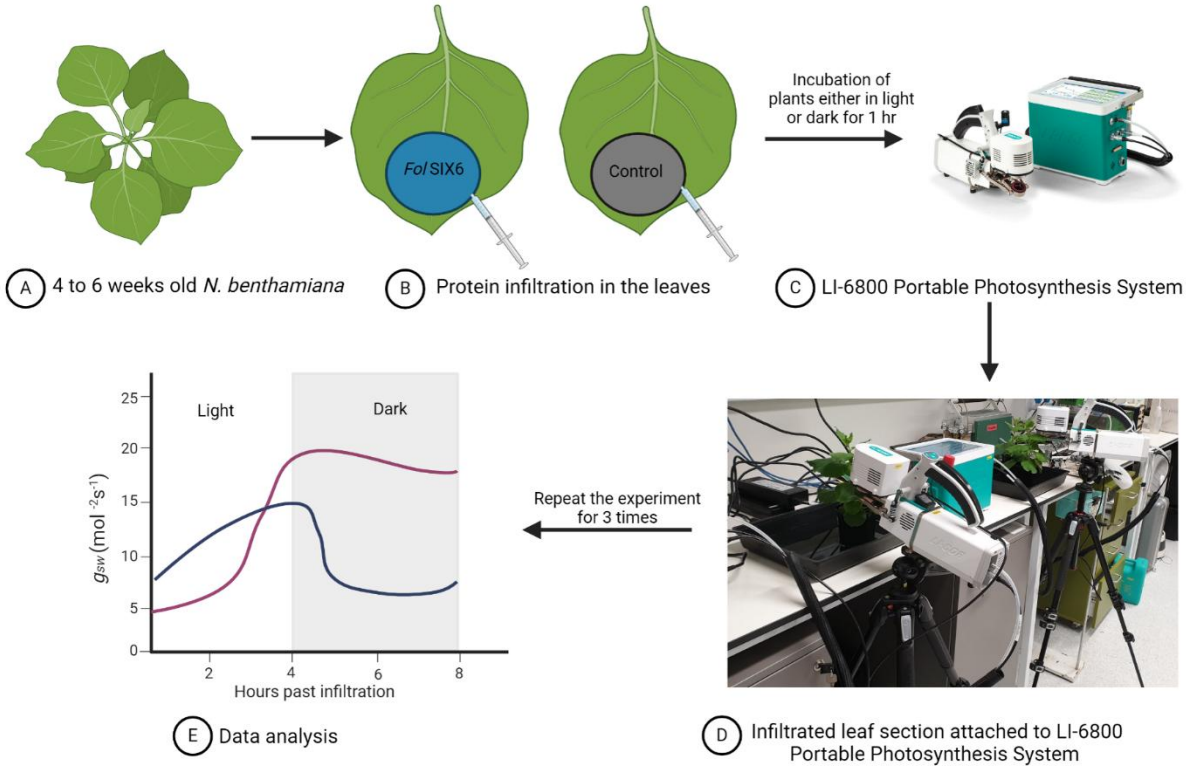

Figure 5.5 Gas exchange measurements of leaves of *Nicotiana benthamiana* infiltrated with *Fol* SIX6 protein.

(A) *N. benthamiana* plants were allowed to grow for 4 to 6 weeks. **(B)** Leaves were then infiltrated with *Fol* SIX6 protein (100 µg/ml) or water (control) and infiltrated plants were kept in light or dark for 1 hour depending on the treatment. **(C)** A LI-6800 Portable Photosynthesis System was used to measure gas exchange. **(D)** The infiltrated area of the leaf was clamped into the Portable Photosynthesis System and gas exchange measurements were taken. **(E)** Gas exchange data were then analysed for all three replicates.

5.2.4 Measurement of electrolyte leakage from leaf discs

Fol SIX6 protein (100 µg/ml) and control (gel filtration buffer and BSA) were infiltrated in *N. benthamiana* or tomato leaves using a 2 ml syringe and kept in a growth room under a 16 h 21°C light 100 µE m^{-2} sec $^{-1}$ and 8 h 16°C dark cycle at 60-65% relative humidity. After 22

hours, for electrolyte measurements, six leaf discs (7 mm diameter) from one plant (three per leaf) were removed using a cork borer. Leaf discs (three leaf discs per well) were then placed in a 6-well plate filled with deionised water (8 ml sterile per well) (Figure 5.6). The plate was then covered with a lid and kept on a shaker at 100 rpm for 10 minutes, and the water was removed by pipette and immediately replaced. Ion leakage was measured by using a hand-held conductivity meter (HM Digital, Model: COM-100) (Figure 5.6). The conductivity meter was calibrated to 0 µS/cm before first use. After each reading, the conductivity meter's sensor was cleaned with deionised water.

Figure 5.6 Measurement of electrolyte leakage from leaf discs taken from leaves of *N. benthamiana* or tomato plants infiltrated with *Fol* SIX6.

Three leaf discs from each infiltrated leaf were placed in 8 ml of sterile deionised water in each well of a six-well culture plate and conductivity was later measured using a hand-held conductivity meter.

5.2.5 Confocal fluorescence microscopy of mTurquoise2-labelled vacuoles

A gene block was synthesised by IDT that contained LIC sites flanking the mTurquoise2 coding sequence (Goedhart et al., 2012) fused to the coding sequence for the C-terminal vacuolar-targeting signal from tomato vacuolar endochitinase 3 as shown in Appendix 5.1. The coding sequence for the fusion protein was transferred to the pSL binary vector (Hellens et al., 2000) by LIC as described in section 2.2.5. The binary vector construct was transferred to *Agrobacterium* strain GV3101 (pMP90) carrying pSOUP as described in section 2.2.9 for use

in agroinfiltration of *N. benthamiana* leaves as described in section 2.2.10. Confocal fluorescence microscopy was conducted on agroinfiltrated leaves expressing mTurquoise2 using a Zeiss confocal LSM 780 microscope with a 40x-water immersion objective lens (LD C-Apochromat 40/1.1W Corr M27). An excitation wavelength of 454 nm and an acquisition wavelength of 475 nm were used for mTurquoise2.

5.2.6 Preparation of *Fol* inoculum

Fol race 3 was grown on PDB (Potato Dextrose Broth) media (Difco, Cat # 254920) at 25°C for 5 days with shaking at 200 rpm. The fungal culture was then filtered through four layers of miracloth and spores were collected in a 50 ml centrifuge tube. The conidial suspension was then centrifuged at 6000 x g for 10 minutes and the pellet was washed three times with deionised water by repeated centrifugation and resuspension. The spore concentration of the final suspension was then checked using a haemocytometer (Fuchs-Rosenthal counter) under a bright light microscope with 10x magnification (Olympus CX22LED). A final concentration of $5x10^7$ conidia/ml was used for plant inoculation.

5.2.7 *Fol* pathogenicity test

Seeds of tomato cv. M82 were germinated and grown in seed raising mix for 18 days in a controlled-environment chamber with 16 h, 25°C day cycle (100 µE m^{-2} sec^{-1}) and 8 h, 20°C night cycle. Seedlings were carefully removed, and roots were washed with deionised water. After trimming 1 to 2 cm from the ends of the roots, the seedlings were dipped into water (mock inoculation) or a spore suspension of *Fol* race 3 ($5x10^7$ conidia/ml prepared as described in section 5.2.6) for 3 minutes. Seedlings were then replanted in potting mix (Martins Fertilizers, Australia) supplemented with Osmocote slow-release fertilizer (Scotts, Australia). Inoculated plants were grown under the same conditions as described above for 21 days.

5.3 Results

5.3.1 *Fol* SIX6 causes stomatal opening in *Nicotiana benthamiana*

To gain a better understanding of the cell death response caused by *Fol* SIX6, a microscopic examination of leaves infiltrated with *Fol* SIX6 protein was performed before the onset of cell death. *N. benthamiana* leaves were infiltrated with *Fol* SIX6 (100 µg/ml) and plants kept at 25°C in light. Leaves of *N. benthamiana* start to show signs of cell death from 24 to 48 hours after *Fol* SIX6 infiltration, so microscopic observations were taken from 6 hours after

infiltration. Surprisingly, stomata from leaves infiltrated with *Fol* SIX6 were found to already be wide open at 6 hours after infiltration compared to stomata from leaves infiltrated with water (Figure 5.7A), suggesting that the stomata were opening in response to *Fol* SIX6. Stomatal pore length and widths were measured, and the mean stomatal pore width was found to be significantly greater ($p<0.0001$) in leaves infiltrated with *Fol* SIX6 (8.4±0.2 µm) than in leaves infiltrated with water alone (2.4±0.1 µm) (Figure 5.7B). The length of the stomatal pore did not differ significantly between treatments ($p>0.05$). Therefore, only the width of stomatal pores was measured in subsequent analyses of stomatal aperture.

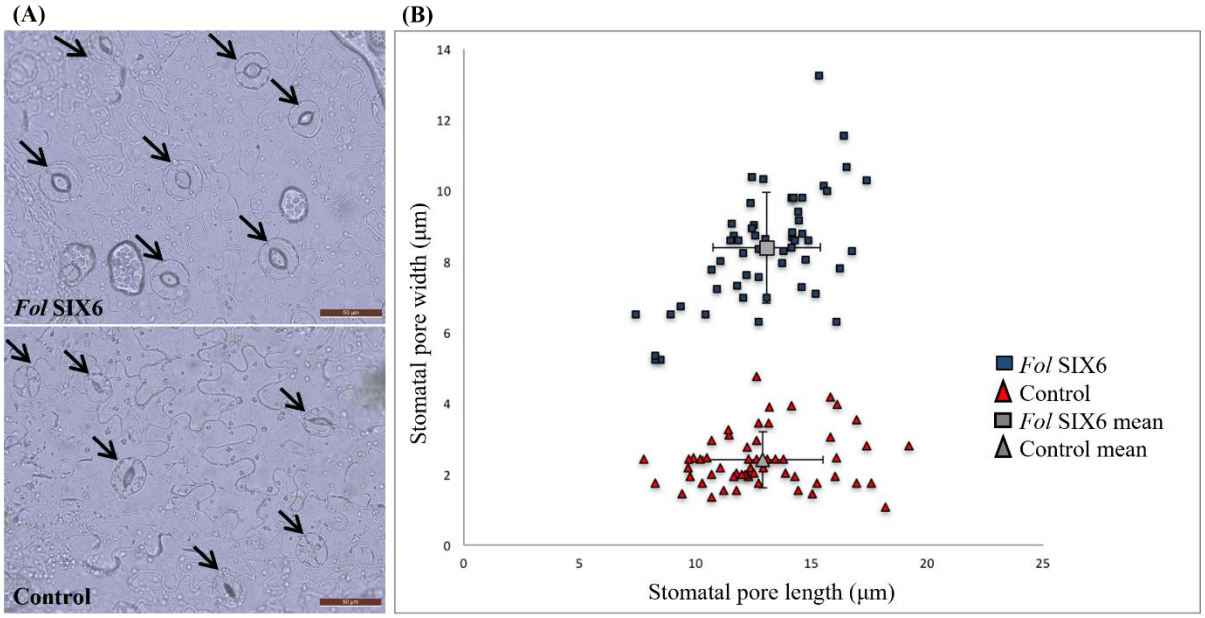

Figure 5.7 *Fol* SIX6 protein induces stomatal opening in *Nicotiana benthamiana*.

(A) Leaves of *N. benthamiana* were infiltrated with *Fol* SIX6 (100 µg/ml) or water (control) and plants were exposed to light for 6 hours after infiltration. Leaf epidermal peels from the area of infiltration were prepared for microscopic analysis as described in Figure 5.4. Stomata are indicated by arrows. Scale bars represent 50 µm. **(B)** Stomatal pore length and widths were measured for 50 stomata from the leaves of three plants using the line tool option from ImageJ software (https://imagej.net/software). Data are shown as scatter plots with means shown using grey symbols and error bars representing standard deviations. Data were analysed using Student's t-test ($P < 0.05$).

To confirm that stomatal opening was caused by *Fol* SIX6, leaves of *N. benthamiana* were infiltrated with protein purified from a vector-only control or with *Fol* SIX6 that had been reduced using dithiothreitol to abolish *Fol* SIX6 activity, as shown previously (Chapter 3). Neither treatment caused stomatal opening (Figure 5.8A and 5.8B). Agroinfiltration of *Avr1*, (*Fol SIX4)* also failed to induce stomatal opening (Appendix 5.2). Collectively, these data show

that stomatal opening was a response specific to *Fol* SIX6 and that stomatal opening could be a precursor to leaf cell death.

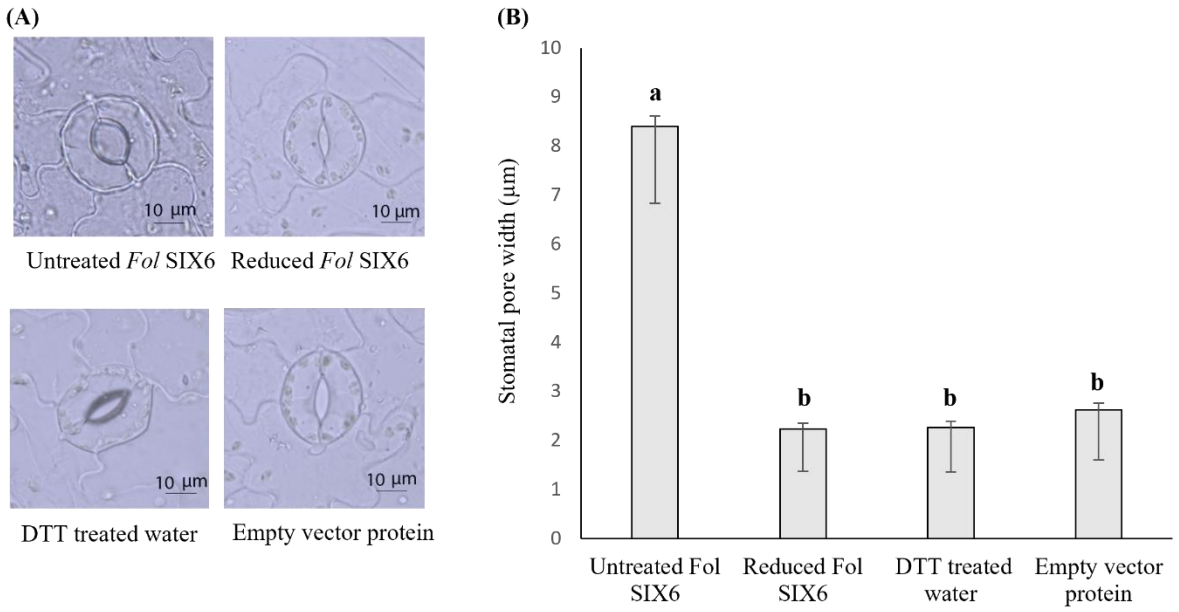

Figure 5.8 Stomatal opening in *Nicotiana benthamiana* is dependent on intact *Fol* SIX6 and is not an artefact of heterologous protein expression and purification.

(A) *N. benthamiana* leaves were infiltrated with recombinant *Fol* SIX6 protein (100 µg/ml), *Fol* SIX6 reduced with 2 mM DTT, DTT-treated water or protein (100 µg/ml) extracted and purified in the same way as SIX6 from *E. coli* carrying an empty vector. Epidermal peels from infiltrated areas were produced and analysed as described in Figure 5.4. **(B)** Stomatal pore widths were measured for 50 stomata from infiltrated leaves on three different plants. Values are the means ± standard errors. Data were analysed using pairwise Student t-tests. Different letters indicate significant differences at $p<0.05$.

To test whether the stomatal opening occurred in tomato (the host of *Fol*), epidermal peels of tomato leaves were also examined by light microscopy 6 hours after infiltration with *Fol* SIX6. Stomata from leaves infiltrated with *Fol* SIX6 were wide open compared to stomata from leaves infiltrated with water (Figure 5.9). To determine whether stomatal opening was correlated with cell death, stomatal opening was also examined in two plant species, zucchini and radish, that did not show cell-death responses to *Fol* SIX6. Stomata from zucchini and radish cotyledons infiltrated with *Fol* SIX6 showed no evidence of stomatal opening compared to stomata from cotyledons infiltrated with water (Appendix 5.3). This result suggested that cell death induction could be a consequence of stomatal opening caused by *Fol* SIX6.

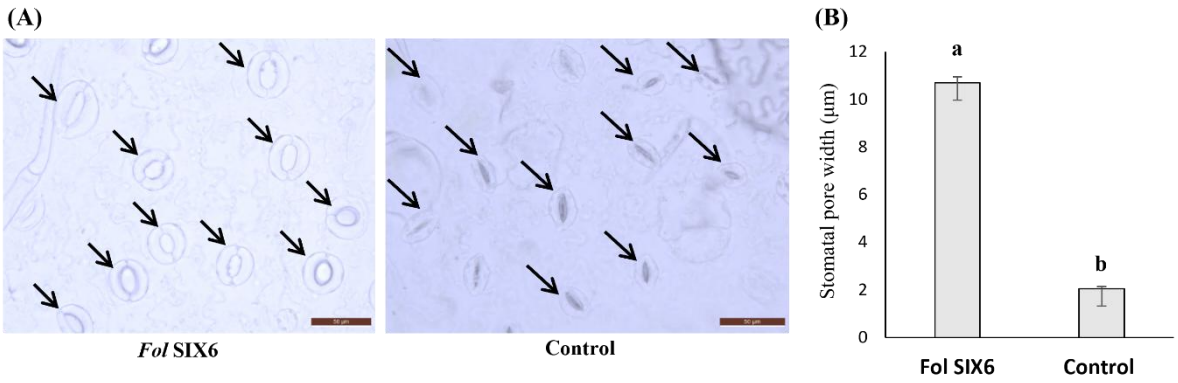

Figure 5.9 SIX6 causes stomatal opening in tomato.

(A) Leaves of tomato cv. M82 were infiltrated with *Fol* SIX6 protein (100 µg/ml) or water (control) and plants were exposed to light for 6 hours after infiltration. Epidermal peels from infiltrated areas were produced and analysed as described in Figure 5.4. Scale bars represent 50 µm. **(B)** Stomatal pore widths were measured for 50 stomata from infiltrated leaves of three different plants in each treatment. Values are the means ± standard errors. Data were analysed using pairwise Student t-tests. Different letters indicate significant differences at $p<0.05$.

5.3.2 *Fol* SIX6 causes stomatal opening in a light-independent manner and increases transpiration

Stomatal opening is normally a light-dependent process that allows the exchange of water vapour (transpiration), carbon dioxide and oxygen between the plant leaf and surrounding air. To test whether stomatal opening triggered by *Fol* SIX6 was light-dependent and resulted in increased transpiration, stomatal conductance was measured in dark-adapted *N. benthamiana* leaves that were infiltrated with *Fol* SIX6 protein or water and then kept in the light or dark as described in section 5.2.3. After a short lag, SIX6-treated plants were found to open their stomata in the light treatment at about twice the speed of control plants, as indicated by a change in stomatal conductance (Figure 5.10A). After the light was turned off, the stomata of SIX6-treated leaves remained open, whereas the stomata of control leaves closed to give minimal stomatal conductance within less than half an hour (Figure 5.10A). In the dark treatment, stomata on control leaves remained closed, but stomata on SIX6-treated leaves opened and maximal stomatal conductance was reached after about 8h (Figure 5.10B). Turning on the light caused stomata on control leaves to open rapidly but had little effect on stomata of SIX6-treated plants, which were already open and showing near-maximal stomatal conductance (Figure 5.10B). In summary, *Fol* SIX6 causes light-independent, irreversible opening of stomata in *N. benthamiana* resulting in a constitutive increase in transpiration.

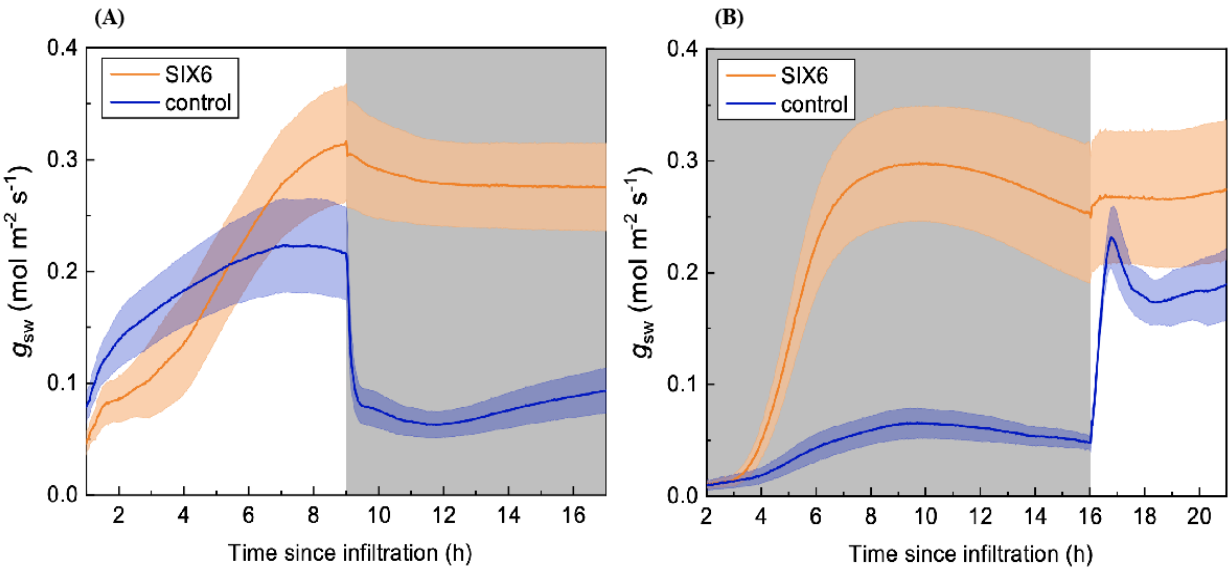

Figure 5.10 *Fol* SIX6 causes irreversible light-independent stomatal opening.

Stomatal opening as indicated by an increase in stomatal conductance (*gsw*) was measured for attached *N. benthamiana* leaves that had been infiltrated with either 100 µg/ml recombinant *Fol* SIX6 protein (SIX6; orange) or with water (control; blue). **(A)** Infiltrated plants were kept for 1 h in the light after which infiltrated leaves were clamped inside the leaf chamber and exposed to light (500 µmol photons m^{-2} s^{-1}). Stomatal conductance was monitored every 2 min for 9 h of light followed by 8 h of darkness. **(B)** Infiltrated plants were kept for 1 h in the dark, after which infiltrated leaves were clamped inside the leaf chamber. Gas exchange measurements were logged every two minutes for 16 h of dark followed by 5 h of light (1000 µmol photons m^{-2} $s^{-1)}$. Note that stomatal opening in response to light in control plants was much quicker after 16h of darkness (B) than 1h (A), possibly because leaves had more time to recover from the infiltration procedure and adapt to the light chamber. Blue and orange lines show means and flanking shaded areas show standard deviations. Grey backgrounds denote dark periods and white backgrounds indicate light periods. n = 4 leaves on 4 different plants in (A) and 3 in (B).

5.3.3 *Fol* SIX6 protein causes electrolyte leakage in leaves of *N. benthamiana* and tomato

Electrolyte leakage has often been associated with the plant hypersensitive response to pathogen attack (Demidchik et al., 2014) and is considered an initial event leading to cell death (Demidchik et al., 2010; Hatsugai et al., 2018). To determine whether cell death induced by *Fol* SIX6 was preceded by ion leakage, leaf discs were taken from leaves of *N. benthamiana* and tomato 24 h after the infiltration with *Fol* SIX6 protein (100 µg/ml) and immersed in water. Aqueous conductivity was measured over 12 hours. Even after just one hour, leaves treated with *Fol* SIX6 were found to show significantly higher conductivity compared to the BSA

control in both *N. benthamiana* (Figure 5.11) and tomato (Figure 5.12), indicating that *Fol* SIX6 protein caused electrolyte leakage in leaves of *N. benthamiana* and tomato.

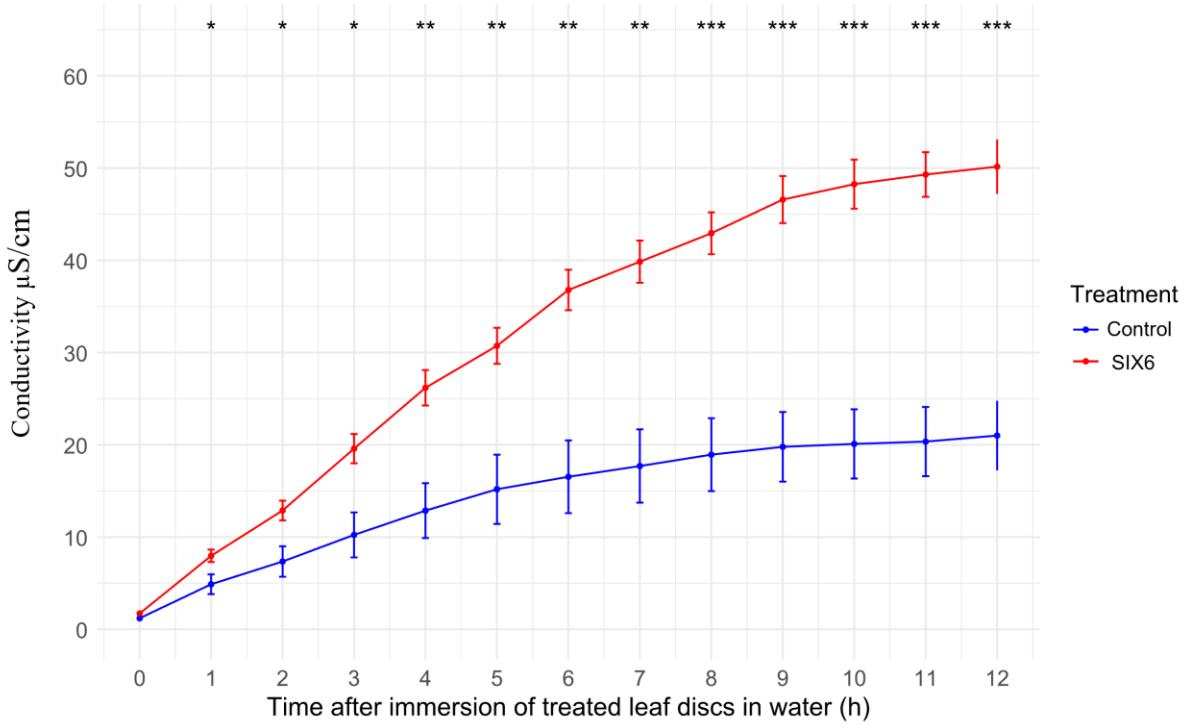

Figure 5.11 SIX6 causes electrolyte leakage in *N. benthamiana* leaves.

Aqueous conductivity was measured at hourly intervals over 12 h for leaf discs of *N. benthamiana* immersed in water 22 h after infiltration with *Fol* SIX6 protein (100 µg/ml) or control (BSA: 100 µg/ml). Means and SEs are shown for six replicates comprising three leaf discs per measurement from each of two leaves on three plants. Conductivity data were analysed using Student's t-test. The numbers of asterisks above the graph indicate significant differences at each time point with * indicating $p< 0.05$, ** indicating $p < 0.01$ and *** indicating $p < 0.001$.

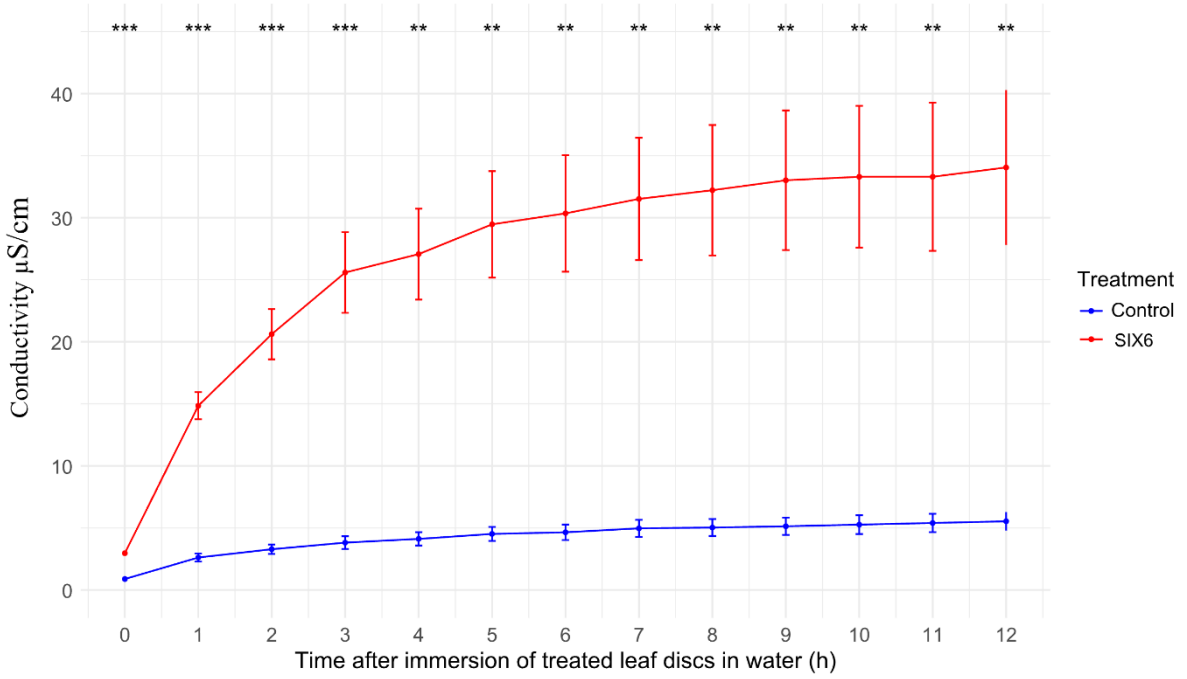

Figure 5.12 SIX6 causes electrolyte leakage in tomato leaves.

Electrolytic conductivity increased in the leaf disc of tomato (c.v. M82) infiltrated with *Fol* SIX6 protein solution (100 µg/ml) from 1 hr to 24 hr as compared to the control (BSA:100 µg/ml). (n = 6 comprising three leaf discs per measurement from each of two leaves on three plants). Means and SEs are shown for six replicates and conductivity data was analysed using Student's t-test. Different numbers of * letters indicate significant differences in the p-value. *: p-value < 0.05, **: p-value < 0.01, ***: p-value < 0.001.

5.3.4 *Fol* SIX6 causes vacuolar shrinkage

Following the analysis of stomatal behaviour, the focus shifted to examining the vacuole, which plays a critical role in regulating stomatal opening and closure and in programmed cell death (Hara-Nishimura and Hatsugai, 2011). During plant programmed cell death (PCD), the vacuole plays a central and dynamic role, exhibiting two distinct behaviours depending on the type of cell death. In developmentally regulated PCD (such as during xylem differentiation or leaf senescence), the vacuole gradually digests cytoplasmic contents through the controlled release of hydrolytic enzymes, resulting in an orderly, autolytic process. In contrast, during pathogen-triggered PCD (such as the hypersensitive response), the vacuole undergoes sudden membrane rupture, releasing a large amount of hydrolytic enzymes into the cytoplasm, leading to rapid cell collapse and death (Hara-Nishimura and Hatsugai, 2011). Given this dual role of vacuoles in both stomatal regulation and cell death processes and considering that SIX6 appears to trigger pathogen-like responses, we investigated whether SIX6 affects vacuolar integrity in

plant cells. To test the effect of SIX6 on vacuoles of leaf epidermal cells, confocal fluorescence microscopy was conducted following agroinfiltration of vacuolar-targeted mTurquoise2 (Appendix 5.1). In control leaves, vacuoles were blue fluorescent and filled almost the entire cell (Figure 5.13A), whereas leaves infiltrated with SIX6 showed vacuolar shrinkage and leakage of mTurquoise2 into the cytosol (Figure 5.13B).

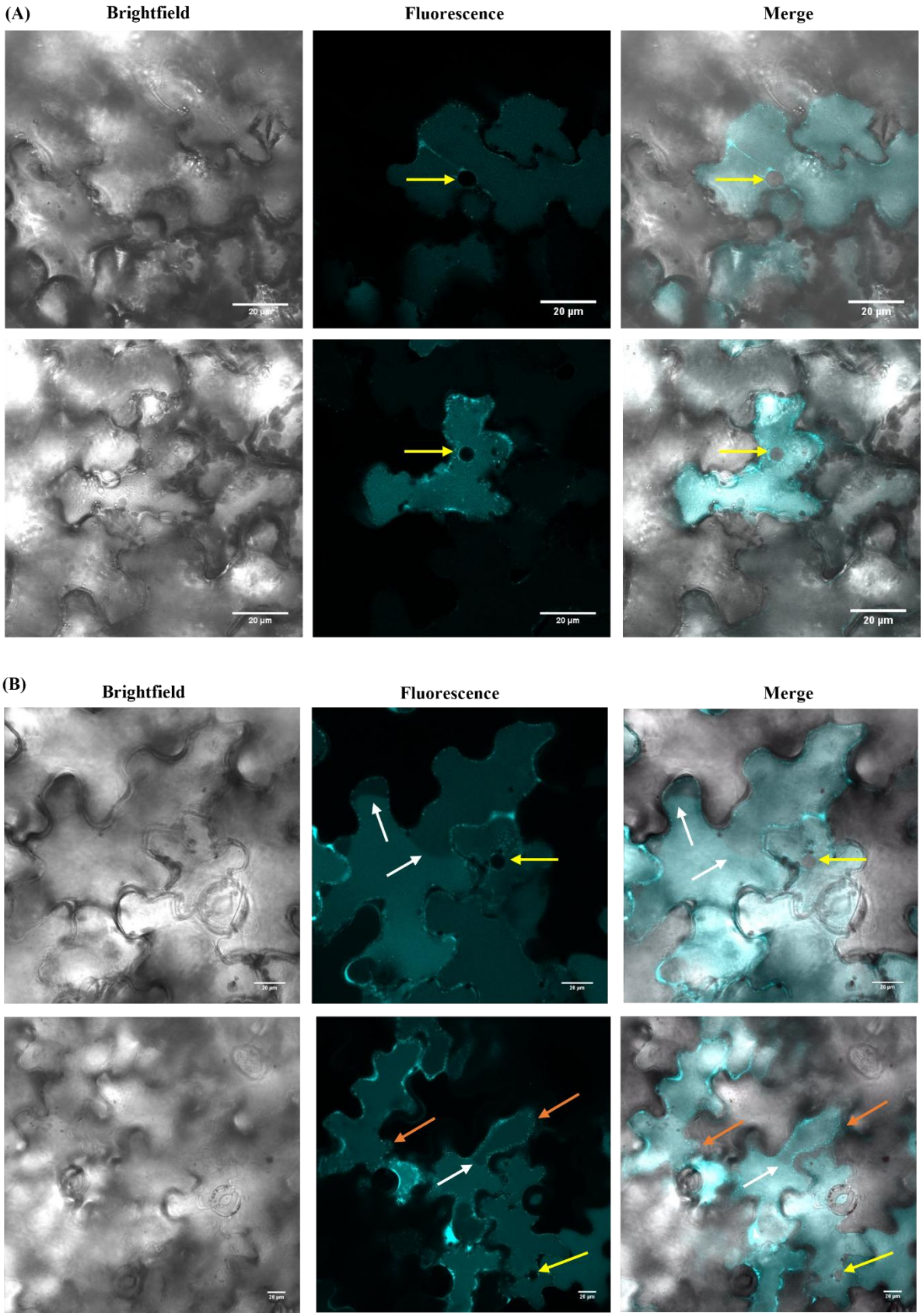
(A)
Brightfield
Fluorescence
Merge
20 µm
(B)
Brightfield
Fluorescence
Merge

Figure 5.13 *Fol* SIX6 causes vacuolar shrinkage in *N. benthamiana.*

Leaves were agroinfiltrated with a vacuolar-targeted mTurquoise2 construct and 2 days later infiltrated with **(A)** deionised water or **(B)** *Fol* SIX6 protein (100 µg/ml). Leaf samples were taken 48 hours after water or SIX6 infiltration. Vacuolar shrinkage after *Fol* SIX6 protein infiltration is indicated by the white arrow and vacuolar leakage by orange arrows. Yellow arrows indicate the nucleus of the cell. Bars = 20 µm.

5.3.5 ABA has a minor effect on the ability of *Fol* SIX6 to open stomata, but does not appear to affect cell death induction

Fol SIX6 causes irreversible stomatal opening, leading to unrestricted transpiration, which may result in leaf cell death. Stomatal closure is the primary mechanism for regulating transpirational water loss (Meinzer 1993; Nilson and Assmann 2007). ABA induces stomatal closure through the regulation of ion fluxes in guard cells (Leckie et al., 1998; Dodd, 2013; Dittrich et al., 2019). ABA acts as a negative regulator of cell death by preventing excessive ROS buildup that could trigger uncontrolled cell death (Xia et al., 2015). Additionally, ABA modulates defence signalling pathways regulated by salicylic acid (SA) and jasmonic acid (JA) (Mauch-Mani and Mauch, 2005; Ton et al., 2009). ABA limits SA-mediated responses like the HR (hypersensitive response), thereby helping to control defence mechanisms by reducing excessive or untimely cell death (Jiang et al., 2010). To determine, whether ABA interferes with the ability of *Fol* SIX6 protein to cause cell death, leaves of *N. benthamiana* were infiltrated with *Fol* SIX6 protein, then sprayed immediately and at 6, 12, 24, 48, 72, 96, 120 and 144 h post infiltration with 50 µM ABA (Sigma Aldrich, Cat # A4906) and assessed at 0, 2, 4 and 6 days after infiltration. Surprisingly, cell death occurred more rapidly in leaves treated with ABA compared to untreated leaves (Figure 5.14).

(A) ABA (0 dpi)

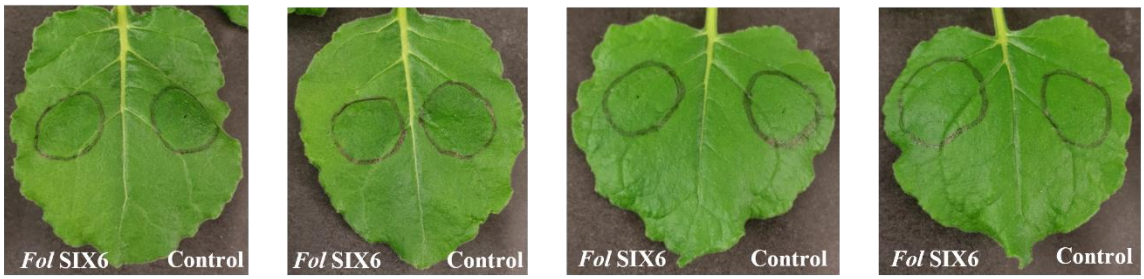

(B) No ABA (0 dpi)

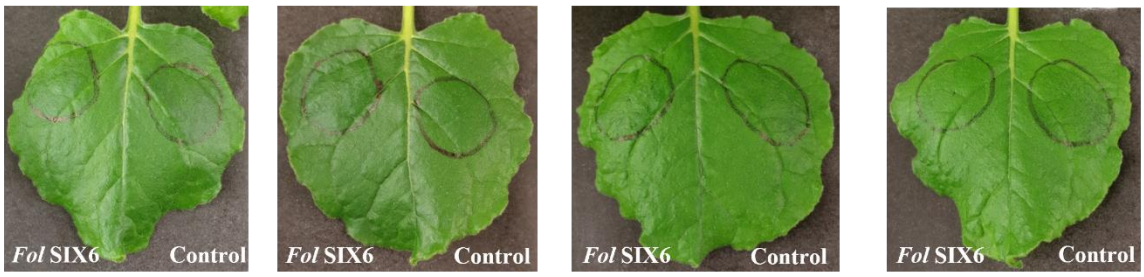

(C) ABA (2 dpi)

(D) No ABA (2 dpi)

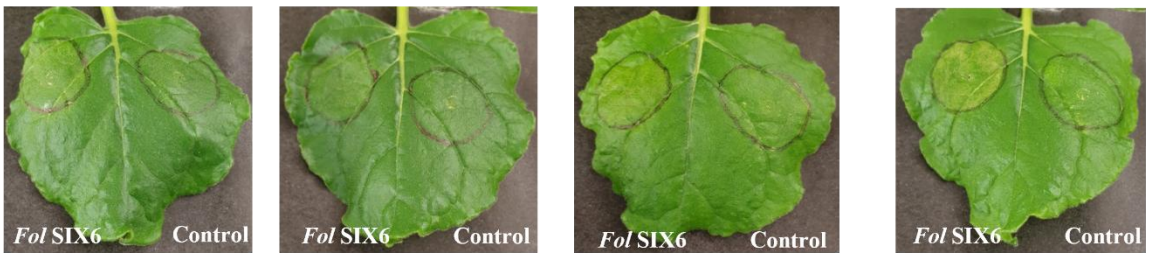

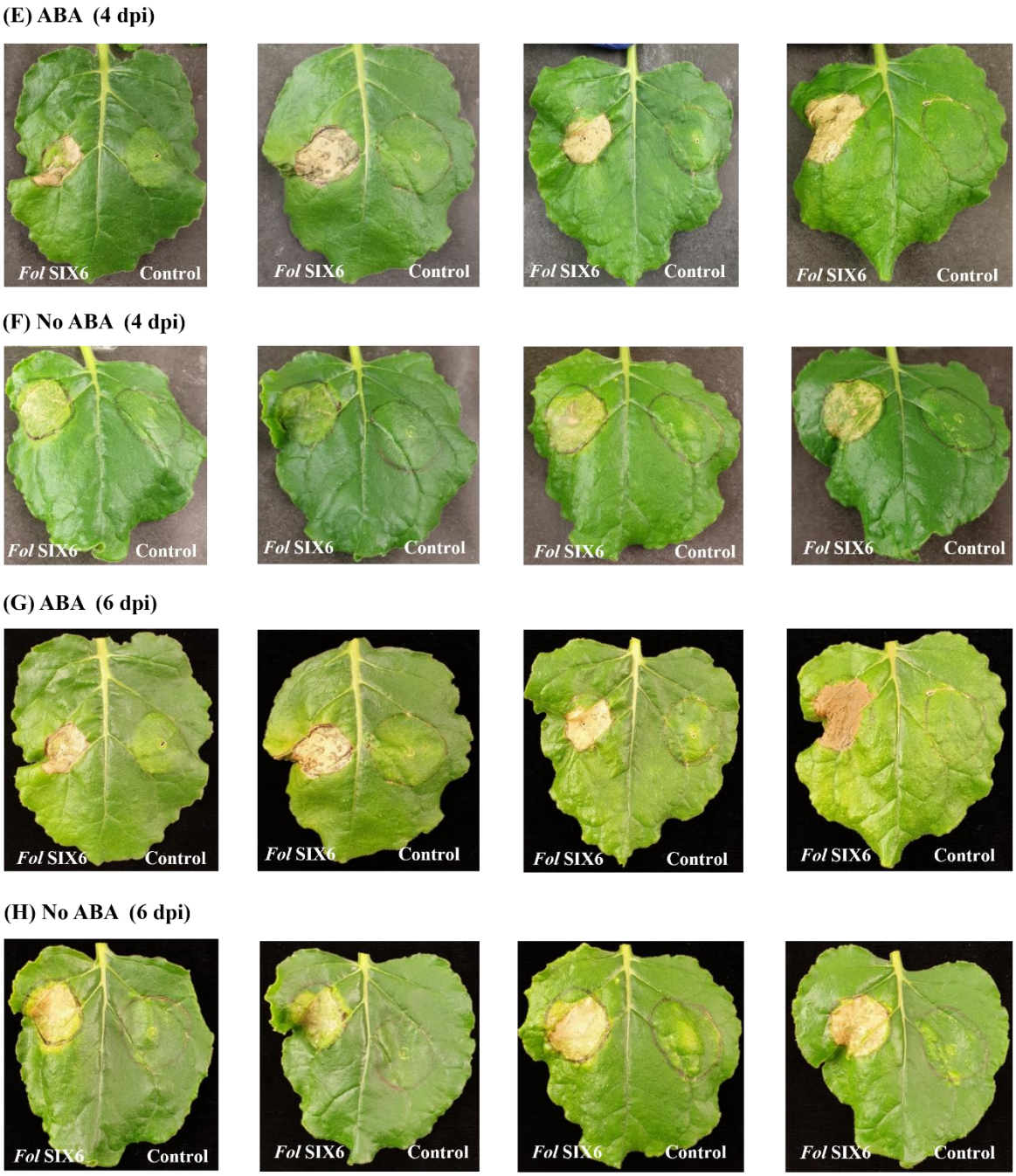

Figure 5.14 Repeated application of ABA did not stop cell death induced by *Fol* SIX6.

Cell death responses induced in *N. benthamiana* leaves following infiltration with 100 µg/ml *Fol* SIX6 protein and **(A) (C) (E) (G)** spraying with 50 µM ABA three times a day or **(B) (D) (F) (H)** no spraying. Photographs were taken at 0, 2, 4 and 6 days after protein infiltration.

To find out whether ABA had any effect on stomatal opening caused by *Fol* SIX6, 50 µM ABA and 50 µg/ml *Fol* SIX6 protein were infiltrated both alone and together into leaves of *N. benthamiana* and stomatal opening was assessed 6 hours after infiltration. A small but significant ($p<0.05$) reduction in stomatal aperture was observed when ABA was coinfiltrated

with *Fol* SIX6 compared to *Fol* SIX6 alone, whereas treatment with ABA alone caused complete stomatal closure (Figure 5.15A and 5.15B).

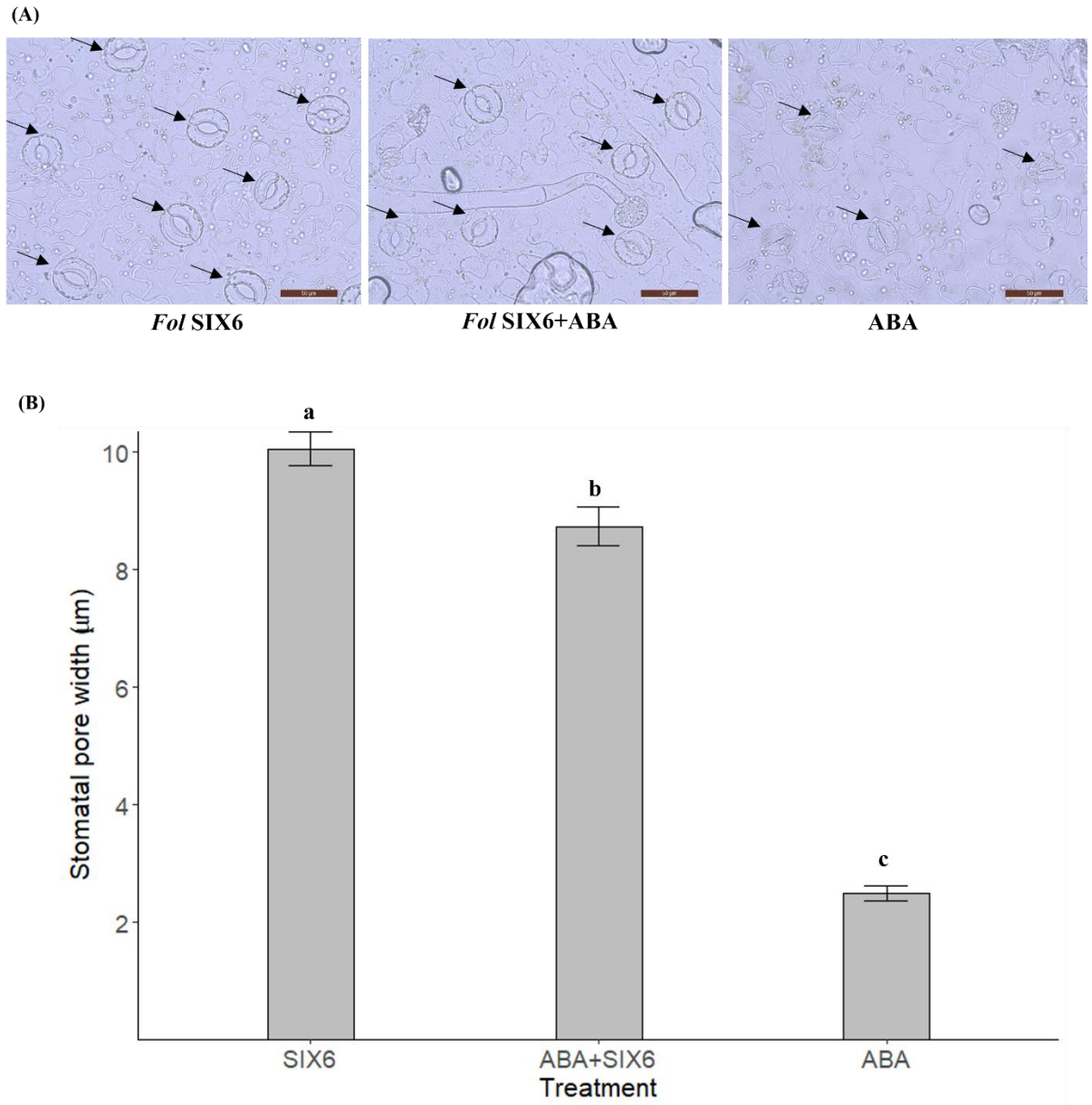

Figure 5.15 ABA causes a small reduction in stomatal opening caused by *Fol* SIX6.

(A) *N. benthamiana* leaves were infiltrated with 50 µg/ml *Fol* SIX6 or 50 µM ABA or both together. Plants were exposed to light for 6 hours after infiltration. Epidermal peels were then prepared from infiltrated leaves and analysed as described in Figure 5.4. Scale bars represent 50 µm. **(B)** Stomatal pore widths were measured for 50 stomata from the leaves of three plants in each treatment. Statistical analysis was done using pairwise Student t-tests. Values are mean ± SEs. Different letters indicate significant differences at $p < 0.01$.

5.3.6 *Fol* SIX6 does not cause stomatal opening during infection

Stomatal opening triggered by *Fol* SIX6 could potentially facilitate *Fol* infection by promoting water loss and subsequent wilting. So far, the effect of *Fol* SIX6 on stomatal opening has been investigated by infiltrating high concentrations of the protein into leaves of *N. benthamiana,* which does not reflect what occurs during infection when *Fol* SIX6 is secreted into the root and stem xylem of an infected plant. To investigate stomatal opening during infection, an infection assay was conducted as described in sections 5.2.6 and 5.2.7 and epidermal peels were taken over a time course and stomata were examined by light microscopy. There were no significant differences in stomatal opening between *Fol* race 3-inoculated and mock-inoculated plants until 18 days after inoculation, when stomata of mock-inoculated plants were significantly more open than stomata of *Fol*-inoculated plants (Figure 5.16). *Fol*-inoculated plants were stunted and showed wilting symptoms after 21 dpi (Appendix 5.4).

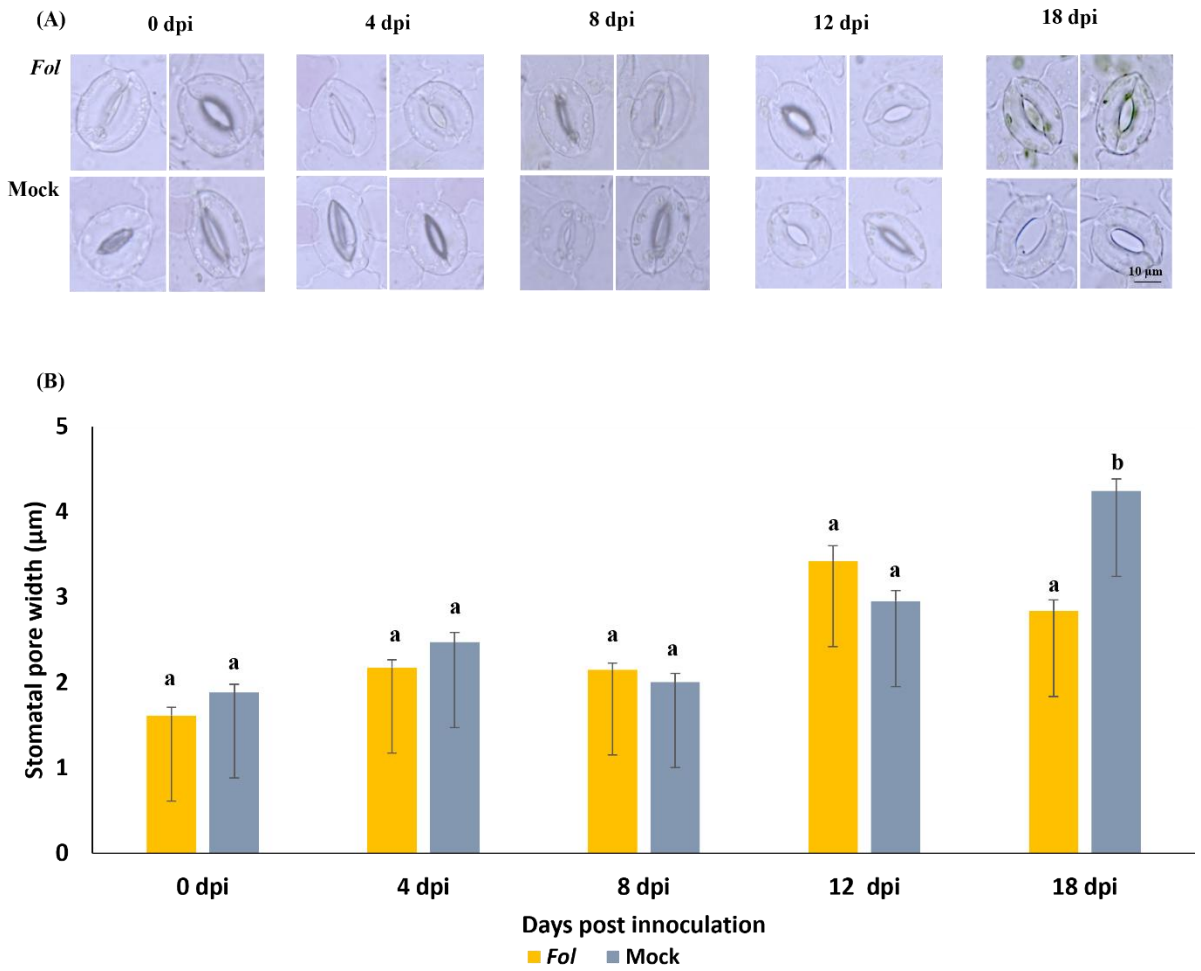

Figure 5.16 Stomatal behaviour during infection.

(A) Epidermal peels from leaves of *Fol* race 3-inoculated and mock-inoculated (dipped in water) M82 tomato plants were prepared at 0, 4, 8, 12 and 18 dpi for microscopic analysis of stomata as described in Figure 5.4. The scale bar represents 10 µm. **(B)** Stomatal pore widths were measured for 50 stomata from the leaves of three plants at each time point. Values are means ± SEs. Statistical analysis was done using pairwise Student t-tests. Different letters indicate significant differences at $p < 0.01$.

5.4 Discussion

5.4.1 *Fol* SIX6 induces stomatal opening

The *Fol* SIX6 protein was found to induce stomatal opening and cell death in *N. benthamiana* (Figure 5.7 and Chapter 3) and tomato (Figure 5.9 and Chapter 3), but neither in some plant species such as radish and zucchini (Appendix 5.3). This suggests that cell death may be associated with stomatal opening. A gas exchange study found that *Fol* SIX6 protein opened stomata independent of light conditions and caused them to stay open (Figure 5.10). Stomata

act as gateways for controlling water and gas exchange in plants. Stomatal opening and closing are controlled by guard cells and the mechanism behind the process is very complex and depends on several environmental factors such as light, CO_2, humidity, temperature and water availability (Hetherington and Woodward, 2003; Lawson and Matthews, 2020) as well as internal factors including ABA, ion channels (Acharya and Assmann, 2009; Kim et al., 2010; Demidchik, 2018; Postiglione and Muday, 2020). The normal mechanism of stomatal opening can be broken down into three steps 1. In response to light, H^+ATPase is activated leading to hyperpolarisation of the membrane 2. This hyperpolarisation then activates voltage-gated K^+ channels, which leads to an increase in osmotic potential 3. This increased osmotic potential draws water into guard cells through aquaporins and makes them swell, which leads to stomatal opening (Daszkowska-Golec and Szarejko, 2013). The overall effect of *Fol* SIX6 on stomatal behaviour strongly suggests that it could be acting on H^+ATPase, but potentially it could act on voltage-gated K^+ channels or aquaporins to open stomata.

Effector proteins can manipulate H^+ATPases, which are proton pumps responsible for regulating ion transport in guard cells. By targeting H^+ATPases, effectors can disrupt ion homeostasis and interfere with stomatal closure (McLachlan et al., 2014). For example, the NIP1 effector from the barley pathogen *Rhynchosporium secalis* stimulates H^+ATPases from barley plasma membranes leading to membrane hyperpolarisation, stomatal opening and leaf cell death (van't Slot et al., 2007). Fusicoccin, a fungal phytotoxin produced by *Fusicoccum amygdali*, specifically activates the plasma membrane H^+ATPase in plants. It binds to the H^+ATPase and stabilisers of 14-3-3 protein interaction with plasma membrane H^+ATPase, leading to an increase in proton pumping across the plasma membrane, which in turn drives stomatal opening that leads to wilting (Oecking et al., 1997; Ohkanda, 2021). RIN4 (RPM1-Interacting Protein 4) is a protein from Arabidopsis that acts as a positive regulator of H^+-ATPase activation and stomatal opening during pathogen invasion (Liu et al., 2009). Several bacterial effectors target RIN4 in Arabidopsis (Buttner, 2016). The *Pseudomonas syringae* AvrRpm1 effector induces phosphorylation of RIN4 and phosphorylation of RIN4 enhances plant plasma membrane H^+-ATPase activity and increases stomatal aperture size, promoting stomatal opening and enhancing bacterial virulence (Liu et al., 2011; Lee et al., 2015).

The phenotype of irreversible SIX6-induced stomatal opening and leaf epidermal cell death closely resembles the phenotype observed for the interaction between the tomato Cf-9 protein and the *Cladosporium fulvum* Avr9 effector (Hammond-Kosack et al., 1998). Paradoxically, this phenotype is associated with irreversible K^+ channel responses resulting in increased

movement of K^+ ions out of guard cells and almost complete suppression of inward movement (Blatt et al., 1999). K^+ efflux is typically associated with stomatal closure rather than stomatal opening. However, Blatt et al. (1999) argue that K^+ efflux in adjacent epidermal cells could lead to a loss of turgor causing stomatal opening as a consequence i.e. pulling stomata open. The Cf-9/Avr9 phenotype of supraoptimal stomatal opening and epidermal cell collapse was found to be inhibited by the protein kinase antagonist staurosporine, indicating a requirement for protein phosphorylation. A similar experiment could be conducted to test whether protein phosphorylation is required for SIX6 induced stomatal opening and leaf epidermal cell death. Inhibition might indicate involvement of a receptor kinase or receptor-mediated activation of a cytosolic kinase in the SIX6 response as has been proposed for the NIP1 response.

AvrPiz-t from *Magnaporthe oryzae* is the only example of a pathogen effector targeting a plant voltage-gated K^+ channel. AvrPiz-t interacts with the rice plasma-membrane-localised K^+ channel OsAKT1 and inhibits its K^+ channel activity, resulting in reduced K^+ uptake (Shi et al., 2018). Suppression of OsAKT1 activity attenuates host immune responses, thereby promoting pathogen colonisation and enhancing virulence. However, evidence of stomatal opening or epidermal cell collapse has not been reported for this interaction.

Pathogen effectors have also been identified that target aquaporins to manipulate host water transport. By modulating aquaporin function, pathogens can influence processes such as osmotic balance, reactive oxygen species (ROS) movement, and stomatal dynamics, ultimately enhancing their ability to colonise and infect host plants. The bacterial blight pathogen *Xanthomonas oryzae* pv. *oryzae* that infects rice produces the *Hpa1* effector, which interacts with the plasma membrane aquaporin OsPIP1;3. *CRN78* effector from the oomycete *Phytophthora sojae* has been found to interact with PIP2-family aquaporins, specifically NbPIP2;2 in *Nicotiana benthamiana* and GmPIP2-13 in soybean (Ai et al., 2021). While aquaporins are primarily known for their role in water transport and stomatal regulation, certain PIP2 subfamily members also facilitate hydrogen peroxide (H_2O_2) transport across cellular membranes. This dual functionality is significant because H_2O_2 serves as a critical signalling molecule in plant defence responses, particularly during pathogen recognition and the oxidative burst that characterises hypersensitive responses. The *CRN78* effector exploits this H_2O_2 transport capability by promoting phosphorylation of PIP2 aquaporins, leading to their degradation (Ai et al., 2021). This targeted reduction in aquaporin levels impairs H_2O_2 movement across membranes, thereby suppressing the host's oxidative defence responses and limiting the spread of immune signals. However, the degradation of these aquaporins raises

important questions about potential secondary effects on plant physiology. Since the same PIP2 proteins targeted by CRN78 also contribute to water transport, their reduced abundance could potentially impact cellular water balance and stomatal function. Whether CRN78-induced aquaporin degradation significantly affects water movement and stomatal regulation, or primarily targets H_2O_2-mediated defence pathways, remains an important area for investigation.

5.4.2 *Fol* SIX6 protein causes vacuolar shrinkage

The response to SIX6 of vacuoles in leaf epidermal pavement and subsidiary cells (hereafter referred to as epidermal cells) was examined by confocal fluorescence microscopy using vacuolar-targeted mTurquoise2. When *Fol* SIX6 protein was infiltrated in leaves agroinfiltrated two days earlier with a vacuolar-targeted mTurquoise2 construct, vacuolar shrinkage was observed in epidermal cells (Figure 5.13B) compared to the control (Figure 5.13A). A background of blue fluorescence outside the vacuole suggests the tonoplast had been compromised allowing vacuolar leakage, whereas the lack of blue fluorescence outside the cell suggested the plasma membrane remained intact (Figure 5.13B). This is consistent with the destructive form of vacuole mediated cell death described by Hara-Nishimura and Hatsugai (2011). Experiments with fluorophores labelling the plasma membrane, cytosol or tonoplast as well as the vacuole could be used to test this interpretation of the images obtained.

Unfortunately, agroinfiltration is ineffective for delivery of transgenes to guard cells, so it was not possible to determine whether vacuolar shrinkage and leakage also occurred in guard cells. However, stomata were fully open and guard cells appeared in cross section to be fully turgid despite exposure to SIX6 protein. One possibility is that guard cells respond differently to SIX6 and that their vacuoles have increased in volume leading to an increase in guard cell volume and stomatal opening. Another possibility, consistent with the suggestion made by Blatt et al. (1999) for Cf-9/Avr9-induced stomatal opening, is that guard cell vacuoles have decreased in volume but stomata have nevertheless been opened despite a concomitant decrease in guard cell volume due to the collapse of adjacent epidermal cells. One way to look at vacuolar responses to SIX6 in guard cells would be to use particle bombardment to deliver vacuolar-targeted mTurquoise2 to both epidermal cells and guard cells or develop transformed tobacco lines expressing vacuolar-targeted mTurquoise2. Although challenging experimentally, it might then also be possible to conduct a study of SIX6-induced changes in epidermal and guard cell volumes over a time course by using confocal fluorescence microscopy to construct three-

dimensional images of double-labelled epidermal cells and guard cells, using mTurquoise 2 to label the vacuole and a different fluorophore to label the cytosol. However, a simpler approach might be to use scanning electron microscopy to look at the surface of SIX6-treated leaves to determine whether epidermal cells have collapsed and guard cells remain turgid.

5.4.3 ABA has a minor negative effect on *Fol* SIX6-induced stomatal opening but a positive effect on cell death induction

ABA application resulted in a slight reduction in stomatal opening induced by *Fol* SIX6 (Figure 5.15) but did not prevent cell death triggered by *Fol* SIX6 (Figure 5.14). In fact, ABA treatment appeared to accelerate the cell death response (Figure 5.14). It is important to note that observation arose from a comparison between ABA-treated leaves and untreated leaves. It is possible, although unlikely, that spraying with water containing the minute amounts of ethanol used to dissolve ABA in the ABA stock solution might have had a similar effect and would have been a better control. Consequently, the accelerating effect of ABA on *Fol* SIX6-induced cell death may not be entirely conclusive. Future experiments with proper controls are necessary to accurately determine the specific effect of ABA on this process. Nevertheless, the minor effect of ABA on stomatal closure suggests that SIX6 is acting at or downstream of ABA perception, e.g. if acting at the level of light perception, ABA should have been able to close stomata.

ABA acts on guard cells to decrease guard cell volume via a decrease in vacuolar volume (described in section 5.1). SIX6 induces a decrease in vacuolar volume in epidermal cells, so it is possible that ABA could exacerbate this effect in epidermal cells, leading to accelerated cell death in ABA treated leaves compared to untreated leaves (Figure 5.14). As indicated above, more carefully controlled experiments would be needed to confirm this observation, including, for example, microscopy experiments using a vacuole-targeted fluorescent protein to look at the effect of ABA on vacuoles in leaf epidermal cells in the presence or absence of SIX6 and vice versa.

5.4.4 *Fol* infection fails to induce stomatal opening

To test whether SIX6 caused stomatal opening during infection, a pathogenicity test was conducted on M82 tomato with *Fol* race 3, which carries *SIX6*, but there was no significant difference between stomatal opening in *Fol*-infected or mock-inoculated plants except for 18 days post-infection (Figure 5.16). One explanation might be that the concentrations of SIX6 are not sufficient in leaves to cause stomatal opening during infection. Agroinfiltration or protein infiltration likely results in high concentrations of SIX6 that simply do not occur in leaves during infection. It is also possible that other *Fol* effectors suppress SIX6-induced stomatal opening during infection. On the other hand, stomatal opening and leaf cell death could be a proxy for something happening in roots and stems during plant infection. Experiments designed to examine the effects of SIX6 on roots are described in the next chapter.

References

Acharya, B.R., & Assmann, S.M. (2009). Hormone interactions in stomatal function. *Plant Molecular Biology, 69*(4), 451-462.

Agurla, S., Gahir, S., Munemasa, S., Murata, Y., Raghavendra, A.S. (2018). Mechanism of stomatal closure in plants exposed to drought and cold stress. *Advances in Experimental Medicine and Biology, 1081,* 215-232.

Ai, G., Xia, Q., Song, T., Li, T., Zhu, H., Peng, H., Liu, J., Fu, X., Zhang, M., Jing, M., Xia, A., Dou, D. (2021). A *Phytophthora sojae* CRN effector mediates phosphorylation and degradation of plant aquaporin proteins to suppress host immune signaling. *PLoS Pathogens, 17*(3), e1009388.

Ayres, P.G. (1984). The interaction between environmental stress injury and biotic disease physiology. *Annual Review of Phytopathology, 22*(1), 53-75.

Bharath, P., Gahir, S., Raghavendra, A.S. (2021). Abscisic acid-induced stomatal closure: an important component of plant defence against abiotic and biotic stress. *Frontiers in Plant Science*, *12*, 615114.

Blatt, M.R., Grabov, A., Brearley, J., Hammond-Kosack, K., Jones, J.D. (1999). K^+ channels of *Cf-9* transgenic tobacco guard cells as targets for *Cladosporium fulvum Avr9* elicitor-dependent signal transduction. *The Plant Journal***,** *19*(4), 453-462.

Boursiac, Y., Chen, S., Luu, D.T., Sorieul, M., van den Dries, N., Maurel, C. (2005). Early effects of salinity on water transport in Arabidopsis roots. Molecular and cellular features of aquaporin expression. *Plant Physiology, 139*(2), 790-805.

Buttner, D. (2016). Behind the lines-actions of bacterial type III effector proteins in plant cells. *FEMS Microbiology Review, 40*(6), 894-937.

Chaumont, F., & Tyerman, S.D. (2014). Aquaporins: highly regulated channels controlling plant water relations. *Plant Physiology,164* (4),1600-1618.

Cosgrove, D.J. (2005). Growth of the plant cell wall. *Nature Reviews Molecular Cell Biology, 6*(11), 850-861.

Danielson, J.A., & Johanson, U. (2008). Unexpected complexity of the aquaporin gene family in the moss *Physcomitrella patens*. *BMC Plant Biology*, *8*(1), 45.

Daszkowska-Golec, A., & Szarejko, I. (2013). Open or close the gate - stomata action under the control of phytohormones in drought stress conditions. *Frontiers in Plant Science, 13*(4), 138.

Demidchik, V. (2010). Reactive oxygen species, oxidative stress and plant ion channels. In *Ion channels and plant stress responses*, 207-232.

Demidchik, V. (2018). ROS-activated ion channels in plants: biophysical characteristics, physiological functions and molecular nature. *International Journal of Molecular Sciences, 19*(4), 1263.

Demidchik, V., Straltsova, D., Medvedev, S.S., Pozhvanov, G.A., Sokolik, A., Yurin, V. (2014). Stress-induced electrolyte leakage: The role of K^+ permeable channels and involvement in programmed cell death and metabolic adjustment. *Journal of Experimental Botany*, *65*(5), 1259-1270.

Dietrich, P., Sanders, D., Hedrich, R. (2001). The role of ion channels in light-dependent stomatal opening. *Journal of Experimental Botany, 52*(363), 1959-1967.

Ding, L., Fox, A.R., Chaumont, F. (2024). Multifaceted role and regulation of aquaporins for efficient stomatal movements. *Plant Cell and Environment, 47*(9), 3330-3343.

Dittrich, M., Mueller, H.M., Bauer, H., Peirats-Llobet, M., Rodriguez, P.L., Geilfus, C.M., Carpentier, S.C., Al Rasheid, K.A.S., Kollist, H., Merilo, E., Herrmann, J., Muller, T., Ache, P., Hetherington, A.M., Hedrich, R. (2019). The role of *Arabidopsis* ABA receptors from the PYR/PYL/RCAR family in stomatal acclimation and closure signal integration. *Nature Plants, 5*(9), 1002-1011.

Dodd, I.A. (2013). Abscisic acid and stomatal closure: a hydraulic conductance conundrum? *New Phytologist, 197*(4), 6-8.

Gao, X.Q., Li, C.G., Wei, P.C., Zhang, X.Y., Chen, J., Wang, X.C. (2005). The dynamic changes of tonoplasts in guard cells are important for stomatal movement in *Vicia faba*. *Plant Physiology, 139*(3), 1207-1216.

Goedhart, J., von Stetten, D., Noirclerc-Savoye, M., Lelimousin, M., Joosen, L., Hink, M.A., van Weeren, L., Gadella Jr, T. W., Royant, A. (2012). Structure-guided evolution of cyan fluorescent proteins towards a quantum yield of 93%. *Nature Communications*, *3*(1), 751.

Hammond-Kosack, K.E., Tang, S., Harrison, K., Jones, J.D. (1998). The tomato *Cf-9* disease resistance gene functions in tobacco and potato to confer responsiveness to the fungal avirulence gene product Avr9. *The Plant Cell***,** *10*(8), 1251-1266.

Hara-Nishimura, I., & Hatsugai, N. (2011). The role of vacuole in plant cell death. *Cell death & differentiation, 18*(8), 1298-1304.

Hatsugai, N., Nakatsuji, A., Unten, O., Ogasawara, K., Kondo, M., Nishimura, M., Shimada, T., Katagiri, F., Hara-Nishimura, I. (2018). Involvement of adapter protein complex 4 in hypersensitive cell death induced by avirulent bacteria. *Plant Physiology***,** *176*(2), 1824-1834.

Hellens, R.P., Edwards, E.A., Leyland, N.R., Bean, S., Mullineaux, P.M. (2000). pGreen: a versatile and flexible binary Ti vector for *Agrobacterium*-mediated plant transformation. *Plant Molecular Biology, 42*(6), 819-832.

Ton, J., Flors, V., Mauch-Mani, B. (2009). The multifaceted role of ABA in disease resistance. *Trends in Plant Science, 14*(6), 310-317.

Hetherington, A.M., & Quatrano, R.S. (1991). Mechanisms of action of abscisic acid at the cellular level. *New Phytologist,119*, 9-12.

Hetherington, A.M., & Woodward, F.I. (2003). The role of stomata in sensing and driving environmental change. *Nature, 21*(424), 901-908.

Hsu, P.K., Dubeaux, G., Takahashi, Y., Schroeder, J.I. (2021). Signaling mechanisms in abscisic acid-mediated stomatal closure. *Plant Journal, 105*(2), 307-321.

Jiang, C.J., Shimono, M., Sugano, S., Kojima, M., Yazawa, K., Yoshida, R., Inoue, H., Hayashi, N., Sakakibara, H., Takatsuji, H. (2010). Abscisic acid interacts antagonistically with salicylic acid signaling pathway in rice *Magnaporthe grisea* interaction. *Molecular Plant Microbe Interaction, 23*(6), 791-798.

Johanson, U., & Gustavsson, S. (2002). A new subfamily of major intrinsic proteins in plants. *Molecular Biology and Evolution, 19*(4), 456-461.

Kim, T.H., Böhmer, M., Hu, H., Nishimura, N., Schroeder, J.I. (2010). Guard cell signal transduction network: advances in understanding abscisic acid, CO^2, and Ca^{2+} signaling. *Annual Review of Plant Biology, 61*(1), 561-91.

Lawson, T., & Matthews, J. (2020). Guard cell metabolism and stomatal function. *Annual Review of Plant Biology, 29*(71), 273-302.

Leckie, C.P., Mcainsh, M.R., Allen, G.J., Sanders, D., Hetherington, A.M. (1998). Abscisic acid-induced stomatal closure mediated by cyclic ADP-ribose. *Proceedings of the National Academy of Sciences*, *Plant Biology, 95*(26), 15837-15842.

Lee, D., Bourdais, G., Yu, G., Robatzek, S., Coaker, G. (2015). Phosphorylation of the plant immune regulator RPM1-interacting protein 4 enhances plant plasma membrane H^+-ATPase activity and inhibits flagellin-triggered immune responses in Arabidopsis. *Plant Cell, 27*(7), 2042-2056.

Leung, J., & Giraudat, J. (1998). Abscisic acid signal transduction. *Annual Review of Plant Biology, 49*(1), 199-222.

Li, Y., Zhang, X., Zhang, Y., Ren, H. (2022). Controlling the gate: the functions of the cytoskeleton in stomatal movement. *Frontiers in Plant Science, 23*(13), 849729.

Lim, C.W., Baek, W., Jung, J., Kim, J.H., Lee, S.C. (2015). Function of ABA in stomatal defense against biotic and drought Stresses. *International Journal of Molecular Sciences, 16*(7), 15251-15270.

Liu, J., Elmore, J.M., Fuglsang, A.T., Palmgren, M.G., Staskawicz, B.J., Coaker, G. (2009). RIN4 functions with plasma membrane H^+ATPases to regulate stomatal apertures during pathogen attack. *PLoS Biology,* 7, e1000139.

Liu, J., Elmore, J.M., Lin, Z.J., Coaker, G. (2011). A receptor-like cytoplasmic kinase phosphorylates the host target RIN4, leading to the activation of a plant innate immune receptor. *Cell Host Microbe, 9*(2),137-146.

Maeshima, M. (2001). Tonoplast transporters: organization and function. *Annual Review of Plant Physiology and Plant Molecular Biology*, *52*(1), 469-497.

Mauch-Mani, B., & Mauch, F. (2005). The role of abscisic acid in plant-pathogen interactions. *Current Opinion in Plant Biology, 8*(4), 409-414.

Maurel, C., & Chrispeels, M.J. (2001). Aquaporins. A molecular entry into plant water relations. *Plant Physiology, 125*(1), 135-138.

McLachlan, D.H., Kopischke, M., Robatzek, S. (2014). Gate control: guard cell regulation by microbial stress. *New Phytologist, 203*(4), 1049-1063.

Meinzer, F.C. (1993). Stomatal control of transpiration. *Trends in Ecology & Evolution, 8*(8), 289-294.

Melotto, M., Underwood, W., He, S.Y. (2008). Role of stomata in plant innate immunity and foliar bacterial diseases. *Annual Review of Phytopathology, 46*(1), 101-122.

Melotto, M., Zhang, L., Oblessuc, P.R., He, S.Y. (2017). Stomatal defense a decade later. *Plant Physiology, 174*(2), 561-571.

Mirasole, F.M., Nastasi, S.P., Cubero-Font, P., Alexis, D.A. (2023). Vacuolar control of stomatal opening revealed by 3D imaging of the guard cells. *Scientific Reports, 13*, 7647.

Nilson, S.E., & Assmann, S.M. (2007). The control of transpiration. insights from Arabidopsis. *Plant Physiology*, *143*(1), 19-27.

Oecking, C., Piotrowski, M., Hagemeier, J., Hagemann, K. (1997). Topology and target interaction of the fusicoccin-binding 14-3-3 homologs of *Commelina communis*. *The Plant Journal, 12*(2), 441-453.

Ohkanda, J. (2021). Fusicoccin: A Chemical Modulator for 14-3-3 Proteins, *Chemistry Letters, 50* (1), 57-67.

Postiglione, A.E., & Muday, G.K. (2020). The role of ROS homeostasis in ABA-induced guard cell signaling. *Frontiers in Plant Science, 30*(11), 968.

Rogers, J. C. (2008). Multiple vacuoles in plant cells. *Plant Physiology***,** *146*(3), 1024-1025.

Sade, N., Shatil-Cohen, A., Attia, Z., Maurel, C., Boursiac, Y., Kelly, G., Granot, D., Yaaran, A., Lerner, S., Moshelion, M. (2014). The role of plasma membrane aquaporins in regulating the bundle sheath-mesophyll continuum and leaf hydraulics. *Plant Physiology, 166*(3),1609-1620.

Schroeder, J.I., Allen, G.J., Hugouvieux, V., Kwak, J.M., Waner, D. (2001). Guard cell signal transduction. *Annual Reviews of Plant Physiology and Plant Molecular Biology, 52*(1), 627-658.

Seo, M., & Koshiba, T. (2002). Complex regulation of ABA biosynthesis in plants. *Trends in Plant Science, 7*(1), 41-48.

Shi, X., Long, Y., He, F., Zhang, C., Wang, R., Zhang, T., Wu, W., Hao, Z., Wang, Y.I., Wang, G.L., Ning, Y. (2018). The fungal pathogen *Magnaporthe oryzae* suppresses innate immunity by modulating a host potassium channel. *PLoS Pathogens*, *14*(1), e1006878.

Swamy, P.M., & Smith, B.N. (1999). Role of abscisic acid in plant stress tolerance. *Current Science, 76*(9), 1220-1227.

Taiz, L., & Zeiger, E. (2010). Plant Physiology.

Tuteja, N. (2007). Abscisic acid and abiotic stress signaling. *Plant Signaling and Behaviour, 2*(3), 135-138.

Tyerman, S.D., Niemietz, C.M., Bramley, H. (2002). Plant aquaporins: multifunctional water and solute channels with expanding roles. *Plant Cell and Environment, 25*(2), 173-194.

van't Slot, K.A.E., Gierlich, A., Knogge, W. (2007). A single binding site mediates resistance- and disease associated activities of the effector protein NIP1 from the barley pathogen *Rhynchosporium secalis*. *Plant Physiology, 144*(3), 1654-1666.

Xia, X.J., Zhou, Y.H., Shi, K., Zhou, J., Foyer, C.H., Yu, J.Q. (2015). Interplay between reactive oxygen species and hormones in the control of plant development and stress tolerance. *Journal of Experimental Botany*, *66*(10), 2839-2856.

ATGGTGAGCAAGGGCGAGGAGCTGTTCACCGGGGTGGTGCCCATCCTGGTCGAGCT
GGACGGCGACGTAAACGGCCACAAGTTCAGCGTGTCCGGCGAGGGCGAGGGCGATG
CCACCTACGGCAAGCTGACCCTGAAGTTCATCTGCACCACCGGCAAGCTGCCCGTG
CCCTGGCCCACCCTCGTGACCACCCTGTCCTGGGGCCGTGCAGTGCCTTCGCCCGC
CTACCCCGACCACATGAAGCAGCACGACTTCTTCAAGTCCGCCATGCCCGAAGGCT
ACGTCCAGGAGCGCACCATCTTCTTTCAAGGACGACGGCAACTACAAGACCCGCGC
CGAGGTGAAGTTCGAGGGCGACACCCCTGGTGAACCGCATCGAGCTGAAGGGCATC
GACTTCAAGGAGGACGGCAACATCCTGGGGCACAAGCTGGAGTACAACTACTTCAG
CGACAACGTCTATATCACCGCCGACAAGCAGAAGAACGGCATCAAGGCCAACTTCA
AGATCCGCCACAACATCGAGGACGGCGGCGTGCAGCTCGCCGACCACTACCAGCAG
AACACCCCCATCGGCGACGGCCCCGTGCTGCTGCCCGACAACCACTACCTGAGCAC
CCAGTCCAAGCTGAGCAAAGACCCCAACGAGAAGCGCGATCACATGGTCCTGCTGG
AGTTCGTGACCGCCGCCGGGATCACCCCTAGGCATGGACGAGCTGTACAAGTCTTT
TTTGGAAACGGACTCTTAGTCGATACTATGTAAGGATCCGTAATTTGGAGAGGA

MVSKGEELFTGVVPILVELDGDVNGHKFSVSGEGEGDATYGKLTLKFICTTGKLPVPWPTLV
TTLSWGVQCFARYPDHMKQHDFFKSAMPEGYVQERTIFFKDDGNYKTRAEVKFEGDTLVNRI
ELKGIDFKEDGNILGHKLEYNYFSDNVYITADKQKNGIKANFKIRHNIEDGGVQLADHYQQN
TPIGDGPVLLPDNHYLSTQSKLSKDPNEKRDHMVLLEFVTAAGITLGMDELYKSFGNGLLVD
TM

Appendix 5.1 Coding and protein sequence of vacuole-targeted mTurquoise2.

The start codon: ATG and N-terminal Methionine highlighted in red. The mTurquoise2 sequence is highlighted in blue, and the vacuole-targeting sequence from tomato vacuolar endochitinase 3 is highlighted in yellow.

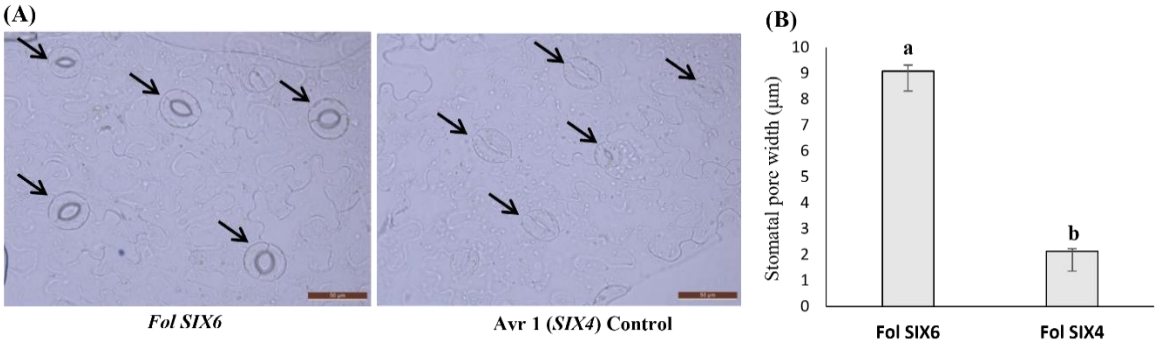

Appendix 5.2 Stomatal response to *Agrobacterium*-mediated expression of *Fol SIX6* and *Avr1* (*Fol SIX4*).

(A) Microscopy of *N. benthamiana* epidermal cells from leaf epidermal peels harvested two days after agroinfiltrated with *Fol SIX6* and *Avr1* (Control). Stomata are highlighted with arrows. Scale bars represent 50 µm. **(B)** Stomatal apertures were measured for 50 stomata from the leaves of three different plants. Statistical analysis was done using Student's t-tests. Values are means ± SE. Different letters indicate significant differences ($p<0.05$).

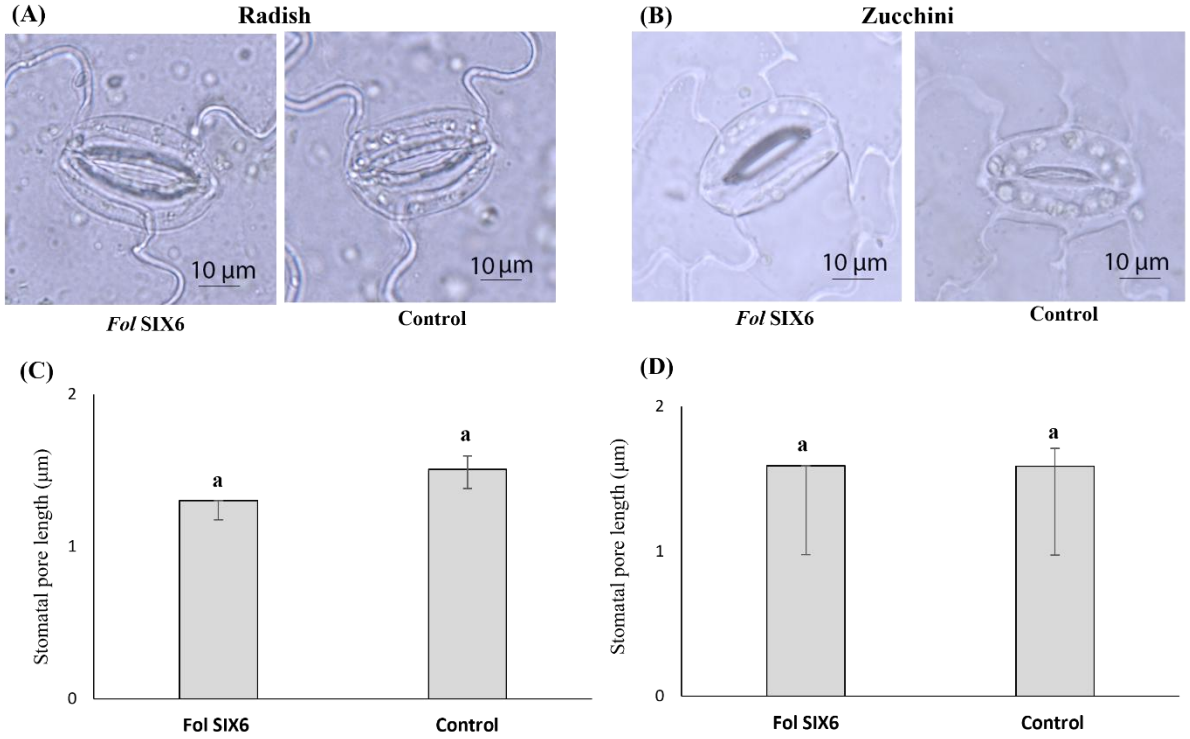

Appendix 5.3 Microscopic analysis of radish and zucchini stomata from leaves infiltrated with *Fol* SIX6.

Leaves of **(A)** radish and **(B)** zucchini plants were infiltrated with recombinant *Fol* SIX6 protein (100 µg/ml) and water (control). Plants were exposed to light for 6 hours, as this time was sufficient for SIX6-induced stomatal opening to occur in tomato and *N. benthamiana* and refer to Figures 5.7 and 5.9. After the infiltration, leaves were harvested and leaf epidermal peels were prepared for microscopy. Stomata are highlighted with arrows. **(C, D)** Stomatal apertures were measured from 50 stomata from the leaves of three different plants. Statistical analysis was done using Student's t-tests. Values are means ± SE. Identical letters indicate no significant differences ($p>0.05$).

Appendix 5.4 Disease symptoms in M82 tomato 21 days after inoculation with *Fol* race 3.

Fol race 3 inoculated and water (Mock) inoculated plants were allowed to grow for 21 days in a controlled environment as described in 5.2.7. Photographs were taken 21 days after inoculation.

Chapter 6: Functional analysis of the effect of *Fol* SIX6 protein on roots

6.1 Introduction

After investigating the effect of *Fol* SIX6 on plants in Chapters 3, 4 and 5, there was still a need for a more comprehensive examination of its function, particularly its effect on plant roots. This was essential for formulating hypotheses regarding its possible role during the infection process. *Fusarium oxysporum* infects through lateral roots or wounds on the roots of the plant and subsequently spreads throughout the xylem of the root (Michielse and Rep, 2009; Gordon, 2017). *F. oxysporum* secretes effectors into the xylem to facilitate its proliferation and dissemination within the plant (Michielse and Rep, 2009; Jangir et al., 2021). Examining the impact of the *Fol* SIX6 protein on leaf tissue has been valuable, but these effects may only be a proxy for activities in cells adjacent to the root xylem. Testing its effect on plant roots is crucial for understanding its role during infection.

Several pathogen effectors have been identified that facilitate root infection. Various root-knot nematode and cyst nematode effectors have been shown to affect the host root system by inducing the formation of feeding sites called giant cells in the case of root-knot nematodes or syncytia in the case of cyst nematodes (Mejias et al., 2019). The *MiPDI1* effector from the root-knot nematode *Meloidogyne incognita* has been well characterised as a protein disulphide isomerase-like effector that targets a stress-associated protein (SAP) in host plants to establish disease and facilitate nematode parasitism in Arabidopsis and Solanaceae (Zhao et al., 2020). *Fgl1* is an effector from *Fusarium graminearum* that contributes to root invasion through its lipase activity, by hydrolysing host cell membrane lipids to release free fatty acids, which act as signalling molecules that inhibit callose deposition and suppress other plant defence mechanisms, thereby weakening cell wall defences and facilitating fungal penetration (Voigt et al., 2005). Recently, the AeSSP1256 effector protein from the root-rot oomycete *Aphanomyces euteiches* was found to target a host RNA helicase and reduce both root number and root elongation in *Medicago truncatula* plants, leading to greater susceptibility (Camborde et al., 2022).

This chapter focuses on examining the effects of the *Fol SIX6* effector on plant roots through analysis of ion leakage and root growth. These experiments are designed to elucidate the impact of *Fol* SIX6 on root physiology and provide insights into its potential role during *Fol* infection.

6.2 Materials and Methods

6.2.1 Measurement of ion leakage from *N. benthamiana* root sections

N. benthamiana plants were sown in pots containing seed-raising mix (Martins Fertilizers, Australia) and grown for 2 weeks before being transplanted to potting mix (Martins Fertilizers) and allowed to grow for another 4 weeks in room with controlled environment condition (16 h 21°C light [100 µE m^{-2} sec^{-1}] / 8 h 16°C dark cycle with 70% relative humidity). Plants were uprooted without damaging the roots, which were then detached and washed in sterile deionised water (Figure 6.1A). Roots were then cut into 1 cm sections and weighed into 300 mg aliquots for each treatment (Figure 6.1B). Roots were then treated by immersion for 24 hours in *Fol* SIX6 protein (100 µg/ml in gel filtration buffer) or control (BSA 100 µg/ml in gel filtration buffer) as a negative control in 5 ml tubes (Figure 6.1C). Each treatment had six biological replicates (Figure 6.1D). Roots were then transferred to six-well plates with 8 ml of sterile deionised water in each well and washed for 10 minutes, after which the water was replaced in each well and conductivity was measured every 3 h for 12 h using a hand-held conductivity meter (Figure 6.1E).

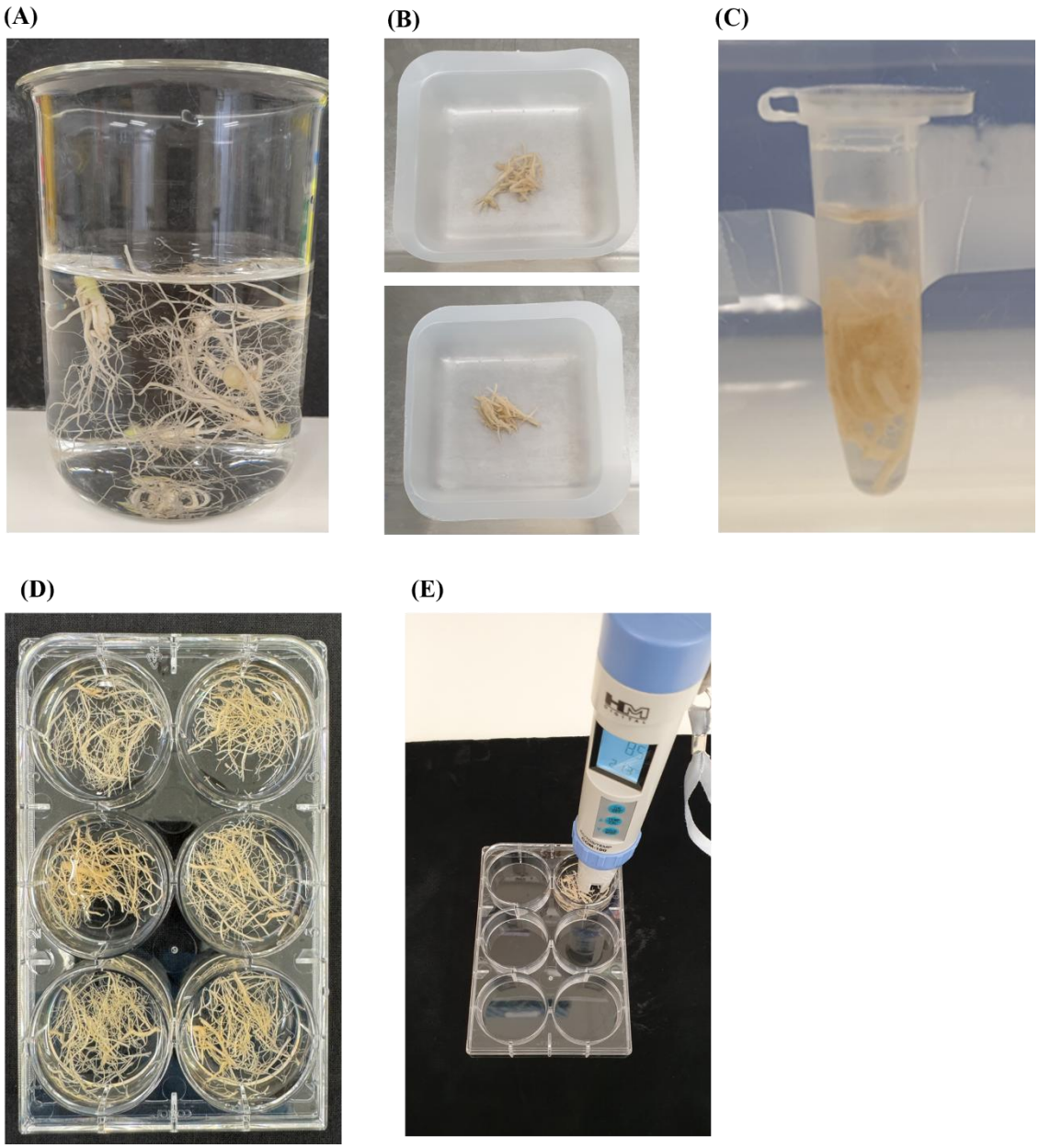

Figure 6.1 Measurement of electrolyte leakage from *N. benthamiana* root sections.

(A) Roots of 6-week-old *N. benthamiana* plants were detached and washed with sterile deionised water for 10 min before cutting into 1 cm sections. **(B)** The root sections were weighed quickly to avoid drying out and the weight was adjusted to approximately 300 mg per sample. **(C)** Root sections were treated by immersion for 24 h. **(D)** Root sections were then rinsed in water and transferred to six-well culture plates holding 8 ml of sterile water in each well. **(E)** Conductivity was measured using a hand-held conductivity meter.

6.2.2 Measurement of ion leakage from tomato root sections

M82 tomato plants were germinated and grown on perlite (Figure 6.2A) supplemented with soluble fertilizer (Thrive, Yates, Australia) and kept in a room with controlled environmental conditions (16 h 21°C light [100 µE m^{-2} sec $^{-1}$] / 8 h 16°C dark cycle with 70% relative humidity) for 45 days. Roots (Figure 6.2B) were then washed in water, cut into 1 cm sections and weighed into 300 mg aliquots for each treatment. Then roots were immersed in *Fol* SIX6 protein (100 µg/ml in gel filtration buffer) or control (BSA 100 µg/ml in gel filtration buffer) as a negative control in 5 ml tubes (Figure 6.2C). Each treatment had six biological replicates (Figure 6.2D). After 24 hours, roots were transferred to six-well plates with 8 ml of sterile deionised water in each well and washed for 10 minutes. The water was then replaced just prior to commencing measurements, and conductivity was measured every hour for 6 hours using a hand-held conductivity meter (Figure 6.2E).

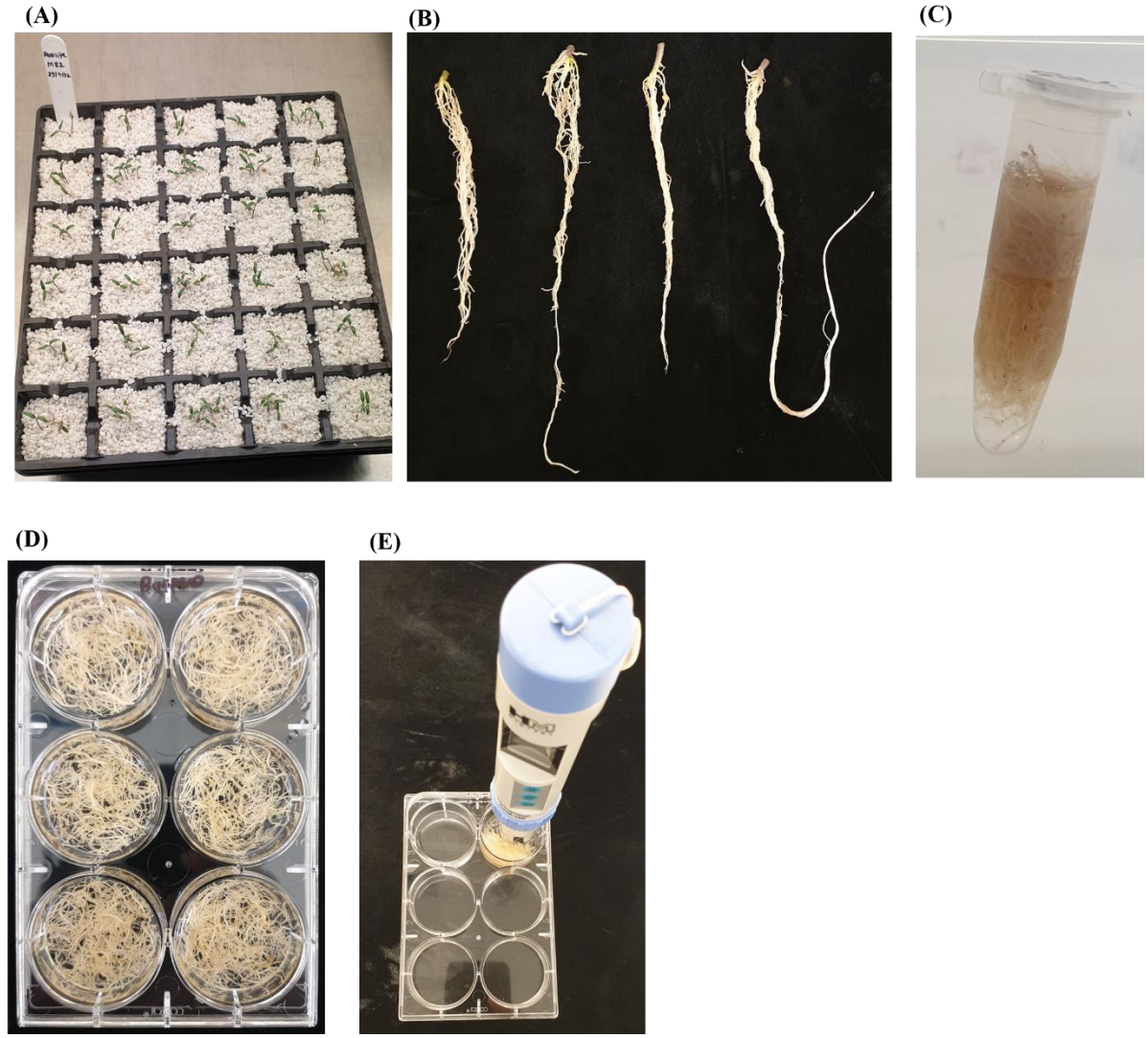

Figure 6.2 Measurement of electrolyte leakage from tomato root sections.

(A) M82 tomato seedlings were grown on perlite. Photographed 15 days after sowing. **(B)** Roots were harvested after 45 days of growth on perlite and washed in water. **(C)** Tomato roots were cut into 1 cm sections and 300 mg aliquots were treated by immersion for 24 h. **(D)** Treated root sections were washed and transferred to a six-well culture plate holding 8 ml of sterile water and an equal amount of root sections treated with *Fol* SIX6 and buffer. **(E)** Conductivity was measured using a hand-held conductivity meter.

6.2.3 Tomato root growth measurement

M82 tomato seeds were surface disinfected with 80% (v/v) ethanol for 2 min and germinated on half-strength MS media (Murashige and Skoog media; Phytotechnology lab, Cat # M519) (2 g of MS media with vitamins, 10 g sucrose and 5 g agar gel, pH 5.7) and grown for 4 days. Seedlings with root lengths of 2 cm were then transferred to half-strength MS medium treatment plates and kept for another 4 days under 16 h 21°C light [100 µE m^{-2} sec^{-1}] and 8 h

16°C dark cycle before primary root lengths were measured and the number of secondary roots counted. Primary root lengths were measured manually with the help of a ruler. Primary root length data were analysed by using Student t-tests, while secondary root number data were analysed using pairwise Mann-Whitney tests.

6.3 Results

6.3.1 *Fol* SIX6 protein causes electrolyte leakage from roots of *N. benthamiana* and tomato

Fol SIX6 was found to cause ion leakage in *N. benthamiana* and tomato leaves (Chapter 3), it would be very interesting to see whether *Fol* SIX6 caused any ion leakage in *N. benthamiana* or tomato roots. Root sections of *N. benthamiana* were treated with *Fol* SIX6 as indicated in Figure 6.1 and conductivity was measured after the roots were washed and immersed in sterile deionised water. Conductivity was found to be significantly higher from 3 h onwards for root sections treated with *Fol* SIX6 compared to those treated with buffer BSA (Figure 6.3).

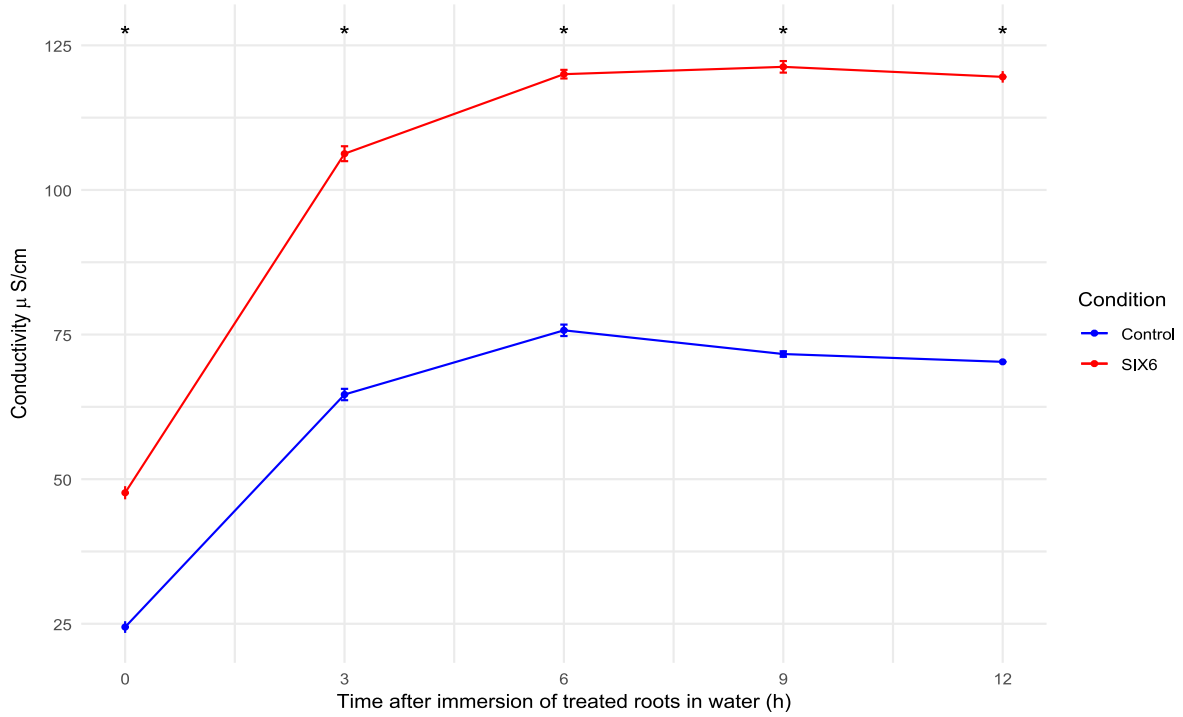

Figure 6.3 Measuring electrolyte leakage from roots of *N. benthamiana* incubated with *Fol* SIX6 or control.

Conductivity was measured following immersion in deionised water of root sections of 6-week-old *N. benthamiana* plants that had previously been incubated for 24 h with *Fol* SIX6 (100 µg/ml in gel filtration buffer) or control (BSA 100 µg/ml in gel filtration buffer).

Conductivity was measured at 3 h intervals for 12 h. Means and SEs are shown for six replicates comprising root sections from six plants. The conductivity data were analysed using pairwise Student t-tests. Asterisks indicate significant differences at $P < 0.001$.

After finding that SIX6 could cause electrolyte leakage in roots of *N. benthamiana*, it was very interesting to see whether roots of the actual host plant (tomato) also showed electrolyte leakage after treatment with *Fol* SIX6 protein. Root sections of M82 tomato were treated with *Fol* SIX6 as indicated in Figure 6.2 and conductivity was measured after the roots were washed and immersed in sterile deionised water. Conductivity was found to be significantly higher from 1 h onwards for root sections treated with *Fol* SIX6 protein compared to those treated with buffer BSA (Figure 6.4). This result was the first indication of an effect of *Fol* SIX6 on the root of its original host, i.e. where the protein is secreted during infection.

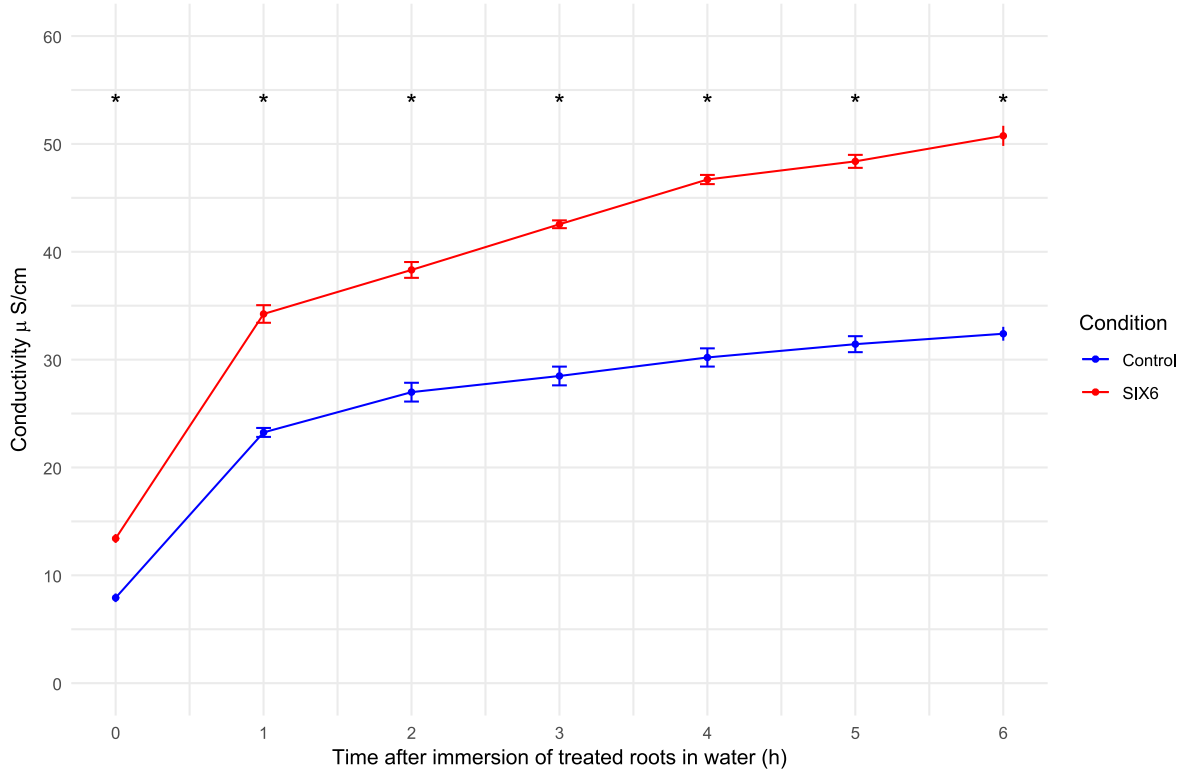

Figure 6.4 Measuring electrolyte leakage from roots of tomato incubated with *Fol* SIX6 or control.

Conductivity was measured following immersion in deionised water of root sections of tomato that had previously been incubated for 24 h with *Fol* SIX6 (100 µg/ml in gel filtration buffer) or control (BSA 100 µg/ml in gel filtration buffer). Conductivity was measured at 1 h intervals until 6 h after immersion in water. Means and SEs are shown for six replicates comprising root sections from six plants. The conductivity data were analysed using pairwise Student t-tests. Asterisks indicate significant differences at $P < 0.001$.

6.3.2 *Fol* SIX6 protein inhibits primary root elongation and promotes the formation of secondary roots of tomato

After finding that *Fol* SIX6 caused ion leakage in root sections, an experiment was set up to see if *Fol* SIX6 had any effect on tomato root growth. From previous experiments, it was known that *Fol* SIX6 remained active after heat treatment (Chapter 3), which meant it could be added to molten agar gel media without affecting its activity. Tomato seedlings were grown on half-strength MS plates for 4 days until roots were approximately 2 cm long. The seedlings were then transferred to half-strength MS plates containing *Fol* SIX6 (20 µg/ml) or controls with water or BSA (20 µg/ml) in place of SIX6 and grown for 4 more days. Roots on the water and BSA controls grew normally, but roots grown on medium containing *Fol* SIX6 showed significant inhibition of primary root elongation (Figures 6.5, 6.6, 6.7, 6.8 and Appendices 6.1, 6.2, 6.3, 6.4). Increased secondary root elongation was evident in one replicate of the SIX6 treatment (Figure 6.6 and Appendix 6.2) but not in three other replicates when compared to the water or BSA controls (Figures 6.5, 6.7, 6.8 and Appendices 6.1, 6.3, 6.4). Reduced secondary root elongation was evident in the third replicate of the SIX6 treatment, possibly due to fungal contamination (Figure 6.7 and Appendix 6.3). Interestingly, when seedlings were grown for 20 days after transfer, inhibition of primary, secondary and tertiary root development was observed along with stunted shoot growth (Figure 6.9). To test whether the effect on primary root elongation was specific to *Fol* SIX6, purified recombinant *Fol* SIX1 (Avr3) and *Fol* SIX8 proteins were also tested, but neither of them showed the same effect as *Fol* SIX6 (Figure 6.8 and Appendix 6.4). The number of secondary roots in *Fol* SIX6 was not significantly different from the BSA control or *Fol* SIX8 (Figure 6.8).

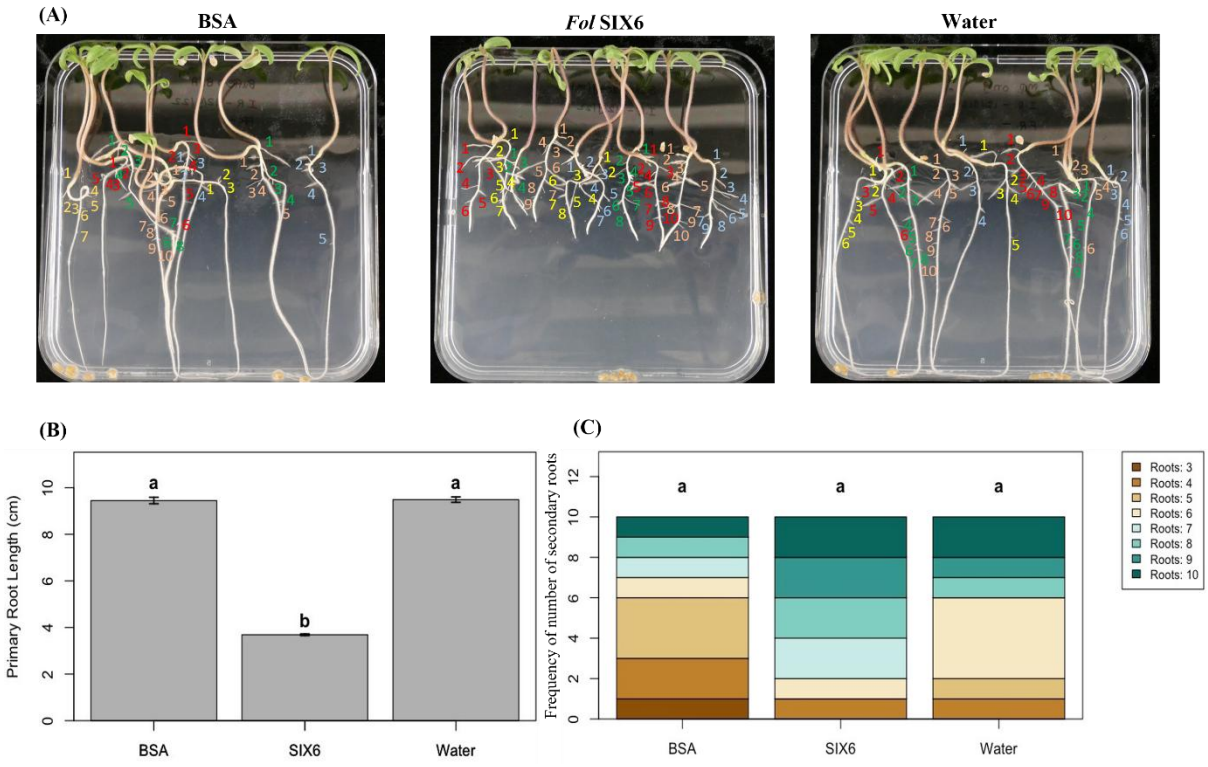

Figure 6.5 Measurement of primary root lengths and numbers of secondary roots for tomato seedlings grown on media containing BSA, *Fol* SIX6 protein or water.

(A) Tomato seedlings (cv. M82) were photographed 4 days after transfer and growth on half-strength MS media containing BSA (20 µg/ml in gel filtration buffer), *Fol* SIX6 protein (20 µg/ml in gel filtration buffer) or water. **(B)** Means and SEs of primary root lengths of seedlings are shown in (A). Root length data were analysed using pairwise Student t-tests. Different letters indicate significant differences at $p < 0.05$. **(C)** Stacked bar graphs showing the distribution of secondary root numbers for seedlings are shown in (A). Secondary root data were analysed using pairwise Mann-Whitney tests. Different letters indicate significant differences ($p < 0.0125$). The P value for significance was adjusted from 0.05 to 0.0125 following application of the Bonferroni correction for four repetitions of the experiment.

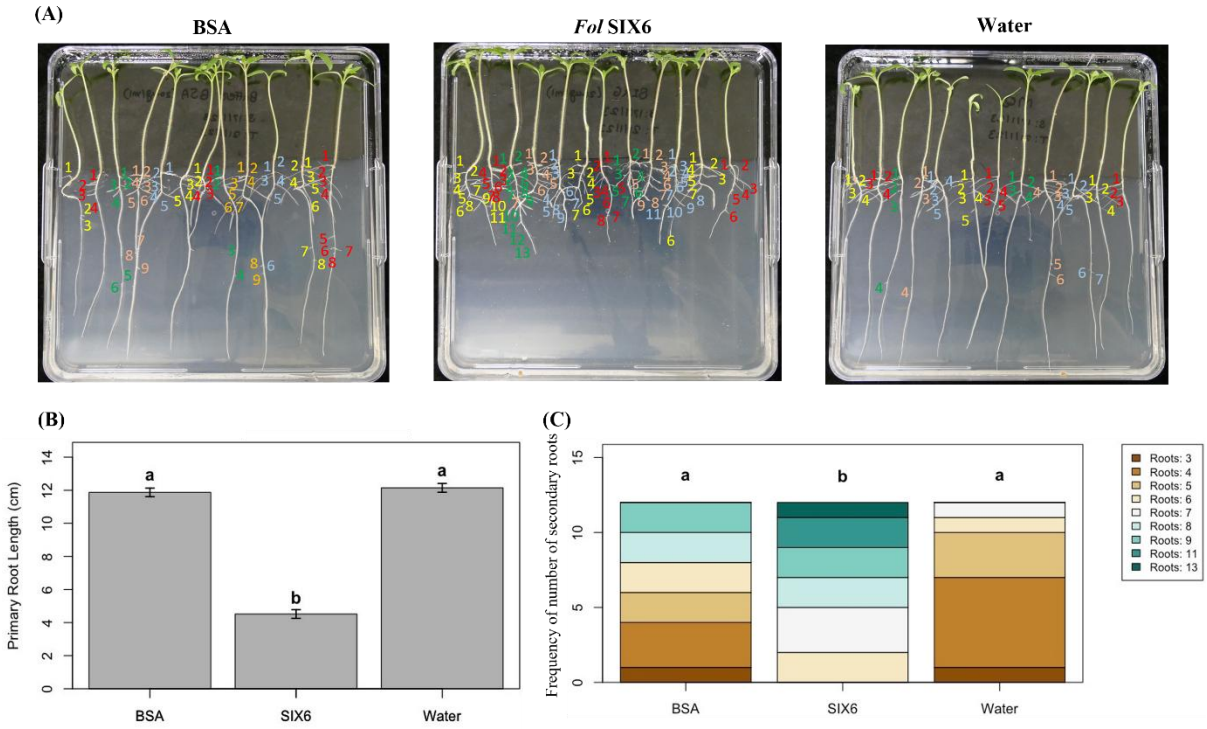

Figure 6.6 Measurement of primary root lengths and numbers of secondary roots for tomato seedlings grown on media containing BSA, *Fol* SIX6 protein or water.

(A) Tomato seedlings (cv. M82) were photographed 4 days after transfer and growth on half-strength MS media containing BSA (20 µg/ml in gel filtration buffer), *Fol* SIX6 protein (20 µg/ml in gel filtration buffer) or water. **(B)** Means and SEs of primary root lengths of seedlings are shown in (A). Root length data were analysed using pairwise Student t-tests. Different letters indicate significant differences at $p < 0.05$. **(C)** Stacked bar graph showing the distribution of secondary root numbers for seedlings shown in (A). Secondary root data were analysed using pairwise Mann-Whitney tests. Different letters indicate significant differences ($p < 0.0125$). The P-value for significance was adjusted from 0.05 to 0.0125 following application of the Bonferroni correction for four repetitions of the experiment.

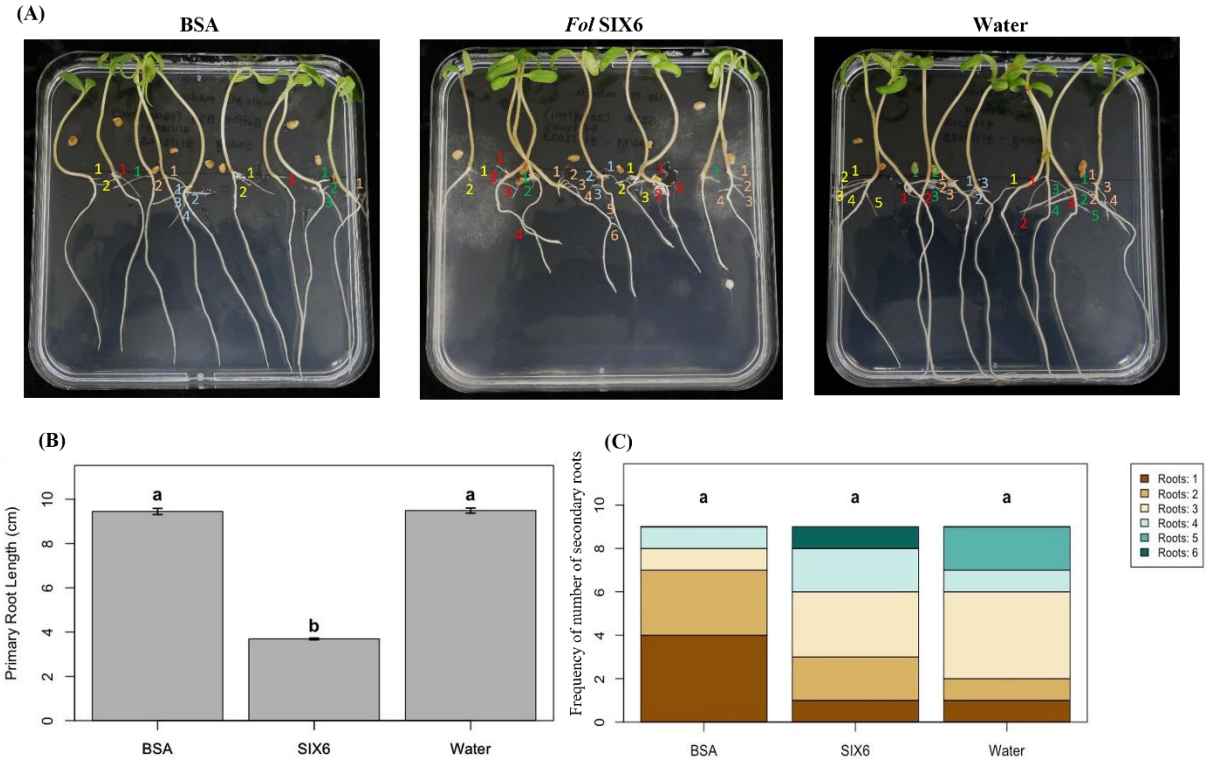

Figure 6.7 Measurement of primary root length and number of secondary roots of tomato c.v. M82 grown on half-strength media containing BSA, or *Fol* SIX6 protein or water.

(A) Tomato seedlings (cv. M82) were photographed 4 days after transfer and growth on half-strength MS media containing BSA (20 µg/ml in gel filtration buffer), *Fol* SIX6 protein (20 µg/ml in gel filtration buffer) or water. **(B)** Means and SEs of primary root lengths of seedlings are shown in (A). Root length data were analysed using pairwise Student t-tests. Different letters indicate significant differences at $p < 0.05$. **(C)** Stacked bar graph showing the distribution of secondary root numbers for seedlings shown in (A). Secondary root data were analysed using pairwise Mann-Whitney tests. Different letters indicate significant differences ($p < 0.0125$). The P-value for significance was adjusted from 0.05 to 0.0125 following application of the Bonferroni correction for four repetitions of the experiment.

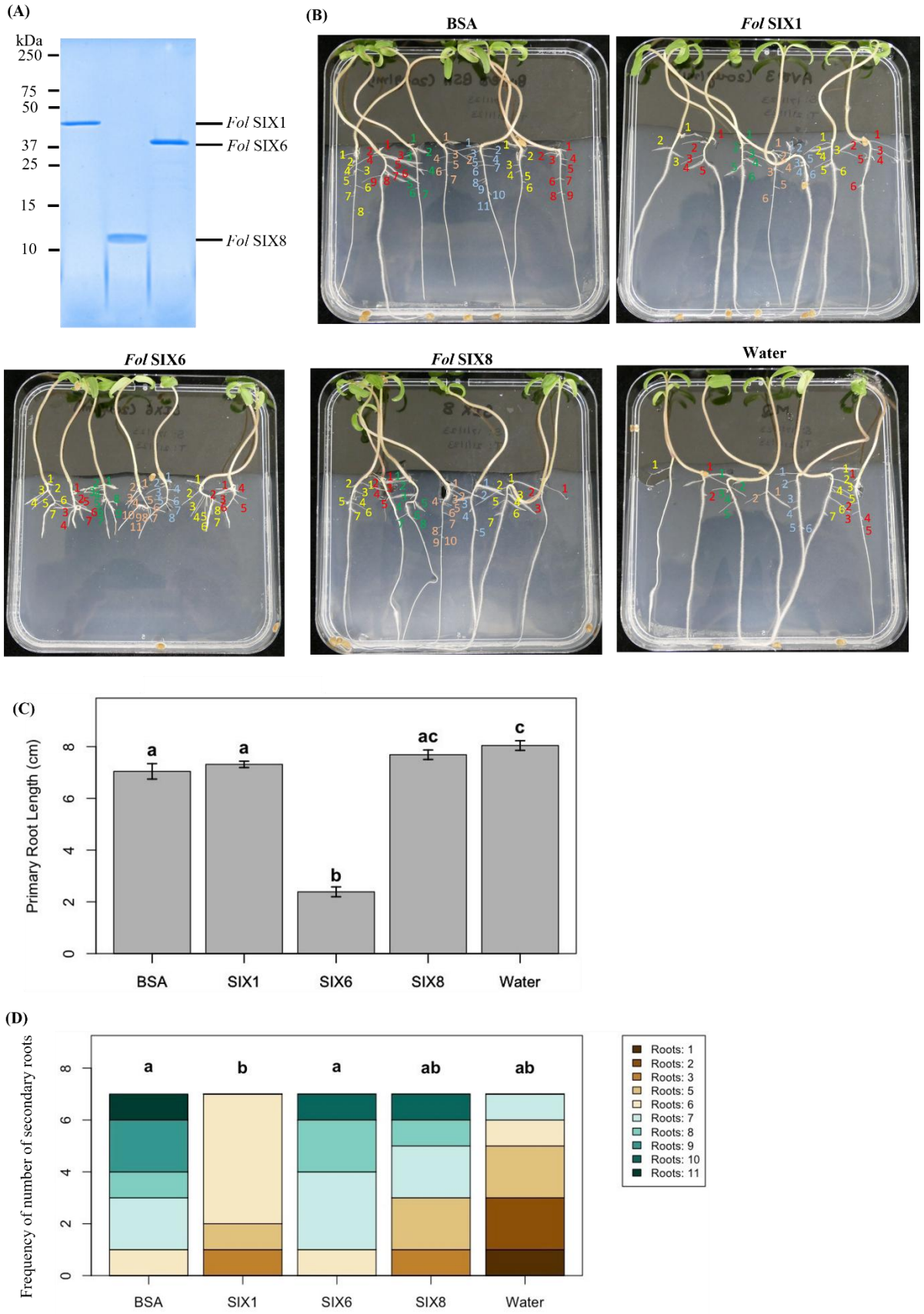
(A)
kDa
250
75
50
37
25
15
10
Fol SIX1
Fol SIX6
Fol SIX8
(B)
BSA
Fol SIX1
Fol SIX6
Fol SIX8
Water
(C)
Primary Root Length (cm)
0
2
4
6
8
a
a
b
ac
c
BSA
SIX1
SIX6
SIX8
Water
(D)
Frequency of number of secondary roots
0
2
4
6
8
a
b
a
ab
ab
BSA
SIX1
SIX6
SIX8
Water
Roots: 1
Roots: 2
Roots: 3
Roots: 5
Roots: 6
Roots: 7
Roots: 8
Roots: 9
Roots: 10
Roots: 11

Figure 6.8 Measurement of primary root lengths and numbers of secondary roots for tomato seedlings grown on half-strength media containing BSA, or *Fol* SIX1, or *Fol* SIX6 or *Fol* SIX8 or water.

(A) Coomassie-blue-stained PAGE gel showing purified *Fol* SIX1, *Fol* SIX8 and *Fol* SIX6 proteins used in root growth assays. **(B)** Tomato (cv. M82) seedlings were photographed 4 days after transfer and growth on half-strength MS medium containing BSA (20 µg/ml in gel filtration buffer), *Fol* SIX1 (20 µg/ml in gel filtration buffer), *Fol* SIX6 (20 µg/ml in gel filtration buffer) protein, *Fol* SIX8 (20 µg/ml in gel filtration buffer) or water. **(C)** Means and SEs of primary root lengths of seedlings are shown in (B). Root length data were analysed by pairwise Student t-tests. Different letters indicate significant differences at $p < 0.05$. **(D)** Stacked bar graph showing the distribution of secondary root numbers for seedlings shown in (B). Secondary root data were analysed using pairwise Mann-Whitney tests. Different letters indicate significant differences ($p < 0.05$). P-values were adjusted using the Bonferroni correction.

Figure 6.9 Phenotypes of tomato seedlings after 20 days of growth on media containing BSA, *Fol* SIX6 protein or water.

Four-day-old seedlings were transferred to half-strength Murashige and Skoog (MS) medium containing BSA (20 µg/ml in gel filtration buffer), *Fol* SIX6 (20 µg/ml in gel filtration buffer) or water. Seedlings were photographed 20 days post-transfer.

6.4 Discussion

6.4.1 *Fol* SIX6 causes electrolyte leakage in roots of *N. benthamiana* and tomato

Fol SIX6 was found to cause electrolyte leakage in roots of *N. benthamiana* (Figure 6.3) and tomato (Figure 6.4). Although the specific ions or ion channels involved in *Fol* SIX6-induced electrolyte leakage have not been identified, the release of electrolytes strongly suggests a disruption of membrane integrity or the activation of ion transport pathways. However, the significance of this observation in terms of the role SIX6 plays in *Fol* infection remains unknown. A study by Demidchik et al. (2010) provides evidence that ion leakage, particularly potassium (K^+) efflux from roots, is closely linked to programmed cell death (PCD) in plants.

Interestingly, a recent study on other fungal effectors, such as PdCDIE1 from *Penicillium digitatum*, which causes citrus green mould, has also shown that it induces electrolyte leakage through the disruption of ion homeostasis by targeting plant calcium signalling pathways and causing ROS-dependent cell death (Lin et al., 2025). Like SIX6, PdCDIE1 demonstrates that fungal effectors can manipulate host ion transport systems as a conserved strategy for promoting infection, suggesting that electrolyte leakage may represent a common cellular response to diverse pathogenic effectors regardless of their specific molecular targets. Further characterisation of the specific ions involved and the temporal relationship between electrolyte leakage and other cellular responses would help clarify whether this phenomenon contributes to disease susceptibility or represents an attempt at pathogen recognition and defence activation.

Despite observing electrolyte leakage, we found no visible signs of cell death in the treated roots, contrasting with the visible necrotic lesions typically observed in leaf infiltration studies. Several factors could explain this difference. The most obvious explanation is that we used a much lower concentration in the root experiments (20 µg/ml) compared to leaf infiltration (100 µg/ml). This lower dose might be enough to disrupt cell membranes without actually killing the cells. There's also a fundamental difference in the mode of protein delivery. In the root assays, SIX6 protein was added to the growth medium and allowed the roots to absorb it naturally, while leaf infiltration protein was pushed directly into the leaf spaces at much higher concentrations. When roots have to absorb SIX6 from the outside, the amount that actually gets inside the cells is probably much lower - sufficient to cause membrane disruption but insufficient to induce visible cell death. Furthermore, root cells might also just respond

differently to SIX6 than leaf cells, including different ion transport systems and cell wall compositions, which may influence their response to the effector protein. The natural infection process of *Fusarium oxysporum* begins in the root system, where the pathogen encounters a different cellular environment compared to above-ground tissues typically used in infiltration studies. It should acknowledge that while leaf infiltration has been established as an effective delivery method for studying SIX effector activity in previous studies (Chincinska, 2021), the effectiveness of root absorption as a delivery mechanism for SIX6 has not been systematically validated in this work, which may contribute to the observed differences in response magnitude.

An examination of apoplastic pH changes in SIX6-treated roots would have provided valuable mechanistic insights into the nature of the observed electrolyte leakage. Apoplastic pH alterations are intimately linked to ion transport and membrane stability, with alkalinization and acidification having distinct physiological implications (Geilfus, 2017; Gamez-Arjona et al., 2022). Apoplastic alkalinization is commonly associated with the hypersensitive response (HR) and programmed cell death in plant-pathogen interactions, often accompanied by rapid K^+ efflux and Ca^{2+} influx (Felle et al., 2001; Felle et al., 2004). Conversely, apoplastic acidification is typically linked to cell wall loosening, growth processes, and can indicate activation of plasma membrane H^+-ATPases in response to stress (Hager, 2003). Given that *Fol* is a vascular pathogen that manipulates host physiology for successful colonisation rather than triggering immediate cell death, SIX6-induced electrolyte leakage might be associated with apoplastic acidification, facilitating pathogen establishment and nutrient acquisition. Future investigations incorporating pH measurements alongside electrolyte leakage assays would help distinguish between defence-related alkalinization and pathogenesis-promoting acidification, thereby clarifying whether SIX6 functions primarily as a virulence factor or triggers host defence responses.

To further investigate the cellular mechanisms underlying SIX6-induced electrolyte leakage in roots, future studies could also employ *Agrobacterium rhizogenes*-mediated transformation to generate hairy root cultures expressing vacuolar-targeted fluorescent markers such as mTurquoise. This approach would enable real-time visualisation of vacuolar integrity and dynamics in response to SIX6 treatment, providing direct evidence of whether the observed electrolyte leakage is associated with vacuolar membrane disruption. Vacuolar leakage would be particularly significant as it would result in the release of vacuolar contents, including

organic acids and inorganic ions, into the cytosol, leading to cytosolic acidification. Such pH changes could have profound implications for root growth and development, as cytosolic pH homeostasis is critical for enzyme function, protein stability, and cellular metabolism (Felle, 2001). Moreover, vacuolar disruption could compromise the plant's ability to compartmentalise toxic compounds and maintain turgor pressure, both essential for normal root function. The hairy root system would provide an ideal experimental platform for these investigations, as it allows for controlled genetic manipulation while maintaining the physiological characteristics of root tissue, potentially bridging the gap between the electrolyte leakage observations and their cellular consequences.

In addition to the above suggestions, the electrophysiological studies of SIX6-treated roots could be used to determine which ions and ion channels are involved, specifically looking for K^+ efflux and Ca^{2+} influx. ROS production could also be examined to provide additional insights into the defence response mechanisms (Demidchik et al, 2006).

6.4.2 *Fol* SIX6 affects root growth in tomato

Fol SIX6 inhibited primary root elongation in tomato (Figures 6.5 to 6.8) but did not appear to significantly affect secondary root initiation in the short term (Figures 6.5, 6.7 and 6.8) but did affect secondary and tertiary root formation and elongation after prolonged exposure (Figure 6.9). However, the latter is only a qualitative observation based on a single experiment. The long-term effect of SIX6 on secondary and tertiary root initiation and elongation warrants verification, perhaps by repeating the experiment using larger plates with fewer seedlings per plate and measuring secondary and tertiary root numbers and lengths after 20 days of growth. One consequence of reduced secondary or tertiary root elongation during infection might be a reduced capacity to absorb water and nutrients from the soil to compensate for root xylem blockages caused by *Fol*. Another consequence might be diversion of nutrients away from root growth for the benefit of pathogen nutrition. It might therefore be interesting and informative to conduct a metabolomic analysis of roots affected by SIX6.

Pyocyanin is a virulence factor from *Pseudomonas aeruginosa* that causes ROS and ethylene-dependent inhibition of primary root elongation and promotion of secondary root formation in Arabidopsis (Ortiz-Castro et al., 2014; Hall et al., 2016). In Chapter 4, *Fol* SIX6-induced cell death was shown to be unaffected in the leaves of the ethylene-insensitive *Nr* mutant of tomato. However, the physiological response to *Fol* SIX6 in roots may differ from that in leaves. To

further investigate a possible role of ethylene in root responses to SIX6, it would be interesting to grow *Nr* tomato on media containing *Fol* SIX6 protein versus a BSA or water control. Additionally, the potential for ethylene-independent formation of reactive oxygen species (ROS) could be tested by assaying ROS production in *Nr* tomato on media containing *Fol* SIX6 versus a water or buffer BSA control. This might provide further insights into the underlying mechanisms of *Fol* SIX6 activity in root tissues.

Interestingly, *Fol* possesses a homologue of plant RALFs (rapid alkalinisation factors) that is expressed during infection of tomato (Thynne et al., 2017). In plants, RALFs interact with plasma-membrane receptor kinases that play roles in both plant growth and plant immunity e.g. RALF1 and RALF23 bind to the receptor kinase FER (FERONIA) (Haruta et al., 2014; Stegmann et al., 2017). In *Catharanthus roseus* RALF23 forms a complex with FER and the LLG1 (LORELEI-LIKE GPI-ANCHORED 1) protein (Xiao et al., 2019). Activation of FER results in phosphorylation of the plasma membrane H^+-ATPase AHA2 leading to inhibition of H^+ transport, extracellular alkalinisation and inhibition of root elongation (Haruta *et al*., 2014). *Fol* RALF peptide has been found to cause FER-dependent extracellular alkalinisation and inhibition of root elongation and root hair formation in tomato seedlings (Masachis et al., 2016; Thynne et al., 2017). However, a contribution to *Fol* pathogenicity found in the study by Masachis et al. (2016) was not evident in the study by Thynne et al. (2017). Based on these reports, it would be interesting to examine root hair formation on tomato roots grown on medium containing *Fol* SIX6. Inhibition of root hair formation would further reduce the capacity of *Fol*-infected tomato roots to absorb water and nutrients from soil and compensate for *Fol*-induced xylem blockage. VIGS or CRISPR-Cas9 mediated deletion of tomato *FER*-like and *LORELEI*-like genes might also yield useful information about the mechanism underpinning *Fol* SIX6-induced induced electrolyte leakage and inhibition of root elongation. Given that *Fol* RALF and *Fol* SIX6 might be targeting similar plant processes, a combined knockout of both *RALF* and *SIX6* genes might reveal a synergistic effect on *Fol* pathogenicity.

References

Camborde, L., Kiselev, A., Pel, M.J.C., Le Ru, A., Jauneau, A., Pouzet, C., Dumas, B., Gaulin, E. (2022). An oomycete effector targets a plant RNA helicase involved in root development and defence. *New Phytologist, 233*(5), 2232-2248.

Chincinska, I.A. (2021). Leaf infiltration in plant science: old method, new possibilities. *Plant Methods, 17*(1), 83.

Demidchik, V., Cuin, T.A., Svistunenko, D., Smith, S.J., Miller, A.J., Shabala, S., Sokolik, A. and Yurin, V. (2010). *Arabidopsis* root K^+ efflux conductance activated by hydroxyl radicals: single-channel properties, genetic basis and involvement in stress-induced cell death. *Journal of Cell Science*, *123*(9), 1468-1479.

Demidchik, V., Sokolik, A., Yurin, V. (2006). Electrophysiological characterization of plant cation channels. In *Plant electrophysiology: theory and methods*, Springer Berlin Heidelberg, 173-185.

Felle, H.H. (2001). pH: signal and messenger in plant cells. *Plant Biology*, *3*(6), 577-591.

Felle, H.H., Herrmann, A., Huckelhoven, R., Kogel, K.H. (2004). Root-to-shoot signalling: apoplastic alkalinization, a general stress response and defence factor in barley (*Hordeum vulgare* L.). *Protoplasma*, *224*(1-2), 33-41.

Gamez-Arjona, F.M., Sanchez-Rodriguez, C., Montesinos, J.C. (2022). The root apoplastic pH as an integrator of plant signaling. *Frontiers in Plant Science*, *13*, 931979.

Geilfus, C.M. (2017). The pH of the apoplast: dynamic factor with functional impact under stress. *Molecular Plant*, *10*(11), 1371-1386.

Gordon, T.R. (2017). *Fusarium oxysporum* and the *Fusarium* wilt syndrome. *Annual Review of Phytopathology, 4*(55), 23-39.

Hager, A. (2003). Role of the plasma membrane H^+ ATPase in auxin-induced elongation growth: historical and new aspects. *Journal of Plant Research*, *116*(6), 483-505.

Hall, S., McDermott, C., Anoop Kumar-Dukie, S., McFarland, A.J., Forbes, A., Perkins, A.V., Davey, A.K., Chess-Williams, R., Kiefel, M.J., Arora, D., Grant, G.D. (2016). Cellular effects

of pyocyanin, a secreted virulence factor of *Pseudomonas aeruginosa*. *Toxins (Basel), 8*(8), 236.

Haruta, M., Sabat, G., Stecker, K., Minkoff, B.B., Sussman, M.R. (2014). A peptide hormone and its receptor protein kinase regulate plant cell expansion. *Science, 343*(6169),408-411.

Jangir, P., Mehra, N., Sharma, K., Singh, N., Rani, M., Kapoor, R. (2021). Secreted in xylem genes: drivers of host adaptation in *Fusarium oxysporum*. *Frontiers in Plant Science, 22*(12), 628611.

Lin, Y., Xu, C., Li, L., Fan, L., Li, R., He, J., Li, H., Deng, W., Kang, Z., Li, Z., Cheng, Y. (2025). A conserved fungal effector disturbs Ca^{2+} sensing and ROS homeostasis to induce plant cell death. *Nature Communications*, *16*(1), 3523.

Masachis, S., Segorbe, D., Turrà, D., Leon-Ruiz, M., Fürst, U., El Ghalid, M., Leonard, G., López-Berges, M.S., Richards, T.A., Felix, G., Di Pietro, A. (2016). A fungal pathogen secretes plant alkalinizing peptides to increase infection. *Nature Microbiology, 1*(6), 16043.

Mejias, J., Truong, N.M., Abad, P., Favery, B., Quentin, M. (2019). Plant proteins and processes targeted by parasitic nematode effectors. *Frontiers in Plant Science, 30*(10), 970.

Michielse, C.B., & Rep, M. (2009). Pathogen profile update: *Fusarium oxysporum*. *Molecular Plant Pathology, 10*(3), 311-324.

Ortiz-Castro, R., Pelagio-Flores, R., Mendez-Bravo, A., Ruiz-Herrera, L.F., Campos-Garcia, J., Lopez-Bucio, J. (2014). Pyocyanin, a virulence factor produced by *Pseudomonas aeruginosa*, alters root development through reactive oxygen species and ethylene signaling in *Arabidopsis*. *Molecular Plant Microbe Interaction, 27*(4), 364-78.

Stegmann, M., Monaghan, J., Smakowska-Luzan, E., Rovenich, H., Lehner, A., Holton, N., Belkhadir, Y., Zipfel, C. (2017). The receptor kinase FER is a RALF-regulated scaffold controlling plant immune signaling. *Science, 355*(6322), 287-289.

Thynne, E., Saur, I.M.L., Simbaqueba, J., Ogilvie, H.A., Gonzalez-Cendales, Y., Mead, O., Taranto, A., Catanzariti, A.M., McDonald, M.C., Schwessinger, B., Jones, D.A., Rathjen, J.P., Solomon, P.S. (2017). Fungal phytopathogens encode functional homologues of plant rapid alkalinization factor (RALF) peptides. *Molecular Plant Pathology, 18*(6), 811-824.

Voigt, C.A., Schafer, W., Salomon, S. (2005). A secreted lipase of *Fusarium graminearum* is a virulence factor required for infection of cereals. *Plant Journal, 42*(3), 364-375.

Xiao, Y., Stegmann, M., Han, Z., De Falco, T.A., Parys, K., Xu, L., Belkhadir, Y., Zipfel, C., Chai, J. (2019). Mechanisms of RALF peptide perception by a heterotypic receptor complex. *Nature, 572*(7768), 270-274.

Zhao, J., Mejias, J., Quentin, M., Chen, Y., de Almeida-Engler, J., Mao, Z., Sun, Q., Liu, Q., Xie, B., Abad, P., Favery, B., Jian, H. (2020). The root-knot nematode effector *MiPDI1* targets a stress-associated protein (SAP) to establish disease in Solanaceae and *Arabidopsis*. *New Phytologist, 228*(4), 1417-1430.

Plant number	Primary root length (cm)		
	BSA	SIX6	Water
1	8.9	3.5	9.5
2	9.0	3.6	9.0
3	9.2	3.7	10
4	9.6	3.6	9.2
5	8.8	3.9	9.4
6	9.6	3.8	9.5
7	9.8	3.6	9.0
8	10	3.7	9.5
9	9.9	3.8	10
10	9.7	3.7	9.8

Plant number	Secondary root number		
	BSA	SIX6	Water
1	7	7	6
2	5	6	6
3	8	4	8
4	10	9	10
5	4	7	4
6	3	8	5
7	6	10	10
8	4	8	9
9	5	10	6
10	5	9	6

Appendix 6.1 Primary root lengths and secondary root numbers used to generate Figure 6.5.

Plant number	Primary root length (cm)		
	BSA	SIX6	Water
1	11.0	5.6	11.0
2	11.3	4.1	12.1
3	12.0	6.0	12.3
4	12.2	3.5	13.0
5	12.6	4.6	12.1
6	12.0	3.6	11.9
7	10.6	4.0	11.8
8	12.8	4.0	13.5
9	13.0	4.1	13.6
10	10.5	5.5	12.5
11	11.4	3.6	11.3
12	13.0	5.6	10.6

Plant number	Secondary root number		
	BSA	SIX6	Water
1	3	11	4
2	4	8	4
3	6	13	4
4	9	7	4
5	5	9	5
6	5	7	5
7	4	8	5
8	4	7	4
9	9	9	6
10	6	11	7
11	8	6	4
12	8	6	3

Appendix 6.2 Primary root lengths and secondary root numbers used to generate Figure 6.6.

Plant number	Primary root length (cm)		
	BSA	SIX6	Water
1	7.6	2.5	9.0
2	7.5	3.5	9.5
3	7.5	3.6	9.7
4	7.6	4.3	9.7
5	7.3	4.3	9.8
6	7.3	3.0	9.2
7	7.2	3.8	8.5
8	7.4	3.6	9.1
9	7.2	3.4	9.1

Plant number	Secondary root number		
	BSA	SIX6	Water
1	2	2	5
2	1	4	2
3	1	2	3
4	2	6	3
5	4	3	3
6	2	3	1
7	1	3	3
8	3	1	5
9	1	4	4

Appendix 6.3 Primary root lengths and secondary root numbers used to generate Figure 6.7.

Plant number	Primary root length (cm)				
	BSA	SIX1	SIX6	SIX8	Water
1	7.3	7.4	2.5	7.8	7.5
2	8.5	7.5	2.1	7.0	8.2
3	6.5	7.2	3.0	7.6	8.4
4	6.0	6.8	2.0	8.0	8.5
5	7.2	7.6	3.1	7.6	8.3
6	6.7	7.7	2.2	8.5	8.2
7	7.1	7.0	1.8	7.3	7.2

Plant number	Secondary root number				
	BSA	SIX1	SIX6	SIX8	Water
1	8	3	7	7	1
2	9	5	7	5	2
3	7	6	7	8	5
4	7	6	10	10	2
5	11	6	8	5	6
6	6	6	8	7	7
7	9	6	6	3	5

Appendix 6.4 Primary root lengths and secondary root numbers used to generate Figure 6.8.

Chapter 7: General Discussion

7.1 *Avr7* gene identification efforts and prospects

An attempt was made in Chapter 2 to identify the *Avr7* gene by screening potential candidate genes, including *SIX2, SIX7, SIX11, SIX12, SIX13*, *FOXG_22509* and *FOXG_17276,* using *Agrobacterium*-mediated co-expression with *I-7* in *N. benthamiana* and looking for cell death induction indicative of effector recognition. However, the attempt to identify *Avr7* was unsuccessful, using the approach described in Chapter 2. Initial annotation of the *Fol* genome by Ma et al. (2010) identified 126 small, cysteine-rich, secreted proteins with a signal peptide lacking transmembrane domains, possessing limited sequence homology to known proteins, and residing on lineage-specific, repeat-rich (conditionally dispensable) genomic regions as possible pathogen effectors (Ma et al., 2010). More recent genomic and transcriptomic work has expanded and refined the pool of candidate *Fol* effectors, with Sun et al. (2022) identifying 40 non-redundant effector candidates beyond the 14 known *SIX* genes, including several novel effector candidates. These 40 effector candidates represent promising targets for future *Avr7* identification efforts, which could use the approach described in Chapter 2 or generate and test *Fol* knockouts of the candidate genes for loss of avirulence on transgenic *I-7* tomato plants lacking any other genes for resistance to *Fol*. It is also important to note that the approach described in Chapter 2 and used previously by Catanzariti and Bru (as indicated in Chapter 2), might not be suitable for the identification of *Avr7*, meaning that the *SIX* genes already tested as *Avr7* candidates should also be retested in any alternative approach used. It is also possible that *Avr7* is not one of the 14 known *SIX* genes or one of the 40 effector candidates identified by Sun et al. (2022), so that a targeted approach to the identification of *Avr7* might not work.

A non-targeted forward genetic strategy using chemical mutagenesis could be used as an alternative to identify *Avr7*. This approach would involve inducing random deletion or point mutations throughout the *Fol* genome using chemical mutagens, followed by screening the resulting mutant population for isolates capable of overcoming *I-7* resistance in tomato plants. The pathogenic mutants could then undergo whole-genome sequencing using high-throughput platforms to identify deletions or mutations responsible for the loss of avirulence (Urban et al., 2015; Li et al., 2020). By comparing mutant genomes against the wild-type *Fol* genome, a candidate *Avr7* gene (or genes) that was disrupted in multiple independent mutants could be identified. This candidate would subsequently require functional validation through knockout and complementation studies looking for loss and recovery, respectively, of avirulence on transgenic *I-7* tomato lacking any other genes for resistance to *Fol* or by testing for its ability to induce *I-7*-dependent cell death as described in Chapter 2.

7.2 SIX6 cell death-inducing activity: potential for novel herbicide development

Chapter 3 showed the cell death-inducing activity of *Fol* SIX6 and its homologues (*Foc, Fom* and *Fov* SIX6) in different plant species (Chapter 3). Testing purified *Fol*, *Foc* and *Fom* SIX6 proteins in foliar tissues of representatives from multiple taxonomic families (Solanaceae, Cucurbitaceae, Brassicaceae and Leguminosae) revealed broad yet differential plant sensitivity (Chapter 3). The effect of *Fol* SIX6 and its homologues was not limited to cell death but also had effects like chlorosis, wilting, curling, and tip cell death (Chapter 3). Notably, SIX6 did not affect the Brassicaeae crop plants tested. Therefore, although Arabidopsis offers extensive genetic and molecular resources, its use as a model system for future SIX6 functional studies is limited. Whilst SIX6 was capable of inducing tip death in Arabidopsis (Chapter 3), this response was insufficient and inconsistent for reliable dissection of the SIX6 response pathway, and no activity was observed in the other Brassicaceae crop species tested. Nevertheless, the tip death phenotype observed in Arabidopsis indicates that the molecular response to SIX6 is present. Since *Fusarium oxysporum* infects plants through the roots, Arabidopsis root tissue may show a more consistent response to SIX6. Future studies could therefore explore root-based assays, which may provide a more biologically relevant system for dissecting the SIX6 response pathway, taking advantage of the extensive genetic resources available in Arabidopsis. Furthermore, if the effect of SIX6 on root growth is conserved in Arabidopsis, a panel of mutants could be tested for resistance to this growth response.

Prior studies show that pathogenic toxins often inhibit the synthesis of proteins and nucleic acids in host plants, resulting in physiological disorders, cell death, and even death of the plant itself, demonstrating the potential for controlled application of such mechanisms (Peng et al., 2021). Developing herbicides with novel mechanisms of action would provide an effective, practical, and rapid solution for managing herbicide-resistant weeds, since new herbicidal approaches would avoid pre-existing resistance patterns or cross-resistance issues found with current herbicide treatments (He et al., 2022). However, in the past 20 years, only a few successful herbicides with new modes of action have been marketed, highlighting the opportunity for innovative approaches like fungal effector-based herbicides (He et al., 2022). The semi-specific cell death-inducing activity of *Fol* SIX6 protein among the different plant families tested makes it an excellent candidate for the development of a selective herbicide targeting specific weed families while sparing the crop. Given that SIX6 did not affect the Brassicaceous crop plants tested, it could potentially be used as a herbicide on Brassicaceous crops such as oilseed rape and possibly a few other field crops like pumpkin and sunflower that

showed little or no response to SIX6 to control non-Brassicaceous weeds. Although Poaceae species were not included in the current screening, a SIX6-based herbicide could potentially be used in cereal crops and other grass crops such as maize if they were found to be non-responsive to SIX6. These are crops of major economic importance that would potentially make the expensive investment in SIX6-based herbicide development worthwhile.

The development of herbicides based on full-length recombinant *Fol* SIX6 protein faces significant economic and logistical constraints that would limit commercial viability. Production of recombinant SIX6 protein in *E. coli* or alternative expression systems would require substantial capital investment in large-scale fermentation facilities, extensive downstream purification processes, and stringent quality control measures to ensure proper protein folding and biological activity (Palomares et al., 2004). Additionally, the inherent instability of proteins requires cold storage and transportation infrastructure, further increasing operational costs and complexity. These problems together make it too expensive to produce full-length proteins for widespread use in agriculture.

Identification of biologically active peptide fragments within SIX6 could overcome these manufacturing constraints by enabling chemical synthesis rather than biological production. Chemical peptide synthesis offers several advantages, including significantly reduced per-unit costs, elimination of protein stability concerns, simplified formulation requirements, and extended shelf life without refrigeration (Kota, 2019). The transition from biological to chemical production methods would facilitate scalable manufacturing processes compatible with existing agrochemical industry infrastructure.

Recent resolution of *Fol* SIX6 protein structure by Yu et al. (2024) using X-ray crystallography provided insights into its molecular architecture, revealing a dual-domain organisation characteristic of FOLD (*Fol* dual-domain) effectors, of which *Fol* SIX6 is one of the founding members. However, translation of this structural information into a commercially viable herbicide would require systematic structure-activity relationship studies to determine which domains are responsible for cell death induction. Subsequent research priorities could include deletion and truncation analyses to map the minimal bioactive region, site-directed mutagenesis to identify functionally critical amino acid residues. Alternatively, the identification of the host target could potentially allow the use of rational design software to design molecules other than peptides that would bind to the SIX6 target site and mimic the effect of SIX6 binding and also potentially enable manipulation of herbicide target plant specificity.

7.3 SIX6 cell death-inducing activity: independence from some defence pathways and future genetic approaches to test others

In Chapter 4, VIGS was employed in *N. benthamiana* to assess the involvement of known plant defence signalling components (*BAK1*, *SOBIR1*, *WIPK* and *SIPK*) in cell death induced by *Fol SIX6* (Chapter 4). Silencing of these genes failed to attenuate cell death induced by *Agrobacterium*-mediated expression of *Fol SIX6*. These results were complemented by experiments using tomato mutant lines deficient in defence signalling pathways, including the ethylene-insensitive *Never ripe* mutant and the *sun1-1* mutant lacking functional EDS1 (Chapter 4). Infiltration of purified SIX6 protein into these mutant lines failed to reduce cell death responses compared to wild-type controls. Whilst these findings indicate that SIX6-induced cell death operates through mechanisms independent of several cell-death pathways associated with effector recognition, including cell death mediated triggered by LRR cell-surface receptors and TIR-NLRs, it does not exclude cell death mediated by CC-NLRs or non-LRR cell-surface receptors such as wall-associated kinases (WAKs), malectin-like receptor kinases (MLRKs aka CrRLK1Ls) or S-domain receptor-like kinases (SRLKs; aka S-locus RLKs). WAKs monitor the cell surface of plant cells, including the cell wall and some are able to trigger plant cell death e.g. Arabidospsis WAK3 and tobacco WAK2 trigger cell death in response to *Erwinia amylovora* and *Xanthomonas citri* pv *glycines* harpins (Held et al., 2024; Held et al., 2025). Interestingly, WAKL22 (WAK-like kinase 22) confers non-race specific resistance to *F. oxysporum* f. sp. *matthioli* in Arabidopsis (Diener and Ausubel, 2005), but other WAKs are involved in race-specific resistance e.g. the *Brassica napus Rlm9* resistance gene encodes a WAKL receptor kinase that triggers BAK1- and SOBIR1-independent cell death following recognition of the *Leptosphaeria maculans* AvrLm5-9 effector (Larkan et al., 2020). MLRKs also monitor the cell surface and some are able to trigger cell death e.g. the MLRK LET1 (lethality suppressor of *mekk1* 1) triggers cell death mediated by the CC-NLR SUMM2 (suppressor of *mkk1 mkk2*) (Liu et al. 2020; Huang et al., 2020). Besides their role in self-incompatibility in the Brassicaeae (Nasrallah, 2023), SRLKs are involved in both biotic and abiotic stress responses (Kim et al., 2009; Chen et al., 2013; Sun et al., 2013). Interestingly, the Arabidopsis *RFO3* gene for resistance to *F. oxysporum* f. sp. *matthioli* encodes an SRLK (Cole and Diener, 2013) and the tomato *I-3* gene for *Fol* resistance encodes an SRLK that recognises the *Fol* Avr3 effector protein (Catanzariti et al., 2015).

Some NLRs are thought to guard cell surface receptors e.g. in Arabidopsis the CHS3/CSA1 sensor-executor TIR-NLR pair guard the co-receptor BAK1 (Yang et al., 2022; Schulze et al.,

2022). Some CC-NLRs like ZAR1, which guards RLCKs (cytoplasmic kinases that resemble the kinase domains of receptor kinases) and the helper NLRS NRC1 and ADR1 form plasma-membrane-penetrating multimers (aka resistosomes) that act as calcium channels allowing a cell-death inducing influx of calcium ions (Contreras et al., 2023). Other CNLs appear to inhibit plasma-membrane H^+ ATPases leading to membrane depolarisation, an influx of calcium ion and cell death (Lee et al., 2022). VIGS or targeted mutagenesis using CRISPR/Cas9 could be used to test the role of genes like these or other candidate genes identified through literature mining, particularly those thought to be involved in cell death pathways. For example, as suggested in Chapter 4, genes encoding proteins such as RAR1, SGT1 and HSP90 required for CC-NLR functionality could be targeted to test whether a CC-NLR might be involved in SIX6-induced cell death. ZAR1 and other so-called ANLs (ancient and autonomous CC-NLRs; thought to be involved in resistosome formation (Lee et al., 2021) could also be targeted.

As was the case for the identification of *Avr7,* it is possible that targeted mutagenesis may not enable identification of a gene encoding a SIX6 target or genes involved in executing the cell death response. A non-targeted forward genetic strategy using chemical mutagenesis of tomato or *N. benthamiana* and screening of M1 seedlings by infiltration with SIX6 protein could be used as an alternative. Whole-genome sequencing of non-responsive mutants could pinpoint specific genes required for SIX6-induced cell death. Complementary studies could focus on identifying the cellular target of SIX6 through protein-protein interaction assays, such as pull-down assays and co-immunoprecipitation (co-IP) assays.

7.4 SIX6 impact on leaves: stomatal opening, water loss and the induction of leaf cell death

Fol SIX6 protein was able to induce irreversible stomatal opening in *N. benthamiana* and tomato (Chapter 5). Gas exchange analyses demonstrated that *Fol* SIX6 infiltration significantly increased stomatal conductance and transpiration rates in *N. benthamiana* leaves, regardless of light conditions (Chapter 5). Cellular-level examination using confocal microscopy following *Agrobacterium*-mediated expression of a vacuole-targeted fluorescent protein in *N. benthamiana* showed that SIX6 treatment induced vacuolar shrinkage and leakage in leaf epidermal cells (Chapter 5).

Whist stomatal opening and associated water loss are unlikely to contribute to the pathogenicity of a root pathogen like *Fol* they could contribute to the pathogenicity of foliar pathogens. Many species of *Colletotrichum*, which cause anthracnose on the leaves and fruit of a wide array of

plants, possess SIX6 homologues, including pathogens of Solanaceous plants such as *C. scovillei* isolated from fruit lesions on chilli pepper (*Capsicum annuum*; Genbank Accession KAG7065108.1) but also able to infect leaves, *C. tamarilloi* pathogenic on leaves and fruit of tamarillo (*Solanum betaceum*; Genbank Accession KAK1493322.1) and *C. chlorophyti* isolated from infected tomato leaves (Genbank Accession OLN97279.1). Like *Fol* SIX6, these SIX6 homologues could be tested for their ability to cause stomatal opening and leaf cell death in tomato and tobacco, and *SIX6* knockouts could be generated in *Colletotrichum* to test their role in pathogenicity. Interestingly, SIX6 homologues have also been identified in *Colletotrichum* species that are pathogens of Brassicaceous plants such as *C. incanum* pathogenic on radish (*Raphanus sativus*; Genbank Accession OHW98556.1) and *C. higginsianum* isolated from infected bok choy leaves (*Brassica rapa* subsp. *chinensis*; Genbank Accession OBR03151.1). Given that *Fol, Fom* and *Foc* SIX6 did not induce cell death in radish (Fig. 3.7–3.9) and *Fol* SIX6 did not induce stomatal opening in radish (Appendix 5.3), it would be interesting to test whether *C. incanum* SIX6 was able to cause stomatal opening and cell death in either radish leaves or tomato leaves. Differential responses might give clues as to SIX6 residues important for host-specific function. Understanding whether *SIX6* effectors from other plant-pathogenic fungi induce comparable responses could broaden our understanding of their virulence strategies and impact on host plants.

The observation that SIX6 induces vacuolar shrinkage and leakage (Chapter 5) is consistent with the induction of leaf cell death via the destructive form of vacuolar-mediated PCD described by Hara-Nishimura and Hatsugai (2011). The question arises as to how an extracellular effector might be linked to activation of vacuolar-mediated PCD. A receptor kinase or a protein translocated from the apoplast to the interior of the cell could generate a cytoplasmic mechanism for activation of vacuolar-mediated PCD. Phytaspase (aspartate-specific subtilisin-like protease) is an example of an apoplastic protein that is imported into the cell during PCD (Chichkova et al. 2010). Phytaspase is essential for PCD associated with TMV-induced HR and osmotic stress in tobacco (Chichkova et al. 2010). Vacuolar processing enzymes (VPEs; aspartate- and asparagine-specific cysteine proteases) play a key role in vacuolar-mediated PCD including TMV-induced HR in *N. benthamiana* (Hatsugai et al. 2004). However, there is no direct connection between PCD controlled by VPEs and that controlled by phytaspases, suggesting that the underlying mechanisms are distinct. VPEs are encoded by a small multigene family with different isoforms controlling PCD in various processes, including xylem formation, pollen dehiscence, senescence and environmental stress responses

as well as pathogen-induced PCD (Wleklik and Borek, 2023). Given their important role in vacuole-mediated PCD, VPEs, especially those involved in pathogen-induced PCD could be tested by VIGS or targeted mutagenesis for a role in SIX6-induced cell death.

7.5 SIX6 impact on root systems: physiological disruption

The effects of *Fol* SIX6 on root tissues were investigated through experiments using both *N. benthamiana* and tomato roots. Measurements from treated root tissues of *N. benthamiana* and tomato showed significant increases in electrolyte leakage following *Fol* SIX6 protein infiltration (Chapter 6). In vitro growth assays using medium containing purified *Fol* SIX6 protein demonstrated substantial inhibition of primary root elongation in tomato seedlings, while secondary root initiation remained largely unchanged within the time frame assessed in three of four experimental replicates (Chapter 6). These results indicate that SIX6 produces physiological effects on root tissues that may contribute to *Fol* pathogenicity during infection.

Potassium efflux via potassium transporters is the predominant cause of biotic and abiotic stress-induced electrolyte leakage and leads to an overall loss of cytosolic potassium, which is important for root growth (Demidchik et al., 2014). Potassium starvation has been found to reduce root elongation (Walker et al., 1998; Zhang et al., 2009). Targeting of potassium channels might explain the inhibition of tomato root elongation caused by SIX6. The *Magnaporthe oryzae* AvrPiz-t effector promotes pathogenicity on its rice host by inhibiting potassium influx mediated via the AKT1 potassium channel protein, but supplementation with potassium was found to counter this effect (Shi et al., 2018). It would therefore be interesting to grow tomato seedlings on media supplemented with SIX6 and various concentrations of potassium to see if inhibition of root elongation could be relieved by increasing concentrations of potassium. A positive response would suggest a possible role for potassium channels in the SIX6 response. Additionally, given that plasma membrane H+ ATPase activity and potassium channel function are closely linked to extracellular pH changes, it would also be informative to test whether SIX6 affects extracellular pH in root growth media. This could be achieved by applying a pH indicator to the medium, which would provide a simple and accessible measure of whether SIX6 disrupts ion transport at the root surface.

The experimental challenges associated with studying root systems warrant additional consideration. Unlike leaf tissues, roots present significant methodological limitations, particularly the inability to use standard techniques such as agroinfiltration or direct protein infiltration that are routinely used for leaf-based studies. Furthermore, roots grown in water or

tissue culture are always in a fully hydrated environment, which makes them unsuitable for using cell death as an indicator of stress or effector impact, since they won't show that response under those conditions. This limitation is particularly relevant given our observations (from Daniel Yu's Honours thesis, ANU) from leaf covering experiments, where cell death was significantly delayed when leaves remained covered, despite stomatal opening continuing to occur in darkness. Since leaf covering would not have affected stomatal aperture, the delayed cell death was likely attributable to reduced water loss, suggesting that water stress may be a contributing factor to the cell death phenotype. This interpretation is further supported by previous observations where *Cf-9* leaves infiltrated with *Avr9*-containing infiltration fluid showed delayed cell death responses when maintained at 95% relative humidity, reinforcing the potential role of water availability in modulating cell death pathways (Wang et al., 2005).

It is likely that SIX6 is acting against the same host target in both leaves and roots, so studying SIX6 function in leaves, in addition to being an easier experimental study system than roots, can still provide information about SIX6 function that can then be explored in roots once progress has been made in leaf systems i.e. SIX6 effects in leaves may still serve as a proxy for SIX6 effects in roots.

7.6 Concluding remarks

Whilst stomatal opening and associated water loss are significant effects of SIX6 on leaves, they may bear little relationship to the effects of SIX6 on roots. Roots do not possess stomata, they have a different morphology and physiology and, in the absence of drought, roots are not subject to the same transpirational water stress as leaves. On the other hand, the ability of SIX6 to trigger a cell death response in leaf epidermal cells that is related to vacuolar shrinkage and vacuolar leakage is likely to be more relevant to roots. Possible models for SIX6-induced cell death are shown in Figure 7.1. These models draw together various possibilities that have been discussed throughout this thesis, including potential roles for plasma-membrane-anchored receptors, H^+ ATPases, potassium channels and calcium channels, as well as cytosolic CC-NLRs and the activation of vacuolar-mediated PCD by VPEs following an influx of calcium ions or an efflux of potassium ions. Various experiments have been proposed throughout this thesis to test the roles of some of these components in SIX6-induced cell death.

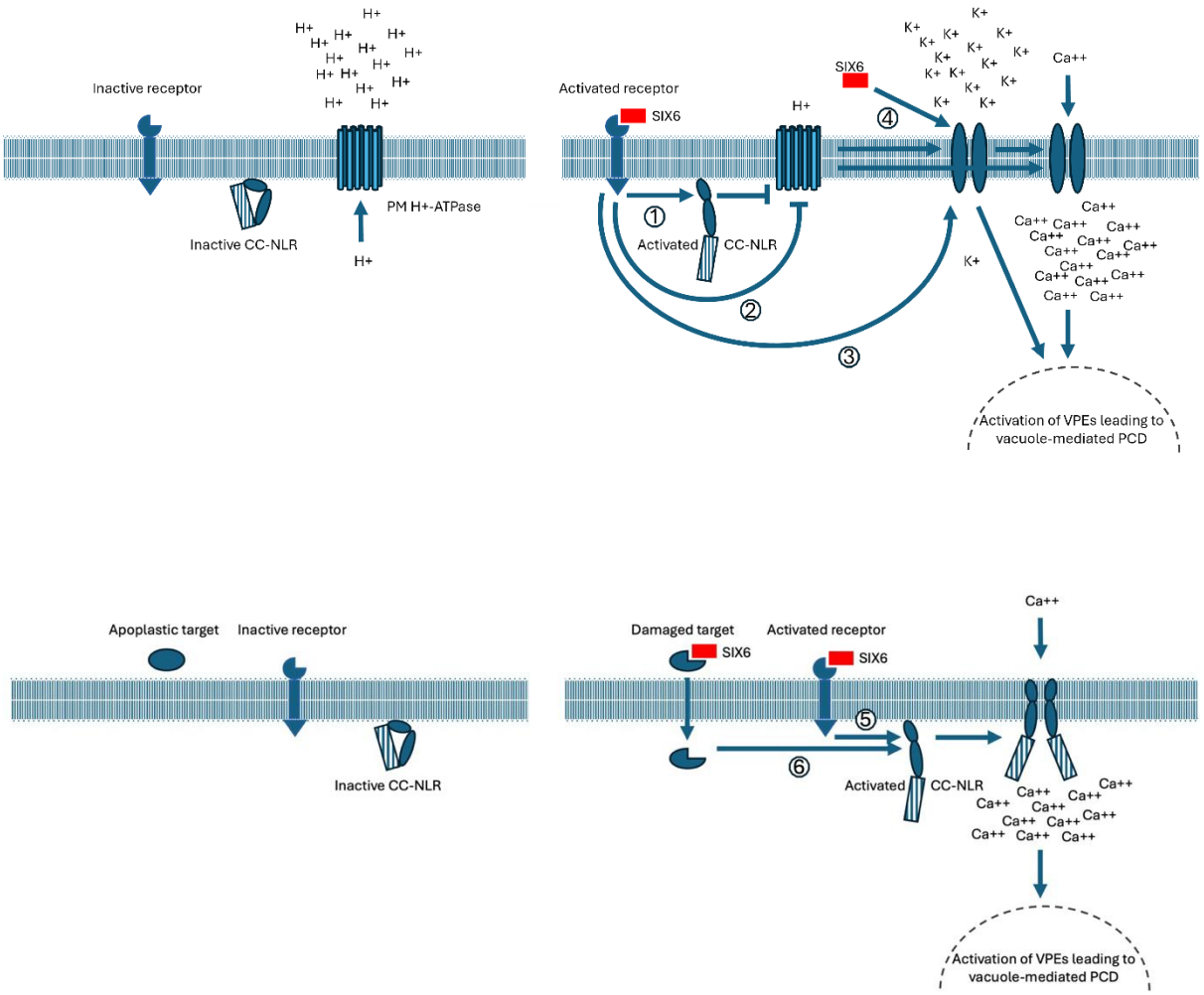

Figure 7.1 Possible models for the induction of leaf cell death by SIX6.

1) SIX6-activated receptor activates a CC-NLR that inhibits PM H^+-ATPase leading to K^+ efflux and/or Ca^{++} influx that activates vacuolar-mediated PCD. 2) SIX6-activated receptor inhibits plasma membrane H^+-ATPase, possibly by dephosphorylation, leading to K^+ efflux and/or Ca^{++} influx that activates vacuolar-mediated PCD. 3) SIX6-activated receptor promotes K^+ efflux and/or inhibits K^+ influx, possibly by phosphorylation, leading a K^+ deficit and/or Ca^{++} influx that activates vacuolar-mediated PCD. 4) SIX6 interacts directly with K^+ channel to promote K^+ efflux and/or inhibit K^+ influx leading to a K^+ deficit and/or a Ca^{++} influx that activates vacuolar-mediated PCD. 5) SIX6-activated receptor activates a CC-NLR which multimerizes and forms a pore in the plasma membrane allowing Ca^{++} influx that activates vacuolar-mediated PCD. 6) SIX6 damages an apoplastic target which is translocated into the cytoplasm and activates a CC-NLR which multimerizes and forms a pore in the plasma membrane allowing Ca^{++} influx that activates vacuolar-mediated PCD or does so by the mechanism described in 1) above.

Whilst the models for SIX6-induced leaf cell death described in Figure 7.1 may provide a focus for future experiments, it is important to remember that leaf cell death is only a proxy for what might be happening in roots. It is also important to remember that the biologically relevant concentration of SIX6 delivered during *Fol* infection may be significantly lower than that delivered by protein infiltration and may well fall below a threshold for activation of cell death responses. It is also important to remember that SIX6 is only one of many effectors delivered during *Fol* infection and some of the other effectors may suppress cell death response and allow SIX6 to carry out its pathogenicity function without adverse consequences. The *Fol* Avr1 effector has been shown to inhibit resistance triggered by the Avr2 and Avr3 effectors in *I* and *I-3* tomato plants, respectively (Houterman et al., 2008). Similarly, the *Fol* Avr2 effector is able to suppress PTI in Arabidopsis (Di et al., 2017; Blekemolen et al., 2023). It would be interesting to test whether co-infiltration of purified Avr1 and SIX6 proteins could suppress SIX6-induced cell death in tomato, or whether prior agroinfiltration of *Avr2* could suppress SIX6-induced cell death in tobacco.

Interference with potassium channel activity is an intriguing possibility for the role of SIX6 in *Fol* pathogenicity, not least because the leaf phenotype triggered by SIX6 resembles the specific effect of *C. fulvum* Avr9 on stomatal opening and epidermal cell collapse in *Cf-9* tomato leaves, which are associated, somewhat paradoxically in the case of stomatal opening, with activation of potassium efflux and inhibition of potassium influx (Blatt et al., 1999). In rice, inhibition of potassium influx via the plasma-membrane AKT1 potassium channel protein by the *Magnaporthe oryzae* AvrPiz-t effector was found to reduce plant immunity whereas supplementation with potassium was found to improve rice resistance to the pathogen (Shi et al., 2018). Cytosolic potassium deficiency also leads to metabolic reprogramming, favouring the production of soluble sugars and non-acidic amino acids (Demidchik et al., 2014), which could potentially favour pathogen nutrition. Targeting of one or more potassium channels by SIX6 could explain many of the leaf and root symptoms observed in this study and, at sub-PCD-threshold levels that might occur in *Fol* infected roots, may help suppress plant immunity and facilitate pathogen nutrition. Potassium channels may therefore be a fruitful area for future investigation into the role of SIX6 in *Fol* pathogenicity.

References

Blatt, M.R., Grabov, A., Brearley, J., Hammond-Kosack, K., Jones, J.D. (1999). K^+ channels of *Cf-9* transgenic tobacco guard cells as targets for *Cladosporium fulvum Avr9* elicitor-dependent signal transduction. *The Plant Journal*, *19*(4), 453-462.

Blekemolen, M.C., Liu, Z., Stegman, M., Zipfel, C., Shan, L., Takken, F.L. (2023). The PTI-suppressing Avr2 effector from *Fusarium oxysporum* suppresses mono-ubiquitination and plasma membrane dissociation of BIK1. *Molecular Plant Pathology*, *24*(10), 1273-1286.

Catanzariti, A.M., Lim, G.T.T., Jones, D.A. (2015). The tomato I-3 gene: a novel gene for resistance to Fusarium wilt disease. *New Phytologist*, *207*(1), 106-118.

Chen, L.J., Wuriyanghan, H., Zhang, Y.Q., Duan, K.X., Chen, H.W., Li, Q.T., Lu, X., He, S.J., Ma, B., Zhang, W.K. Lin, Q. (2013). An S-domain receptor-like kinase, OsSIK2, confers abiotic stress tolerance and delays dark-induced leaf senescence in rice. *Plant Physiology*, *163*(4), 1752-1765.

Chichkova, N.V., Shaw, J., Galiullina, R.A., Drury, G.E., Tuzhikov, A.I., Kim, S.H., Kalkum, M., Hong, T.B., Gorshkova, E.N., Torrance, L., Vartapetian, A.B. (2010). Phytaspase, a relocalisable cell death promoting plant protease with caspase specificity. *The EMBO Journal*, *29*(6), 1149-1161.

Cole, S.J., & Diener, A.C. (2013). Diversity in receptor-like kinase genes is a major determinant of quantitative resistance to *Fusarium oxysporum* f. sp. *matthioli*. *New Phytologist*, *200*(1), 172-184.

Contreras, M.P., Lüdke, D., Pai, H., Toghani, A., Kamoun, S. (2023). NLR receptors in plant immunity: making sense of the alphabet soup. *EMBO Reports*, *24*(10), 57495.

Demidchik, V., Straltsova, D., Medvedev, S.S., Pozhvanov, G.A., Sokolik, A., Yurin, V. (2014). Stress-induced electrolyte leakage: the role of K^+-permeable channels and involvement in programmed cell death and metabolic adjustment. *Journal of Experimental Botany*, *65*(5), 1259-1270.

Di, X., Cao, L., Hughes, R.K., Tintor, N., Banfield, M.J., Takken, F.L.W. (2017). Structure–function analysis of the *Fusarium oxysporum* Avr2 effector allows uncoupling of its immune-suppressing activity from recognition. *New Phytologist*, *216*(3), 897-914.

Diener, A.C., & Ausubel, F.M. (2005). *Resistance to Fusarium oxysporum 1*, a dominant Arabidopsis disease-resistance gene, is not race specific. *Genetics*, *171*(1), 305-321.

Hara-Nishimura, I., & Hatsugai, N. (2011). The role of vacuole in plant cell death. *Cell Death and Differentiation*, *18*(8), 1298-1304.

Hatsugai, N., Kuroyanagi, M., Yamada, K., Meshi, T., Tsuda, S., Kondo, M., Nishimura, M., Hara-Nishimura, I. (2004). A plant vacuolar protease, VPE, mediates virus-induced hypersensitive cell death. *Science*, *305*(5685), 855-858.

He, B., Hu, Y., Wang, W., Yan, W., Ye, Y. (2022). The progress towards novel herbicide modes of action and targeted herbicide development. *Agronomy*, *12*(11), 2792.

Held, J.B., Rowles, T., Schulz, W., McNellis, T.W. (2024). *Arabidopsis wall-associated kinase 3* is required for harpin-activated immune responses. *New Phytologist*, *242*(3), 853-857.

Held, J.B., Sinn, J.P., Kvitko, B.H., McNellis, T.W. (2025). The harpin-induced hypersensitive reaction in *Nicotiana tabacum* requires wall-associated kinase 2. *Molecular Plant Pathology*, *26*(5), 70096.

Houterman, P.M., Cornelissen, B.J., Rep, M. (2008). Suppression of plant resistance gene-based immunity by a fungal effector. *PLoS pathogens*, *4*(5), 1000061.

Huang, Y., Yin, C., Liu, J., Feng, B., Ge, D., Kong, L., Ortiz-Morea, F.A., Richter, J., Hauser, M.T., Wang, W.M., Shan, L. (2020). A trimeric Cr RLK1L-LLG1 complex genetically modulates SUMM2-mediated autoimmunity. *Nature Communications*, *11*(1), 4859.

Kim, H.S., Jung, M.S., Lee, S.M., Kim, K.E., Byun, H., Choi, M.S., Park, H.C., Cho, M.J., Chung, W.S. (2009). An S-locus receptor-like kinase plays a role as a negative regulator in plant defense responses. *Biochemical and Biophysical Research Communications*, *381*(3), 424-428.

Kota, S. (2019). Peptide Therapeutics: strategy and tactics for chemistry, manufacturing and controls, *The Royal Society of Chemistry,* 111-150.

Larkan, N.J., Ma, L., Haddadi, P., Buchwaldt, M., Parkin, I.A., Djavaheri, M., Borhan, M.H. (2020). The *Brassica napus* wall-associated kinase-like (WAKL) gene *Rlm9* provides race-specific blackleg resistance. *The Plant Journal*, *104*(4), 892-900.

Lee, H.Y., Mang, H., Choi, E., Seo, Y.E., Kim, M.S., Oh, S., Kim, S.B., Choi, D. (2021). Genome-wide functional analysis of hot pepper immune receptors reveals an autonomous NLR clade in seed plants. *New Phytologist*, *229*(1), 532-547.

Lee, H.Y., Seo, Y.E., Lee, J.H., Lee, S.E., Oh, S., Kim, J., Jung, S., Kim, H., Park, H., Kim, S., Mang, H. (2022). Plasma membrane-localized plant immune receptor targets H^+-ATPase for membrane depolarization to regulate cell death. *New Phytologist*, *233*(2), 934-947.

Li, Y., Xia, C., Wang, M., Yin, C., Chen, X. (2020). Whole-genome sequencing of *Puccinia striiformis* f. sp. *tritici* mutant isolates identifies avirulence gene candidates. *BMC Genomics, 21*(1), 247.

Liu, J., Huang, Y., Kong, L., Yu, X., Feng, B., Liu, D., Zhao, B., Mendes, G.C., Yuan, P., Ge, D., Wang, W.M. (2020). The malectin-like receptor-like kinase LETUM1 modulates NLR protein SUMM2 activation via MEKK2 scaffolding. *Nature Plants*, *6*(9), 1106-1115.

Ma, L.J., van der Does, H.C., Borkovich, K.A., Coleman, J.J., Daboussi, M.J., Di Pietro, A., Dufresne, M., Freitag, M., Grabherr, M., Henrissat, B., Houterman, P.M., Kang, S., Shim, W. B., Woloshuk, C., Xie, X., Xu, J.R., Antoniw, J., Baker, S.E., Bluhm, B.H., Breakspear, A., Brown, D.W., Butchko, R.A.E., Chapman, S., Coulson, R., Coutinho, P.M., Danchin, E.G.J., Diener, A., Gale, L.R., Gardiner, D.M., Goff, S., Hammond-Kosack, K.E., Hilburn, K., Hua-Van, A., Jonkers, W., Kazan, K., Kodira, C.D., Koehrsen, M., Kumar, L., Lee, Y.H., Li, L., Manners, J.M., Miranda-Saavedra, D., Mukherjee, M., Park, G., Park, J., Park, S.Y., Proctor, R.H., Regev, A., Ruiz-Roldan, M.C., Sain, D., Sakthikumar, S., Sykes, S., Schwartz, D.C., Turgeon, B.G., Wapinski, I., Yoder, O., Young, S., Zeng, Q., Zhou, S., Galagan, J., Cuomo, C.A., Kistler, H.C., Rep, M. (2010). Comparative genomics reveals mobile pathogenicity chromosomes in *Fusarium*. *Nature, 464*(7287), 367-373.

Nasrallah, J.B. (2023). Stop and go signals at the stigma–pollen interface of the Brassicaceae. *Plant Physiology*, *193*(2), 927-948.

Palomares, L.A., Estrada-Mondaca, S.S., Ramírez, O.T. (2004). Production of recombinant proteins challenges and solutions. *Methods in Molecular Biology, 267, Recombinant Gene Expression: Reviews and Protocols* (2nd ed.). Humana Press.

Peng, Y., Li, S.J., Yan, J., Tang, Y., Cheng, J.P., Gao, A.J., Yao, X., Ruan, J.J., Xu, B.L. (2021). Research progress on phytopathogenic fungi and their role as biocontrol agents. *Frontiers in Microbiology, 12*, 670135.

Schulze, S., Yu, L., Hua, C., Zhang, L., Kolb, D., Weber, H., Ehinger, A., Saile, S.C., Stahl, M., Franz-Wachtel, M., Li, L. (2022). The Arabidopsis TIR-NBS-LRR protein CSA1 guards BAK1-BIR3 homeostasis and mediates convergence of pattern and effector-induced immune responses. *Cell Host and Microbe*, *30*(12), 1717-1731.

Shi, X., Long, Y., He, F., Zhang, C., Wang, R., Zhang, T., Wu, W., Hao, Z., Wang, Y.I., Wang, G.L., Ning, Y. (2018). The fungal pathogen *Magnaporthe oryzae* suppresses innate immunity by modulating a host potassium channel. *PLoS Pathogens*, *14*(1), 1006878.

Sun, X., Fang, X., Wang, D., Jones, D.A., Ma, L. (2022). Transcriptome analysis of Fusarium–tomato interaction based on an updated genome annotation of *Fusarium oxysporum* f. sp. *lycopersici* identifies novel effector candidates that suppress or induce cell death in *Nicotiana benthamiana*. *Journal of Fungi, 8*(7), 672.

Sun, X.L., Yu, Q.Y., Tang, L.L., Ji, W., Bai, X., Cai, H., Liu, X.F., Ding, X.D., Zhu, Y.M. (2013). GsSRK, a G-type lectin S-receptor-like serine/threonine protein kinase, is a positive regulator of plant tolerance to salt stress. *Journal of Plant Physiology*, *170*(5), 505-515.

Urban, M., King, R., Hassani-Pak, K., Hammond Kosack, K.E. (2015). Whole-genome analysis of *Fusarium graminearum* insertional mutants identifies virulence associated genes and unmasks untagged chromosomal deletions. *BMC Genomics, 16*(1), 261.

Walker, D.J., Black, C.R., Miller, A.J. (1998). The role of cytosolic potassium and pH in the growth of barley roots. *Plant Physiology*, *118*(3), 957-964.

Wang, C., Cai, X., Zheng, Z. (2005). High humidity represses *Cf-4*/*Avr4* and *Cf-9*/*Avr9*-dependent hypersensitive cell death and defense gene expression. *Planta*, *222*(6), 947-956.

Wleklik, K., & Borek, S. (2023). Vacuolar processing enzymes in plant programmed cell death and autophagy. *International Journal of Molecular Sciences*, *24*(2), 1198.

Yang, Y., Kim, N.H., Cevik, V., Jacob, P., Wan, L., Furzer, O.J., Dangl, J.L. (2022). Allelic variation in the *Arabidopsis* TNL CHS3/CSA1 immune receptor pair reveals two functional cell-death regulatory modes. *Cell Host and Microbe*, *30*(12), 1701-1716.

Yu, D. (2019). Structural and functional characterisation of SIX6: A cell death-inducing effector. (Honours thesis, The Australian National University, Australia).

Yu, D.S., Outram, M.A., Smith, A., McCombe, C.L., Khambalkar, P.B., Rima, S.A., Sun, X., Ma, L., Ericsson, D.J., Jones, D.A., Williams, S.J. (2024). The structural repertoire of *Fusarium oxysporum* f. sp. *lycopersici* effectors revealed by experimental and computational studies. *eLife, 12*, RP89280.

Zhang, Z.Y., Wang, Q.L., Li, Z.H., Duan, LS., Tian, X.L. (2009). Effects of potassium deficiency on root growth of cotton seedlings and its physiological mechanisms. *Acta Agronomica Sinica*, *35*(4), 718-723.